Integrated Evaluation of a Wet Gas Reservoir: Minimizing Volumetric Uncertainties Using Dynamic Analysis

Bello Saidu

Ph.D. Thesis **2019**

Integrated Evaluation of Wet Gas Reservoir: Minimizing Volumetric Uncertainties Using Dynamic Analysis

Bello Saidu

School of Science, Engineering and Environment (SEE)

University of Salford, Manchester, UK

Submitted in Partial Fulfilment of the Requirements of the Degree of Doctor of Philosophy, November 2019

Abstract

There is a growing research effort to understand the most reliable approach in estimations of oil and gas reserves, through different procedures such as the volumetric, Material Balance, Reservoir Simulation, Decline Curve Analysis (Production performance analysis), which depends on the understanding of the physical flow characterization of the formation, production data, and recently dynamic nature of reserves. While most researchers were motivated by static nature of dry gas reserves and hence, their reserve estimations consider parameters typical of such reservoirs, formations where associated gas is found has continued to be a challenge particularly in sandstone reservoirs.

In this study a novel approach of adopting integrated experimental and analytical techniques, using digital core flooding system to establish dynamic properties of the reserves was used in combination with analytical techniques including Volumetric, Decline Curve Analysis, Reservoir simulation and Material balance.

Experimental study was conducted in phase I to determine rock properties, such as effective porosity, permeability and distribution of pore size, generally regarded as petrophysical properties, the core characterization measurement of the dimensions and weight were performed using the Vernier calliper, weight measurement balance.

In Phase II PVT (Pressure, Volume and Temperature) analysis for gas composition and fluid properties were also carried for a wet gas field case study (Ogba Essale). A sub set of the sample was flashed from reservoir condition to atmospheric condition (758.31 mmhg and 82.4 f). The products (i.e. gas and oil) were analysed by gas chromatographic technique and then mathematically recombined to obtain the reservoir fluid composition. Constant composition expansion (CCE) test, Constant volume depletion (CVD) test were performed at the reservoir temperature of 224.6 f. multi-stage separation test was performed at the specified surface processing condition, the results were subsequently inputted for reserve evaluation into various method

Phase III Involved Modelling and computer simulation Static geologic models in Petrel and Reservoir simulation models in Eclipse 100 and 300 were built and utilized to estimate the hydrocarbon volumes. Similarly, in this phase Declining Curve Analysis using Oil Field Manger (OFM), Material Balance and Volumetric calculations was carried out.

Phase IV focused on Single Phase flow of Buff Bera using Navier-Stokes equations and Darcy`s law to describe single-phase gas transport and free gas at the pore spaces. The models were developed using water salinity representation of the wet gas field in the case study, to simulate the performance of the natural gas reservoir in assessing the performance of production from natural gas reservoir.

Phase V: Core flooding for two-phase liquid movements under unsteady state or steady state circumstances and single-phase gas steady-state experiments, was conducted.

Phase VI involved the application of COMSOL-Physics, constitute the creation of a pore-scale finite element mesh of sandstone core samples from SEM images and based on the numerical simulation of sandstone at a pore-scale level based on experimental results

Phase 7: Results analysis and discussions: The findings indicated from the characterization (phase I) indicated for porosities of the respective core samples: Buff bera 24.55% and 20-22%, Castle gate 29.31% and 27-29%, Boise 30.35% and 28%, Bandera Grey 19.67 and 19-21%, and Grey Beira 20.18% and 18-21% for experimental and factory values respectively. While permeabilities values indicated Buff Beira 458.1mD and 350-600mD, Castle gate 1434.8mD and 1300-1500mD, and Boise 2196.4mD and 2000-4000mD for experimental and factory values respectively, the porosity and permeability values by the experiment deviated slightly from the factory porosity values. The experimental result showed good agreement with the literature data under dynamic conditions, subsequent data of the Buff Berea experiment result was implemented into COMSOL multi physics software to characterize gas transport of single-phase flow at pore scale level. Also, for this study, the Buff Bera values of porosity and permeability were imputed for all the reservoir evaluation technique except for Reservoir simulation of which porosity was estimated from the bulk density and sonic logs using average grain density of 2.65g/cc, 1.00g/cc and 0.85g/cc for fluid density, 53msec/ft. for average grain velocity and 189msec/ft. For pore fluid velocity, the net sand of the reservoirs was estimated by applying Petro-physical cut-off (vsh=0.52, porosity=0.12). The results from the aquifer salinity confirms that the higher the salinity of the aquifer the higher the natural gas production and the lower the produced water as seen in the gwr vs time graph. there was a production increase of about 50% when 0 wt% salt encroached the reservoir compared to when 10 wt% Nacl. With this leading finding, a better characterisation of the natural gas reservoir will be carried out for adequate evaluation of the performance of the reservoirs in the phase II of the study.

Consequently, 75.9132 MMSTB of oil and 2,188.54 BCF of gas was obtained from reservoir simulation, do nothing case: an additional recovery for the field is about 30.23MMSTB and 27.8BSCF of oil and gas respectively. case 1: an additional recovery for the field was about 37.21MMSTB and 26.0BSCF of oil and gas respectively. STOOIP of 1548.297365 MMSTB and GIIP of 3007862.483 MMSCF from volumetric, EUR of 52261BSCF gas and EUR of 452.6MMSTB from decline curve analysis, and GIIP of 370.47MMSCF and STOOIP of 377.26MMSTB from material balance. the volume of initial hydrocarbon obtained from material balance analysis and static model volume estimates are comparable and within 2 -6% difference. The declining curve analysis and production performance analysis were carried out and compared with a slight variation of the end volumes.

This study has utilised dynamic reservoir data integrated with various models, which can be valuable in improving reserve estimation using multiple models compared to single models adopted by many research and industry practices.

Acknowledgement

In the name of Allah, the beneficent, the merciful, all thanks be to you, the master of universe, without you nothing under this earth is possible I am grateful for gift of life, health and the ability to undergo this programme successfully in this regard I say Allahuma Salli Ala Muhammadin Wa Ala Ali Muhammadin Kama sallaita Ala Ibrahima Wa Ala Ali Ibrahima Innaka Hammedun Majeed Allahuma Barik Ala Muhammadin Wa Ala Ali Muhammadin Kama Barakta Ala Ibrahima wa Ala Ali Ibrahima Innaka Hameedun Majeed.

At this juncture, I would like to express my sincere appreciations and gratitude to my supervisor, Doctor Abubakar Abbas Jibril, for his indefatigable academic sustenance in all imaginable way he could during my PhD programme. My sincere thanks to Professor Ghasem Ghaveni Nasr for his succour and sustenance during the period of my study, as my co-supervisor. I will not hesitate to mention the valuable contribution to all other academic and technical staff in the Department; Dr Godpower Chimagwo Enyi, Dr M. Burby, Dr A.Nourian N, Mr Ali Kadir, Mr Alan Mappin among others numerous to mention I said thank you for your generous support throughout this study. To Petroleum Technology Development Fund (PTDF), for the studentship. To Federal Ministry of Petroleum Resources-Abuja and my office colleagues and friends there Thank you for the enormous support

In this regard I cannot forget to mention my good friends and colleagues in the School of Computing Science and Engineering and other school as well, exclusively, Aminu Abba Yahya, Mohammed Abba Kabir, Hamid Adamu Abubakar, Abdullahi, Alhaji Umaru, Emmanuel, Kabir Jega, Murtala, Mahmud, Ibrahim Sadiq, my study colleague Hamza Muhammed and all others whose names were not stated for their assurance, commonality, friendship and being there always for me whenever the need arises.

My heartfelt appreciation goes to my parents Alhaji Saidu Abubakar Ardo Asura and Hajia Maryam Aliyu Baware, I owed all my success to your prayers support and everything I have achieved in life by Allah through you, words could hardly express my gratitude to you all I can say may Allah reward you with aljanatul Firdausi hereafter to all my family members who helped with everything they could for me to succeed in life may Allah reward with Janatul Firdausi as well. My deepest appreciation goes to Ahmed Tijani Galadima who has helped me in numerous ways to mention, I will be forever grateful.

To my darling wives from Zainab Chubado Labaran nee Zainab Bello Saidu the pillar and the foundation of the house to Nabila Ibrahim Hussain the midfielder {Hayatti}of the house and to the youngest wife Fatima Bayero Waziri nee Amariya for your care, comfort and moral support, thanks for the valour, sustenance and tolerance, perseverance, through this journey. You complete my heart glimmerings when being at home. To my carbon copies Muhammed Ardo Asura and Abdullahi Bayero Waziri for being the most extraordinary part of this voyage, your beams, carrying you and always picturing you in my mind and heart you are indeed a jewel given to me by Allah`s mercies.

To my friends, and colleagues too numerous to mention, you have my most sincere appreciation. Particularly, Alim Adamu, Danladi Mumini Abubakar Muazu Garga, Adamu Sanda TATA Aliyu Abubakar Madawaki, Isa Ahmadu Sarki Power and to my Mentor Muhammed Umar Jabu {Talban} Madagali, the Distric head of Madagali Alhaji Bakura Iya Gaji May all your visions come true. You have been contributory to the triumph and completion of this PhD. Most especially Late Muhammed Bappa Madagali. Time and space will not allow me to reckon the individuals in my life who made this mission conceivable, by Allah's will. ALLAH, the almighty recognises you all.

Declaration

I, Bello Saidu, declare that this thesis is my original work, and has not been submitted elsewhere for any award. Any section, part or phrasing that has been used or copied from other literature or documents copied has been clearly referenced at the point of use as well as in the reference section of the thesis work.

……………………… ………………………….

Signature Date

……………………… ………………………….

Approved by

Dr A. J. Abbas (Supervisor) Date

……………………… ………………………….

Approved by

Prof. G. G. Nasr (Supervisor) Date

List of Symbols

A	Reservoir area (acres),
API	American Petroleum Institute
B	Decline exponential,
Bcf	Billions cubic feet
Bgi	Initial gas formation volume factor
B_{hi}	Hydrocarbon Formation Volume Factor (FVF)
BHP	Bottom Hole Pressure (psi)
BHT	Bottom Hole Temperature (^{o}C)
B_{tt}	Bottle
Cn+	Group of components heavier than n-1 (paraffin with n carbon atoms)
C_o	Isothermal Compressibility
cP	Centipoise
dP	Differential pressure (atm).
E_A	Areal sweep efficiency
E_D	Displacement efficiency
E_V	Vertical sweep efficiency
F	Fahrenheit
FVF	Formation Volume Factor
g/cm^3	Gram per cubic centimetre
g/mol	Gram per mole
GDT	Gas down To
GIIP	Gas Initial in Place
GOC	Gas Oil Contact

GOR	Gas Oil Ratio
GR Log	GR of formation measured from log,
GR Max	Maximum GR reading in zone of interest,
GR Min	Minimum GR reading in zone of interest,
GWC	Gas Water Contact
H	Net pay thickness (ft.),
IGR	Gamma Ray Index
K	Integration constant
k	Permeability of the porous media.
L	Length of porous medium (cm).
MMscf	Millions standard cubic feet
MMstb	Millions stock tank barrels
MW	Molecular Weight
N	Fitting Curve parameter
N/A	Not Available
ODT	Oil down To
OGIP	Original Gas in Place
OML	Oil mining license
OOIP	Original oil in place
OWC	Oil Water Contact
P	Pressure (psi)
PC	Capillary Pressure,
Pce	Capillary Pressure Entry
Pd	Dew point pressure
PIIP	Petroleum Initial in Place

Psat	Saturation pressure
PSIA	Pounds per Square Inch Absolute
PVT	Pressure Volume Temperature
q	the flowrate (cm^3/s).
Q_t	Production rate (STB/D, STB/month or STB/year),
SCF	Standard Cubic Feet
STB	Stock Tank Barrel
STO	Stock Tank Oil
STOIP	Stock Tank Oil in Place
S_w	Water Saturation,
S_{wi}	Initial average water saturation (%),
S_{wirr}	Irreducible Water Saturation,
T	Temperature
V_{gp}	Volume of natural gas produced
Vi	Initial gas because of pressure drop
vol/svol	Volume at pressure and temperature per standard volume
V_{sh}	Volume of Shale
W_e	The water influx
W_p	the volume of water produced
Z	Gas deviation factor
Φ	Porosity (fraction)
➡	Resulting to
μ	Dynamic viscosity of the fluid (cP)

Table of Contents

List of Figures

List of Tables

List of publications

A list of publications resulting from this study and contributing to its development is outlined below:

- Saidu, Bello, Abbas, Jibril Abubakar, Abba, M.K Nasr, G.G Pore scale gas flow modelling in sandstone rocks using scanning electron microscopy (SEM) images for structure mapping. Journal of Engineering Technology 2019 (Accepted)
- Saidu, Bello, Abba, M.K, Abbas J. Abubakar, Nasr, G. G. Effect of aquifer salinity on the performance of natural gas reservoir during influx: An experimental approach Journal of Engineering Technology 2019 (Accepted)
- Abba, M. K., Saidu, B., Al-Othaibi, A., Abbas, A. J., & Nasr, G. G. (2018). Effects of gravity on flow behaviour of supercritical CO2 during enhanced gas recovery and sequestration. Fifth CO2 Geological Storage Workshop, (November), 2–6. Fifth CO2 Geological Storage Workshop, (November), 2–6. (Accepted and Published)
- Abba, M. K., Al-Othaibi, A., Abbas, A. J., & Nasr, G. G., Saidu B. (2018). Solubility Trapping as a Potential Mechanism for CO2 Sequestration during Enhanced Gas Recovery by CO2 Injection. Journal of Natural Gas Science and Engineering. (Accepted and Published)
- Emmanuel Udofia Akpan, Godpower C. Enyi, Nasr, G. G, Aminu A. Yahaya, Abdullahi A. Ahmadu, Bello Saidu. Water-based drilling fluids for high-temperature applications and water-sensitive and dispersible shale formations Journal of Petroleum Science and Engineering; 2019. (Accepted and Published)
- Muhammad Kabir Abba, Abubakar J. Abbas, Ghasem G. Nasr, Athari Al-Otaibi, Martin Burby, Bello Saidu, Salihu M. Suleiman Solubility Trapping as a Potential Secondary Mechanism for CO2 Sequestration during Enhanced Gas Recovery by CO2 Injection in Conventional Natural Gas Reservoirs: An Experimental Approach (Accepted and Published)

Chapter 1 Introduction

1.1 Preamble

The role of petroleum products in shaping the requirements of human energy cannot be denied. Although the term 'natural gas' is synonymous with petroleum gas, few comprehend the physical characteristics of' natural gas in terms of estimating its reserves, and it becomes even more complex in knowing the geology of its reservoirs, and thus appreciating the function of' natural gas' in a natural reservoir setting. While there was no ambiguity in terms of what is natural in both physical and chemical constituents, which apart from its environmental advantages as fuel, its substantial abundance but very limited availability of assessment methods. Energy security and sustainability have continued to challenge the development of more reliable methods for predicting quantities of gas reserves, allowing investment decisions in project development to harness abundant gas resources.

The demand of natural gas will continue to grow globally, aggregating its market segment of total primary energy depletion. For the high energy utilising nations, natural gas is projected to provide the utmost increase in energy consumption, due to its usage in industrial, civil, transportation and power generation segments (Stefano, 2007). Over the years, the Nigerian gas sector has seen an increase in achievements, encouraging both local and transnational stakeholders as well as Nigerian companies. What is immediately compulsory, however, is a legal framework and domestic petroleum policy to give direction, rationality and continuous efficiency to the industry and nation (Anthony, 2013). In view of these, the need to estimate or quantify quantities of Nigerian natural gas reserves using an appropriate international standard for reserve assessment is not negotiable. Moreover, the bulk of current assessment methods are predominantly model based, but the integration of both model-based and experimental techniques can be more reliable in confirming real accessibility. It will have a direct effect on the GDP of the country and add value to the life of Nigerians. Since the very beginning of the oil industry, approximating petroleum, gas and related constituents' reserves has been a burning subject. The understanding of reserves has meant distinct stuff to distinct individuals within this sector over the consequent centuries. Each evaluator, petroleum and gas corporation, financial agency, securities commission and department of state uses its range of categories (Aguilera, et al, 2014) and Reserves and Resources assessment effect both capital investment decision-making advancement and control of important country performance measures. The suitability and accuracy of the evaluations may also have a significant impact on how the asset public identifies the nation. Consequently, the significance of these concerns cannot be over-defined (NNPC, 2012).

Gas reserves are recorded in Trillions of Cubic Feet of Oil (tcf). Where available, prices of production are reported in millions of cubic feet of gas per day (mm cf / day). Reserves can be retained as proven, produced and produced unless additional data is accessible (Adelman & Watkins, 2005). Reserves are those amounts of oil and gas predictable to be commercially recoverable under specified circumstances by applying development projects to known accumulations from a specified date forward. Furthermore, reserves must meet four requirements: they must be found, recoverable, commercial, and maintained (as of the date of assessment) based on the project(s) being implemented. Reserves are further categorized by the level of certainty connected with the estimates and can be sub-classified based on project maturity and characterized by growth and status of manufacturing (SPE, 2007).

1.2 Problem Statement

Several methods are available for estimating hydrocarbon reserves in the oil and gas industry. The following are methods of quantifying reserves: The volumetric, Material Balance, Reservoir Simulation, Decline Curve Analysis (Production performance analysis) and History Matching. The choice of which depends on several reservoir and fluid properties and their inherent dynamics and behaviour because of changes in their nascent conditions. Hence, each method is suited for application to a hydrocarbon resource. Furthermore, accurate estimation of the hydrocarbon reserves of a given demographic is vital to the overall economics of an oil producing state whose economy is heavily reliant on hydrocarbon exports.

The growing demand for greener energy has awoken interest in natural gas utilisation for energy generation. This trend has shown a significant surge in natural gas markets. So current natural gas reserve estimation approach utilises seismic modelling data with limited experimentally supported data which tends to underestimate or overestimate the natural gas reserves. This problem can only be tackled through an integrated approach using experimental special core analysis, production data, and seismic data to project an accurate estimation of the natural gas resources in-situ. A typical of this gross underestimation of natural gas reserves is Nigeria, whose oil and gas operators estimated its reserves at about 190 tcf according to the Department of Petroleum Resources Nigeria (DPR) while the United States Geological Survey estimated the reserves more than 600 tcf. This necessitated further research into way in which natural gas reserves in Nigeria are accurately determined to meet the greener energy route requirement and make informed decision on the economy.

Therefore, this research is geared towards using offset well data, experimental (SCAL), and analytical techniques to estimate and calculate the natural gas reserves in place. This will help to accurately determine the volumes of gas in a specified locality to meet the domestic and international gas supply demand with a potential economy of scale derivable.

1.3 Benefits of the study

a) Nigeria Energy Policy Making can be improved buttressed with precise and dependable data on Gas reserves both in the civic and private sectors. Specifically, reserve data for Gas and other energy resources should be directly comparable so that decision makers can easily understand the relationship among variable resources. Gas Projects are capital intensive accurate reserve data will boost investors' confidence; domestically and internationally.

b) Generate greater awareness among both private and public organisations on the importance of having a proper and reliable reserve data as a vehicle to economic recovery, and revenue generation;

c) Resource availability for Domestic Supply Obligations (DSO), LNG (Liquidified Natural Gas) OK, LNG (Liquidified Natural Gas) Brass, Trans-Sahara Gas Pipeline West African Gas Pipeline Power generation using Gas-powered turbines. Moreover, boost employment for Nigerians.

1.4 Research contribution

Integrated experimental and analytical gas reserve estimation, PVT (Pressure, Volume and Temperature) analysis using Gas Chromatograph for fluid composition and properties evaluation of wet gas field. Pragmatic analysis of relevant parameters, improving core flooding reserve using dynamic reserve analysis

1.5 Research aims and objectives

1.5.1 Aim

The main aim of this research is to use experimental and analytical information from a moist gas field to perform an integrated natural gas reserve estimation.

1.5.2 Objectives

To achieve the aim of the research, the following objectives will be realised:

a. Data collection and mining
b. To conduct characterisation of petrol physical properties of the core samples the objectives are;
   i) the bulk volume, grain volume, pore volume and effective porosity of interconnected pores of a core sample with the use of helium Porosimetry.
   ii) To determine the permeability of the core samples of interest
   iii) Using techniques such as numerical imaging technology such as Scanning Electron Microscope (SEM) of the given core samples of interest.
c. Effect of aquifer salinity on the performance of natural gas reservoir during influx: An experimental approach
d. To develop a reservoir simulation model with PETREL using experimental and wet gas field data.
e. To incorporate experimental and field data into MBE for gas reserve quantification. Material Balance Equation (MBE) tool was used to interpret and predict reservoir performance. Material balance analysis of OGBA Field objectives are as follows:
   i) Estimating the volume of hydrocarbons in place
   ii) Determining the presence, type and size of aquifers, encroachment angles etc.
   iii) Investigating reservoir drive mechanisms
   iv) History matching of the past performances of the reservoirs.
   v) Predicting the reservoir pressure for a given production
   vi) Exploiting other reservoir analysis issues possible with the material balance approach
f. To evaluate experimental and field data using Decline Curve Analysis for gas reserve estimation. The objectives of the production performance analysis are as follows:
   i) Identification of reservoir and well performance problems.
   ii) Identification of scope for well repairs.
   iii) Investigation of opportunities for improving well productivity.
   iv) Recommendation of reservoir management strategies.
g. To carry out PVT Analysis for gas composition and fluid properties

1.6 The thesis has the following structure:

Chapter 1- Introduction

Introduces the general purpose and objective of research work.

Chapter 2- Literature Review

Presents a review of fluid flow dynamics in gas reservoir, numerical research, porosity and permeability, as well as prior work. This section offers the context needed for the following chapters.

Chapter 3- Background of the Field case study

Detailed assessment of the wet gas field has been conducted.

Chapter 4- Material and Methods

Presents the models and equation used to carry out the research. Simulation runs are discussed. Model design, procedures and calibration that were adopted in this research are presented.

Chapter 5- Equipment Description

An approach used in the thesis is described.

Chapter 6- Results and Discussion

Results obtained and discussion from experimental and simulation (modelling) are elaborated.

Chapter 7- Conclusions and recommendations

1.7 Chapter Summary

The conclusion drawn from different sections of the thesis are summarized. In addition, recommendations are provided in this region for future inquiry.

The chapter presents the insight of natural gas reserves with emphasis on wet gas reserves estimation as a major oil and gas reserve quantification problem. It then provides a brief description of the existing state of knowledge and provides an appreciation of the function of' natural gas in a natural reservoir setting. Furthermore, how reserves and resources assessment affect both capital investment decision-making advancement and control of important country performance measures are highlighted. Moreover, the chapter suggests a different methodology, namely an integrated approach in evaluating wet gas reserves which improves significantly the traditional method employed in petroleum reservoir engineering for reserves estimation. This chapter also sheds more light on how the research conducted is geared towards using offset well data, experimental (SCAL) and analytical techniques to estimate and calculate the natural gas reserves available. This optimized approach is shown to more accurately determine the volumes of gas in a specified locality to meet the domestic and international gas supply demand with a potential economy of scale derivable. Details of the intrinsic stages inherent to developing a research approach for enhancing the accuracy of reserves using the integrated method are provided. Research contributions, aims and objectives are also provided. The thesis outline is succinctly summarised in this chapter. The next chapter contains the in-depth literature survey relevant to the topic under investigation.

Chapter 2 Literature review

2.1 Overview

There are numerous publications in the Oil and Gas Industry regarding the definitions, classifications, techniques and applications of reserve estimation and terminologies. However, very limited articles are available which shed more light on this research and its case study (World-Energy-Resource-full-report-2016).

The industry has made tremendous efforts since the 1930s to date to standardise petroleum reserve definitions, classifications and evaluation. The International accepted guidelines for reserve definitions, classification and assessment which is used in this research is formally known as Petroleum Resource Management System (PRMS-SPE 2011). A petroleum resource management system provides a consistent approach to estimating oil quantities, evaluating development projects and presenting results within a comprehensive classification framework. This scheme entered into force in 2007 and was endorsed by the Petroleum Engineers Society (SPE) and commonly used today as standard rules by the Petroleum Industry professionals. The definitions, the associated system of classification, are now widely used in the petroleum sector. They provide a measure of comparability and reduce the subjective nature of resource estimation. Additionally, the technologies used for the exploration, growth, processing and processing of oil and gas continue to develop and improve. The SPE Committee on Oil and Gas Reserves operates closely with other organizations to preserve definitions and problems regular revisions to keep up to date with evolving technologies and changing business possibilities (SPE 2007).

These standardize definitions and recommendations assistance create a normal global reference for the international petroleum sector, including national reporting organizations and regulatory disclosure authorities. This is intentionally indented to promote requirements for Oil and Gas projects and portfolio management. For improved clarity on petroleum and gas resources in international communication. In the long run, the aim is to supplement this document, along with the Petroleum Industry programs and application rules, in addressing their implementation in a wider range of technical and commercial environments. Moreover, the definitions and guidelines provide enough flexibility for end customers and organisations to tailor the request to their individual requirements. A dominant debate will later be the Petroleum Resource Management System (PRMS).

The interpretation of quantities and values in relation to petroleum and gas reserve estimation is generally inherent in a specified degree of uncertainty. These amounts are engaged in any specified petroleum development project from the design and execution phases. Adopting classification systems increases project comparisons, a project group, and complete business portfolios based on manufacturing profiles and recoveries. However, the scheme must consider a technical and commercial factor that could affect the economic feasibility of the project, the life cycle of manufacturing, and the money flows concerned. Uncertainty is a recurring characteristic in estimating natural gas reserves and their potential role in the gas-dependent global economy. Recent modelling attempts have substantiated this shift and variety in terms of manufacturing costs, upstream emissions, etc. concerning future natural gas market circumstances (Huntington, 2013). These and more of this uncertainty are described as the structural and actual extent of the reservoir's accumulation and inner architecture (Akinwunmi, Arochukwu, & Abdul-Kareem, 2004). For development purposes, the writers converted the uncertainties into a range of static field quantities in the Niger Delta the magnitude of the danger often reduces as manufacturing begins, but this is not always the case (Wright, 2003) He presents some real-world instance which disproves this hypothesis. Operating settings for investments such as power plants may differ from the context in which they are scheduled, given the lengthy lifetimes and elevated adjustment expenses of energy assets. These vibrant and stochastic components are particularly applicable to natural gas-related hazards as these uncertainties are unlikely to be addressed before choices are made soon. Insufficient accounting for uncertainty can therefore have financial and environmental consequences for a range of stakeholders (Bistline, 2014).

Any assessment of accumulation resource amounts or collection group (a project) is subject to uncertainty and should be expressed as a range. The role of the three primary reserve classifications (proven, likely, feasible) in the "SPE / WPC Petroleum Reserve Definitions" is to demonstrate the variety of uncertainty from a known accumulation in estimating the possibly recoverable amount of petroleum. Such estimates can be produced deterministically or probabilistically for each well or reservoir and are then aggregated for the entire collection/ project. Provided a comparable logic is applied to all volumetric estimates (including conditional and prospective assets), the estimation of uncertainty for each accumulation can be monitored over time from exploration through discovery, growth, and manufacturing. This strategy offers an extremely effective foundation for assessing the validity of the methodology used to estimate quantities that could be recovered. The range of uncertainty for an individual accumulation or project represents a fair variety of estimated possibly recoverable quantities. In the event of reserves, and where applicable, this range of uncertainty can be expressed in estimates of proven reserves (1P), proven plus probable reserves (2P), and proven plus probable plus possible reserves (3P) scenarios. The similar terms low estimate, best estimate, and high estimate are recommended for other resource categories. ("Petroleum Reserve and Resource Assessment Guidelines, "n.d.)

A standard deterministic procedure or a strict probabilistic procedure can represent the variety of uncertainty. The later can be used using Monte Carlo simulation and has several intrinsic issues as described in (Kamali, Omidvar, & Kazemzadeh, 2013). Monte Carlo simulation is a methodology used to understand the impact on financial, project management, cost, and other forecasting models of risk and uncertainty. A simulation allows Monte Carlo to imagine most or all the possible outcomes to get a better idea about the risk of a decision.(J.E. Gentle, in International Encyclopaedia of Education (Third Edition), 2010).
The writers demonstrate these issues that are mostly impacted by input parameters where no one can ensure that the precise result will be produced when the same input parameters have been recalculated. Another problem is that it is hard to estimate the dependencies between the related parameters and not to visualize the spatial place and the variability of uncertainties. Monte Carlo simulation applications are described in several journals such as (Mata, Rojas, Salil, & Camacho, 1997), (Komlosi & Komlosi, 2009).

Alternatively, the probabilistic procedure strategy is to use a 3D geological model as the basis for volumetric calculations in which the dependencies between parameters are properly handled with the spatial variability of the related uncertainties as mentioned in the (MacDonald & Tollesfrud, 2008). The primary source of opportunities, therefore can be categorized anywhere within the modelling workflow when using a 3D model (Zabalza-Mezghani, Manceau, Feraille, & Jourdan, 2004). Such dangers include static modelling, upscaling of petrophysical and assets, modelling of fluid flow, manufacturing information, creation of manufacturing schemes, and financial assessment. The authors classified the various statistical behaviours of uncertainty as deterministic, discrete and stochastic changes.

In the oil industry, reservoir simulation has become the norm for solving tank engineering issues. Several simulators have been created and methods of recovery are being created for fresh activities of oil recovery. Reservoir simulation is the art of mixing physics, mathematics, reservoir engineering, and computer programming to create a tool to predict hydrocarbon reservoir efficiency in different methods of activities.

Modelling systems or oil tanks therefore play a major role in developing and implementing mathematical and stochastic models for characterizing petroleum reservoirs. It comprises of constructing an oil reservoir computer model for enhancing reserves assessment and making choices about field growth. They are called mathematical, and geostatistical models and their primary objective are to characterise petroleum reservoirs worldwide That is, a precise image of the field permeability, porosity and the quantity of current oil can be obtained through digital deposit pictures. These models represent not only the understanding of the reservoir's internal features (porosity, permeability, fracture structures and flaws, oil / water contact) but their related uncertainty. The following list summarises some of the principal uncertainties associated with the performance of the overall reservoir model. The type of data can, for example, be subdivided into two aspects - "static" and "dynamic" data: Static Properties 1. reservoir structure 2. reservoir properties 3. reservoir sand connectivity 4. impact of faults 5 "thief" sands Dynamic Properties 1. relative permeability etc. 2. fluid properties 3. aquifer behaviour 4. well productivity (fractures, well type, condensate drop out etc.), (Heriot-Watt University Institute of Petroleum Engineering Reservoir Engineering Manual book 2019).

This research involves studying the characterization of the reservoir and quantifying the uncertainties of a gas field by analysing two methods to be implemented in a practical case study Resource Definition and Classification.

Many nations and businesses further subdivide resource categories by project status or maturity to create a more comprehensive resource reporting scheme that can provide the foundation for portfolio management. This represents the concept that there will be a greater likelihood that the collection will reach commercial output as an accumulation moves to a greater maturity level. The categories of project status are independent of the related uncertainty.

Guidelines for the range of possibly recoverable quantities; however, changes are anticipated to decline as maturity rises for an individual accumulation.

For illustrative reasons only, the following categories of project status are given. SPE (Society of Petroleum Engineers), WPC (World Petroleum Congress), and AAPG (American Association of Petroleum Geologists) do not endorse the use of any subdivision of reserves, contingent resources, or potential resources because it is recognized that nations and businesses will want to create their categories in accordance with their classification systems ' goals. Each accumulation is categorized according to its project status / maturity in the classification scheme shown in Table 2.1, which represents the activities (business / budget decisions) needed to push it towards commercial manufacturing.

Table 2-1: Illustrates the entire spectrum of in-place and recoverable hydrocarbons (PRMS-SPE 2011).

<table>
<tr><td rowspan="11">Total petroleum initially in place</td><td rowspan="8">Discovered petroleum initially in place</td><td rowspan="4">Commercial</td><td colspan="3">Production</td><td>Project status</td><td></td></tr>
<tr><td rowspan="3">proved</td><td rowspan="3">Production

Proved
+
Probable</td><td rowspan="3">Proved
+
Probable
+
Possible</td><td>On production</td><td rowspan="10">low risk
↑
Project maturity

high risk</td></tr>
<tr><td>Under development</td></tr>
<tr><td>Planned for development</td></tr>
<tr><td rowspan="4">Sub commercial</td><td rowspan="3">Low estimate</td><td rowspan="3">Contingent resources
Best estimate</td><td rowspan="3">High estimate</td><td>Development pending</td></tr>
<tr><td>Development on hold</td></tr>
<tr><td>Development not viable</td></tr>
<tr><td colspan="3">Unrecoverable</td><td></td></tr>
<tr><td colspan="2" rowspan="3">Undiscovered petroleum initially in place</td><td rowspan="3">Low estimate</td><td rowspan="3">Prospective resources
Best estimate</td><td rowspan="3">High estimate</td><td>prospect</td></tr>
<tr><td>Lead</td></tr>
<tr><td>play</td></tr>
<tr><td></td><td colspan="2"></td><td colspan="3">← Range of uncertainty →</td><td></td><td></td></tr>
</table>

The groups used as examples reflect the following concepts:

- **Reserves**

✓ **On Production**— The project is presently producing and marketing oil. Under Development— All needed approvals were acquired, and the project is being developed.

- ✓ **Planned for Development**— Satisfies all reserve requirements and a strong intention is to create, but thorough development planning and required approvals / contracts have yet to be finalized.
- ✓ · Other development restrictions, such as technical, economic or political limitations.
  - ✓ Contingent Resources
  - ✓ **Development, not Viable—** Due to restricted production potential, no present plans to develop or obtain extra information at this moment.
  - ✓ Prospective Resources
  - ✓ **Prospec**t—Potential accumulation is sufficiently well-defined to represent a viable drilling target.
  - ✓ **Lead**—Potential accumulation is currently poorly defined and requires more data acquisition and evaluation to be classified as a prospect.
  - ✓ **Play**—Recognized prospective trend of possible candidates, but which requires more data acquisition and evaluation to define specific leads or prospects.
- This instance scheme offers a foundation for resource classification and therefore portfolio management, with the aim of balancing the resource base across the different classifications while concentrating on shifting individual accumulations from low maturity (such as lead) to projects in manufacturing and income generation. Contingent resources are particularly important in that they should be minimized; despite being found, resources in this category are identified as needing specific intervention to realize value. Budget choices should concentrate on growing project maturity. ("Petroleum Reserve and Resource Assessment Guidelines, "n.d.).
- Project— This is the connection between the accumulation of petroleum and the decision-making process, including budget distribution. For example, a project may involve the development of a single reservoir or field, or incremental development for a producing field, or the integrated development of a multi-area group. In particular, an individual project will constitute the level at which a choice on whether to proceed (i.e. spend cash) is made, and for that project there should be a related range of estimated recoverable quantities.

Note that the reservoir, known accumulation, and field of the term are not associated with commercial connotations. Commerciality.

The difference between recognized business and sub commercial accumulations (and therefore between stocks and contingent assets) is of basic significance in maintaining a decent amount of reserve reporting consistency. The accumulation must be evaluated as commercial by the SPE / WPC / AAPG classification scheme before any reserves are allocated. It is recognized that there may be some ambiguity between contingent resource definitions and unproven reserves. This represents differences in present practices in the sector.

It is suggested to classify the estimated recoverable quantities for accumulation as contingent assets if the degree of engagement is not such that the accumulation is anticipated to be developed and put on production within a reasonable timeframe. A sensible timeframe for development initiation relies on the conditions but should generally be restricted to about five years. For instance, if a group of gas areas are committed to a sales contract (and are therefore explicitly commercial), a longer period could be implemented, but some of them will not be created until they are needed to fulfil contractual commitments. In particular, a project must be described in the form of a commercially feasible development plan in order to assign reserves of any category, and there should be proof of a strong intention to continue with that plan. Reserve amounts would then be the estimated recovery arising from that plan being implemented. **Table 2.2:** is a graphical depiction of the classification scheme of SPE / WPC / AAPG / SPEE assets. The scheme describes the main classes of recoverable resources: production, reserves, contingent resources, prospective resources, and unrecoverable oil The "Range of Uncertainty" reflects a range of estimated quantities that can potentially be recovered from a project's accumulation, while the vertical axis represents the "Chance of Commercialization," i.e., the chance that the project will be developed to achieve economic producing status. For the main subdivisions within the resource classification, the following definitions apply:

Table 2-2: Resources Classification Framework. (PRMS SPE, 2007).

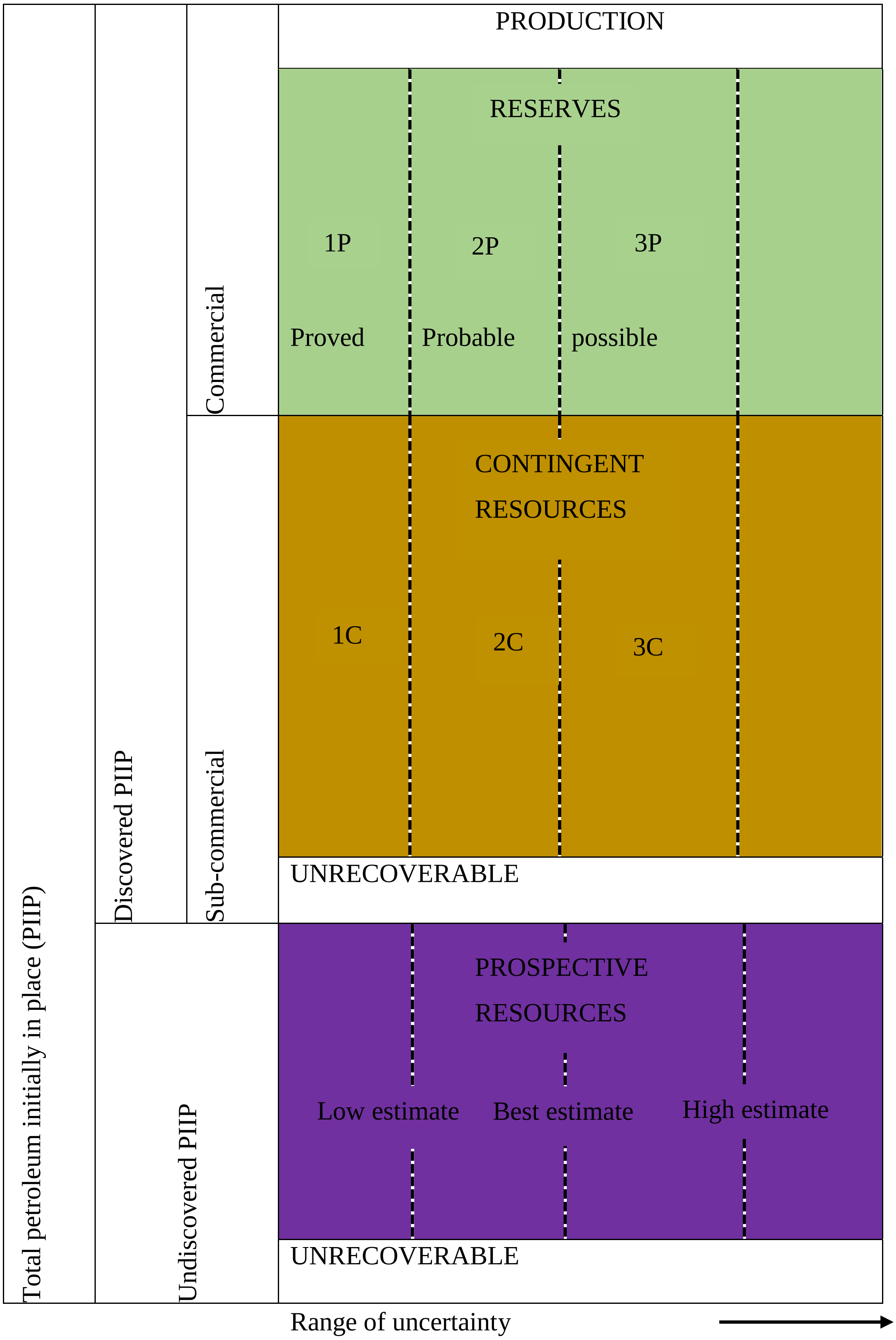

Table 2-3: SPE-System sub-classification options (PRMS SPE, 2007).

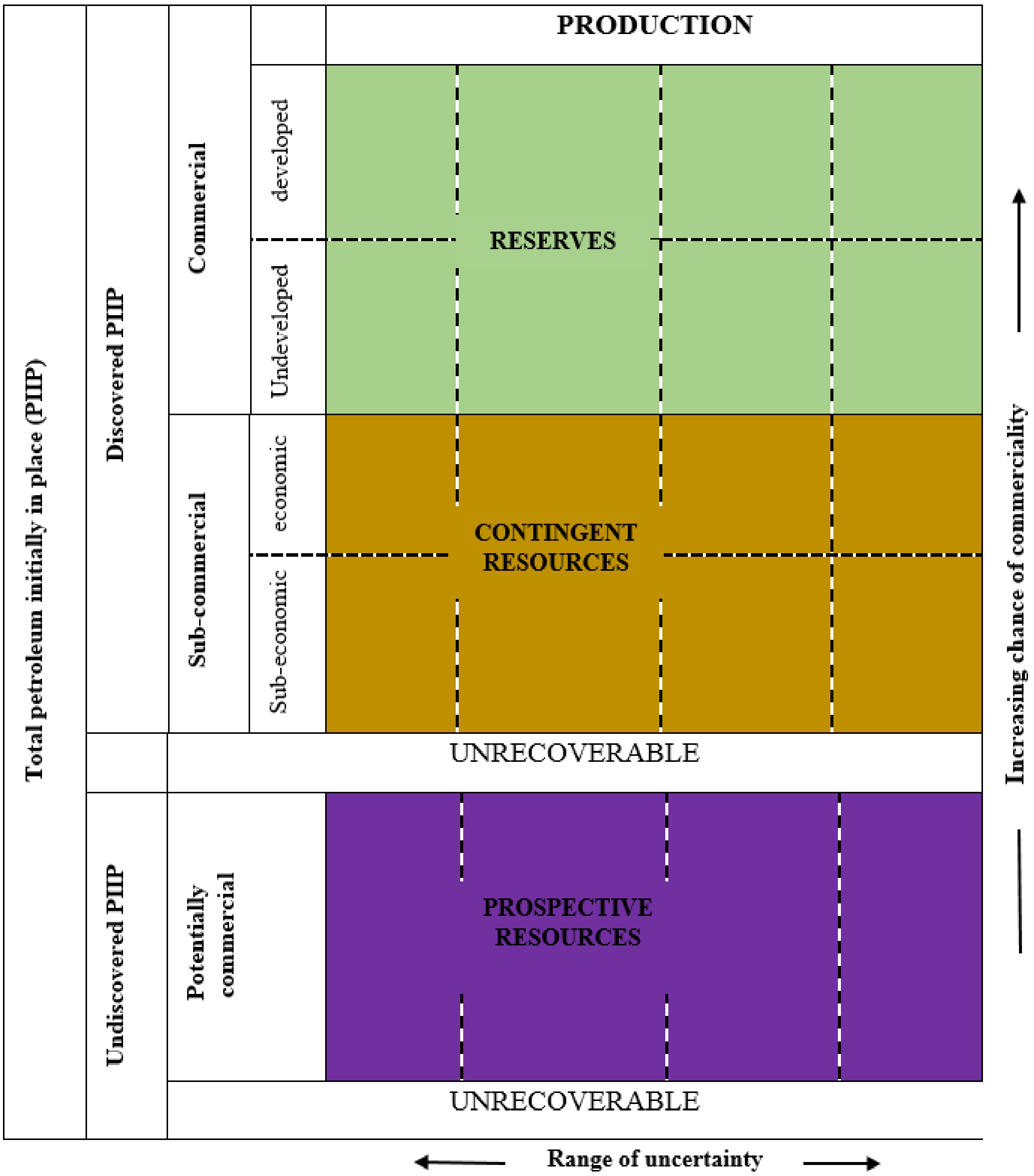

a) Operational and Economics

b) Decision based

Project maturity Sub-classes

On production

Approved for development

Justified for development

Development pending

Development unclarified or on hold

Development not viable

Prospect

Lead

Play

2.2 Range of uncertainty

- Petroleum resources are an important component of the external assets of a company and are the basis of its upstream present and future operations. Often, there are uncertainties connected with quantifying certain hydrocarbons in location when discovering a fresh field or extending a current field. The following are be linked to these problems;
- structure,
- aerial extent of the accumulation,
- unseen fluid contacts to delineate the vertical extent,
- the internal architecture of the reservoir
- and the characteristics of the resident fluid(s).

Based on the degree of uncertainty, reserves may fall into either proven or unproven one of the two major categories. Reservoir uncertainty is attributed to insufficient or unreliable information due to limited sampling of the heterogeneity of the subsurface. Well data and seismic data are incomplete and are finite. Unproven reserves are less certain to be recovered than proven reserves and may be further subclassified as likely and possible to denote increasing uncertainty about their recoverability.

The spectrum of uncertainty in SPE-PRMS is characterized by three possible situations that reflect the project's low, best and high case results. Depending on which is suitable for the project, terminology is distinct, but the underlining principle is the same regardless of maturity level. In summary, if the project met all the reserve criteria, the low, best, and high criteria are designated as proven (1P), proven plus probable (2P), and proven plus probable (3P), respectively. The equivalent conditions are 1C, 2C, 3C for contingent funds, while the terms "Low estimates," "Best estimates" and "High estimates are used for potential funds. The range of uncertainty can be represented by either a deterministic procedure or a probability distribution procedure. Further description of these methods is discussed in detail later. The probalistic distributions that account for the range of uncertainty have gained widespread approval in the petroleum Industry. Figure 2.1**,** the probalistic definition of reserve is as follows:

The following summarizes the definitions of both the deterministic incremental strategy and the scenario approach for each Reserves category and gives the criteria of probability when applying probabilistic methods.

• **Proved Reserves** Are those amounts of petroleum which can be estimated commercially recoverable from known reservoirs and under specified financial circumstances, working techniques and public laws with reasonable certainty, by analysing geoscience and engineering information. The word sensible certainty, if deterministic methods are used, is designed to convey a high degree of confidence that the amounts will be retrieved. If probabilistic techniques are used, the likelihood of the retrieved amounts being equivalent to or exceeding the estimate should be at least 90%.

• **Probable Reserves** The extra reserves indicated by geoscience assessment and engineering information are less probable to be recovered than Proved Reserves but more certain to be recovered than Possible Reserves. It is equally probable that the real retrieved amounts will be higher or lower than the estimated Proved plus Probable Reserves (2P) sum. In this context, when probabilistic methods are used, the probability that the actual quantities recovered will be equal to or exceed the 2P estimate should be at least 50 percent.

• **Possible Reserves** These extra reserves are less likely to be recoverable than Probable Reserves, suggesting the evaluation of geosciences and engineering information. The total quantities finally recovered from the project have a low likelihood of exceeding the sum of Proved plus Probable plus Possible (3P) Reserves, which is equivalent to the high estimate scenario. In this context, when probabilistic methods are used, the probability that the actual quantities recovered will be equal to or exceed the 3P estimate should be at least 10 percent.

Based on extra information and updated interpretations indicating enhanced certainty, parts of Possible and Probable Reserves may be reclassified as Probable and Proven Reserves. (Parliament, 2007).

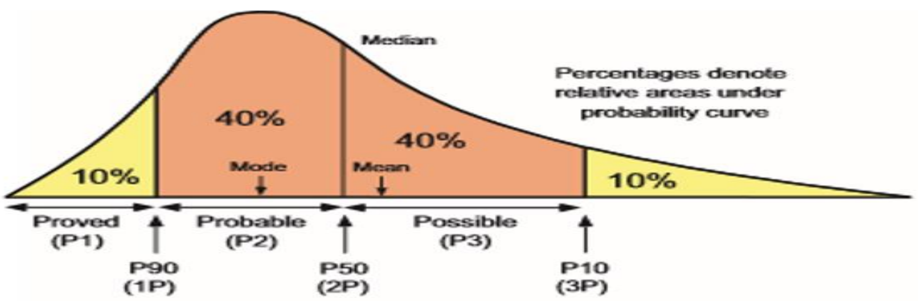

Figure 2-1: Illustration of the probalistic reserves definition, (Demirmen, 2007)

When using one of the two deterministic processes, the approximations should typically be small, best, and high as well. The evaluation relies on a qualitative assessment of relative uncertainty using coherent interpretation rules when using the deterministic scenario (cumulative) method. While, under the incremental (risk-made) deterministic strategy, the amounts are estimated individually and discreetly at each stage of difficulty.

2.2.1 Technical uncertainty

In some respects, uncertainty assessment of the technical element of the assessment of stocks can be accomplished. Either the sensitivity analysis of the geological and reservoir stream model (by creating deterministic assumptions and then recalculating the outcome) is involved in the most popular methods, or a probabilistic evaluation can be performed by identifying the variety of possible results for several factors and then conducting an analysis of Monte Carlo. In either scenario, it is essential to identify and evaluate the principle of unknown to determine a fair variety of opportunities that are physically meaningful for example, it was not possible to set the deepest oil occurrence below the reservoir spill point, and the combined flow of the wells could not exceed the inlet capacity of the facility. The use of geostatistical methods combined with strong computers in this study will enable the generation of various realization of geological and flow models to generate a fully integrated confidence assessment of recoverable hydrocarbons (Wilkinson, 1996). Figure 2.2 shows how changes in technical uncertainty could influence the selection of appropriate resource evaluation methods for any petroleum restoration project over its financial E&P life cycle. Any oil project's range of Estimated Ultimate Recovery (EUR) reduces over time as the accumulation is found, evaluated, developed and generated, with the degree of uncertainty decreasing at each point. More importantly, the evaluation of reserves and assets is based on the integrity, abilities and judgement of the qualified professional assessors.

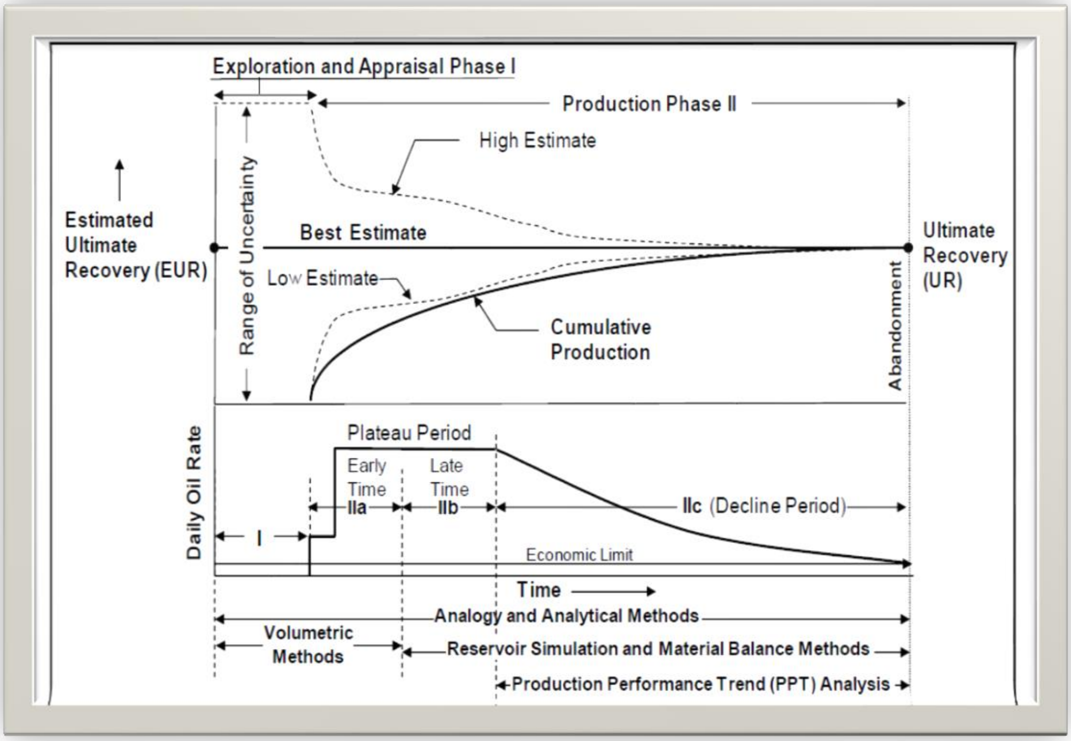

Figure 2-2: Change in uncertainty and assessment methods over the project's E&P lifecycle (PRMS SPE, 2011)

Figure 2-2 shows that the range of estimated ultimate recovery (EUR) of any oil project decreases over time as accumulation is discovered, assessed (or delineated), developed and produced, with the degree of uncertainty declining at each stage. Once identified, the length of each duration differs both on the size of the depletion (e.g. duration of assessment) and the potential of development in terms of the annual rate of depletion of the reservoir (e.g. as portion of the reserves generated annually). For example, projects with low levels of depreciation would support a significantly longer time of plateau accompanied by a longer period of decline, and vice versa.

2.2.2 Commercial uncertainty

One of the most complex procedures is the evaluation of financial variables and how they could affect reserves. The lesson of the 1980s is that product pricing is both unsure and extremely volatile, and that dropping prices have more than offset improvements in technology developments to a big extent or degree would probably have enhanced field development profitability. Recently, we have seen that physical stability and exchange rates play an important part in the project's general economy. This is motivated by the significant investment taken during the development stage in several currencies and, in the event of European gas sales, also receiving product revenue in several currencies (Wilkinson, 1996).

Costs for development are an important consideration as they happen during the field's early life. Plateau rates are often determined by optimizing the investment needed to construct a processing plant and then by drilling wells to satisfy the inlet ability. In turn, the original production rate will influence the recoverable reserves realized within the specified permit term. However, later in the field life, the impact of tariffs, government take, and license expiry becomes more significant in that the minimum economic rate for the area and loss of the license will become the determining factors in estimating the ultimate recovery This assessment should also consider the option of extending field life through the use of current infrastructure or, conversely, the need to shorten field life as a result of raising rigid environmental regulations. The estimate of late-life reserves may also be affected by choices to delay abandonment for cost or environmental reasons (Wilkinson, 1996).

Also, as time progresses in a field's life, the technical uncertainty of the assessment of reserves is decreased, but the business threat rises as manufacturing levels fall and profitability decreases.

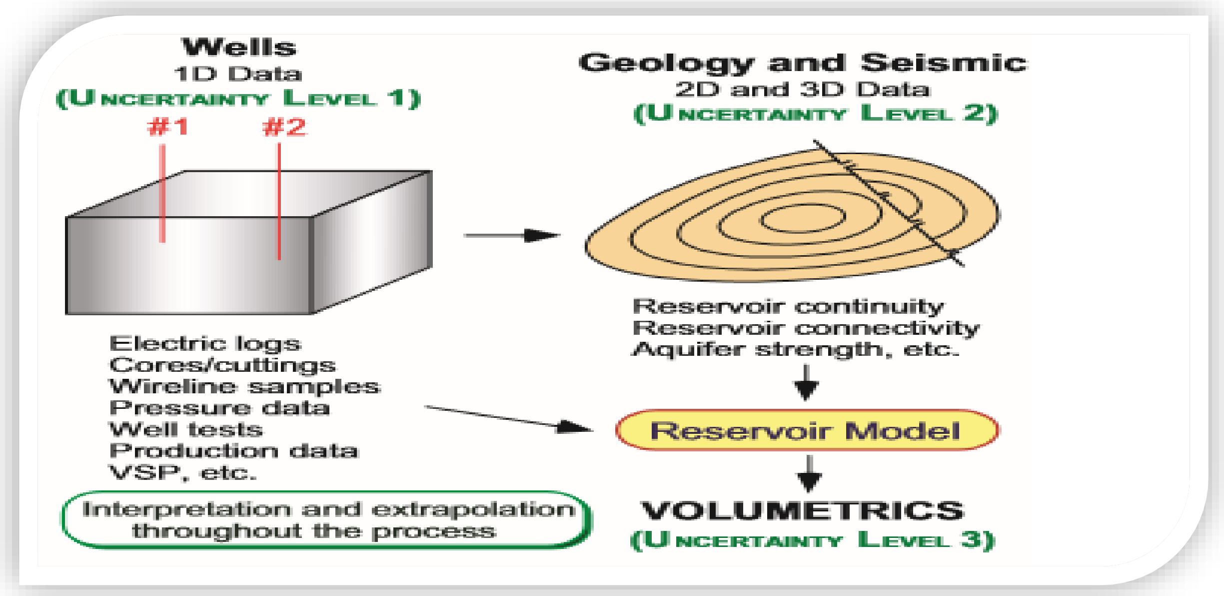

Figure 2-3: The sources of technical uncertainties (Demirmen, 2007).

2.2.3 Sources of technical uncertainty reserves

As for the above, the uncertainty range and consequently the reserve estimates are affected by certain factors. The cause of these factors can be technical or commercial (non-technical). Divide sources of uncertainty into three concentrations as shown in Figure 2.4 (Demirmen, 2007). The level of technical uncertainty is related to one-dimensional data such as important samples, well tests, well logs, etc. The one-dimensional data provides the reservoir's main features including porosity saturation, permeability, fluid viscosity, and moisture

The second level of uncertainty occurs when the reservoir characteristics are extrapolated from one-dimensional information to two or three-dimensional information. Without seismic, geological and long-term production tests, this extrapolation cannot be accomplished. At this stage, errors caused during the first stage are compounded.

Consequently, collecting the laboratory measurement with the accessible information helps to construct a reservoir model that is static or dynamic. This is due to the intrinsic information uncertainty and the assumption that the tank design itself was originally produced is imperfect. Moreover, a 2/3D depiction of the complicated rock / fluid / geology scheme is the reservoir model. The process of reserve estimation itself forms the third level of uncertainty. These shortcomings in this stage compound the imperfections in the reservoir model. In this regard, one can conclude the technical difficulties are inherent when estimating reserves.

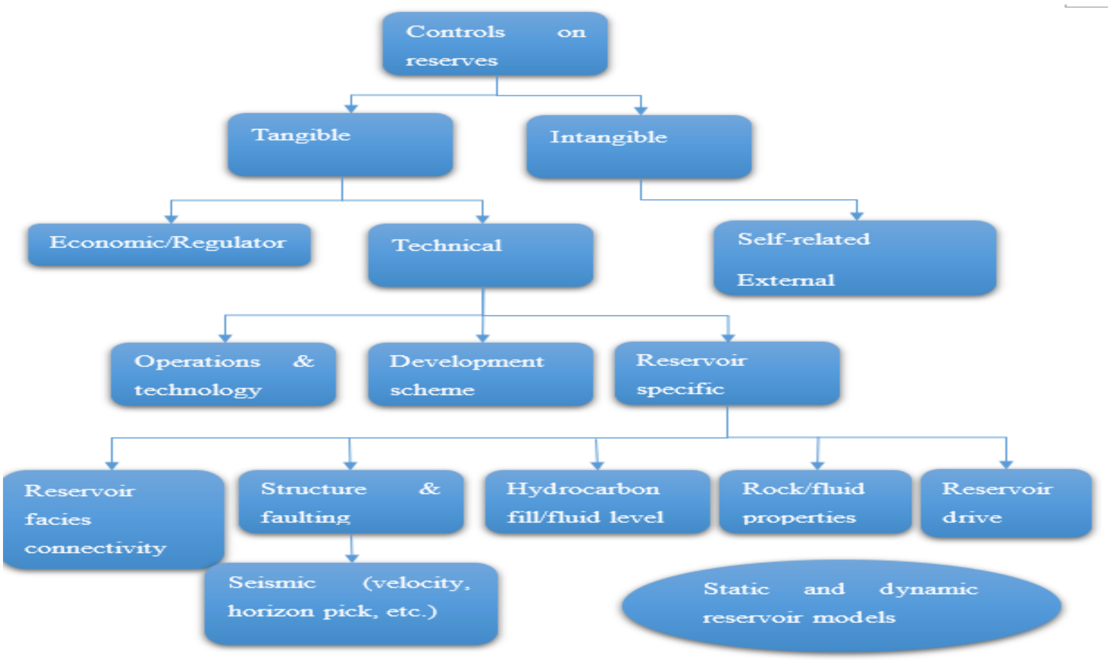

Figure 2-4: Technical and non-technical factors control on reserves estimates (modified and adopted from (Demirmen, 2007)).

The above figure shows all the technical and non-technical factors that may influence the determination of reserves. The primary variables are those linked to the reservoir including the geological, fluid and rock structure and the basics of static or dynamic models of the reservoir. Furthermore, the activities, technology and growth schemes which also play a part. Further than the technical factors, economic and regulatory (Including contractual) have an overall role in reserve estimation/determination.

Interestingly, factors such as those linked to technical sources, as well as regulatory and financial, can be described as concrete because their roles are well recognized and transparent. Intangible factors are not easily recognized and less transparent, not to be ignored. One sort of intangible variables is self-related, such as integrity, knowledge, problem solving attitude, and ability. Professional judgement is very critical at this juncture.

Most importantly, external to the evaluator is the second form of intangible factor. These include factors such as obsolete regulatory rules and leadership or customer pressure to provide the' correct numbers' and the statistic nature of the third type. The subsequent distortions are one of the underestimations causes of reserve, and they often add to the development of stocks. Often the distortions join the determination without the unwary estimator's understanding.

2.3 Deterministic and probabilistic procedures

Because the project was characterized by maturity (for instance, the project meets all requirements to be categorized as stocks). In estimating the associated recoverable quantities and their assignments, the uncertainties are based solely on the analytical method used. Regardless of the procedure, a level estimate (proven, 1p), the highest estimate (proven plus likely, 2p) and a large estimate (proven plus probable plus possible, 3p) should always be available. The analytical method can be used using the deterministic procedure, probabilistic process, or both techniques combined. The two relationships highlighted by the following declaration in SPR-PRMS. A deterministic estimate is a single discrete situation within a range of possible results obtained from probalistic assessment " (PRMS SPE, 2011).

2.3.1 Deterministic procedure

About acceptability of a wide spectrum, the deterministic process has achieved broad acceptance and is by far the most prevalent technique used in the sector. Basically, the method is to select a discrete value for each parameter (geoscience and engineering information) based on the simulator's choice of input in the most suitable equation to derive a single result from the related recoverable amounts. To assess the reserves, SPE-PRMS adopts two equally valid solutions to the deterministic method; scenario and incremental methods. For discrete increments and specified situations, deterministic volumes are determined. Although deterministic estimates may have generally inferred levels of confidence, they have not correlated quantitatively determined probabilities (PRMS SPE, 2011).

2.3.1.1 Scenario Approach

In this technique, three discrete analyses (scenario) are ready and created to curb uncertainty through sensitivity assessment. The three scenarios represent low, best, and elevated estimates of the related oil recoverable amounts. These situations must be combinations of plausible and realistic sets of important parameters, and care must be taken to ensure that a fair range of uncertainty is used in reservoir property measurements (e.g. average porosity) and parameter interdependencies connected with the average (PRMS SPE, 2011).

2.3.1.2 Incremental approach

Professional judgment, experience and expertise are used in the step-by-step approach to determine the reserves of recoverable amounts of petroleum as distinct amounts. In mature onshore settings, this technique is commonly used. When the incremental approach is used in the volumetric estimate, for instance, a single value of each key input parameter is selected based on a well-defined description of the reservoir at various points to calculate the reserves in-place. In such approach, the project must be defined correctly, and all uncertainties associated with the key parameters including Recovery Factor (RF) should be appropriately addressed (PRMS SPE, 2011).

2.3.1.3 Advantages and disadvantages

The deterministic method defines an individual physical situation as it is possible to remove and spot the input parameter's inconsistent mix of chosen values. It is an effective, direct and easy-to-use workforce. Long and good use history with reproducible and reliable estimates in the sector. The primary disadvantage of this operation is that there is no quantification of the probability of low, best and high estimates, and each is treated in isolation. Therefore, sensitivity analysis is required to evaluate the low, best and high estimates by utilising the different key reservoir parameter values to a reasonably reflect that scenario.

2.3.2 Probabilistic procedure

The user defines the uncertainty distribution curves in the probabilistic method by representing the full range of values that could reasonably occur for each input parameter and the correlations (relationships) between them to generate a full range of possible output distribution for reserve volumes (recoverable quantities) based on the combination of input data and assumptions. Typically, using stochastic process, this method is frequently performed using Monte Carlo Simulation. Using the stochastic method (shown schematically in Figure 2.6), it is necessary to identify all the associated input parameters of the reserve estimate and then the software determines the uncertainty associated with each parameter based on the data expressed in relation to a Probability Density Function (PDF). A random number (0 to1) is selected for each parameter and the related value of the parameter is read from its PDF where the software determines a mixture of parameters for each iteration produced. Each iteration is a single, discrete deterministic scenario (usually several thousand iterations) for the development and recovery of PDFs for the Stock Tank Oil In-Place (STOOIP)and recoverable reserves. Real input data and assumptions leads to a lot of qualifying information that can be obtained from the statistical calculations resulting from it. The data obtained in figure 2.7 includes the mode value (most probable), the mean value (centre), mean value (average), minimum and maximum values, standard deviation and percentiles (Kamali, M R; Omidvar, A; Kazemzadeh, E;, 2013). The results are generally represented by three discrete values (P90, P50, and P10) (John et al., 2008) and expressed in a curve of expectation (EC) (i.e. a cumulative probability density factor, PDF representation) as shown in Figures 2.5 and 2.6.

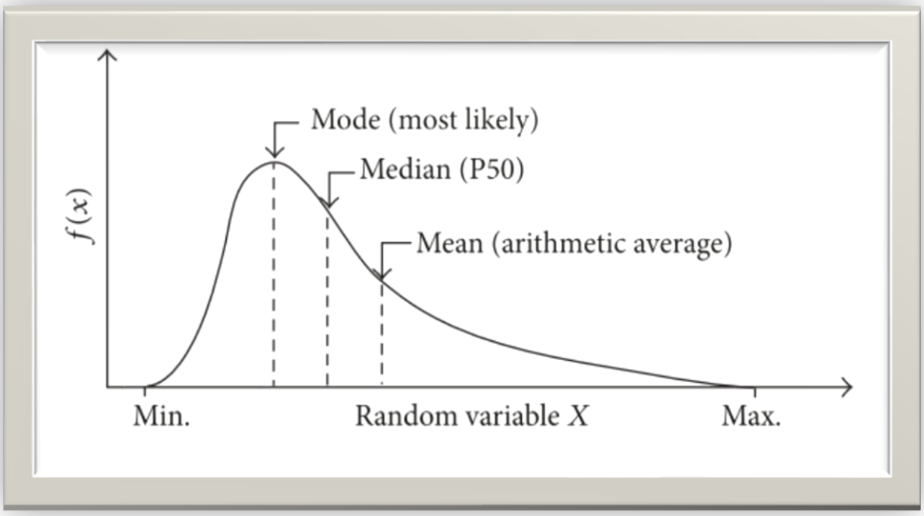

Figure 2-5: Probability Density Factor (PDF) (Kamali et al., 2013).

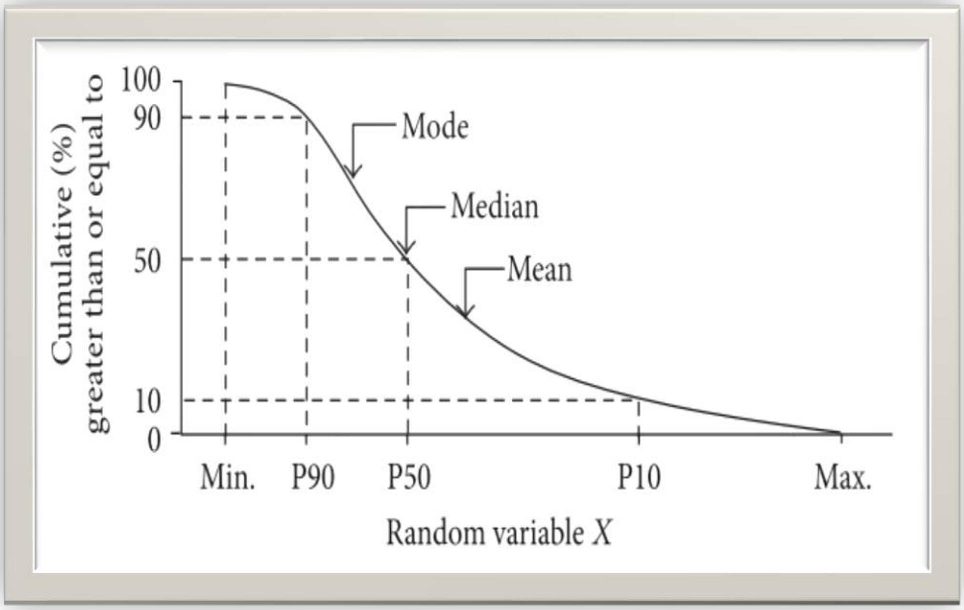

Figure 2-6: Expectation curve represented by three discrete values (P10, P50 and P10), (Kamali et al., 2013.)

Based on the stochastic reservoir modelling technique, each single, physically coherent result is called a sub-surface realization. It is possible to generate multiple understandings. Impossible physical achievements, however, must be excluded from the model as the constraints on the parameters imposed by the proven reserve's PRMS guideline and the related business uncertainties. This ensures that the unrealistic case is not considered in the assessment as they are inappropriately skew and outside the range of outcomes.

2.3.2.1 Advantages and Disadvantages

- ✓ Basic range of parameter uncertainties will drive the result of the uncertainty range
- ✓ Straightforwardly provides a numerical treatment
- ✓ It can be applied during the whole project cycle
- ✓ Possible outcomes are generated even inadequate data available

2.3.2.2 The disadvantages are as follows

- ✓ It may result in a complicated and extensive calculation work
- ✓ A technical judgement may be needed due to limitation on PDFs of some parameters
- ✓ Difficult assessment of the dependencies between parameters.

2.3.3 Multi scenario procedure

A comparison of the outcomes of probabilistic and deterministic processes can provide a quality assurance of either method. Results trust is improved if the two values agree. However, if a strategy combines the power of the two techniques, high confidence and more sensible outcomes of estimating reserves can be achieved. The multi-scenario method is an evolving method that tries to combine determinist scenario approach components with probabilistic process forces.

In the multi-scenario procedure, the evaluator develops a range of possible discrete deterministic outcomes / scenarios that are physically consistent with the observed data (called as a sub-scenario realization) and assigns the probabilistic of each possible discrete input parameter and assumption to give a likelihood for that outcome / scenario. The scenario collection can also be converted by related occurrence opportunities into a pseudo-probability curve (PRSM SPE, 2011).

2.3.3.1 Advantages and disadvantages

The advantages of the multi-scenario procedure as stated in the SPE-PRMS guidelines are: sub-surface realizations are generated from a consistent set of parameters. The concept of development is easily identified and can be examined under all possible reservoir results and conditions.

A drawback of the procedure is that a limited range of the results/scenarios may typically be handled, with a risk that under samples the possibilities range. Allocating a probability to each outcome/situation depend heavily on the petroleum and geological engineering judgement. Experimental design methods that are described by (Al Salhi et al., 2005) tackled those shortcomings. (SPE, 2011).

2.4 Analytical method for reserve estimations

i) One project was characterized by maturity, the estimation of related hydrocarbon recoverable amounts and their comparative uncertainties is based on one or a mixture of analytical methods. These techniques can be used by one of the two processes of calculation, deterministic, probabilistic, or a mixture. The analytical techniques can be categorized as follows:

ii) Analogy method

iii) Volumetric method

iv) Performance production analysis methods
   a) Material balance method
   b) Production declines analysis
v) Reservoir simulation**.**

The evaluation of PIIP and reserves is limited to the analogy technique and volumetric estimates based on static-data at the early point of the project (pre-and post-discovery phases). The dynamic-data-based performance estimates are implemented after starting manufacturing or in subsequent manufacturing phases where more data is accessible (such as reservoir stress and manufacturing rates). More confidence in the results of estimated PIIP and reserves increases when the calculations are supported by more than one analytical method

2.4.1 Reserves calculations terms

OOIP: Original oil in place, STOIP: Stock Tank Oil in Place, OGIP: Original Gas in Place

GIIP: Gas Initial in Place, PIIP: Petroleum Initial in Place

Recovery Factor: Fraction of oil that can be recovered from the initial in place volume

2.4.2 Analogy method

The" direct" measurement of information is restricted during the exploration and initial design phases, similarity technique is preferable at this time for reserve estimation. The reserves estimated by this strategy are guided" indirect" and are based on the premise that the similar reservoir is like the reservoir subject in terms of reservoir and fluid characteristics that regulate the ultimate petroleum recovery. By selecting appropriate analogues, where performance data based on comparable development plans (including well type, well spacing and simulation) are available, a similar production profile may be forecast.

Analogous reservoirs are described by characteristics including, but not restricted to, approximate depth, pressure, temperature, reservoir drive mechanism, original content fluid, pool extent, gross width, pay volume, net-to-gross ratio, lithology, heterogeneity, porosity, permeability, and growth schedule. Analogous basins are created by the same, or very similar, sedimentation, diagenesis, pressure, temperature, chemical and mechanical history, and physical distortion method "(SPE, 2007)

The uncertainty range is predicted to be PIIP and reserves can be enhanced by comparing several analogies with the reservoir or field subject. Analogous reservoirs with the same geographic region and age with close-to-abandonment can provide better analogy and approximation. In all cases, evaluators should document the analogy and subject reservoir / field similarities and differences. Review of analogy reservoir efficiency is helpful at all phases of growth in the quality assurance of resource evaluation. Such a technique is most helpful when conducting basic tank / field economics.

2.4.3 Volumetric method

The so-called ' volumetric calculation of resources ' is usually made before any output is obtained. Geological and geophysical data are mixed in order to obtain several contour maps and volumetric measurement

The static-data-based volumetric method (also known as the geologist's method) can be used to estimate PIIP and reserves indirectly in the absence of actual reservoir performance data and during the exploration, assessment and initial development phases of the project's E and P-life cycle where the dynamic-data-based performance production method cannot be used. The operation in this technique is called" indirect" because it is not possible to directly drive the Estimated Ultimate Recovery (EUR), i.e. it needs an autonomous estimate of PIIP values and a suitable recovery factor (RF).

The method is expressed regarding a simple classical volumetric relationship expressed as follows.

$$EUR(STB\ orSCF) = PIIP(STB\ or\ SCF) * RF(Fraction\ of\ PIIP \tag{2.1}$$

Regarding average variables, the generalised classic volumetric equation for the PIIP is expressed at standard conditions as;

$$PIIP(STB\ or\ SCF) = Ah\phi\frac{1-\mathrm{swi}}{\mathrm{Bhi}} \tag{2.2}$$

Therefore;

Original Oil – In – Place (OIIP), Oil Initial In-Place (OIIP) or Stock Tank Oil Original In-Place (STOOIP)

$$\mathrm{STOOIP} = 7758\ \mathrm{A\ h}\ \phi\frac{1-\mathrm{swi}}{\mathrm{Boi(STB)}} \tag{2.3}$$

Original Gas in – Place (OGIP) or Gas Initial In-Place (GIIP)

$$GIIP = \frac{43560Ah\phi(1-\text{swi})}{\text{Bgi(SCF)}} \tag{2.4}$$

Whereas;

7758 and 43560= conversion factors to convert acre-feet to stock tank barrel and standard cubic feet respectively, A = reservoir area (acres), h = net pay thickness (ft.), ϕ = porosity (fraction), Swi = initial average water saturation (%), Bhi = Hydrocarbon Formation Volume Factor (FVF), Boi = initial oil formation volume factor (RB/STB), Bgi = Initial gas formation volume factor (Rcf/scf).

- Using the generalized classic volumetric equation for the PIIP, however, determines the reserves volumetrically, so to calculate the EUR, RF is estimated separately. Based on an analogous development project, RF is determined using analytical methods or using published empirical correlations and simulation studies using reservoir data variables. SPE–PRMS promotes RF assignment using accessible analogues.
- Reservoir geometry and trap limits that impact gross rock volume
- Geological characteristics that define pore volume and permeability distribution
- Evaluation of the fluid contacts
- Combinations of reservoir quality, fluid types, and contacts that control fluid saturations.

Estimated Ultimate Recovery (EUR) is not a resource category, but a term that can be applied to any accumulation or group of accumulations (discovered or undiscovered) to define the estimated quantities of petroleum as a date to be potentially recoverable under the definition of technical and commercial conditions plus the quantities already produced (total recoverable). Reserves and EUR are the same before production begins.

Recovery Factor (RF) is a numeric expression of that portion of in – place quantities of petroleum estimated to be recoverable by specific processes or projects, most often represented as a percentage. See Table 2-4**:** for ease of reference.

Table 2-4: Estimation of primary recovery factor (DPR)

Drive mechanism	Primary Recovery Factor Drive Mechanism (%)
Depletion	
Solution gas	18-25
Expansion	2-5
Gas cap drive	20-40
Water drive	
Bottom	20-40
Edge	35-60
Gravity	50-70

Recoverable reserves are a fraction of the OOIP or OGIP and are dependent on the efficiency of the reservoir drive mechanism. The basic equation used to calculate recoverable oil reserves is

$$Recoverable\ of\ oil\ reserves(STB) = OIIP * RF \quad (2.5)$$

The primary recovery factor, RF_P, is estimated from the type of drive mechanism (Table 2).

The secondary recovery factor, RF_S, equals

$$\boldsymbol{RF_s = E_D * E_A * E_V} \quad (2.6)$$

- E_D = displacement efficiency
- E_A = areal sweep efficiency
- E_V = vertical sweep efficiency

These 3 conditions of effectiveness are affected by: residual petroleum saturation, relative permeability, heterogeneity of the reservoir, and reservoir manufacturing and management operational constraints.

Directly using these conditions, it is hard to calculate the retrieval factor and other techniques, such as curves of decrease, are often implemented.

Reserves of Gas Recoverable:

$$Recoverables\ gas\ reserves(SCF) = OGIP * RF \tag{2.7}$$

The gas recovery factor (RF) is typically higher than for oil reservoirs; it is often near unity for dry gas reservoirs.

Hydrocarbon Formation Volume Factor (FVF) or (B_o) is defined as the ratio of the volume of the oil (plus gas in solution) or gas at the reservoir conditions (pressure and temperature) to the volume at standard conditions.

2.4.4 Material balance method

Material balance technique for interpreting and predicting reservoir performance is component of the dynamic-data-based performance production assessment and one of the reservoirs engineers' key techniques. Method efficiency information includes analysing pressure behaviour as reservoir liquids are removed, production and injection profiles, rock characteristics, and reservoir-specific liquid characteristics all depending on reservoir pressure and temperature.

In optimal circumstances such as depletion–drive gas tanks in comparable, high-permeability reservoir rocks, and where there are enough and high-quality pressure information available, estimation based on material equilibrium can provide very accurate estimates of ultimate recovery at multiple dropout pressures. In a complicated situation, such as those involving water flow, multi-phase behaviour, and multi-layered or low-permeability reservoirs, estimates of material balance can produce erroneous outcomes on their own.

Regardless of volumetric methods, the methods of material balance can be used directly and simultaneously to determine PIIP, the size of its gas cap(m), or its volume in-place (Gas Cap Initially In-place, GCIIP) and the water flow (W_f). A well-established and reasonable assumption is that the use of the material balance analysis to estimate the PIIP I'd is often considered valid if the cumulative production exceeds 10% PIIP providing the accumulation development is such that the pressure used in the analysis is an average over the entire reservoir. Uncertainty in the estimate is anticipated to decline over time as historical information on production efficiency cover at least the early period of production and beyond.

Modelling of the computer tank or simulation of the tank can be regarded a advanced form of assessment of the material equilibrium. While such modelling can be a reliable predictor of reservoir behaviour under a specified development program, reliability of input rock characteristics, reservoir geometry, relative permeability features, and fluid characteristics is critical. Predictive models are most reliable in estimating recoverable quantities when there is enough production history to validate the model through history matching. The material balance technique mathematically models the reservoir as a tank. This method uses limiting assumptions and attempts to equilibrate changes in reservoir volume because of production.

Aquifer support and gas cap expansion can be accounted for by using this method Change in the pore

Volume = Change in Oil Volume + change in Free gas volume + change in water volume: (2.5)

Change in Pore Volume = $\frac{NB_{oi}}{(1-S_{wi})} C_f P$ (2.6)

Change of Volume in Oil = $NB_{oi} - \left(N - N_p\right)B_{oi}$ (2.7)

Change in Gas Volume = $(((GB)\_gi - (GB)\_g) + [N\_p\ R\_p\ (N - N\_p\ ) - NR\_si]B\_$ (2.8)

Change in Water Volume = $\frac{-NB_{oi}S_{wi}}{(1-S_{wi})} C_w P - W_e + W_p B_w$ (2.9)

B_g = formation volume factor of free gas, B_{gi} = formation volume factor of free gas at initial conditions, c_f = formation (rock) compressibility (psi^{-1}), c_w = water compressibility (psi^{-1}), N = Original Oil in Place, OOIP (STB)

- Np = cumulative oil produced (STB); from production history data
- P = Change in reservoir pressure due to production, that is, initial pressure minus current pressure; taken from field pressure surveys
- R_p = cumulative gas-oil ratio, or total produced gas (in SCF)/ total produced oil (in STB); from production history data
- R_{si} = initial solution gas-oil ratio (SCF/STB)
- S_{wi} = initial connate water saturation (decimal)
- W_e = cumulative amount of water encroachment; from map and field data
- W_p = cumulative water produced; from production history data

General material balance equation

$$N = \frac{N_p[B_t + (R_p - R_{si})B_g] - (W_c - W_p)}{(B_t - B_{ti}) + \frac{MB_{ti}}{B_{gi}}(B_g - B_{gi}) + \frac{B_{ti}(C_t S_{wi} + Q)P}{1 - S_{wi}}} \quad (2.10)$$

B_t = total (two-phase) formation volume factor

B_{ti} = total formation volume factor at initial conditions

M = gas cap size expressed as a fraction of initial reservoir oil volume; from map data

This equation assumes a thermodynamic balance between oil and gas, a uniform distribution of pressure, and a uniform distribution of saturation in the reservoir. Additional equations for kinds of reservoirs can be obtained from the overall equation of material balance.

Simplified equation for a quick estimate of initial oil in place. This equation assumes a closed tank system (no active water drive), no original gas cap, and the original tank pressure close to the bubble point

$$N = \frac{N_p B_{ob} V_t + \frac{(R-R_s)B_g}{5.61}}{B_{ob}(V_t - V_i)} \quad (2.11)$$

- 5.61 = conversion factor from volume/volume to ft^3/bbl.
- B_{ob} = formation volume factor for oil at the bubble point; determined for specific separator conditions
- R = gas-oil ratio, or GOR, equal to produced gas (in SCF)/produced oil (in STB); from production history data
- R_s = solution gas-oil ratio (SCF/STB) or gas solubility in oil
- V_i = initial volume of oil plus liberated gas as a function of pressure measured at reservoir temperature

V_t = volume of oil plus liberated gas as a function of pressure measured at reservoir temperature; determined under flash liberation conditions

This equation can also be used to predict N_p (how much a reservoir can produce, or recoverable reserves) assuming N is determined by an independent method and R, the gas-oil ratio, can be controlled throughout the life of the field.

$$N = \frac{N_p B_{ob} V_t + \frac{(R-R_s)B_g}{5.61}}{B_{ob}(V_t - V_i)} \quad (2.12)$$

- Material balance estimation for gas

- The material balance technique for calculating gas reserves, like material balance for oil, attempts to mathematically equilibrate changes in reservoir volume because of production. The basic equation:

Weight of Gas Produced = Weight of Gas Initially in the Reservoir – Weight Gas Remaining in the Reservoir

Volume of Gas Produced = Volume of Gas Initially in the Reservoir – Volume of Gas Remaining in the Reservoir

Material balance equations for gas reservoirs:

For a gas reservoir with active water drive:

$$G = \frac{G_p B_g - (W_c - W_p B_w)}{B_g - B_{gi}} \qquad (2.13)$$

Gas reservoir with no water drive ($W_C = 0$)

$$G = \frac{G_p B_g + (W_p B_w)}{B_g - B_{gi}} \qquad (2.14)$$

Where

G = Original Gas in Place, OGIP (SCF)

G_p = cumulative gas produced (SCF)

These equations can also be used to predict G_p (recoverable reserves) assuming *G* is determined by an independent method and the production conditions remain constant

2.4.5 Production Decline Analysis method

Production Performance Trend (PPT) analyses are frequently referred to as Decline Curve Analyses (DCAs), which have proven to be very helpful techniques for estimating and predicting the ultimate recoverable amounts for a reservoir / field directly. The technique includes analysing changes in manufacturing rates and ratios of production fluids versus moment or cumulative manufacturing as liquids are removed from the reservoir.

Historical trends in manufacturing efficiency noted in mature wells, reservoirs, or projects can be extrapolated at the financial limit to aggregate production and provide a sensible EUR evaluation. The expected production rate profiles acquired through analytical or reservoir simulation research, however, could create performance patterns that are not long enough to include the financial life of the project. The DCA can also be used in these instances to best fit these trends and extrapolate them to the economic limits of the project and to determine the EURs. To better understand or understand the constraints of the PPT Analysis (Harrell, Hodgin, & Wagenhofer, 2004), the following circumstances under which manufacturing decline trends would provide acceptable manufacturing profile predictions and the resulting reserve estimates for the assets being studied;

- Production conditions, methods, and the overall production strategy are not changed significantly over the projected remaining producing life
- The reservoir has been fully developed, and therefore, the right count is relatively stable
- Wellbore Interventions and other remedial work can be classified solely as maintenance.

Production Performance Trends are not only precise in the tank but also rely on the specific reservoir management and manufacturing methods used. Any substantial change in these methods could readily lead to incorrect outcomes. Therefore, the reliability of output profiles using DCA depends not only on the quality and quantity of past production data but also on the evaluator's professional experience gained through working on many hands-on assessments and reconfirmations of the results over time with actual performance, including the use of appropriate analogy reservoirs (SPE, 2011)

Decline analysis is based on the solution of the following differential generalised hyperbolic equation defining the nominal drop rate (D) as the fraction of ``change in production rate with time (t) `` (also known as loss ratio) as;

$$Dt = -\left(\frac{dQ}{dt}\right)Qt = KQ^{b} \qquad (2.15)$$

Where; Dt =nominal (or continuous) decline rate (slope of the line) at any given time (t) and is a fraction of production rate (Qt) with a unit of reciprocal time (1/t) in per month, per year, etc., which must be consistent with the units of production rate, Qt = Production rate (STB/D, STB/month or STB/year), b = decline exponential, K = integration constant.

A variety of curves can be used (Figure 2.8), the most common being a semi-log plot of rate of production versus time (Figure 2.9).

These data are easily obtained through operator records or state regulatory agencies.

Three mathematical models can be used to describe decline curve (usually rate versus time) behaviour. They are

- Exponential decline
- Hyperbolic decline
- Harmonic decline

Table 2-5: Decline equations

Solving for	Exponential	Hyperbolic
Rate of production	$Qt = Q_I e^{-Dt}$	$Qt = Q_i(1 + nD_{it})^{-\frac{1}{n}}$
Cumulative production	$N_p = \dfrac{(Q_i - Q_t)}{D}$	$N_p = \dfrac{Q_i^n}{[(1-n)D_i]}(Q_i^{1-n} - Q_t^{1-n})$
Life of reservoir	$t = \left(\dfrac{1}{D}\right)\ln\left(\dfrac{Q_i}{Q_{ec}}\right)$	$t = \left(\dfrac{Q_i}{Q_{ec}}\right)^n - \dfrac{1}{nD_i}$

Where

qt = Rate of production at time t (BOPD), qi = Rate of initial production (BOPD), qec = Economic limit rate of production (BOPD), D = Decline rate (decimal), Di = Initial decline rate (decimal), t= Time (years), n = Exponent (usually between 0 and 0.7), Np = Cumulative production (STBO).

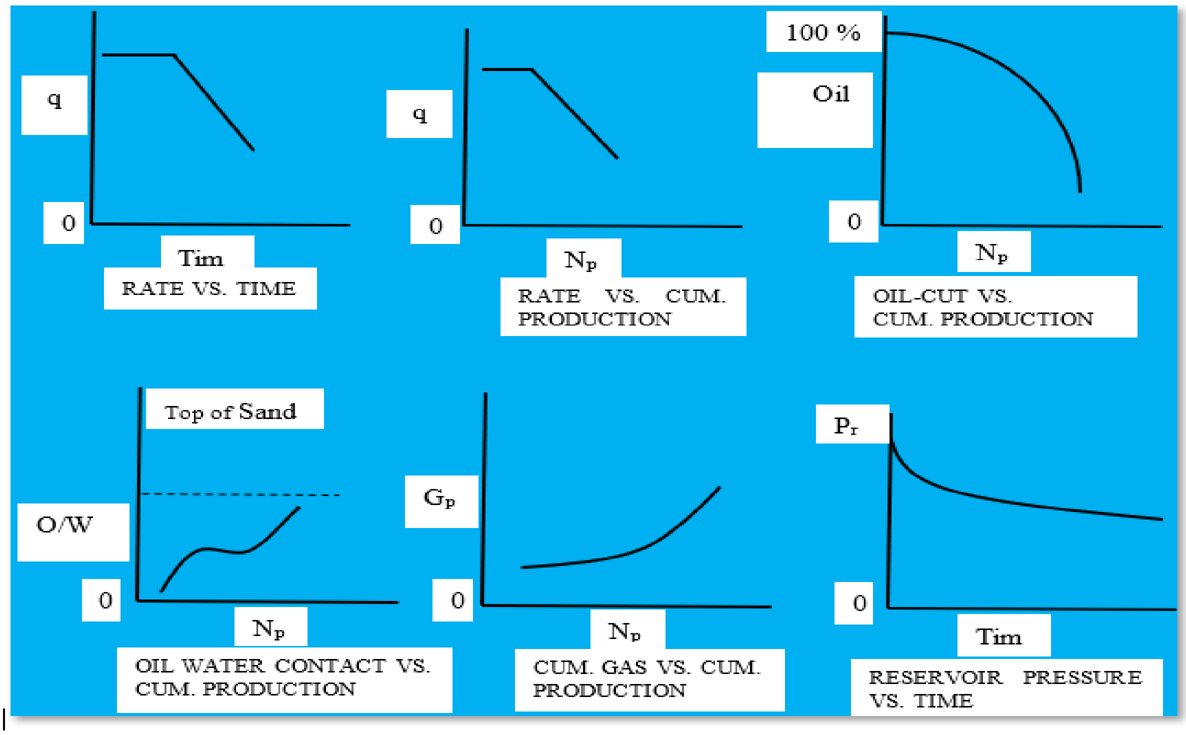

Figure 2-7: Production history curves

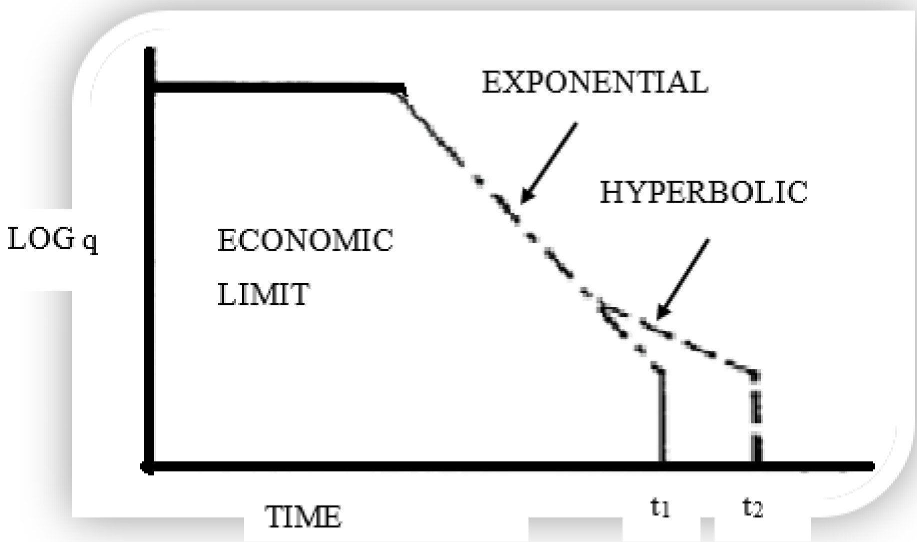

Figure 2-8: Semi-log plot of rate of production versus time from (Fetkovich, M. J., Fetkovich, E. J., & Fetkovich, M. D. 1996)

It is common to use exponential and hyperbolic decrease to define reservoirs. Harmonic decrease is a unique case of hyperbolic decrease rarely applied. For this study, only the Exponential and Hyperbolic will be applied to reservoirs with long late prolonged manufacturing.

2.4.5.1 Production history analysis

• There is no mutual exclusion of distinct kinds of decline behaviour.

• Different decrease curve features are often connected to distinct phases of reservoir growth and general trends may be considerably influenced by workover or stimulation, infill drilling, lift mechanics alter, or secondary or tertiary flood initiation.

2.4.6 Reservoir simulation method

The tremendous advances in computer innovation and technology have simplified the use of widespread applications in the construction of a 3D model (as shown in Figure 2.8:) built with an I million cells representing the static geophysical, geological, petrophysical and engineering data characterizing the structure of the subsurface reservoir. A simulation reservoir model reflects the grid pool or a set of interconnected tanks each with fluid and rock characteristics.

The model characterizes the reservoir by integrating the basic geological model and the dynamic flow model with the actual performance data of the reservoir (such as PVT data, rate of production, pressure, tests, etc.).

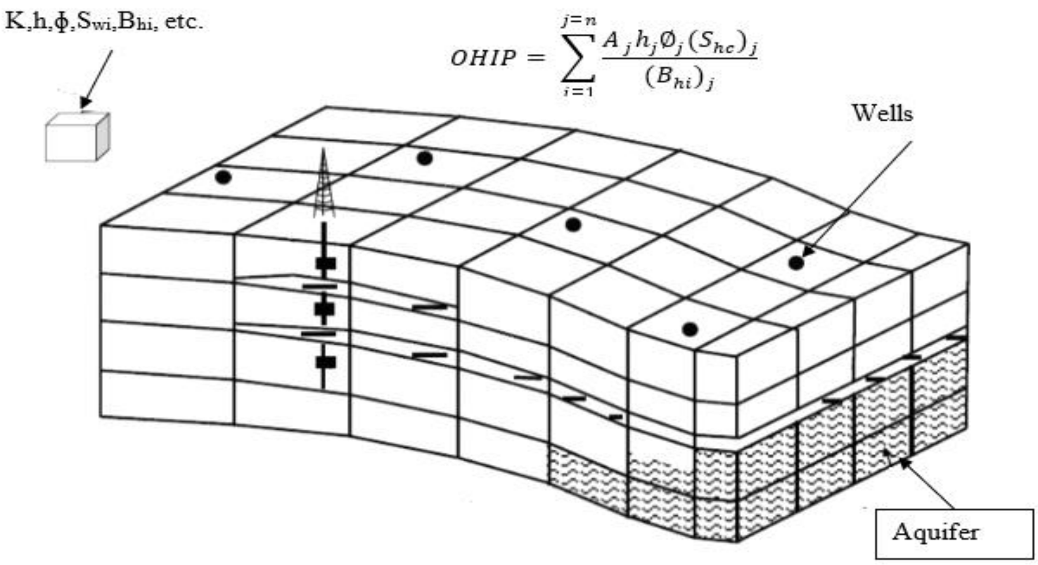

Figure 2-9: 3D geological (adopted from Petroleum Society of CIM, 1994; and modified by SPE, 2011)

The parameters in the Petroleum Initial In-Place (PIIP) or Original Hydrocarbon In-Place (OHIP) equation shift from cell to cell where the computer model conducts a sequence of material equilibrium (or volumetric estimates) calculations in each cell and enables fluid migration between the adjacent cells using Darcy's flow equations. Then the total OHIP is achieved by summing the matched and calculated individual values for each cell.

The system is superimposed by a design scheme and working circumstances. A excellent match between observed history and simulated performance is crucial for accurate outcomes. Moreover, the result of integrated reservoir simulation models can be used with increased confidence as the amount and quality of static geoscientific and dynamic reservoir performance data increase.

For any oil and gas recovery project, reservoir simulation can be used during any production phase to estimate directly both the original in-place and the recoverable quantities of petroleum or the EUR. Any recovery technique, including a main drive system, secondary pressure maintenance and displacement systems, and multiple possibly relevant Enhanced Oil Recovery (EOR) processes, may derive estimates from any oil recovery project.

The guidelines of SPE-PRMS (2011) recommend considering consideration the following two key points when reservoir simulation is used to estimate reserves regardless of the assessment methods.

1) The degree of uncertainty in estimates (or scope of results) is anticipated to reduce the quantity and quality of information on geosciences, engineering and manufacturing performance.
2) Compare estimates collected using various techniques (e.g. volumetric, material balance, reservoir simulation and trend analysis of manufacturing efficiency) and similar projects, if accessible, prior to reservation.

Consequently, in actual practice, one may have the following two extreme cases in which to assess and categories the estimate using the estimates using simulation models (SPE, 2011);

- ❖ **Case 1.** One may have the three-different geological realizations (representing the low, best, elevated scenarios) and related reservoir simulation models that can be used directly to assess individual in-place quantities, EURs, Reserves (e.g., the EURs reduced realized for cumulative manufacturing, if any), and Contingent Resources. This is preferred, but not a normal practice given the moment and cost of several strict models being developed.
- ❖ **Case 2.** One may have only one embedded simulation reservoir model, which can be used to predict straight a single most probable (or best) value of the PIIP, EUR,

Reserves, and Contingent Resources project. It is normal practice in deterministic assessment to carry out projections of sensitivity to know the variety of uncertainty and to assign the categories 1P and 3P accordingly.

Table 2-6: Summary of methods use to drive hydrocarbon reserves

Method	Application	Accuracy	
Volumetric	OOIP, OGIP Recoverable reserves. Use early in the life of the field.	Dependent on the quality of reservoir description. Reserve estimate is often high because this method does not consider problem of reservoir heterogeneity.	
Material balance	OOIP, OGIP (assumes adequate production History available) recoverable reserves (assumes OOIP and OGIP known). Use in mature field with abundant geological, petrol physical, and engineering data.	High dependent on the quality of reservoir description and amount of production data available. Reserve estimate is variable.	
Production History	Recoverable reserves. Use after a moderate amount of production data is available	Dependent on the amount of production history available. Reserve estimates tends to be realistic	
Analogy	OOIP, OGIP, recoverable reserves. Use early in exploration and initial field development	Highly dependent on the similarity of reservoir characteristics. Reserve estimates are often general.	

2.5 Selection of reserves estimate method

The selection of an appropriate method to estimate PIIP and reserves with satisfactory accuracy depend primarily on the following factors;

i) The type, quantity, and quality of geosciences, engineering, and economic data available and require for both technical and commercial analyses.

ii) Reservoir-specific geological complexity, the recovery mechanism, stage of development, and the maturity or degree of depletion.

Research and development attempt as well as technology implementations in the sector were vibrant due to the proven potential of sandstone reservoirs as a long-term energy source. A review of the literature will be given in this section with a summary of the most appropriate events.

2.6 Rock properties of sandstone formation

Sandstone reservoirs account for over 60% of oil and gas reserves throughout the global world. They are formed when the sand grains transport to far distances and are deposited in deposition environment. The Quartz (SiO2) are the main mineralogical components of sandstone reservoir. Sandstones are of different colours with brown and tan as the most common colours. This is due to the impurities within the sandstone minerals. It is a sedimentary rock composed of mainly quartz sand and some small amount of feldspar, clay and silt. Quartzose sandstone is made up of more than 90% quarts while Arkosic sandstone contains above 25% feldspar. Geologists refer to the rock as argillaceous sandstone when there is significant amount of clay or silt (Anon, 2017).

2.7 Porosity of sandstone reservoir

The most important aspect of fluid-bearing rock is called Porosity (Dibbie et al., 1983). The Porosity determine the quality of a reservoir rock (Chengzao et al., 2012). The pore space between the grains in sandstones is referred to as Porosity (Lyons & Plisga, 2005). Total porosity is important because of its involvement in gas reserves such as sandstone. It determines the pore structure connectivity, which regulate the transport and fluid-flow through these formations (Anovitz and Cole, 2015). Sandstone porosity is a hard variable to measure, and a high deviation result between the same sample is possible. The sandstone total porosity is reported to be within the range of 2 to 15 % (Hinckley et al., 2012) (Arogundade et al, 2003). Porosity is affected by factors such as sandstone minerology, compaction, grain size and maturity. The techniques applicable when quantifying porosity include mercury injection capillary pressure (MICP) porosimetry, grain density/helium psychometry, scanning electron microscopy (SEM) images, and gas sorption techniques (Rexter et al, 2014). Among these techniques, helium Pycnometry is one of the most accurate, precision tested and latest in technology for measuring the porosity of microporous materials (Kazimierz et al, 2004). This method gives a very precise result because of the advantages of helium such as access to fine pores and high diffusivity (Ross & Bustin, 2009; Anovitz and Cole, 2015).

Scientific studies on porosity have long been reported for over a decade with early studies by Moore (1904), Fuller (1906), Sorby (1908), Wheeler (1896), Buckley (1898), Kessler (1919), Schwarz (1870–1871), Grubenmann et al. (1915) and Cook (1878) which are mainly about clays and rocks of commercial utility (Manger., 1963, Anovitz and Cole, 2015). In recent times, research has been conducted using advanced methods with differing conclusions as reviewed: Manger (1963) made measurements of porosity of sedimentary rock in a survey report for the U.S. Atomic Energy Commission. He used above 900 items of bulk density data and porosity for sedimentary rocks with up to 2,109 porosity determinations per item.

Manger (1963) summarised the methods used for porosity determinations. He divided these techniques into seven to find total porosity. Total porosity measurements are mostly differences on bulk volume/grain volume or bulk density/grain density methods whereas apparent porosity measurements use different absorption methods for unlike fluids or gases.

Kazimierz et al, (2004) used the Core lab PORG200 and the HGP100 type porosimeter when conducting an inter-laboratory porosity determination with the purpose of getting precision and accuracy of these apparatus. The results from the experiment demonstrate repeatability of measurements from these instruments, high precision and a small error of results obtained in repeatable conditions. They conclude that the methods and calibration procedures are the main problems which decide the result correctness and system error levels.

Cnudde et al., (2011) presented the high-resolution X-ray with 3D analysis software for a Belgium Bray sandstone sample. The total porosity was determined using two different approaches for the Bray sandstone. The result from this study shows 14% average porosity determined with water under vacuum and a minimum and maximum of 4% and 24% respectively. Using the MIP, the pore diameter average was 15.7 μm which ranged from 4.7 to 20.1 μm. The average porosity of a micro CT scanned sample in pore volume analysis was 18% over a volume of 343 mm^3. Due to limited resolution, pores less than 7.4 μm are not in the volume analysis. They conclude that the high-resolution for analysed volume is very low to represent data. (Cnudde et al., 2011)

Khan et al., (2012) used helium porosimeter to assess six sandstone sample porosity from different locations of the Khewra Gorge and the Khewra Choha Sudden Shah road section; cores samples were prepared based on the instrument standard. This study shows that the Khewra sandstone upper horizon formation gives a good porosity ranging from 18.76% to 21.07% with different porosity in some part of the formation. The results agree with the international petroleum reservoirs of Cambrian Sandstone. The Khewra sandstone porosity values determined by the helium porosimeter ranges from 18.76% to 21.07%. This represent a potential petroleum reservoir formation. They conclude that the obtained porosity values are greater than the values reported through well logs and other methods, which suggest more petroleum reservoir exploration on the Cambrian sequence from Potwar Plateau. (Khan et al., 2012)

Jenkins., (2015) analysed the porosity and permeability of a tight sand core sample from the Cooper basin, Big Lake field, South Australia. They conclude that the tight sand reservoir result is higher in size than expected, the data trend fit the expected trend by modelled data for the region. SEM imaging and optical microscope are the two methods of photomicrography used in porosity analysis. The pore structure analysis focused on the pore size distribution and porosity. He concluded that the sample of the 'tight' reservoir rock on the porous side of the rock gives an average porosity of 10.22% and more permeable fractures than expected in the sample. The SEM photomicrography is more useful in pore analysis than optical microscope because of higher magnification capabilities. These discoveries improved the tight rock analysis in Australia both in the developing and the new field.(Rezazadeh and Technology, 2015)

Klaja et al., (2015) presented a work to investigate microporous work using the helium porosity measurement. This study showed that the conditions for measurement are important, which include the grain size and the pressure measurement. The measurement performed on samples crushed to < 0.5 mm fraction gives the high porosity values. Porosity measured values are underrated on the entire plug, which relate to the grain density underestimated value. In most cases, porosity increase is caused by increase in the pressure measurement from 19.50 psi to 100psi. These values are far lower than the crushed samples result. This shows that helium molecules cannot penetrate the plug pore spaces for rocks of low permeability at a specific time of measurement. The only way to dry the sample and access the pores is crushing of the sample. For the same grain size fraction (Kp < 0.5 cm), the values of porosity using the volumetric method (KpV) are greater than those when using the density method but in some cases, have lower porosities than the grain size fractions (Kp < 0.5 mm). This confirms that the factor affecting porosity value is the pore space available in the grain size fraction.

There was no connection between the clay minerals and porosity which is because both the clay minerals and the organic matter are associated with the studied rock pore space. Instead, quartz content increase was noticed with a porosity growing trend. The effect of quartz resistance grains in the clay matrix prevents the closing of the pores. Under optimum conditions, the porosity values for sample crushed to < 0.5 mm fraction ranges from 1.5% to 4.5%. This way of measuring porosity is necessary because crushing the sample does not need to make so much pore space available; inaccessible helium pores due to drying and small dimensions of the sample can be in the crushed sample. The combination of helium porosimetry with nitrogen adsorption measurements are studies on the pore space which reaches the nanopores of the organic matter and gives the total porosity value.(Klaja and Przelaskowska, 2015)

2.8 Permeability of sandstone reservoir

Permeability and porosity determine the quality of a reservoir rock. (Chengzao, Min& Yongfeng, 2012). The interconnection between a rock pores which provides a way for flow of trapped hydrocarbon is termed as Permeability. (Lyons & Plisga, 2005). In geophysical research, the transport properties of rocks on the field or laboratory scale is important. One of the main parameters which predicts the recovery capability of reservoir rocks is permeability. (David & Darot., 2013).

Tye & Hickey., (2001) used the core horizontal well (ARCO 18-34 PBU) in Alaska Prudhoe Bay Field. The distribution of lithofacies was established using collected cores to find the petrophysical rock-derived data in a completed well of Triassic Ivishak Formation. Permeability and porosity values ranges from 0.1 to 197.9 md and 10.4 to 25.9% respectively from the vertical and horizontal core plugs. The lithofacies grouped statistical mean-permeability values reveals two different populations: (1) permeability smaller than 40mD and (2) Permeability between 40 and 130mD. Also, the two groups of porosity data (with 95% assurance level) have means of 20.2 and 24.7%. Fractures and faults made no influence to distributary mouth bar permeability. The difference in permeability of the mouth bar lithofacies are determined by fabric and sediment texture variations as improved by preferential diagenesis. In sandstone containing lignite laminae and clay, cementation and compaction to a high extent degrade permeability. For well sorted fine-grained sandstone lithofacies correspond to high permeability values. Under sedimentary conditions, the lithofacies deposited make it possible for geomorphic data from modern-depositional example to deduce the amount, level, and shape of high-permeability streaks. In geostatistical models, sandstone lithofacies 7 form continuous beds in distributary mouth bar deposits which should be treated as separate objects. (Tye and Tye, 2015)

Lock et al., (2002) used a model based on two-dimensional image analysis of its pore structure that gives the accurate permeability of core samples of sedimentary rocks. The pore structure consists of network of pore tubes, with the tubes having distributed cross-sectional shapes and areas. The image analysis of the scanning electron microscope of thin sections estimates the perimeters and areas of the individual pores, with introduced stereological corrections to account for the thin section plane and angle between the pore tube axis. Using the hydraulic radius approximation, the measured perimeter and area estimates each tube individual conductance. The pore diameter variations on the tube length are accounted with a ‘‘constriction factor’’ which is derived using steady flow through an irregular tube. Based on individual conductance’s measured distribution, effective-medium theory is used to find the effective tube conductance. This technique applies to some North Sea reservoir sandstones with permeability range of 20 to 1400 mD. The permeability’s falls within the measured value factor of 2 and error in logK of 0.168.

Intrinsic gas permeability (kg) and intrinsic liquid permeability (kl) ranges from 32 to 159 mD and 12 to 47 mD respectively. The ratio of the gas permeability to liquid permeability gives two groups: (1) For 65% samples, ratio ranges from 1 to 2 (2) For 35% samples, ratio ranges from 4 to 5. The physicochemical, mechanical and experimental phenomenon reduce the liquid permeability during permeability measurements. This study shows more accuracy of gas permeability because it measures close permeability for clay-rich rock than liquid permeability. Furthermore, gas is a replacement fluid because experiment is conducted faster than liquid flow experiments. (Baraka-lokmane, 2002)

To relate liquid and gas permeability’s, the analytical derived Klinkenberg correction is incorporated in the models and a Klinkenberg factor for analytical expression is proposed for each model. The permeability estimates produce a way to compare the sandstone percolation data.

Raza et al., (2015) states that a formation ability to produce hydrocarbons which is affected by pore size, cementing, clay swelling, compaction, sorting and layering is known as Permeability. The literature reports the texture effect of permeability when considering the sphericity, grainsize, degree of cementing and sorting. Furthermore, this study looked separately at the permeability effect on pressure displacement, capillary pressure, water saturation and pore geometry constant. The results of eight experimental sample describes the texture factor effects of permeability as presented by this study. It can be said with the knowledge of these result, the permeability is affected by the effect of texture material, grain size, porosity, cementation and sphericity except when sample from different depositional environment are considered. In the literature, the result also demonstrates the impact of pressure displacement, pore geometry index, water saturation and capillary pressure as similar as published.

The permeability is in positive correlation with the rock texture parameter known as sorting. There is an increase in the permeability sample when the sorting degree from poor sorted grains to well sorted grains is increased. The permeability variation is influenced by parameters such as texture, grain size, degree of sphericity, porosity, degree of cementing but permeability relationship with few numbers of samples can be observed. Permeability variation have great effect on pore geometry index, water saturation, displacement pressure and capillary pressure. (Raza *et al.*, 2015)

Akinlotan., (2016) studied the Wealden sandstones petrophysical properties in the southeast of England which is barely known in the literature regardless of the possibility to study permeability, porosity and sedimentary architecture in three dimensions. The Weald Basin in the southeast of England present the permeability and porosity of the Wealden Sandstone within the Wadhurst Clay Formations and Ashdown for the first time. The Weldon porosity sandstone ranges from 6.3% to 13.2% and the permeability ranges from 0.4 mD to 11.9 mD and both have an average of 9.9% and 3.1 mD respectively. The sandstone with the best quality in terms of high porosity and permeability is the Wadhurst Clay Formation, then by the Top Ashdown, Upper Ashdown and Lower Ashdown. The permeability and porosity in these sandstones are mainly controlled by the grain shapes, grain sizes and sorting which are linked directly to their depositional environment. This study aims to investigate more in the Wealden sandstones petrophysical properties and their potential analogues for fluvial reservoirs. (Akinlotan, 2016)

Saadi et al., (2017) studied the Fontainebleau sandstone petrophysical characteristics based on experimental work. The results are from a sandstone sample block of $0.018m^3$, from a specific layer and site. These results are compared with the result from the whole outcrop area of France. The porous media was characterize using the image analysis technique and experimental laboratory methods. The summary of the result and the technique used are as follows: The Fontainebleau sandstone permeability and porosity values do not vary and are constant for the sample bock. The literature does not cover the data set range of porosity from 0.05 to 0.15. An improved phi/k-relation is developed by combining the literature data; $K = 106,5+4,6*\log(\phi)$; R2 = 0.95. (Saadi *et al.*, 2017)

2.9 Numerical simulation at pore scale

In sandstone reservoirs, pore scale flow mechanism is studied on several topics based on flow models. The pore scale flow component in sandstone reservoir is based upon flow models from few proposed studies. The entire studies use the Darcy's mathematical statement, which is based on the integration of physics at molecular level brings higher permeability value (Ozkan, R, & O.G., 2010). In the oil and gas industry, Computational Fluid dynamics (CFD) is applied to study several industrial problems. It is used for modelling flow of fluid through reservoirs, wells and completion which enables modelling of fluid flow physics through restricted media (Bryne et al, 2011). In recent years, CFD have drawn much attention because of the wide development and computer capability in the simulation field. It is an effective way for solving flows which are complex in nature and used to model 2 or 3-dimensional complex problem due to its strength (Bokane et al, 2013). Recent studies of Comsol Multiphysics software review are presented below;

Debenest et al., (2006) provided a transport analysis from two-region heterogenous porous systems using the COMSOL software. Considering the problems involved from a physicist view point, many questions are raised. Specifically, which models are used in the Darcy-scale equation to avoid high direct computation? A theoretical analysis is required to answer these questions. Several sets of PDE's arises from these analyses with many peculiarities causing a problem in computational implementation: periodicity conditions, integral-differential equations, coupling between different dimension domains.

Fourie et al (2007) showed that using robust modelling and X-ray computer tomography to model the pore scale fluid flow with Navier-Stokes equation is used to derive Darcy's law macro parameters, such as the hydraulic conductivity.

2.10 : Chapter Summary

This chapter summarises the literature survey that was conducted and provides comprehensive definitions, classification, techniques and application of reserves, concepts and procedures of reserves estimation methods, uncertainty (both technical and commercial), sources and how to minimise them, reserve estimation methods (including advantages and disadvantages), and an enumeration of the entire spectrum of in-place and recoverable hydrocarbons/Resources Classification Framework. The selection of an appropriate method to estimate PIIP (Petroleum Initially In Place) and reserves with satisfactory accuracy are also highlighted. Rock properties of sandstone formation, porosity of sandstone reservoir, permeability of sandstone reservoir and numerical simulation at pore scale have also been elaborated in detail. The next chapter will introduce in detail the geological and other characteristics of the Ogba Wet Gas Field as a case study.

Chapter 3 Background of the Wet Gas Field

3.1 Case study

This field consists of several reservoirs of the Agbada formation, a succession of alternating deltaic or near-shore sands and marine shales of Oligocene-Miocene age. A total of eighteen (18) wells have so far been drilled in the field, which found about twenty-four (24) hydrocarbon bearing sands (levels), out of which five (5) are oil bearing and nineteen (19) contain gas condensate.

This reservoir study was undertaken to evaluate the hydrocarbon potentials and recoverable reserves in reservoirs of the Ogba Main field. Static geologic models in Petrel and reservoir simulation models in Eclipse 100 and 300 were built and utilized to estimate the hydrocarbon volumes in place. The total oil-in-place for the twenty-four (24) reservoirs Main field, grounded on the investigation of the information made available for this research, are estimated at about 75.9023MMSTB and 2068.7059BSF of oil and gas respectively. This Field programme was prepared with considerable input and support from NPDC-PED (Nigerian Petroleum Development Company-Petroleum Exploration Department). This chapter covers detailed geological and historical information about the field as the basis of this study special equations used in the study were highlighted and explained several petrophysical properties including reservoir fluid contacts used in the study has been discussed.

The Ogba Egase Ishelle (gas field) is an onshore gas field, for this research **Ogba Egase Ishelle** will be used as the name, a moniker, of the field in question. This is in accordance with the Agreement entered with the data provider through confidentiality agreement signed. This field has some oil reservoirs situated at about 34km southeast of a City in Delta state, in the Niger Delta province of Nigeria. OML AAA block is bound by OML BB to the north, OML CC and DD to the south, OML EE to the east and OML F to the west. The field was discovered in December 1963 and has about 24 hydrocarbons bearing sands between 9405.48 ftss to12440.72 ftss (4 oil bearing reservoirs and 20 gas bearing reservoirs). To date, eighteen wells have been drilled in Ogba Egase Ishelle to further appraise and develop the field. The wells drilled in the field have been completed on one or more of the hydrocarbons bearing intervals. Production from the field started in 1996 and reached a peak of 6,536.4 stb/d and 96028.44 Scf/d in 1996 and 2013 respectively and as at April 2014, a cumulative of 18.02 MMstb of oil, 119.42 Bscf of gas and 2.27MMstb of water have been produced from the field. Structurally, Ogba Egase Ishelle is controlled by a NW-SE trending major growth fault which formed an east-west trending rollover anticline, with crystal faults resulting in a collapsed crest- the main hydrocarbon trapping system in the field. There are several synthetic and antithetic intra-reservoir faults within the field.

3.2 Geological location

Ogba Egase Ishelle is a gas field, with some oil reservoirs, located in the Greater Ughelli Depobelt system, which is an area within the Niger Delta hydrocarbon province characterized by NW–SE trending macro and micro-structural building listric faults from Oligocene to Recent (20Ma-36Ma), Niger Delta litho-stratigraphic units (Benin, Agbada and Akata Formations), Extensional, Translational and compressional structures. The Greater Ughelli Depobelt, which recorded great depositional rates coupled with the variable rates of subsidence accounted for the numerous syn-depositional faulting that range from simple rollover to collapsed crestal fault pattern that contributed to the hydrocarbon traps in the Ogba Egase Ishelle field.

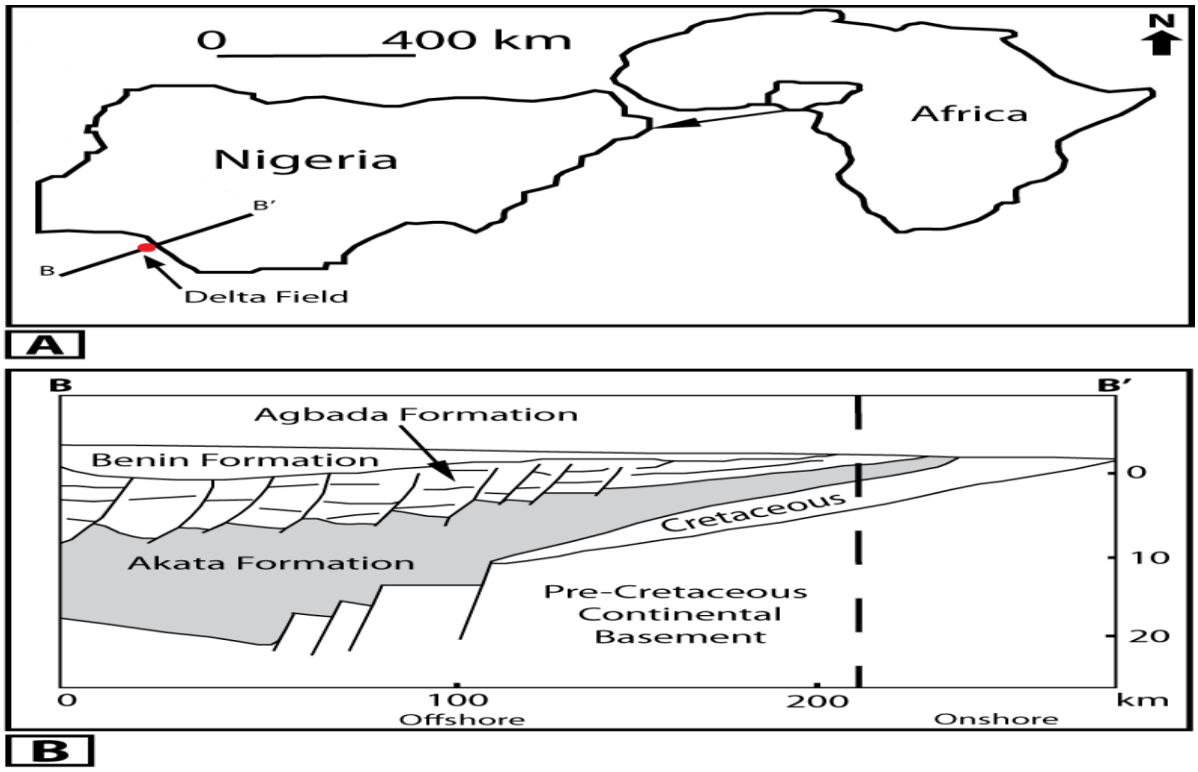

Figure 3-1: (A) Location of the Delta Field, which is located within the Niger Delta (B) Cross section across the Niger Delta, which has been modified from Nyantakyi et. al (2003) and Stacher (1995)

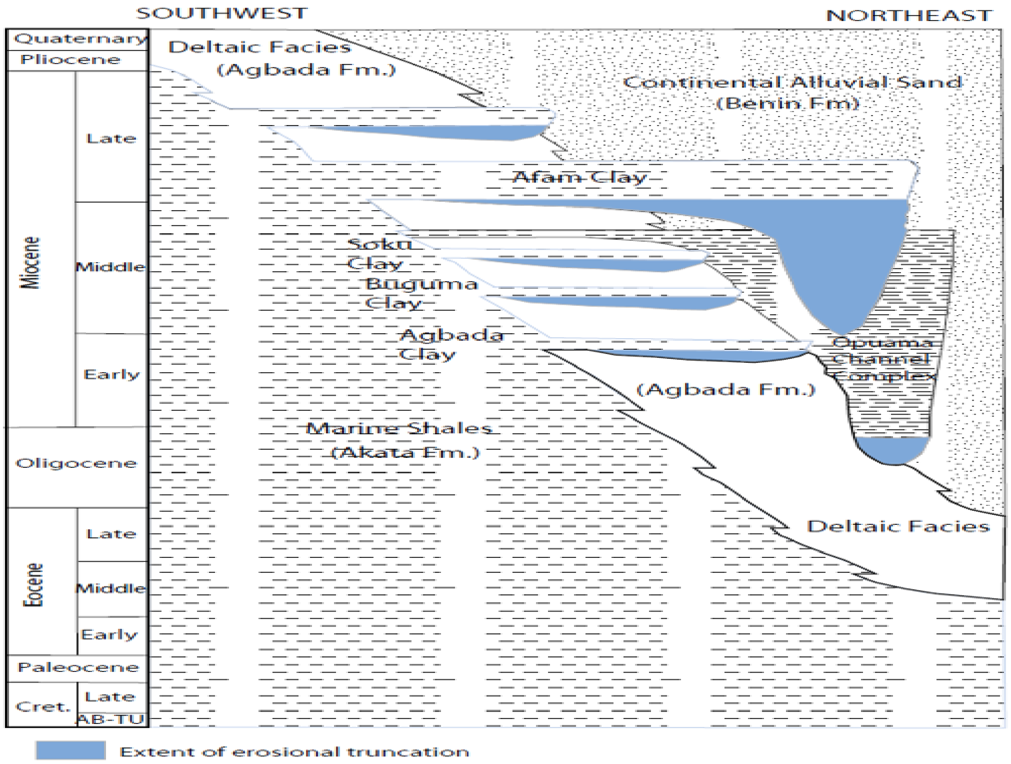

Figure 3-2: Generalized Litho-stratigraphy of Niger Delta. Source: Doust and Omatsola, 1990.

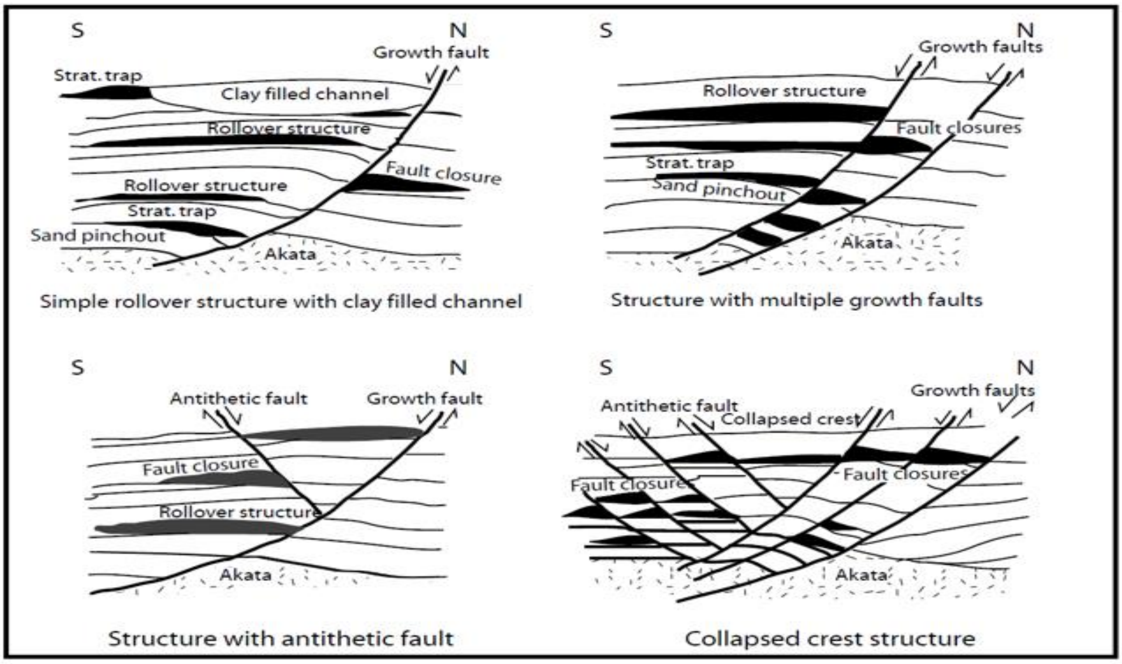

Figure 3-3: Generalized Structural traps of Niger Delta (Nwangwu, 1990).

3.3 Reservoir Geology

3.3.1 Stratigraphy and sedimentology

Ogba Egase Ishelle is located within the geological setting of the Niger Delta where clastic wedges were deposited along the failed arm of a triple junction system. Originally, the Delta was formed during the breakup of the South American and African plates in the late Jurassic (Burke, 1972; Whiteman, 1982). The two rift arms that followed the south-western and south-eastern coast of Nigeria and Cameroon developed into passive continental margin of West Africa. Also, the third failed arm formed the Benue Trough, which is located under the Gulf of Guinea, offshore Nigeria. After an early history of rift filling in the late Mesozoic, the clastic wedge steadily prograde into the Gulf of Guinea during the Tertiary as drainage expanded into the African Craton with consequent subsidence of the passive margin. These upward-coarsening strata, which off lapped this continental margin, was divided into three diachronous lithostratigraphic units. These are Akata, Agbada and Benin Formations (Short and Stauble, 1967; Doust and Omatsola, 1990).

The *Akata* Formation is the oldest of the units and composed mainly of marine shale, which range in age from Paleocene and through the recent (Doust and Omatsola, 1990). The Agbada Formation overlies the Akata Formation and comprises mainly of alternating deltaic sandstones with shale. It ranges from Eocene to Recent. The Benin Formation is the youngest, Oligocene to Recent, in the lithostratigraphic succession and comprises loose sandstone, grits, claystone and streaks of lignite. Ogba Egase Ishelle Wells penetrated two main classical geologic lithostratigraphic formations of the Niger Delta; Agbada and Benin Formations. (NPDC Benin, November 2015).

- ***Benin* formation*:* -** Characterized by massive unconsolidated continental sands with few intercalating clay materials. The relatively high values observed on the resistivity logs from the Wells are indicative of fresh water sands. This section did not encounter any hydrocarbon in all the Wells drilled.
- ***Agbada* formation*:*** - The top is characterized by the first major shale break from the overlying Benin formation while the base (top of Akata formation) was not reached by any of the Wells. The interval is typically made up of alternating sand and shale sequence. The sand/shale ratio generally decreases with depth. The sands encountered are a combination of transgressive (upward fining of sand), regressive (upwards coarsening) phases and tidal channels. Major shale breaks separate each sequence. The

interval of interest in the Agbada formation is interpreted to be near-shore marine with variable weak to strong continental influence. The sands consist of alternating beds of shale and relatively thick sands with shale inter beds. The general log motif of the sands is coarsening upwards in shape. The Field is entirely composed of normal faults whose pattern is consistent with exclusively southerly dipping synthetic faults. The structure is a roll-over anticline controlled by a large growth fault that forms the boundary fault of the field. In the absence of core data facie characterization, the environment of deposition was inferred, relying on well log motifs and the sediment logic description of logs.

3.4 Petro-physics

The petrol physical evaluation was performed to identify hydrocarbon bearing reservoirs and study rock and fluid properties that are essential for the economic accumulation of hydrocarbon and its general characterization, based on the available data from the wells. This evaluation was carried out with Techlog Software. The log suite contained a reasonable set of data, consisting GR, Sonic, Density and Resistivity curves as shown in Table 1.1. These logs were considered enough to allow the evaluation of the reservoir properties (Volume of shale (Vsh), Porosity, Water saturation and NTG) to be carried out. Porosity was calculated directly from both density and sonic logs correcting both for fluid density, matrix density and matrix interval transit time. The Formation Resistivity was obtained from the Resistivity log. The normalized volume of shale (Vsh) in the reservoir was calculated from the Gamma Ray logs in all the Wells using the Gamma Ray Index (Equation 3.1).

$$IGR = \frac{GR_{\log log} - GR_{min}}{GR_{\max log} - GR_{\min}} \tag{3.1}$$

3.4.1 Volume of Shale (Vsh)

The Larinov equation for tertiary sands was employed to determine the percentage of shale and implicitly, the dominant lithology. This was achieved by determining the clean sand line and shale line from Gamma-Ray logs for each of the reservoirs. However, correction was made on the gamma ray index to compensate for the unconsolidated sand of the Niger Delta (Tertiary). (Equation 3.2).

$$V_{sh} = 0.083 * 2^{(3.7 * IGR)} - 1.0 \tag{3.2}$$

Where,

GR Log = GR of formation measured from log, GR Min = minimum GR reading in zone of interest, *GR* Max = Maximum GR reading in zone of interest, *IGR* = Gamma Ray Index Vsh = Volume of Shale

The volume of shale (Vsh) also served as an input data in the porosity and saturation model for shaly sand.

3.4.2 Porosity

The porosity of 0.12% was estimated from density log and sonic log (where density log is unavailable). The effective porosity was further deduced by introducing the shale volume percentage into the equation. Comparison was made between density porosity and different sonic porosity estimation models in well 8 (methods by Wyllie, Raymer et al and Raiga-Clemenceau), meanwhile Raymer-Hunt Gardner method was the closest match to density porosity and was therefore adopted as the Sonic porosity estimation method. In Ogba Egase Ishelle Well 8, density log terminated at a depth of about 3419.63m and the Well has a total depth of about 3659.7m, with some reservoirs occurring beyond 3419.63m where the density log terminated. Sonic porosity was therefore combined with the Density porosity to account for the porosity of reservoir bearing sands below the depth of 3419.64m, where the density porosity of the well ended. Porosity was estimated from the bulk density and sonic logs (Equation 3.3 and 3.4) using average grain density of 2.65g/cc, 1.00g/cc and 0.85g/cc for fluid density, 53msec/ft. for average grain velocity and 189msec/ft. for pore fluid velocity.

$$\emptyset_D = \frac{\rho_{ma} - \rho_{log}}{\rho_{ma} - \rho_{fluid}} \tag{3.3}$$

$$\emptyset_s = C\,\frac{\triangle t_{log} - \triangle t_{ma}}{\triangle t_{l}} \tag{3.4}$$

$\emptyset_D$= density porosity (effective)

$\emptyset_s$ = sonic porosity (Raymer-Hunt equation)

ρ_{ma}=matrix density

ρ_{log}=bulk density log reading

ρ_{fluid}=density of fluid

V_{sh}=Density of adjacent shale

V_{sh}= volume of shale

GR_{log} = sonic log reading

GR_{max} = interval transit time of the matrix material

C = empirical correlation factor.

3.4.3 Water saturation (S_w)

Indonesia model and modified Simandoux equations were used to estimate effective water Saturation for the reservoirs. A comparison was made between the two effective water saturation methods used, and the observed difference fell within less than 3% margin. However, Indonesia model was preferred as it appears to have less spikes than modified Simandoux. Meanwhile, Pickett plot was used to determine Rw for the different reservoirs, which served as an input for water saturation estimation. Saturation Height Models were used to generate a liquid inundation prototypical. This method uses capillary pressure to justification for the hydrocarbon shift zone, together with any dependence on rock quality and pore-throat geometry. It is trained by the calculated water saturation model.

The Saturation Height Model was built based on Brooks Corey's method.

(Brooks Corey's Method)

$$S_w = S_{wirr} + (1 - S_{wirr}) * \left\{\frac{P_{ce}}{P_c}\right\} \frac{1}{N} \tag{3.5}$$

Where;

S_w = Water Saturation, S_{wirr} = Irreducible Water Saturation, Pce = Capillary Pressure Entry PC = Capillary Pressure, N = fitting Curve parameter

3.4.4 Net-To-Gross Ratio

The net sand of the reservoirs was estimated by applying Petro physical cut-off (Vsh=0.52, Porosity=0.12). The Net-to-Gross ratio was used to define the net pay for evaluating the Hydrocarbon – in – place. Volume of shale and porosity cut-offs were applied to define the Reservoirs.

3.4.5 Field cut-off determination

To determine the field cut off, a plot was made of porosity thickness versus porosity and volume of shale respectively see figure3-4. A field average cut off 0.11 was determined for porosity, while volume of shale was fixed at 0.52.

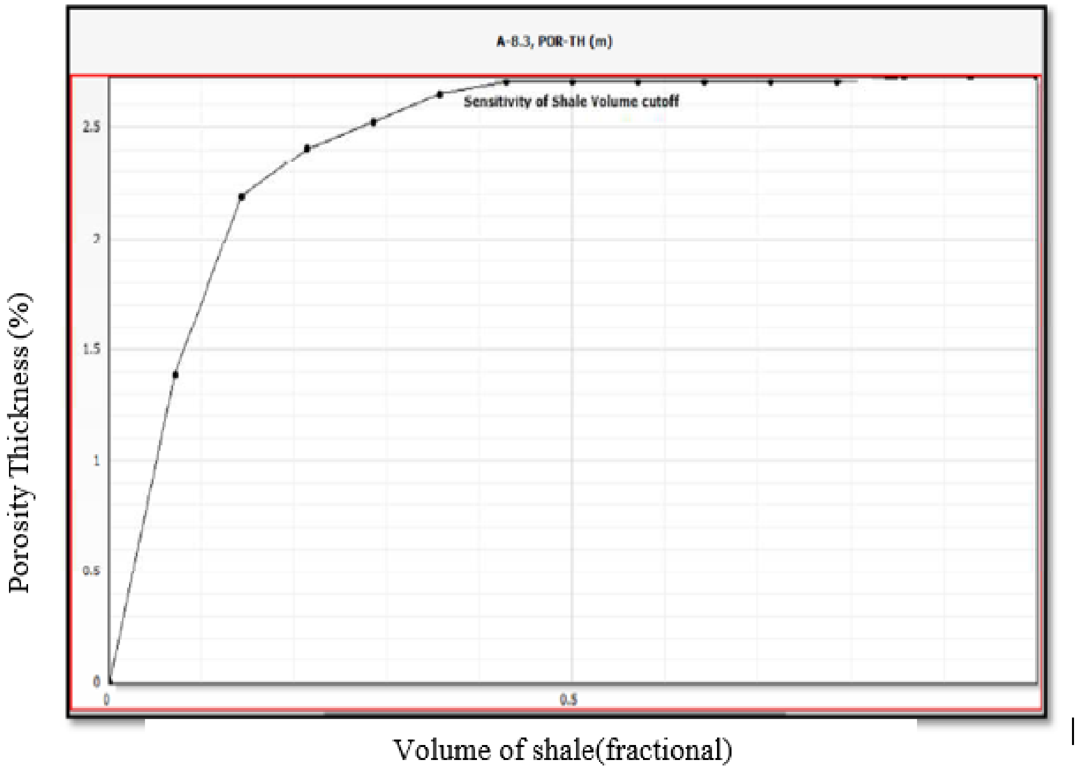

Figure 3-4: Plot of Porosity Thickness vs V-shale for Field Cut-Off determination

3.4.6 Permeability

Permeability was derived from the calculated porosity using the FZI equation developed for the Niger Delta. The FZI is an intrinsic reservoir quality parameter that represents the cumulative effects of pore throat sizes and shapes, tortuosity and surface to grain volume ratio on the hydraulic behaviour of a reservoir rock. However, reservoir rocks with identical FZIs have the same permeability-porosity relationship and thus have a predictably distinct hydraulic behavioural pattern, thus reservoir sections with identical FZIs form a distinct Hydraulic Flow Unit. From analyses of core data in the Niger Delta, it has been revealed that various geological facies/genetic units found in the Niger Delta are characterized by a predictable range of FZI values. Some of the average FZI values that characterize the genetic units found in the Niger Delta have been computed and are presented in this report shown in Table 3.0**.**

With the FZIs known, the permeability at all points in the reservoir segment of interest is given by**:**

$$k = 1014(FZI)2\frac{\Phi^3}{(1-\Phi)^2} \quad (3.6)$$

Where, K = permeability, Φ = Total porosity, FZI = Flow Zone Indicator

Table 3-1: Some average FZI values of genetic units found in the Niger Delta (NPDC)

Some Generic Units Identified in Ogba Egase Ishelle	Min FZI No.	Mean FZI No.	Max FZI No.
Upper Shore face	6.02	7.54	9.06
Fore Shore	14.57	19.35	24.13
Proximal Lower Shore face	1.39	2.10	2.81
Channel Sands	6.04	8.88	11.72
Transgressive Sand	2.72	3.76	4.80
Marine Shale	-	0.10	-

Table 3-2: Summary of average Petro physical parameters for reservoirs (DPR)

SAND	POROSITY	NTG	SW
X7.1	0.2105	0.96640	0.24360
X8.0	0.1883	0.85960	0.37053
X8.1	0.2467	0.82410	0.22905
X9.0	0.1900	0.82000	0.34000
X9.1	0.2200	0.92000	0.15000
X10.1	0.2000	0.90000	0.36220
X10.0a	0.2000	0.82000	0.16000
X10.0b	0.1710	0.90840	0.46770
Y1.1	0.2140	0.86430	0.31720
Y2.1	0.1927	0.70700	0.42362
Y3.0	0.2673	0.91900	0.24510
Y5.0	0.1645	0.83430	0.63427
Z1.0	0.2359	0.88500	0.30310
Z2.0	0.2167	0.89070	0.32049
Z2.1	0.1770	0.68020	0.31880
Z3.0	0.1288	0.90520	0.66630
Z4.1	0.1691	0.89000	0.33590
Q2.0	0.1438	0.83850	0.37840
Q3.0	0.1535	0.85140	0.23660
X8.2U	0.2100	0.88000	0.35000
X8.2L	0.1561	0.90290	0.42480
X8.3	0.2197	0,8969	0.3804
X11	0.2230	0.8969	0.2985
Y1.0	0.1904	0.8133	0.3684

3.4.7 Reservoir fluid contact

The fluid contact is the fluid-to-fluid or fluid-to-formation interface of the hydrocarbon column in the reservoirs. The common contact types found in the field are Gas Water Contact (GWC), Gas Oil Contact (GOC), Gas down To (GDT), Oil down To (ODT) and Oil Water Contact

(OWC). These fluid contacts were determined using the Deep Resistivity and a combination of Neutron-Density Logs where available.

Table 3-3: Shows the fluid contacts for the reservoirs

RESERVOIR	CONTACT	
	OWC/ODT	GOC/GDT
X7.1	-	2908.85 GDT
X8.0	-	2958.45 GDT
X8.1	-	2967.64 GDT
X9.0	-	3046.15 GDT
X9.1	-	3050.88 GDT
X10.1	-	3086.10 GWC
X10.0a	-	3082.59 GWC
X10.0b	-	3089.15 GWC
Y1.1	-	3217.99 GWC
Y2.1	-	3271.30 GDT
Y3.0	-	3262.77 GDT
Y5.0	-	3425.08 GDT
Z1.0	-	3572.31 GDT
Z2.0	-	3607.04 GWC
Z2.1	-	3614.22 GDT
Z3.0	-	3601.67 GDT
Z4.1	-	3732.39 GDT
Q2	-	3745.1 GDT
Q3	-	3791.93 GDT
X8.2U	2986.79 OWC	2967.27 GOC
X8.2L	2989.22 ODT	-
X8.3	3003.47 OWC	3000.53 GOC
X11	3129.41 OWC	3124.72 GOC
Y1.0	3204.07 ODT	3187 GOC

Consequently, having sated the background of the field in this chapter the next chapter will introduce the material, and detailed procedures, precautions etc that was followed during the research.

3.5 Chapter summary

This chapter elucidates the concept of the field lithology of the reservoirs of the Ogba Egase Ishelle main field and the generalized litho-stratigraphy of Niger Delta. The geological location and reservoir geology (stratigraphy and sedimentology) have been discussed in detail. The concept of petro-physics evaluation of the entire field has been emphasised with the related rock and fluid properties such as Volume of Shale (Vsh), Porosity (Porosity Thickness vs V-shale for Field Cut-Off determination), Water saturation (S_w), Net-To-Gross Ratio (NGR), Field cut-off determination, permeability and reservoir fluid contact (i.e. fluid-to-fluid or fluid-to-formation interface of the hydrocarbon column in the reservoirs) which are all essential for the economic accumulation of hydrocarbon and its general characterization. Furthermore, some average FZI (Fluid Zonation Isolation) values of generic units found in the Niger Delta and a summary of average petro-physical parameters for reservoirs are also highlighted. Consequently, having described pertinent details of the background of the field in this chapter the next chapter will introduce the material methods, detailed procedures, precautions and other processes employed during the research.

Chapter 4 Materials and Methods

4.1 Overview

This chapter introduces the research methodology which focuses on the analysis of experimental and computational fluid dynamics output obtained through flow dynamic methods. This chapter was divided into five phases:

The experimental set up involved, procedures and description of detailed steps involved to ensure precise and accurate results are obtained. The Chapter covers the six phases including:

(1) **Phase 1**: The core characterization measurement of the dimensions and weight were performed using the Vernier calliper, weight measurement balance.

(2) **Phase 2:** The application of COMSOL-Physics, constitutes the creation of a pore-scale finite element mesh of sandstone core samples from SEM images and based on the numerical simulation of sandstone at a pore-scale level based on experimental results.

(3) **Phase 3**: Presents the methodology employed in determining the porosity of sandstone core samples using helium Porosimetry,

(4) **Phase 4:** Presents the methodology employed in determining the permeability of sandstone core samples using Prog 200 model from core laboratories. To measure the permeability of rock samples using a gas Permeameter and to apply Klink Enberg effect corrections to obtain the liquid permeability.

(5) **Phase 5**: core flooding for two-phase liquid movements under unsteady state or steady state circumstances and single-phase gas steady-state experiments

(6) **Phase 6**: PVT Analysis for gas composition and fluid properties

(7) **Phase 7**: Modelling and computer simulation

The experimental set ups, procedures as well as precautionary measures and sources of error are detailed in each respective section below.

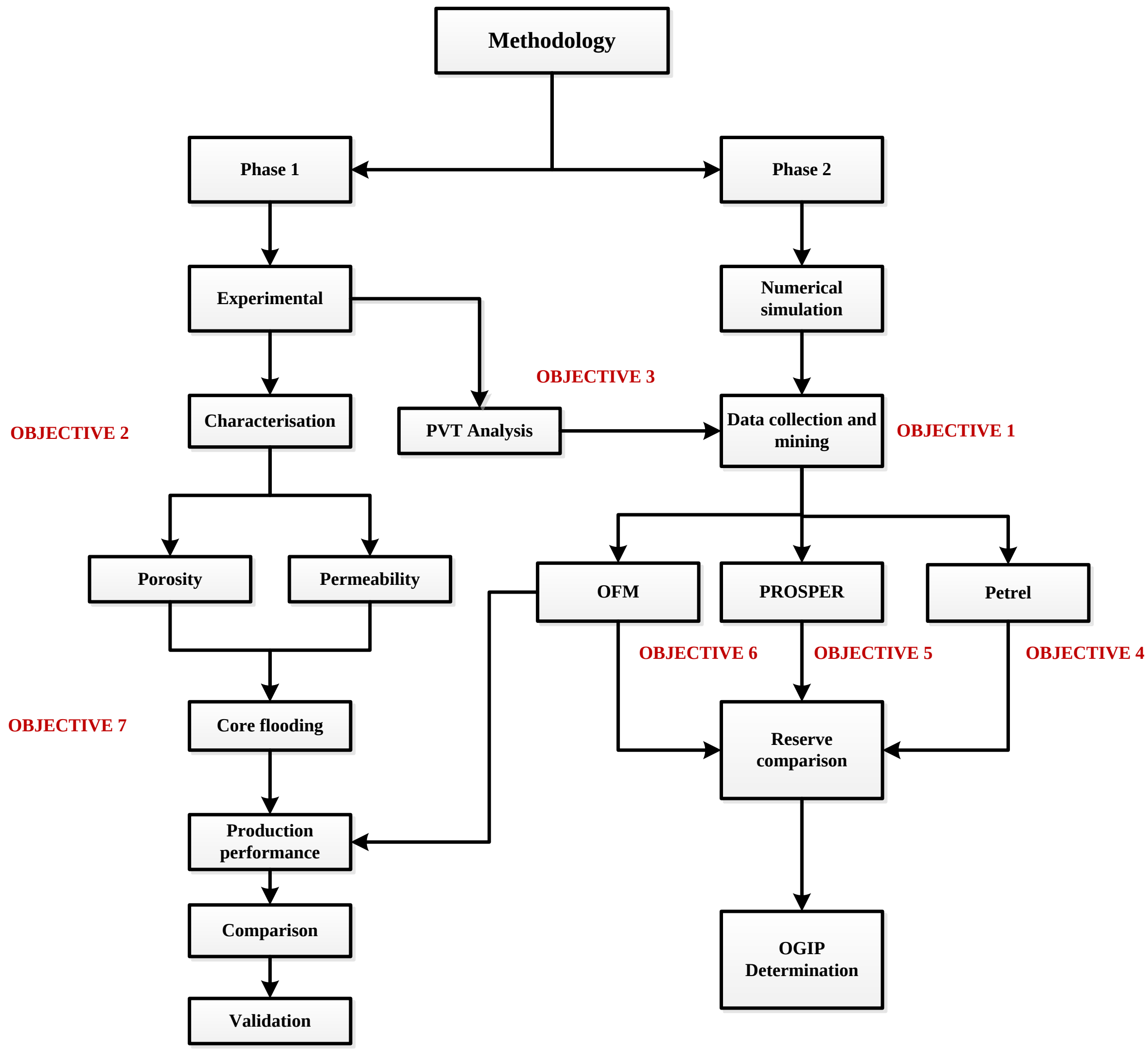

Figure 4-1: Schematic showing stages involve for conducting current studies

4.2 Sandstone materials

Buff Brea, Boise and Castle gate core sandstone were obtained from Kocurek Industries INC, Hard Rock Division, 8535 State Highway 36 S Caldwell, TX 77836) and were used for this study. Using the Vernier calliper for core characterization, weighing balance. The core samples have the following weight and dimensions:

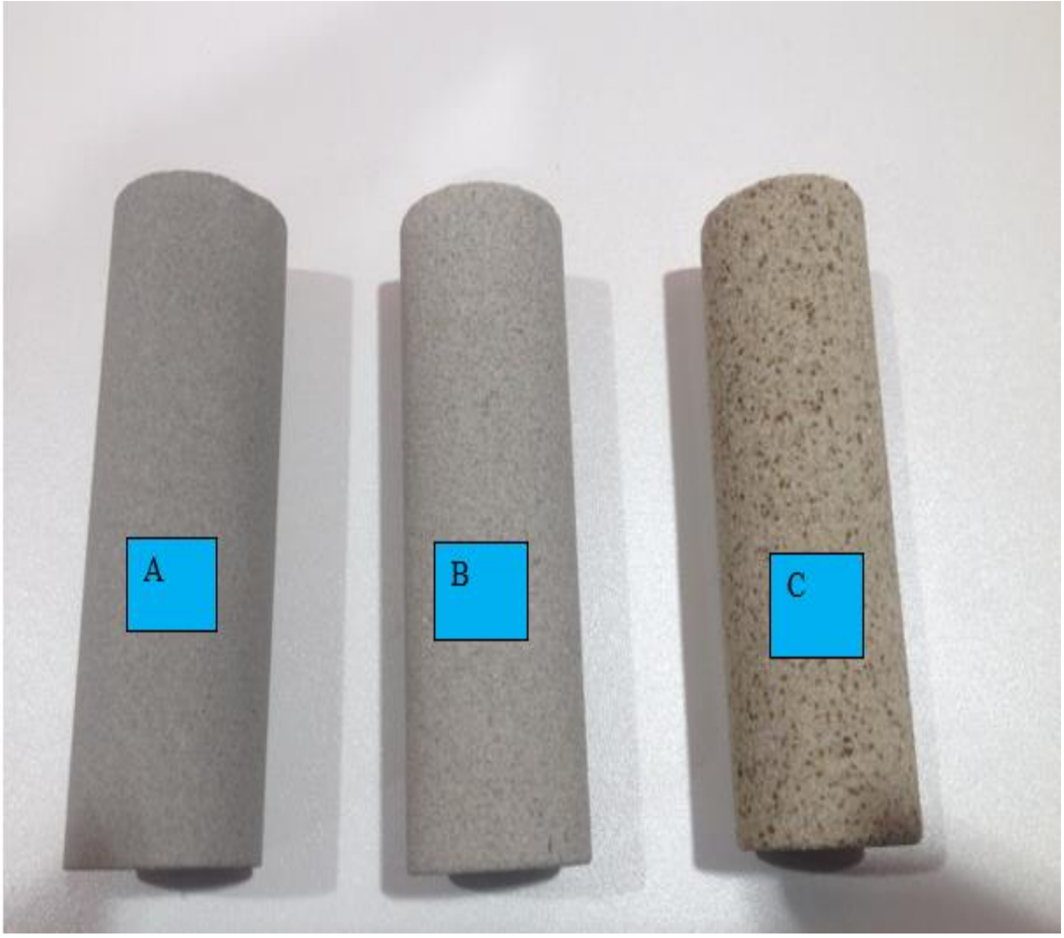

Figure 4-2: core samples for porosity determination.

A. Castle gate
B. Buff Bera
C. Boise

Table 4-1: Sample characterization for both A, B, and C

S/N	Weight (kg)	Diameter (in)	Length (in)
A	69.95	0.9795	2.9965
B	75.77	0.9920	3.0025
C	66.77	0.9755	2.9940

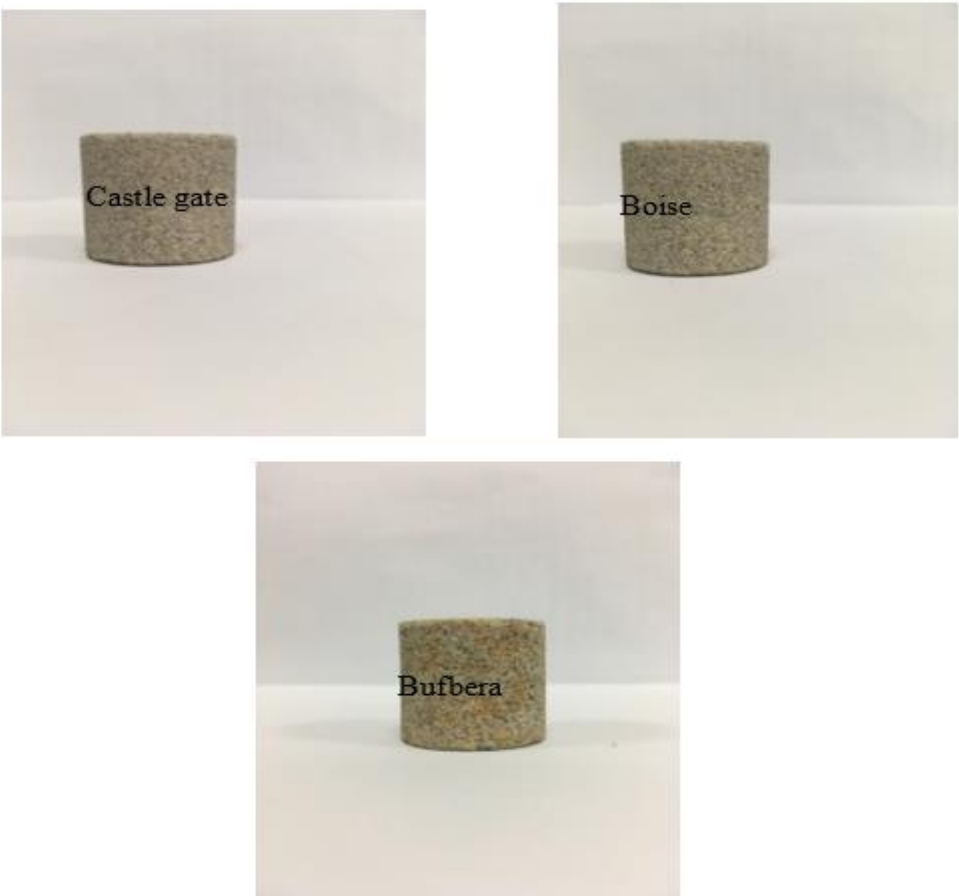

Figure 4-3: Core samples for permeability determination.

4.3 Pvt study on Ogba Essale-8 Sub Surface sample Procedure

XYZ 200 sample chamber was among the loaded chambers that were delivered to the laboratory on October 19, 2017 for PVT analysis. Results of the various analysis and measurements are presented in this report.

4.3.1 Sample validation and transfer

The opening pressure of the chamber was measured at room conditions of 761.9 mmHg and 78.8 F. The chamber was compressed to 7015 psia and heated to the reservoir temperature of 224.6 F. The sample was homogenized and restored to its original reservoir status through rocking for 12 hours.

A subset of the Gas condensate sample was introduced into a high pressure and high temperature visual PVT cell. The sample was heated and stabilized at 224.6 F. The gas condensate sample exhibited a saturation pressure of 5621 psia at the reservoir temperature of

224.6 F. A complete PVT study was subsequently performed on the sample. The validation result of the samples is presented on page 5 of this report

4.3.2 Phase behaviour studies

A sub set of the sample was flashed from reservoir condition to atmospheric condition (758.31 mmHg and 82.4 F). The products (i.e. gas and oil) were analysed by gas chromatographic technique and then mathematically recombined to obtain the reservoir fluid composition.

Constant Composition Expansion (CCE) test, Constant volume Depletion (CVD) test were performed at the reservoir temperature of 224.6 F. Multi- stage separation test was performed at the specified surface processing condition.

4.4 Digital Imaging

4.4.1 SEM imaging and principle

Scanning electron microscope (SEM) focuses electron beam in the direction of the Buff Bera sandstone to analyse the sample. An electron gun at the top of the device is used to shootout concentrated electron beam. The SEM consist of a vacuum chamber which ensures no obstruction of the beam from the gun within the microscope to the sample under analysis. The sample emits X-rays and 3 different types of electrons when incident electron beam hits it. The SEM uses the secondary electron and primary backscatter among these electron types. An electron recorder picks up the rebounded electron and records the imprints of the electrons. This information is interpreted onto a screen as a 3-dimensional image.

4.4.2 Sample preparation

Several procedures described by the manual on how to clean up the sustained damage due to coring and plug extraction. The figure below shows that the area of interest for the microscale imaging was determined. To confirm the difference is not impacted negatively by the charging due to routine use of electron microscopy, a plan was established to electron charge mitigation. The sample prepared as shown in the figure below gives a large field of view image of mineralogy and porosity without any damage.

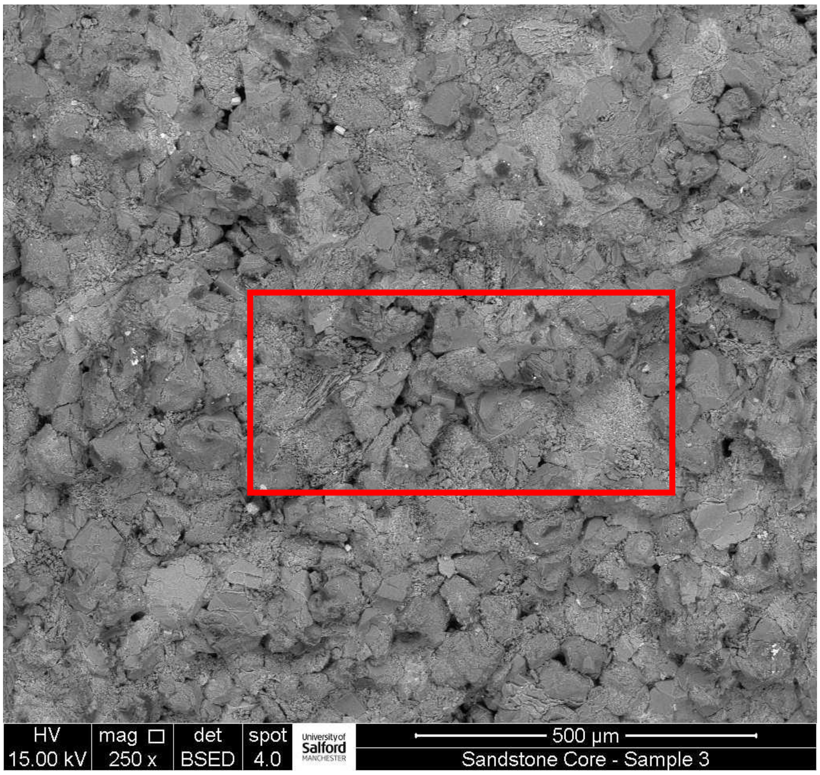

Figure 4-4: The image of Scanning electron microscope of the Grey Berea sandstone.

4.5 Experimental Procedure for porosity determination

The experiment is ready for grain volume calibration when a transducer zero check and leak test are performed. The Bandera grey sample stabilized into the matrix cup. The gas inlet is turned on and the sample valve is turned to vent position. This system is pressurized to about 90psi by adjusting the regulator handle. The gas inlet valve is turned off to record the upstream pressure (P1) on the screen. Helium is directed to the matric cup by turning the sample valve to vent position. The upstream pressure is observed till a steady value is attained. This is recorded as the stabilised pressure reading (P2). The sample valve is turned off to vent out helium from the apparatus. The same procedure is repeated to the Castle gate, Buff Brea core sandstone samples. The spreadsheet (Appendix A) can be used to plot P1/P2 versus the "grain" volume of the disks in the cup. (See Appendix A for calibration disk volumes.) The equation of the line obtained is used to determine the grain volume for core plugs. Prior to measurement of core sample on each suite, the following sequence was performed

4.6 Computational Fluid Dynamics (CFD) modelling using COMSOL Multiphysics

COMSOL Multiphysics is a powerful interactive environment for modelling and solving all kinds of scientific and engineering problems. The software provides a powerful integrated desktop environment with a Model Builder where you get full overview of the model and access to all functionality (T.J Bogar, 1983). With COMSOL Multiphysics one can easily extend conventional models for one type of physics into Multiphysics models that solve coupled physics phenomena—and do so simultaneously.

Using the built-in physics interfaces and the advanced support for material properties, it is possible to build models by defining the relevant physical quantities—such as material properties, loads, constraints, sources, and fluxes—rather than by defining the underlying equations (F.A.L.Dullien, 1991). One can always apply these variables, expressions, or numbers directly to solid and fluid domains, boundaries, edges, and points independently of the computational mesh. COMSOL Multiphysics then internally compiles a set of equations representing the entire model.

Using these physics interfaces, one can perform various types of studies including:

- Stationary and time-dependent (transient) studies
- Linear and nonlinear studies
- Eigenfrequency, modal, and frequency response studies

When solving the models, COMSOL Multiphysics uses the proven finite element method (FEM). The software runs the finite element analysis together with adaptive meshing (if selected) and error control using a variety of numerical solvers (R.D.Bird, 2002).

Partial differential equations (PDEs) form the basis for the laws of science and provide the foundation for modelling a wide range of scientific and engineering phenomena.

4.6.1 How to Develop Simulation and Modelling.

These calculations are at the core of the simulation of fluid flow. Attempting to solve them for a specific set of initial conditions (such as inlets, exits, and walls) determines the velocity and pressure of the fluid in a given geometry (T.J Bogar, 1983). These equations accept only a relatively small number of quantitative solutions due to various their complexity. For example, solving these equations for a flow between two parallel plates, or for the flow in a circular tube, is relatively easy. Nevertheless, the equations must be solved for even more complicated systems.

4.6.2 Laminar Flow Past a Backstep

In the following example, we solve numerically in a computational domain the Navier-Stokes equations (hereinafter also referred to as "NS equations") and the equation of mass conservation. These equations must be solved under a set of boundary conditions.

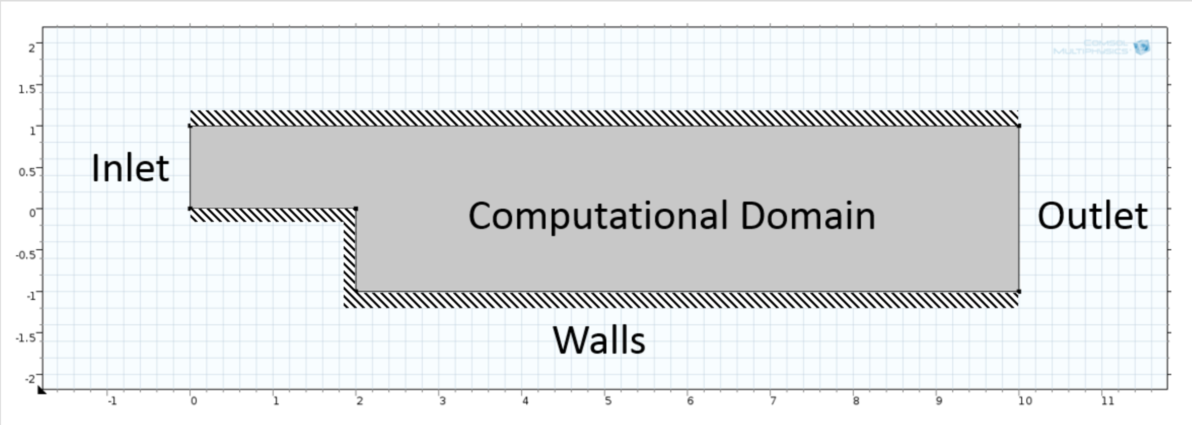

Figure 4-5: Laminar Flow Past a Backstep from COMSOL Multiphysics manual 2019.

The speed of the fluid is defined at the inlet and at the outlet pressure is prescribed. The no-slip boundary condition (i.e. the velocity is set to zero) is specified on the walls. The mathematical solution of the stable-state NS (the time-dependent derivative is set to zero) and the calculations in the laminar regime are executed (O.Anwar Beg M. U., 2016).

4.6.3 Low Reynolds number / Creeping flow

The inertial forces are quite low when the number of Reynolds is very small in comparison to the viscous forces and can be ignored when solving the NS equations ((M.Saiben, 1977). To demonstrate this flow system, we first examine pore-scale flow studies carried out by the University of California, Santa Barbara, USA by Professors Arturo Keller, Maria Auset, and Sanya Sirivithayapakorn.

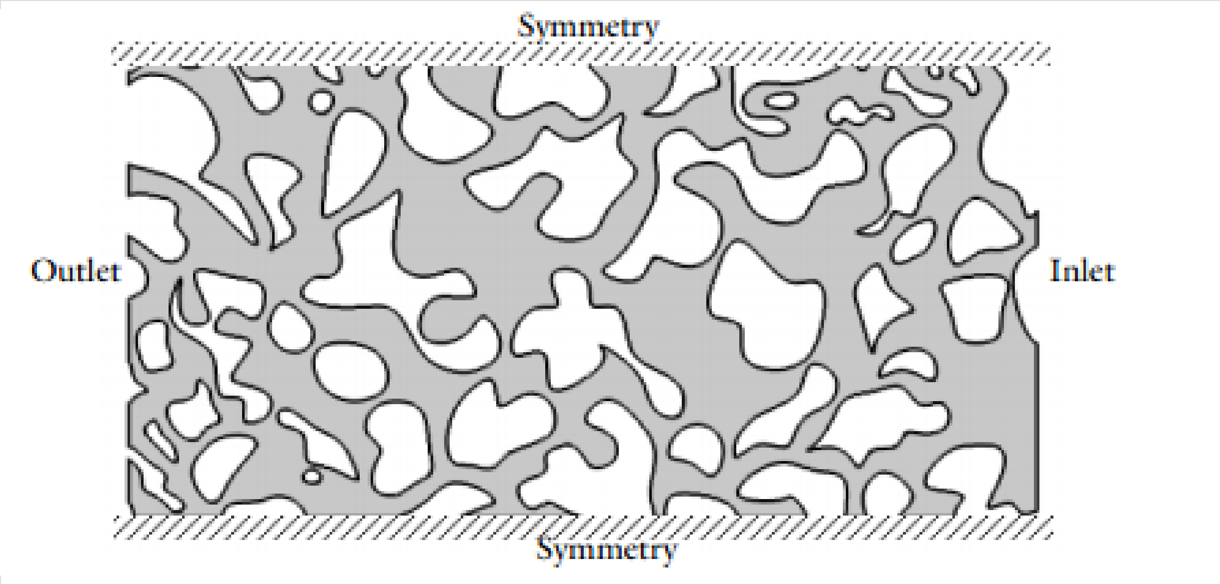

Figure 4-6: Graphic showing the boundary conditions in the pore-scale flow experiment. from COMSOL Multiphysics manual 2019.

4.6.4 An Introduction to the Finite Element Method

The description of the physics laws for space-and time-dependent issues is usually expressed as partial differential equations (PDEs). Such PDEs cannot be solved with analytical methods for most geometries and issues. Rather, it is possible to construct an approximation of the equations, usually based on different discretization forms (T.J Bogar, 1983). Such methods of discretization approximate PDEs with mathematical model equations that can be solved with numerical methods (T.J Bogar, 1983). In addition, the solution for the numerical model equations approximates the real solution for the PDEs. The system of finite elements (FEM) is used to measure these approximations.

Consider, for example, a function u which may be the dependency variable in a PDE (i.e. temperature, electrical potential, stress, etc.) The variable u can only be approximated by a process uh using linear combinations of basic functions in the following terms.

$$u \approx u_h \qquad (4.1)$$

$$u_h = \sum_i u_i \psi_i \qquad (4.2)$$

Here, ψ_i denotes the basic functions and u_i denotes the coefficients of the functions that approximate u with u_h. The figure below illustrates this principle for a 1-D problem. u could, for instance, represent the temperature along the length (x) of a rod that is nonuniformly heated. Here, the linear basis functions have a value of 1 at their respective nodes and 0 at other nodes. In this case, there are several elements along the portion of the x-axis, where the function *u* is defined (i.e. the length of the rod). One of the advantages of the finite element method is its capacity to select optimised basic function (Beg, 2019)s.

4.6.5 Finite Element Mesh Refinement

In order to build predictive computational models of real-world scenarios, engineers and scientists use finite element analysis (FEA) technology. The use of FEA software begins with a model of computer-aided design (CAD) representing the simulated physical parts as well as knowledge of the material properties and the loads and constraints applied (J.T. Salmon, 1983). This insight helps real-world behavioural predictions, even with very high precision points.

The precision that can be gained from any FEA model is directly linked to the mesh used for finite elements. The finite element mesh is used to partition the CAD model into simpler regions called elements that solve a sequence of equations. These equations depict the governance equation of relevance approximately through set of given polynomial functions over each variable. The simulated solution will follow the true solution as these components are made smaller and smaller as the mesh is refined (T.Hsieh, 1987).

This mesh refinement process is a key step in validating any model of finite elements and gaining trust in software, models and results.

4.6.6 The Mesh Refinement Process

A good analysis with finite elements begins with both an understanding of the system's physics to be analysed and a complete description of the system's geometry (C.A.Balanis, 1989). A CAD design reflects this geometry (Buff Berea). A standard CAD model may accurately describe the shape and structure, but often also include cosmetic features or specifics of produce that may prove to be foreign to finite element modelling (J.T. Salmon, 1983) The analyst should use some engineering judgement to examine the CAD model and decide whether to remove or simplify these features and details before meshing. It is almost always easier to start with a simple model and add complexity rather than starting with and simplifying the complex model.

The analyst should also be aware of all the physics applicable to the problem, the properties of the materials, the loads, the constraints, and any elements that may affect the outcomes of interest (M.Saiben, 1977). There may be ambiguity in these outputs. For example, the properties and loads of the material may not always be accurately understood. During the modelling process, it is important to keep this in mind as there is no advantage in trying to solve a model to greater accuracy than the data input admits.

4.6.7 CFD Module

The CFD Module is an optional package that extends the COMSOL Multiphysics modelling environment with customized user interfaces and functionality optimized for the analysis of all types of fluid flow (R.D.Bird, 2002). Ready-to-use interfaces allow the simulation of both laminar and turbulent flows in single or multiple phases. Functionality for treating coupled free and porous media flow, stirred vessels, and fluid-structure interaction are also included (T.Hsieh, 1987).

- Laminar and turbulent flow using several established turbulence models
- Single-phase and multiphase flow
- Isothermal and non-isothermal flow
- Compressible and incompressible flow
- Newtonian and non-Newtonian flow

The ready coupling of heat and mass transport to fluid flow enables modelling of a wide range of industrial applications such as petroleum reservoirs, heat exchangers, turbines, separations units, and ventilation systems.

Together with COMSOL Multiphysics, the CFD Module takes flow simulations to a new level, allowing for arbitrary coupling to physics interfaces describing other physical phenomena, such as structural mechanics, electromagnetics, or even user-defined transport equations (J.A.strong, 1989)

COMSOL Multiphysics excels in solving systems of coupled nonlinear PDEs that can include:

- Heat transfer
- Mass transfer through diffusion, convection, and migration
- Fluid dynamics
- Chemical reaction kinetics
- Varying material properties

The Multiphysics capabilities of COMSOL can fully couple and simultaneously model fluid flow, mass and heat transport, and chemical reactions.

In fluid dynamics one can model fluid flow through porous media, characterize flow with the incompressible Navier-Stokes equations. It is easy to represent chemical reactions by source or sink terms in mass and heat balances (T.J Bogar, 1983). These terms can be of arbitrary order. The physics interfaces in this module cover the following areas:

- Chemical Species Transport

  - Reaction engineering

  - Transport of diluted species through diffusion, convection, and migration in electric fields

  - Transport of concentrated species using one of the following diffusion models: mixture-averaged, Maxwell-Stefan, or Fick's law

  - Nernst-Planck transport equations

- Heat Transfer in fluids, solids and porous media
- Fluid Flow **-** Single-phase flow (incompressible Navier-Stokes equations)

  - Darcy's law **-** Brinkman equations

  - Free and porous media flow

Because of the nature of the simulation used in this work (reservoir flow), the evaluation of the single or multi-phase velocity is conducted using the Navier-Stokes equation adopting the PDE module in the CFD physics. A summary of the governing equations is discussed next.

4.6.8 Governing equations

The Navier - Stokes equations are the fundamental governing equations for fluid dynamics and can be regarded as the extension of Euler equations and includes the effects of viscosity on the flows. This non-linear set of PDEs are difficult to solve analytically due to the non-linear and coupled nature. Therefore, it has no general solution so far (Wang, 1991), but mathematicians and engineers made further approximations and simplifications to the equations. However, recently high-speed computers have been used to solve numerical approximations and this procedure is called Computational Fluid Dynamics (CFD) (Feynman, 2013). However, mathematicians and physicists continue to search for the existence of analytical solution to the equations but yet to obtain the general analytical solution for the equation so far. The Navier-Stokes Equation is just Newton's law ($f = ma$) where f stands for force, m refers to the mass and a stands for acceleration for a liquid component respond to unknown force and pressure and resistance influences. (Fefferman, 2006). The Navier-Stokes equations for an incompressible fluid are given as:

$$\rho\frac{\partial u_i}{\partial t}+\rho u_j\frac{\partial u_i}{\partial x_j}=-\frac{\partial p}{\partial x_i}+\mu\frac{\partial^2 u_i}{\partial {x_j}^2}+f_i. \tag{4.3}$$

$$\frac{\partial u_i}{\partial x_i}=0, \tag{4.4}$$

where u_i is the fluid velocity, p is the pressure, ρ is the density of the fluid, μ is the fluid viscosity and f_i are the body forces. However, from (4.1) above, it can be seen that the Navier-Stokes equations for incompressible flow consist of four (4) basic quantities namely; Local (unsteady) acceleration ($\rho\frac{\partial u_i}{\partial t}$), convective acceleration represented by $\rho u_j\frac{\partial u_i}{\partial x_j}$, pressure gradients ($\frac{\partial p}{\partial x_i}$) and viscous forces given by $\mu\frac{\partial^2 u_i}{\partial {x_j}^2}$. These quantities are very important in analysing the flow type (Feynman, 2013).

Nevertheless, the complexity and type of flows depends on these quantities. The table below shows some types of flows and the corresponding important quantities in the flows.

Table 4-2 Types of flows with their corresponding quantities (Source: Andre Baker, 2002)

Flow type/Quantity	$\boldsymbol{\rho\frac{\partial u_i}{\partial t}}$	$\boldsymbol{\rho u_j\frac{\partial u_i}{\partial x_j}}$	$\boldsymbol{\frac{\partial p}{\partial x_i}}$	$\boldsymbol{\mu\frac{\partial^2 u_i}{\partial {x_j}^2}}$
Pipe (steady flow) viscous low Re	N	N	S	S
Pipe (Unsteady) inviscid at large acceleration	S	N	S	N
Cylinder (Steady viscous)	N	S	S	S
Airfoil (Inviscid) steady	N	S	S	N
Airfoil (Unsteady) inviscid	S	S	S	N

Note: N stands for not significant and S stands for significant.

As indicated in the table above, for instance in the steady viscous laminar flow in a horizontal pipe, there is a balance between the pressure forces along the pipe and viscous forces making the flow to be steady called a Stokes flow (Fefferman, 2006). Hence, the local and the convective acceleration are not significant because the velocity profiles are identical at any section along the pipe.

Meanwhile, for an inviscid fluid in a pipe undergoing large acceleration, there is a balance between local (unsteady) acceleration effects and pressure differences (J.T. Salmon, 1983). Unlike the steady flow in a pipe, there is no viscous forces thus making the fluid to slip along the pipe wall. The convective acceleration is not significant, but the local acceleration is since the fluid velocity at any point is a function of time.

4.6.9 Model development

Considering the approach in this study, a laminar time dependent compressible Navier-Stokes equation was solved to obtain a steady state solution by marching time(Wang, 1991). As already stated, the Navier-Stokes equation consist of mass conservation law and momentum for compressible Newtonian fluids is:

$$\rho\,(\frac{\partial u}{\partial t} + u\ \cdot \nabla u) \ = \ -\nabla p + \nabla \cdot (\mu(\nabla u + (\Delta u)^{T} - \frac{2}{3}\mu(\nabla \cdot u)I) \ + F \qquad (4.5)$$

This is usually solved together with the continuity equation

$$\frac{\partial \rho}{\partial t} + \nabla \cdot (\rho u) = 0 \qquad (4.6)$$

But FEM tool uses a non-conservative form of the governing equation shown described below:

$$\frac{\partial \rho}{\partial t} + \rho \cdot \nabla \cdot (u) + (u \cdot \nabla)\rho \ = \ 0 \qquad (4.7)$$

For this study, an insert from the SEM image of the core sample depicted from figure 4-4, was converted into pore scale model at the magnification the SEM was carried out. Here, the interstitial velocity, u, of the gas through the porous media, as developed for the experimental core flooding, was in the range of $1x10^{-5}$m/s, therefore, the Reynolds number ($Re < 0.001$) is very small (Adler, 1992). Hence this shows that the inertial forces are small compared to the viscous forces and these can be neglected when solving the Navier-Stokes equation (4.3). Also, given that the there are no external forces, the force terms *F* in Eq. 4.3 can also be neglected since gravity is neglected. This Navier Stokes equation is therefore reduced to:

$$0 \ = \ -\nabla \cdot p \ + \ \nabla \cdot (\mu(\nabla u + (\nabla u)^{T} \qquad (4.8)$$

Using the above equation, the SEM image was converted and used as the pore scale model for the porous medium to simulate the gas velocity distribution in the pore spaces during the transport. Finite element mesh was used to subdivide the porous medium into elements for accurate definition of the finite element analysis which will enable the equation to the solved (Y.C.Fung, 1965). Fine meshing was chosen to refine the pathways of the porous medium so that the computed solution to the Navier Stokes equation approached the true solution with the adopted constraints and assumptions. This the model is shown in Figure 4-7.

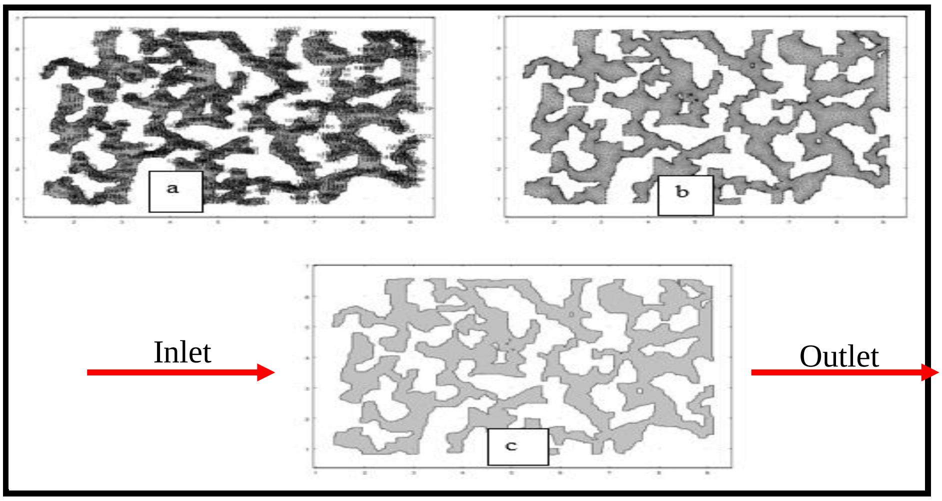

Figure 4-7: Converting a rock SEM image to Pore-scale finite element mesh (a) CAD image imported into COMSOL software; (b) Coercing to solid; (c) Pore scale model.

Creating a Pore-scale finite element mesh (Figure 4.5) from a Scanning electron beam (Figure4.10) is the first step in CFD modelling so that it should reproduce a computer-aided engineering software package. The Scanning electron microscope/Focused ion beam (SEM/FIB) models generated were imported into the COMSOL software. This is converted into solid by the CAD format to create a finite volume meshing (J.T. Salmon, 1983). To avoid errors, the final meshing and the geometrical shape of the model must be accurately defined. The defined flow domains and files are imported into the software for solving of flow equations. The outlet pressure, fluid properties and flow domains are the main variables and parameters inputted into the software to solve flow equations (R.D.Bird, 2002). By applying the fundamentals of fluid dynamics and defining the solver controls, boundary conditions and convergence monitors, the COMSOL software solves the numerical variables.

4.6.10 COMSOL model assumptions

The following assumption were taken to develop the model for this study:

i) The model presents a single-phase flow.
ii) The reservoir temperature is constant.
iii) The formation has the same permeability.
iv) The gas follows ideal gas laws.
v) The study does not consider the effect of desorption.
vi) Gas flow effect of gravity and heterogeneity are neglected.

vii) The model has a uniform and rectangular formation.

4.7 Procedure for core flooding

The core flooding experimental aspect of this thesis was carried out using the standard branded core flooding system provided by Core Lab Oklahoma as already discussed in chapter 3. A methodical step by step procedure to perform a concise displacement process is as follows;

i) Wall mount power ON
ii) Compressed air taps fully opened
iii) Turn ON the system console
iv) Power ON the PC
v) 1A set the air pressure on the system using the air regulator to 90psi
vi) Launch the smart flood software in the PC and power ON the digital balance to clear the error on the smart flood software.
vii) ON the smart flood software, main tool bar and click online to interface the software with the console.
viii) Apply the back pressure to the required value.
ix) Open pump to BPR (6A) making sure (6B) drains overburden is closed/shut.
x) Using (6G) Air to overburden regulator apply a pressure of about 20psi and monitoring BPR DOME pressure gauge.
xi) At the desired applied back pressure, close (6A) pump to BPR.
    i) Set the Isco pressure to desired bottle pressure.
    ii) Open/Close valves shown.
    iii) Slowly open purge pump valve until no water bleeds into beaker
    iv) Close Gas bottle valve and 3 – way valve connected to bottle.
    v) Set Isco to desired gas pressure.
    vi) Open accumulator valve after reaching pore pressure with A/B pump
    vii) Begin gas flow

4.8 Precautions for gas flooding equipment operations

i) The working pressure (system pressure or maximum allowed pressure shot NOT exceed 5,000psg
ii) The pump pressure should NOT exceed 3,750psg

iii) Ensuring tight connections around the joints or fittings to avoid leakages. Leaks can be detected with gas detector this is because Methane is highly flammable.

iv) The Back pressure MUST be applied before pressurizing the system or equipment to avid failure of the Wet test meter (Volumetric Flow Meter) which has a working pressure of 50mbar (milli bar) = 0.75psi Therefore, 1bar = 14.7psi X = 0.72psi. Anything above 0.72psi will destroy or rapture the wet test meter. More so, the back pressure should be at least 300psi higher than the accumulator pressure.

v) The overburden pressure should be at least 500psi higher than the pore pressure to avoid rapturing of the sleeves enclosing the core sample.

vi) Making sure the fan number 4 is on when conducting the experiment to vent the effluent gas.

vii) To initial flow the back pressure MUST be reduced gradually or gently.

4.9 Procedure for core cleaning

During the process, the following procedure is followed; the toluene was heated to almost 110 ^{0}C at this temperature the toluene will evaporate upwards into the condenser. Condensation takes place in the condenser as the vapor settles, with the aid of cold water circulating through the system and then drips into the thimble where the core sample resides, this also serves as the receiver of the fluids extracted from the core sample. Consequently, the core sample becomes saturated the vapor from the toluene and eventually the re-condensed toluene fills up the thimble until it reaches the fluid/liquid within the Soxhlet tube which drains itself by siphon tubes as arranged and flow to the Pyrex flask housing the boiling toluene. The operation allows the toluene to clean the impurities in the core sample in a reflux manner. This procedure can take place continually for Forty- Eight hours(48HRS) for a proper cleaning to take place. A modest temperature was allowed so that the toluene will not evaporates. The equipment set up is shown in the figure 4.18**.**

4.10 Modelling procedure

Data used to estimate the gas reserve are seismic, well log, core data, bottom hole pressure and temperature data, fluid sample information, well test result. The data is used to develop various sub-surface maps (structural, isopach), cross sections. These graphics helps to establish the reservoir areal extent and contribute to identifying reservoir discontinuities. Consequently, to meet the objectives for this research, a certain methodology was followed and summarised in the following steps.

i) Data Collection and analysis
ii) Building of a 3D model using Petrel
iii) Running uncertainty and sensitivity analysis

4.11 Data collection

All the data for Ogba Egase Ishelle Field used in this work has been released for this research officially by the regulator, DPR (Department Petroleum Resources) a parastatals/Department of the Federal Ministry of Petroleum Resources.

4.12 Building A 3D model using petrel

In this project, a 3D geological (static) model of Ogba Egase Ishelle Field will be built. All steps will be shown in detail with screen shots of the necessary figures. Petrel software was developed in Norway by a company called Techno guide. Techno guide was formed in 1996 by former employees of Geomatics, some of whom were key programmers involved in the early development of RMS. Petrel was developed specifically for PCs and the Windows OS, it was commercially available in 1998. Petrel was developed to have a familiar Microsoft like interface, with a pre-arranged workflow that enabled less experienced user to follow, Techno guide made 3D geologic modelling more accessible to all subsurface technical staff, even those without specialist training. In 2002, Schlumberger acquired Techno guide and the Petrel software tools, and they currently support and market Petrel. Newer versions of Petrel include additional functionality such as geological modelling, seismic interpretation, uncertainty analysis, well planning, and links to reservoir simulators.The project is divided in steps as indicated in the Petrel Workflow Tools shown in Figure 4.6. After some modifications and enhancements to the Petrel Workflow, the steps will be presented as follows:

i) Introduction
ii) Data Import
iii) Input Data Editing
iv) Well Correlation
v) Fault Modeling
vi) Pillar Gridding

vii) Vertical Layering

viii) Geometrical Property Modeling

ix) Upscaling in the Vertical Direction-Well Logs up scaling

x) Facies Modeling

xi) Petro physical Modeling

xii) Defining Fluid Contacts

xiii) Volume Calculation

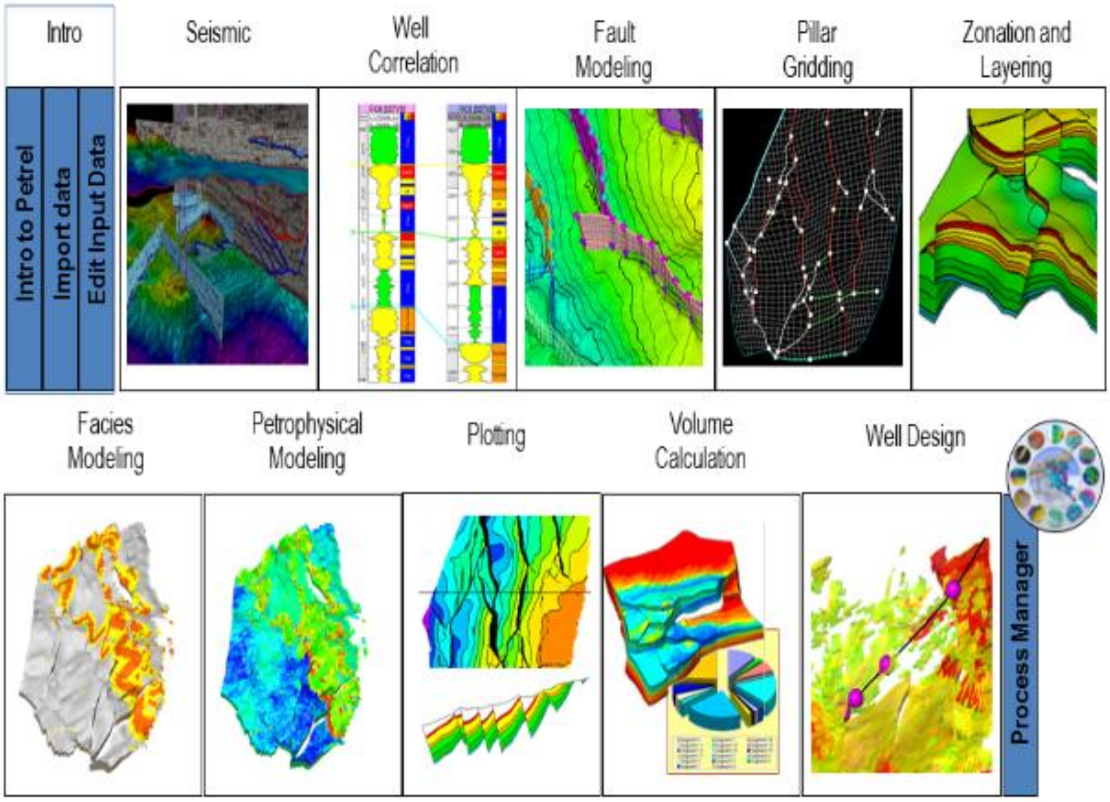

Figure 4-8: Petrel Workflow Tools for Building 3D static model

4.12.1Petrel User Interface and tool bars

When starting Petrel, it displays all Panes along with an empty 3D window as shown in Figure 6.2 as appended. All windows are either docked or float. Double-clicking the window toggles its docking state. If one of the Panes is not shown, it can be displayed from the View menu command using Panes. On the other hand, if a 2D/3D window is not shown, it can be displayed using the Windows Panes as shown in Figure 6.3 as appended

i) Client Area

The Client Area is the parent window of Petrel (grey area). It forms the area where a variety of windows, which are listed under the **Windows** menu command, can be hosted. Examples are 3D and 2D windows, well section windows (for well correlation), interpretation windows (for seismic interpretation), map/intersection windows (for plotting), etc.

ii) Input Pane

The input data is imported from files - one file for each data object. All input data are organized in the Input Pane as shown in Fig.6.2. Import Data describes the data import procedure and the various data formats supported. Imported data such as wells, well tops, interpreted lines, polygons, gridded surfaces and SEG-Y data is stored here.

iii) Models Pane

Internally created data connected with a 3D model (such as faults, trends and 3D grids) is stored here. Imported grids (3D models or parts of models) and properties will also be put here.

iv) Processes Pane

This pane contains a list of all available processes in Petrel. They are sorted in the order they should be used, and the first processes will have to be executed before you get access to other processes down the list. For example, you must create a 3D grid before you can insert horizons into it, and you must create zones before you can insert layers into them. Activating a process will cause the tools associated with that process to appear on the Function bar. Double clicking a process will open the process dialog.

v) Cases Pane

Gives access to all cases defined for simulation and volume calculation.

vi) Workflows Pane

Provides access to the workflow manager and any workflows which have been created in the current project.

vii) Windows Pane

Provides access to the windows and plots that have been created in the

4.12.2 Import data

New project was created before any data was imported as follows;

i) Petrel was opened, and a new project was selected from the file menu.

ii) A new Display Window was appeared with a black bag round color.

iii) The option save Project As was selected from the file menu and the project was named and the location was specified.

The following table displays the different types of input data required for Petrel along with their formats and types.

Table 4-3: Different types of input data imported to petrel along with their formats and types

Data	Format	Type
1. Well Data		
a. Well Headers	Well heads (*. *)	**Well**
b. Well Deviations	Well Path/deviation (ASCII) (*. *)	**Well**
c. Well Logs	**Well Logs (LAS 3.0) (*.las)**	**Well**
2. Well Tops	**Petrel Well Tops (ASCII) (*. *)**	**Well Tops**
3. 3D Seismic Data	**General lines/points (ASCII) (*. *)**	**Lines**
4. Fault Data		
a. Fault Polygons	ZMapp+ lines (ASCII) (*. *)	**Lines**
b. Fault Sticks	**ZMapp+ lines (ASCII) (*. *)**	**Lines**
5. Isochore Data	**ZMapp+ grid (ASCII) (*. *)**	**Surface**

4.12.3 Well attribute description

i) *** Well Symbol -** The type of well. This attribute is a label for the well symbol (discrete attribute).

ii) *** Surface X -** The X location (in project units) of the well at the well head (continuous).

iii) *** Surface Y -** The Y location (in project units) of the well at the well head (continuous attribute).

iv) *** Kelly Bushing (KB) -** The Z value (in project units) of the Kelly Bushing (continuous attribute).

v) *** TD (TVD) -** The vertical depth value (in project units) of the last point in the well (continuous attribute).

vi) *** TD (MD) -** The measured depth value (in project units) of the last point in the well (continuous attribute).

vii) **UWI -** The Unique well identifier (string attribute).

viii) **Max Inc -** The value of the highest inclination from vertical (in project units) in the well path (continuous).

ix) **Cost -** The cost of the well (string).

x) **Spud Date -** The date the well was spudded (date attribute).

xi) **Operator -** The name of the organization operating the well.

The attributes proceeded by an asterisk (*) are required fields, the other attributes are non-mandatory and can be ignored if desired.

4.12.4 Correlation

To establish the lateral extent of the reservoirs across the field, reservoir sands were correlated across the wells using a combination of Gamma ray (GR) log, Spontaneous potential (SP) log, Resistivity (ILD) log, Neutron (NPHI) and Density logs (RHOB). Reservoir X-8.2 was divided into Reservoir X-8.2U (upper) and X-8.2L (lower) because of a thick laterally extensive shale intercalation, which was found to have bridged communication between the two (2) halves of the reservoir. In recently drilled Wells such as Well 8B, the fluid saturation in the lower half of the reservoir was seen not to have moved significantly, even after years of production from nearby wells. Meanwhile, all the Wells producing from the reservoir were perforated in the upper half of the reservoir. These correlated sand tops were used as input in the synthetic seismogram process.

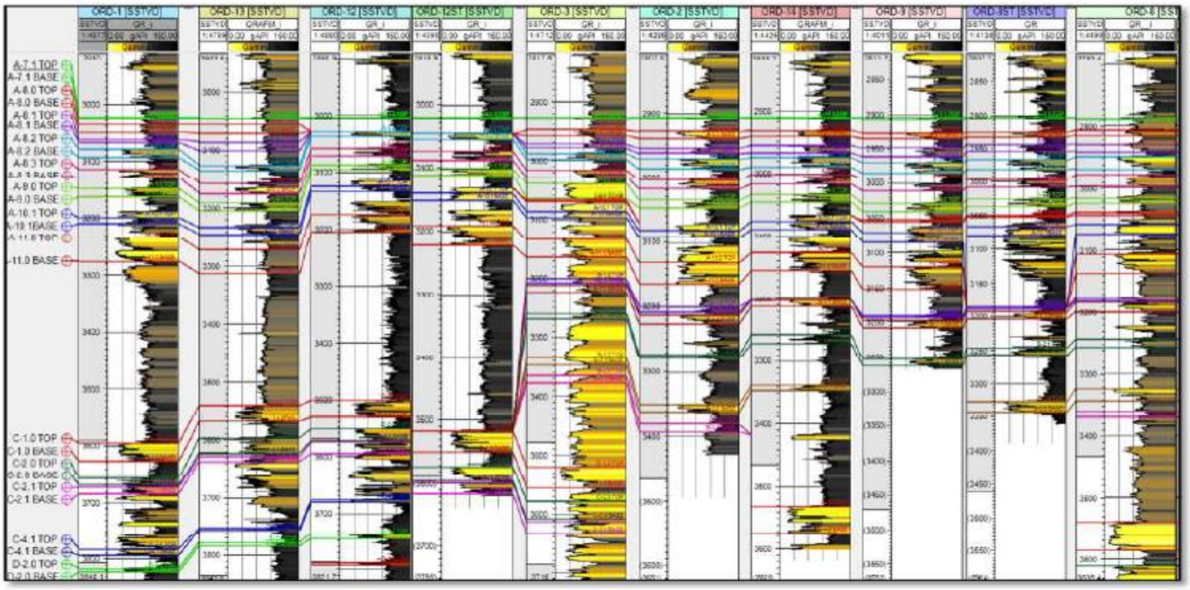

Figure 4-9: Well Section correlation panels

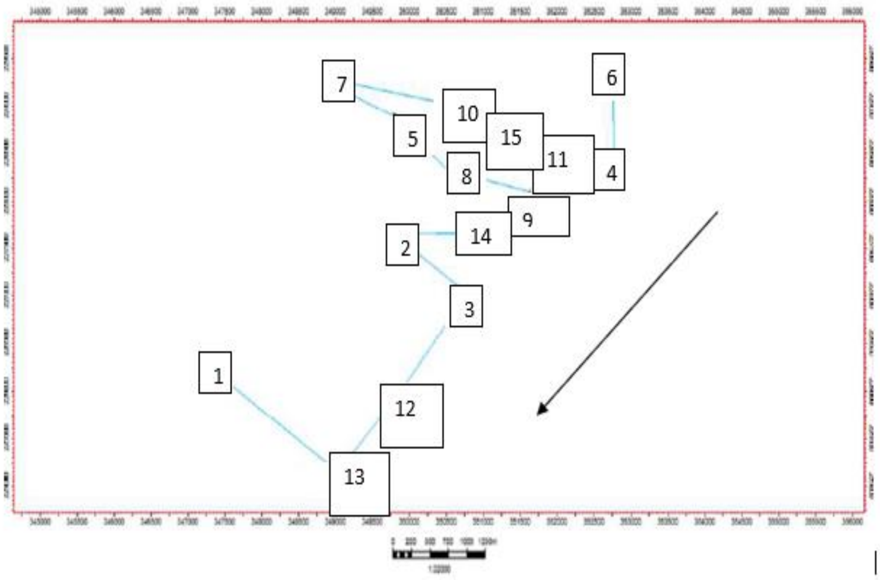

Figure 4-10: Fence Diagram showing all the Wells of Ogba Egase Ishelle in accordance with the dipping direction of field

The seismic data covered the Ogba Egase Ishelle field and its interpretation captured the hydrocarbon bearing intervals in the field. Check shot was provided for Ogba Egase Ishelle Wells 3 and 5 and both were confirmed to be in the same velocity domain. As a result, Ogba Egase Ishelle Well 3 Check shot as indicated in Figure 4-9 which has more depth coverage, was adopted and shared to other Wells for the Well to seismic tie.

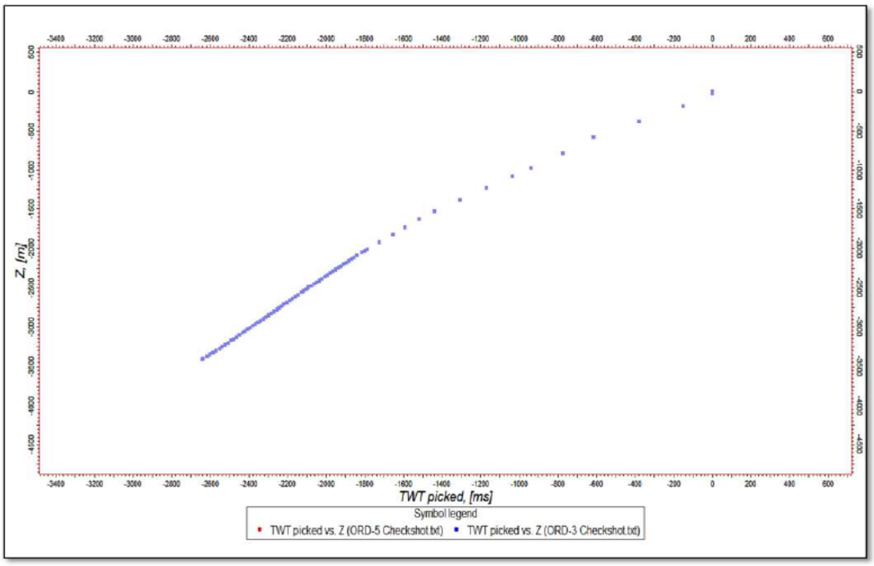

Figure 4-11: Showing T-Z Cross-Plot for Well 3 Check shot

Synthetic seismogram was generated for Wells X- 2, X- 3 and X- 8 and was subsequently used to tie the Well picks to the seismic. These Wells have the complete log suite (Density and Sonic logs) required for the synthetic seismogram generation. The generated synthetic seismograms were matched with the well seismic for the three (3) Wells and good ties were established with the maximum time shift of about 29.08 milliseconds

4.12.5 Fault Interpretation

Faults were interpreted across Ogba Egase Ishelle field using the 3D seismic vintage provided for the study. Variance Edge seismic attribute was generated and was subsequently used to unravel the structural trend of the reservoirs and for the fault picking as shown in Figure 6.8. The interpreted faults are normal and listric in nature, with a major boundary fault trending NW-SE of the field**.** To the East of the field, a prospect (Eastern Prospect) is created by a structural closure between the main growth fault and a normal fault branching out of the major fault (further studies should be carried out here to determine the presence and integrity of the hydrocarbon seal and trap mechanism). Generally, the field is structurally controlled by the roll-over anticline formed by the NW-SE trending major growth fault. The field is also characterised by minor synthetic and antithetic faults and the deeper reservoirs (C and D-series) were seen to be less faulted than the shallower reservoirs. These series were also observed to have recorded a more pronounced saddle towards the boundary fault.

4.12.6 Horizon Interpretation

The horizon interpretation of Ogba Egase Ishelle field was carried out to define the geometric framework of the field, the individual reservoirs and generate the top structural maps (Time and Depth) of the reservoirs in Ogba Egase Ishelle field. This was achieved using the given Well information and the 3D Seismic Data. Fifteen (15) reservoir sands *(X-7.1, X-8.0, X-8.3, X-9.0, X-9.1, X-10.0a, X-11.0, Y-1.0, Y-2.1, Y-3.0, Y-4.0, Y-5.0, Z-1.0, Z-4.0 and Q-2.0*) were interpreted out of a total of twenty-four reservoir sands. This is because the remaining reservoirs were not resolvable due to the short time window between the already interpreted reservoir sands or because of the quality of the Seismic vintage provided within those intervals. To account for the non-interpreted reservoir horizons, a depth/time-shift of the interpreted tops to the other conformable layers was carried out while also strongly considering their proximity. After the horizon interpretation, time maps were generated for the reservoirs using the interpreted horizons as shown in Figure 4-11.

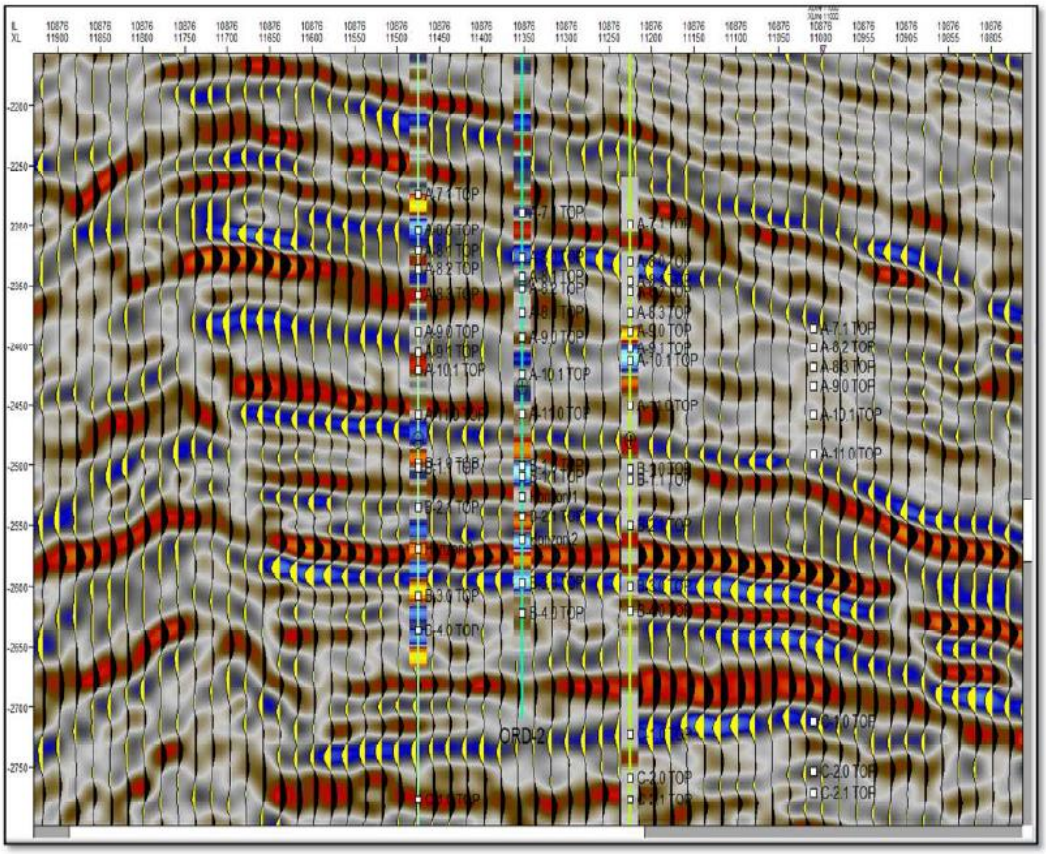

Figure 4-12: Showing Matched of Synthetic seismogram with Seismic along Well path

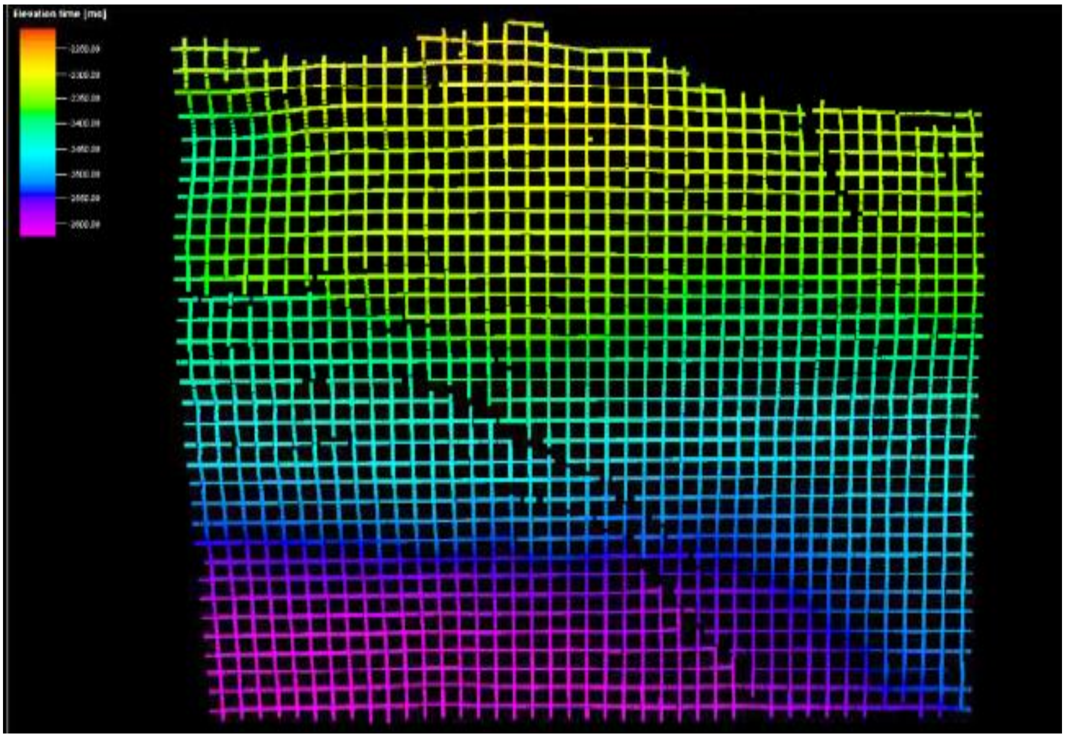

Figure 4-13: Showing the Interpreted horizons on 3D (reservoir A-8.3)

4.12.7 Time-depth conversion

The time maps generated from the interpreted horizons were finally depth converted using Linvel Velocity modelling function as it had the lowest residual among Adlinvel and 2nd Order Polynomial velocity modelling functions, which were also adopted for comparison.

$$V = Vo + K * Z \tag{4.1}$$

Where;

Vo = Velocity at datum, Z = Distance of the point from datum, K = factor showing velocity change in the vertical direction

4.12.8 Structural uncertainty

The Standard Deviation of the residuals was calculated to account for the Structural Uncertainty. Thus, the High, Base and Low Cases were generated for all the reservoir depth maps. The base case was however adopted for the modelling.

4.12.9 Remark on structural interpretation

The structural seismic interpretation carried out in Ogba Egase Ishelle field has revealed the structural trend of field, beginning from the NW-SE trending regional fault, to several synthetic and antithetic normal faults, which resulted in a collapsed crest structure in the shallower sands. The deeper sands were observed to be less faulted with simple roll over structure. A good structural uncertainty analysis resulted in the identification of the velocity models that could generate the low, mid (base) and high cases for the depth maps. With this interpretation, the structural challenges of Ogba Egase Ishelle field can easily be solved.

4.12.10 Static reservoir modelling

The 3D Static models of the reservoirs in Ogba Egase Ishelle field were built using Schlumberger Petrel software to distribute reservoir properties within the 3D structural grid. This involved using the estimated Petro physical data as input to generate the geo-cellular models. Sequential Gaussian Simulation is the modelling algorithm used for the distribution of continuous properties, while Sequential Indicator Simulation was used to distribute discreet properties across the entire 3D grid while honouring data input points. This algorithm is dependent on the up scaled well log data, defined Variogram, and frequency distribution of up scaled data points. Porosity and Net-to- Gross were up scaled using arithmetic average while permeability was up scaled using geometric average. The model architecture was constrained by structural map interpreted from the 3D seismic survey provided, after it had been tied to the wells. The internal stratigraphy was also incorporated into the geologic model and Petro physical properties were assigned to each layer. The Petro physical Properties were geo-statistically distributed across the grid. In line with geology of Niger Delta and in agreement with the seismic interpretation, the model revealed some growth faults together with simple antithetic and synthetic faults in the reservoirs. These constitute the main hydrocarbon trapping mechanism. Reservoir properties show a high variability within the lithological zones due to pronounced heterogeneity.

4.12.11 Structural modelling

Structural modelling of the reservoir was carried out with the depth converted faults and surfaces from seismic interpretation as input. This process was divided into five sub-processes, namely; fault modelling, pillar gridding, horizons making, zone making and layering. The Fault modelling formed the basis for generating the 3D grid. The faults were used to define breaks in the grids. This was followed by pillar gridding which is the process in which 3D grids are generated. The Vertical layering of the 3D grid was done with a process called make horizon.

4.12.12 Fault modelling and pillar gridding

The faults were modelled, and pillar gridded to generate 3D grids as shown in Figures 4.12 and 4.13. The faults were modelled, and quality checked with the depth converted seismic interpreted fault sticks for accuracy. A grid dimension of 50m by 50m was used in the pillar gridding process and the modelled Structure was quality checked with general geometry interpreted on Seismic by taking cross sections.

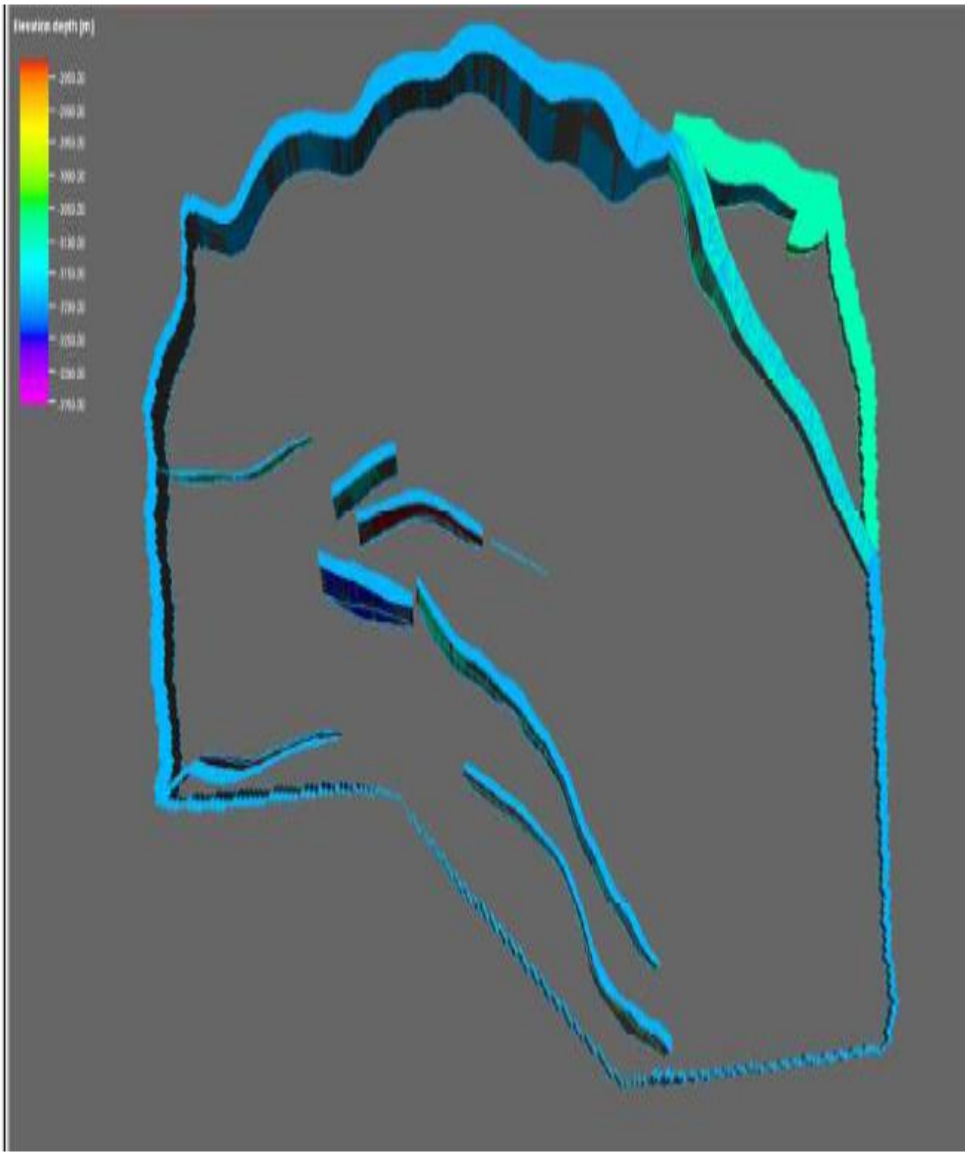

Figure 4-14: Fault Modelling

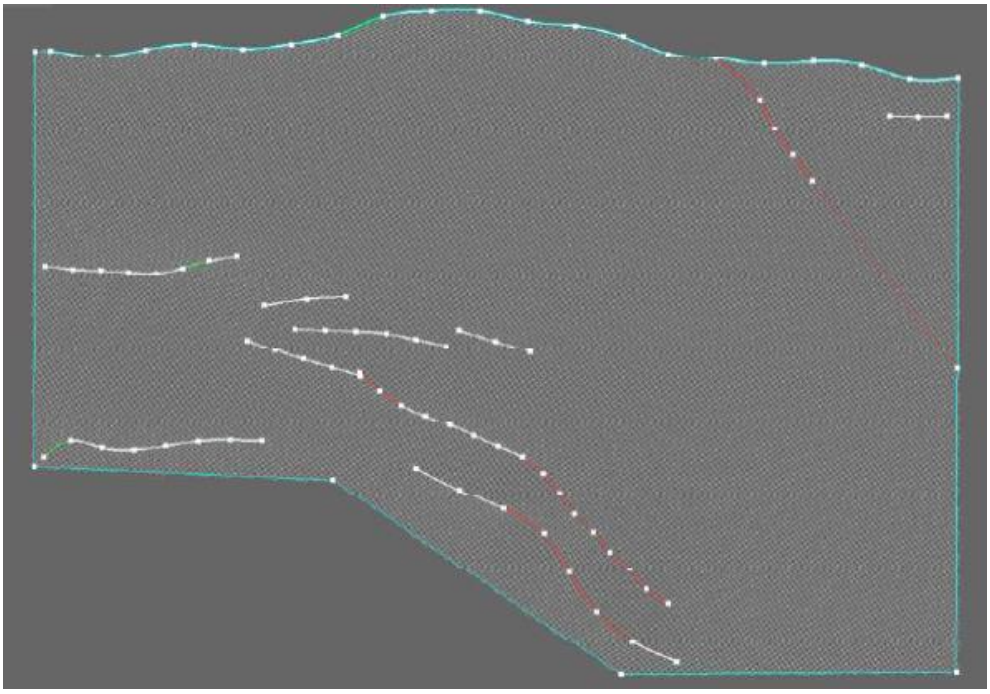

Figure 4-15: 3D Grids from Pillar Gridding

4.12.13 Stratigraphic modelling

The Niger Delta lithostratigraphic units penetrated by the Ogba Egase Ishelle wells are the Benin and Agbada Formations. The Agbada formation, which is the main hydrocarbon bearing lithostratigraphic unit in the Niger Delta, is characterized by multiple condensed paralic lithologic facie sequence of shale, siltstones and sandstones. Competent shale breaks of high sealing capabilities overly the reservoir sands. The interval is typically made up of alternating sand and shale sequence. The basal Akata marine shales provide hydrocarbon source for overlaying Agbada paralic sandstone reservoirs. The section is overlain by continental to shallow marine sandstones of the Benin Formation. The stratigraphy of the reservoir was established using Gamma Ray log and correlated it across the wells.

4.12.14 Reservoir zonation and layering

Stratigraphic Modified Lorenz (SML) Plot was used in delineating the zones of Ogba Egase Ishelle reservoirs. The zonation process considered the depositional facies and their quality in each of the reservoir. Poor flow units show low gradient while good flow units show high gradient. The resulting zones were correlated across the wells and used as input in zone making. The zonation process considered the depositional facies in each of the reservoir. The areas with thick field wide marine shale, that can create barrier to flow, were captured as a single zone with one layer especially where it was generically laterally extensive, to help in the streaking off process of shale where need be. The SML plot and the corresponding reservoir zones for reservoir Y-1.0

The zones were layered according to their relative thicknesses; however, sensitivity was running to establish the optimum number of layers within the zones of the reservoirs this was carefully carried out with due consideration of the optimum Reservoir engineering grid simulation run time and was also quality checked using the histogram plot of Petro physical properties.

4.12.15 Facies modelling

Facie Models for Ogba Egase Ishelle field were created from the input Facies interpreted based on Environment of deposition (EOD). These Facies include; Lower Shore face, Upper Shore face, Transgressive sand, Foreshore and Marine Shale. The identified and interpreted Facies were quality checked using Niger Delta conceptual analogue model. Facies at well points were scaled-up and distributed using Sequential Indicator Simulation (SIS). Calculated vertical Variogram and thickness proportions were carried out in Data Analysis.

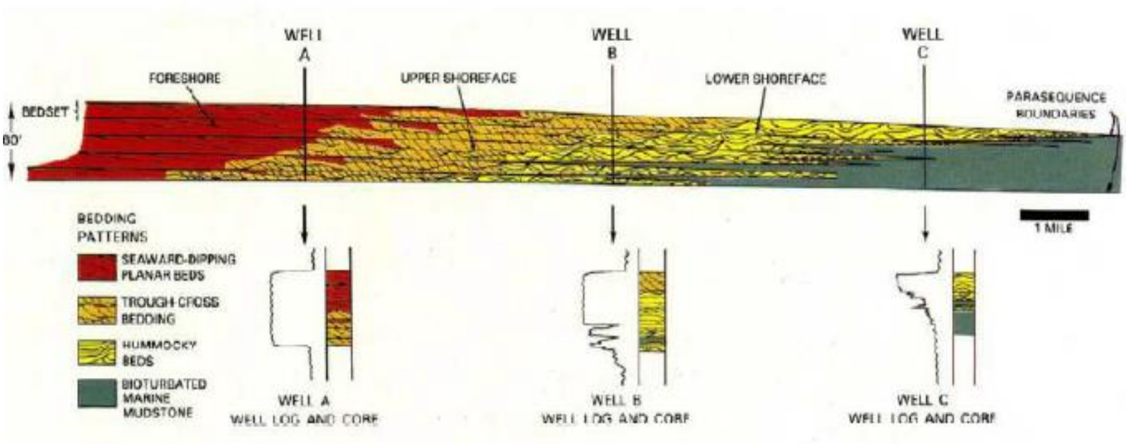

Figure 4-16: Lateral Facies relationship and Well Log response for Shallow Marine Environment

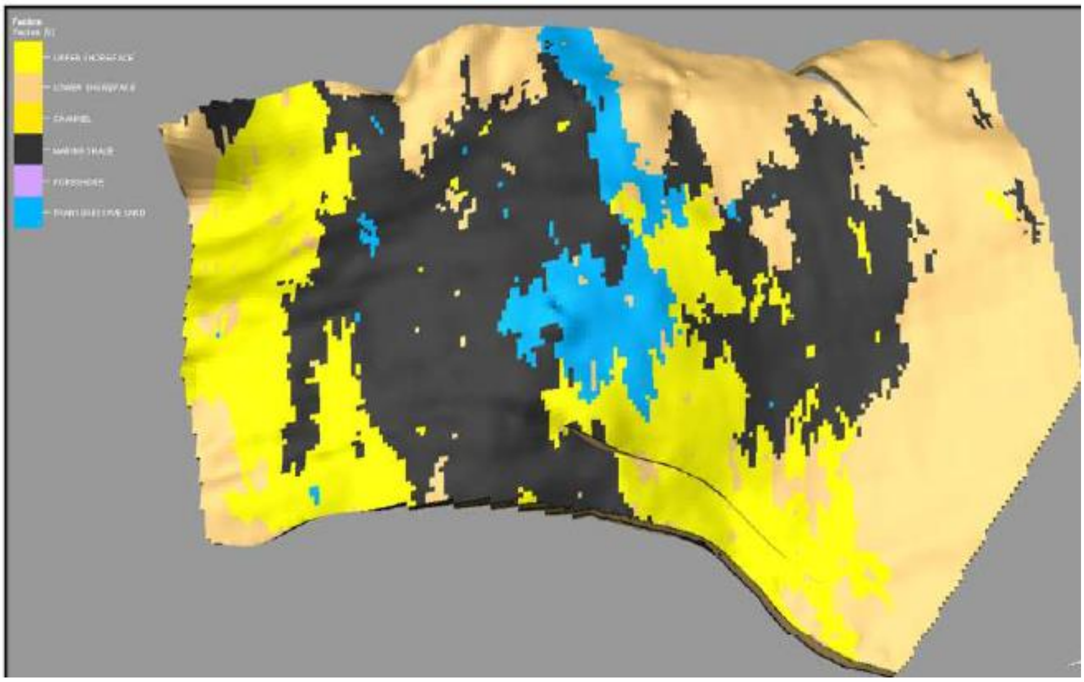

Figure 4-17: showing the Facie model for reservoir Y-1.0

4.12.16 Property modelling

The workflow used for property modelling of the Ogba Egase Ishelle reservoirs:

i) Scale up of well logs into grids;
ii) Data Analysis:
iii) Vertical Proportion curve analysis
iv) Data Transformation
v) Variogram Analysis
vi) Property Distribution

The facies model was used to condition the facie-dependent porosity. This reflects in their consistency in trending with the facies distribution in the models for individual reservoirs. The porosity model was then used in co-kriging scaled-up permeability and Net–to-Gross data to generate permeability and NTG models. Water saturation was modelled using Brooks-Corey saturation height function. Sequential Gaussian simulation (SGS) was used to model the continuous properties while Sequential Indicator Simulation was used to model discreet properties. Generally, the Petro physical properties were highly consistent with facies type in all models. 35 realizations of all the properties were generated to get all the possible scenarios and probabilities attainable in the reservoirs.

4.12.16.1 Porosity modelling

Porosity log (Φ) data was used for porosity modelling. The log porosity data was scaled-up to the 3D grid using arithmetic averaging method and quality checked in terms of statistical parameters. The scaled-up porosity data was conditioned with Facies and modelled with Sequential Gaussian Simulation algorithm (SGS). However, detailed data analysis of porosity at the zone level was done to capture data distribution (histogram) and spatial variations

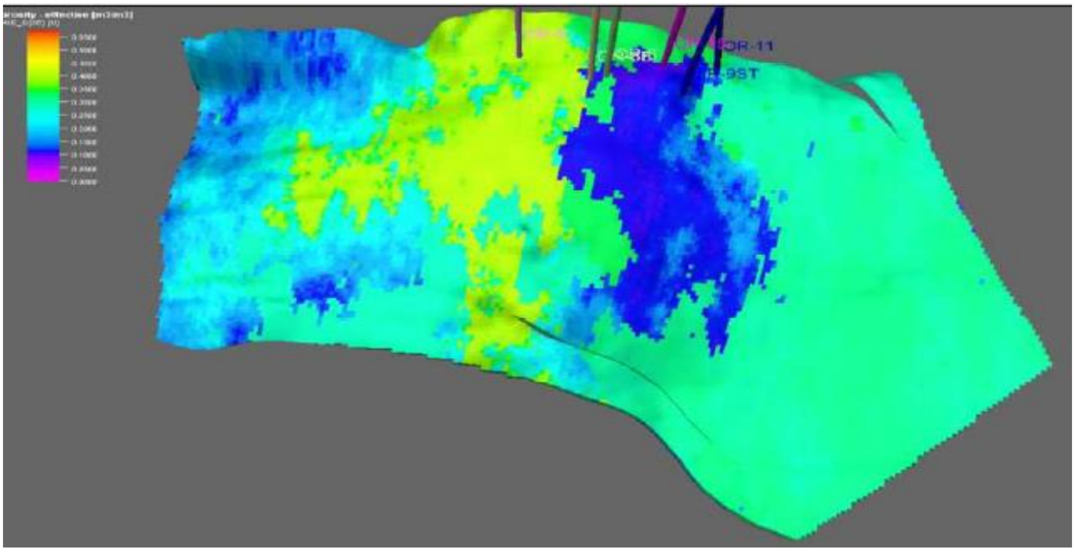

Figure 4-18: The log porosity data was scaled-up to the 3D grid

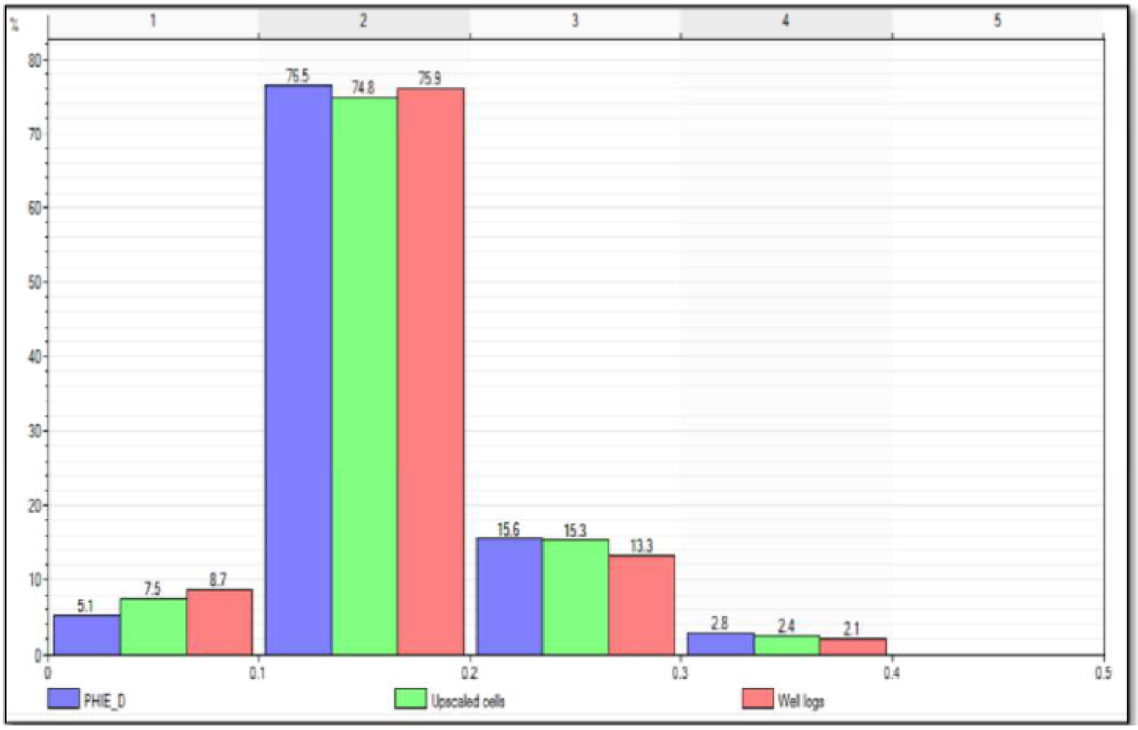

Figure 4-19: Data analysis of porosity at the zone level distribution (histogram) and spatial variations.

4.12.16.2 Net - to - gross modelling

Net-to-Gross log data was used for Net-to-Gross modelling. The Net-to-Gross log data was scaled-up to the 3D grid using arithmetic averaging method and quality checked in terms of statistical parameters. The scaled-up Net-to-Gross data was co-kriged with the modelled porosity and distributed using Sequential Gaussian Simulation algorithm (SGS). However, detailed data analysis of Net-to-Gross at the zone level was done to capture data distribution (histogram) and spatial variations.

4.12.16.3 Permeability modelling

Permeability log data was used for permeability modelling. The permeability log data was scaled up to the 3D grid using geometric averaging and quality checked in terms of statistical parameters. The scaled-up permeability data was co-kriged with the porosity model and distributed using Sequential Gaussian Simulation algorithm (SGS). Detailed data analysis of permeability at the zone level was done to capture data distribution (histogram) and spatial variations.

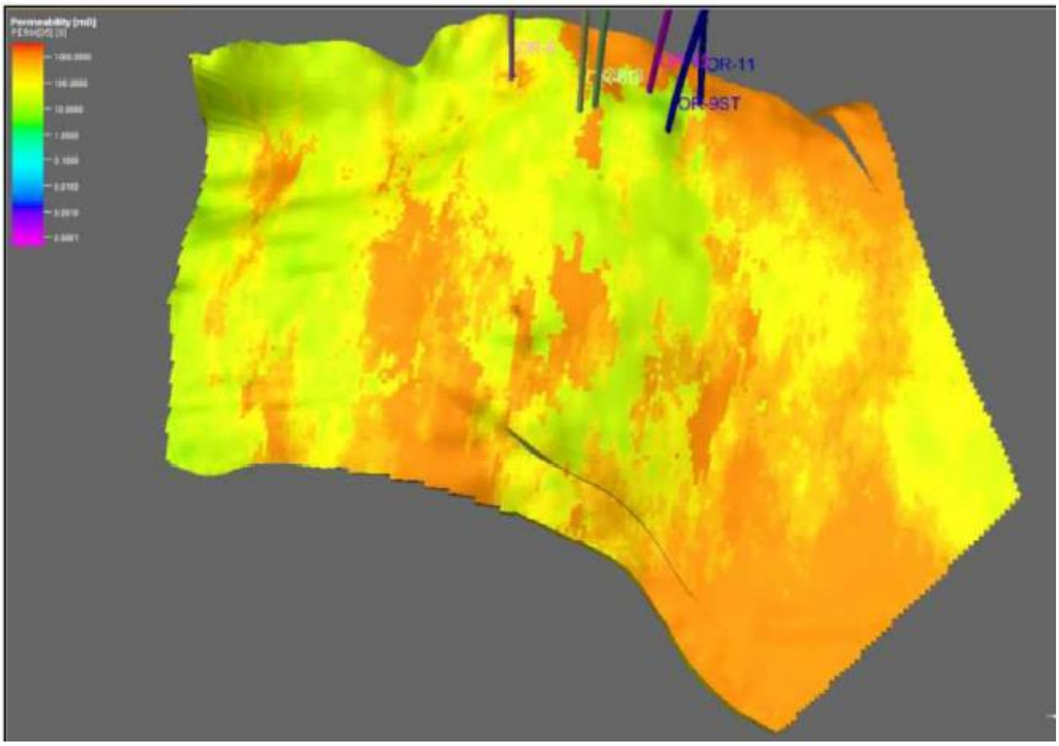

Figure 4-20: The permeability log data was scaled up to the 3D grid.

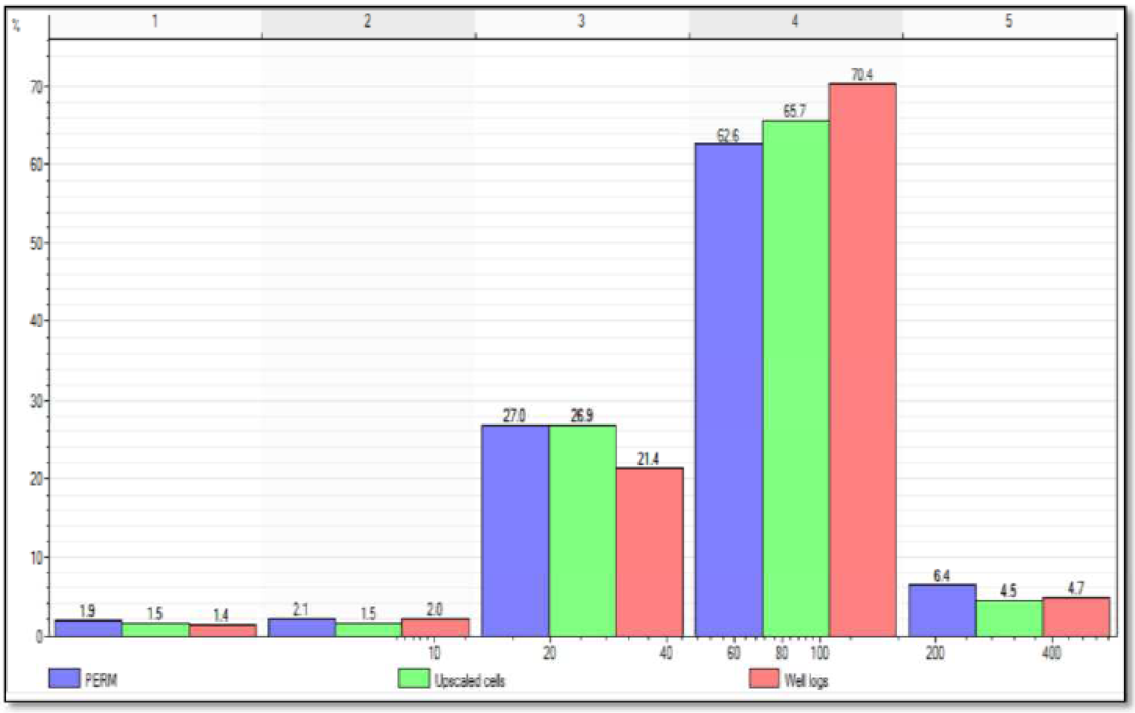

Figure 4-21: Permeability at the zone level data distribution (histogram) and spatial variations.

4.12.16.4 Water saturation modelling

The Brookes-Corey water saturation height function was used for water saturation modelling. Modelled parameters like porosity, permeability and height above free water level were used as inputs to generate the 3D model of the water saturation from the Brookes-Corey water saturation height function. The statistical parameters of the model were quality checked.

4.13 Static volumes estimate

Stochastic volumetric estimates, based on the estimated, distributed and realized properties were made. Initial volumes of oil and gas were estimated based on the Equations 4.1 to 4.6. Stochastic estimations within the range of petrol-physical variations of the thirty-five (35) realizations showed that Ogba Egase Ishelle Field has a total volume of about 75.9023MMSTB and 2068.7059BSF (P50), of oil and gas respectively. The optimal realization case was selected for each reservoir as the closest value to P50 using the Histogram skewness.

$$V_{NNET} = Bulk\ Volume * \frac{N}{G} \tag{4.1}$$

$$V_{PORE} = \text{Net Volume} * \text{Porosity Ø} \tag{4.2}$$

$$HCPV_o = \text{Pore Volume} * \text{So} \tag{4.3}$$

$$HCPV_S = \text{Pore Volume} * \text{Sg} \tag{4.4}$$

$$GIIP = \frac{HCPV_g}{B_g} + \left(\frac{HCPV_o}{B_o}\right) * R_s \tag{4.5}$$

$$STOIIP = \frac{HCPV_O}{B_O}. + \left(\frac{HCPV_g}{B_g}\right) * R_v \tag{4.6}$$

Where:

So = Oil Saturation, Sg = Gas Saturation, Bo = Oil Formation Volume Factor, Bg = Gas Formation Volume Factor, Rs = Solution Gas-oil Ratio, RV = Vaporized Oil-Gas Ratio

The volumetric estimates were generated using the populated Petro physical properties (Net-to-gross, Water saturation and porosity), the established hydrocarbon contacts and the PVT parameters (Formation Volume Factor) are shown in Table 6.8.

4.14 Production Performance Analysis procedure

The Production performance/declining curve analysis as detailed in sub-section 2.4.5 of the wells in OGBA Field was carried out to ascertain the causes of non-conformance issues like high GOR, high BSW, decline in production and reservoir pressure. Perforation panel plots were constructed for the Levels with respect to the initial fluid contacts to diagnose for high water cut and GOR. Well models were built with PROSPER® system analysis software and good matches were obtained with the available test data. Sensitivity runs were made on some parameters; water cut and reservoir pressure, to investigate their impact on future performance scenarios and productivity of the currently producing wells.

4.14.1 Data availability

The available data used for this review are from reports provided by The Ministry of Petroleum Resources, these includes:

- ✓ Production History.
- ✓ Flow Test data
- ✓ Well Completion Schematics.
- ✓ PVT Reports.
- ✓ Static BHP pressure data for some Reservoirs

4.15 Methodology for Decline curve analysis

Hypothetically, the field production data acquired for the investigation corresponds to the pressure transient analysis. To recover the production data analysis, we analyse, examine, and deduce the production data by means of the following procedure,

1. Change stream occurrence. For a high Gas–Liquid Ratio (GLR), modify the condensate oil into condensate gas, and conduct dispensation as per pseudo-single phase; if the flowing time is less than A DAY, change the flow rate into daily rate.
2. Convert flowing pressure. If there are no bottom hole flowing pressure (BHFP) data, use the related wellbore conduit flow software to alter the tubing compression or casing pressure data into BHFP data under the restraint of the measured pressure gradient.
3. Evaluate information. Appraise the data superiority/correlativity of the production curve.
4. Eliminate/decrease information. Confiscate the uncharacteristic statistics arguments in the log–log plot used by analyses.
5. Categories distinctive flow regime. Matching the pressure derivative curve in the well test analysis (WTA), use the pressure curve and rate integral derivative curve to categories the flow features in the historical of transient flow, for e.g. the normalized pressure integral (NPI) method and Blasingame method.
6. Curve Type Match. Tie the restrained data with the corresponding academic decline curves in the basin model to get relevant parameters.
7. History Match. Conduct ultimate "history matching" of prototypical and exclusive information of sole well routine (pwf and q).
8. In the event the analytic solution cannot be matched well, convey mathematical studies based on it to spring relevant parameters.
9. Estimate production performance. Founded on building the dynamic model from the above analysis, we can conduct performance prediction of constant pressure or constant rate based on the matching results, to direct the production. As mentioned by Mattar and Anderson (2003), the production decline curve analysis technique is developed at a very high swiftness, where a variability of approaches can be pragmatic. More so, there is no technique that can always be accomplished of awarding the most dependable explanation. In practice, various methods can be collective realistically, compelling

each other and complementing each other, to reduce the uncertainty in reserve evaluation.

4.16 Material Balance Introduction

MBAL® software was used for the material balance analysis. MBAL® software allows analysis, evaluation and prediction of the response of hydrocarbon reservoir systems using fundamental material balance principles. It also uses analytical method, a non-linear regression approach based on reservoir pressure decline against cumulative production (void age).

4.16.1 Data requirements

The following data were used for Material Balance Analysis using MBAL® software:

• PVT Data.

• Initial Reservoir Pressure.

• Reservoir Average Pressure History.

• Production History.

• All available Reservoir Parameters.

4.16.2 Data analysis and validation

Due to errors (sampling, systematic and random errors amongst others) field data are subjected to, it has become imperative to perform a QA/QC on all the data available for analysis. The Reservoir PVT parameters were calculated using empirical correlations for black oil. Production history data were found to be adequate and consistent. The reservoirs considered for Material Balance Analysis with their respective years of production are shown in the results section at chapter 6 (six).

4.16.3 Methodology

The reservoir fluid system was defined, and PVT was modelled for each reservoir. Production history data were screened, formatted and imported into production history data section of the software. Also, reservoir static pressure history data were entered the reservoir production history data section. Initial reservoir pressure and temperature were defined, and reservoir rock properties (porosity and fluid saturation) were entered the reservoir input data. Rock compressibility was estimated from in-built correlation using connate water saturation, porosity and initial reservoir pressure. SCAL models were built with an in-built Corey correlation using connate water saturation, end-point saturations and exponent. Campbell's plots were used to investigate the presence of aquifers. Using Analytical Method, regression was carried out until an acceptable reservoir voidage match was obtained.

MBAL® also allowed the regression "best fit" to be compared with the classical graphical material balance methods such as Havlena and Odeh, Campbell, etc. Simulation was then run to validate the pressure history match.

4.17 : Chapter Summary

In this section, the plan for experimental work conducted in this study has been described in detail, explained and summarised. The apparatus used for the experiment, procedures, safety measures, sources of error, and calibration are also included in this chapter. The next chapter will provide further details of the experimental set-up and design for this research.

.

Chapter 5 Experimental Set-Up and Design

5.1 Helium porosimetry

5.1.1 Porosity

The ratio of the total pore space to the bulk volume within the reservoir rock is referred to as the absolute or total porosity which is given by the expression below;

$$\emptyset = \frac{Pore\ Volume}{Bulk\ Volume} \tag{5.1}$$

Where the void space in the rock is the Pore volume and the volume which the rock occupies is the Bulk volume. Grain volume is the volume of the rock grains or solids (not including the pore volume). Porosity is the fraction of void space in the total rock. Thus, pore volume can be calculated from the bulk volume and grain volume measurements:

$$\text{Pore Volume} = \text{Bulk Volume} - \text{Grain Volume} \tag{5.2}$$

5.1.2 Principles of Operation for Helium Porosimetry for porosity determination

The PORG-200^{TM} determine the grain volume of a sample using the ideal gas law. A known volume of helium is expanded in a calibrated holder (Matrix Cup).

$$\frac{p_1 v_1}{t_1} = \frac{p_2 v_2}{t_2} \tag{5.3}$$

Where

P1 = Initial absolute pressure, (Psig) V1 = Initial Volume, (cm^3) T1 = Initial absolute temperature, (^{O}C) P2 = Expanded absolute pressure, (Psig) V2= Expanded Volume, (cm^3) T2= Expanded Absolute Temperature, (psia)

The reference volume is expanded into a Matrix cup holder and pressured to 95 psig for the sample to be investigated. The unknown volume is calculated from the second pressure reading. The grain volume is derived from the following equation:

$$V_g = V_c - V_r\left[\frac{p_1 - p_2}{p_2 - p_a}\right] + V_r\left[\frac{p_2}{p_2 - p_a}\right] \tag{5.4}$$

Where:

Vg = Grain Volume, (g/cm^3) Vc = Sample Chamber Volume, (cm^3) Vr = Reference Chamber Volume, (cm^3) Vv = Valve Displacement Volume, (cm^3) P1 = Absolute Initial Reference Volume Pressure, (Psig) P2 = Absolute Expanded Pressure, (Psig) Pa = Absolute Atmospheric Pressure Initially in Sample Chamber, (psia)

The relationship between the resultant pressure and the calibrated disk volume is experimentally determined by the PORG-200^{TM}. Due to temperature changes and other factors, this approach considers any variability of the Matrix Cup volumes.

For the PORG-200^{TM} the relationship between the calibrated disk volumes and the resultant pressure is ascertained experimentally. This direct approach considers any variability of the reference or Matrix Cup volumes due to changes in temperature or other factors.

The PORG-200^{TM} is a helium porosimetry operated manually which have a digital technology to give the grain volume for core plugs samples. It consists of 3 inches in length and 1 inch in diameter for core samples and different calibration disks. The Helium port outlet is connected to the matrix cup of the PORG-200^{TM} for measurement of grain volume. The temperature sensor on the helium port measures the helium temperature. The helium inlet pressure (psig) is displayed on the regulatory inlet pressure. The reference pressure (psig) fine-tunes on the Digital Pressure Inlet. The input gas pressure fine-tune to the desired pressure is allowed by the gas regulator. The flow of helium from the regulator to the reference cell is controlled by Valve (V1). The Valve (V2) vents out the helium in the matrix cup when the measurement is complete. It also directs helium flow from the reference cell to the Matrix cup. The PORG-200^{TM} apparatus is connected to the Helium inlet port for helium regulation. The power connector of the apparatus is on the back panel. The experimental setup is shown below.

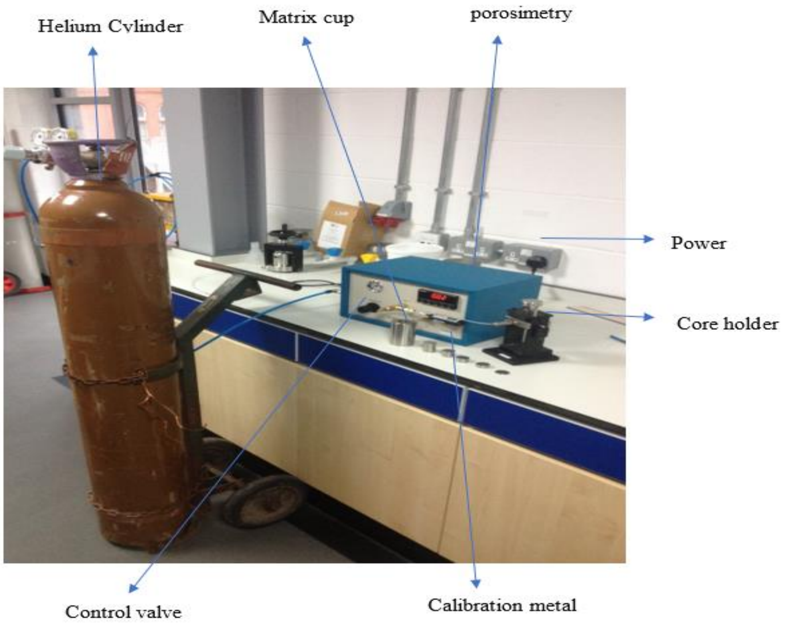

Figure 5-1: Experimental set-up used in porosity determination.

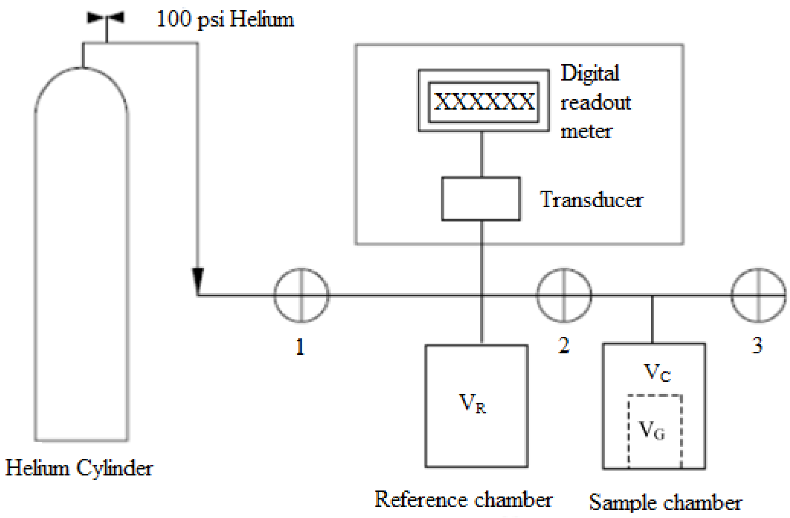

Figure 5-2: Schematic diagram of Helium porosity measurement.

$V_{C=}$ Volume of chamber, V_G=Grain Volume of sample, V_R = reference volume

5.1.2.1 Leak testing

This test is performed to ensure that the system is leak tight. The system calibration and pressure testing procedures are described as follows:

The transducer can reach equilibrium by powering the PORG-200^{TM} for up 30minutes before running a sample. At the same time, the helium supply pressure is set at 120psi. The helium outlet on the front of the panel is attached to the matrix cup. The regulator is set to about 95psi. Valve 1 grey and Valve 2 is turned on for expansion. Immediately the pressure drops and stabilizes in few seconds. The pressure is observed for about 10 to 20 minutes. There is an indication of a leak in the system if the pressure continues to drop. The location of any leak is detected with soapy water or liquid leak detector. Proper check on the valves packing, at the matric cup O-ring and the vent valve opening are assured.

5.1.2.2 Pressure transducer zeroing

The helium source is turned off before the start of the pressure transducer zeroing. Valve V1 is opened and Valve V2 is turned to expand the matrix cup. The pressure showed a zero reading on the digital readout. The procedure is repeated to release out all the pressure when a zero reading is not shown on the digital readout. Adjustment on the zero screw brings down the readout value to zero in cases where the value has decreased but it still not zero.

5.1.2.3 Pressure transducer calibration

The factory calibrates the pressure transducer which is not changeable except by the user (zero adjustments). Using the procedure in the following section, the instrument is calibrated to run effectively. The transducer should be replaced if the procedure cannot produce reliable, repeatable result.

5.1.2.4 Bulk volume determination

The sample total volume which consists of the internal pore volume, particle volume, and inter-particle void volume is referred to as the bulk volume. This is accurately calculated from core samples dimensions when there are no surface loopholes and it is a true cylinder. A caliper is used to find numerous length and diameter measurements. The average length and diameter are used to find the sample bulk volume in the caliper method:

$$B_v = \pi r^2 \mathrm{L} \tag{5.5}$$

Where

L = length, r = cylinder radius, π = 3.142

5.2 Gas permeameter (PERG- 200$^{\mathrm{TM}}$)

5.2.1 Permeability

Permeability is the rate of fluid flow through a rock sample and is given by the expression below:

$$\mathbf{k} = \frac{\mathbf{q\mu L}}{\mathbf{\Delta PA}} \tag{5.6}$$

Where: K = permeability, (Darcies)

q = Flow Rate, (cc / sec) μ = Viscosity, (centipoise) L =Length of Core, (cm)

ΔP = Difference in Pressure Drop, A = Area, (cm^2)

5.3 Flow in porous media theory

Henry Darcy derived from or guided by experience or experiment defined fluid flow in a porous media as being proportional to the differential pressure per unit length. The connexion was derived from data collected during series of experiments on the vertical flow of water through gravel packs. Consequently, numerous works carried out has proved the validity of Darcy`s Law for the flow in all directions and confirmed the experimental observations by derivation from the fundamental laws of physics. Equation (4.7) known as Darcy`s Law

$$Q = \frac{kA(P_1 - P_2)}{\mu L} \tag{5.7}$$

Where:

K = Permeability, (Darcie's), μ = Viscosity. (Centipoise), Q = Flow Rate. (cc/sec), L = Length of Flow. (cm), A = Cross- Sectional Area of Flow. (cm3), P_1= Upstream Pressure, atmospheres, P_2 = Downstream Pressure, atmospheres

Darcy's law has always been the basis of reservoir engineering methods. In its infancy, reservoir engineering consisted mostly of predictions of fluid production as a function of the amount of drawdown in the production well. For this purpose, Darcy's law could be used in its simplest form which points out that the flow rate of any fluid through a porous medium of any type or geometry is directly proportional to the pressure drop across the system (Tiab and Donaldson, 2015).

Darcy`s law has been found to be effective only at low flow rates, and it is now known as a distinct case of Forchheimer Equation where the second order term has been reduced to zero. Conservatively, the Darcian section of the flow is stated to as the `linear laminar or Darcian flow and that the region designated by the complete Forchheimer Equation (5.8) as `non-linear-laminar or Non-Darcian flow.

$\frac{\delta P}{\delta L} = \frac{\mu V}{k} + \beta \rho v^2$ (5.8)

Where:

$\frac{\delta P}{\delta L}$ = Pressure Drop across Sample (Pascals), μ = Viscosity (centipoise), v = Darcian Velocity (Q/A). (m/s), k = Permeability. (Darcie's), β = Forchheimer Factor, ρ = Density. (gm/cc)

5.3.1 Factors affecting permeability measurement

Gas slippage is one of the phenomena which affects permeability of a core sample, more so, pore content, confining pressure, turbulence and improper cleaning and drying can be considered few other examples. In this connexion, certain precautionary measures must be taken while preparing the core samples and when conducting the experimentation.

Gas slippage. Klink Enberg (5.9) has stated discrepancies in measured permeability when relating data which were collected using no-relative liquids versus gases. These variations were related with a laboratory effects termed gas spillage, which can be pronounced as the capability of a gas molecule of more easily retain forward velocity along a solid interface compared to a liquid molecule. Liquid velocities normally tend to zero at the solid wall. More so, gas molecules have a no-zero wall velocity this may result in two different dimension of rock permeability dependent on the liquid used in the experiment, since permeability is a rock property, it should be autonomous of the fluid injected into the system, therefore data gotten through gas injection should be corrected.

Klink Enberg exhibited that measured permeability values are higher at low mean pressures, since the gas molecules do not follow to the pore walls as liquids molecules do and hence the slippage of gas along the pore walls occurs

In 1942 Klink Enberg applied these principles to porous media and discovered permeability to a gas to be dependent upon molecular size, mean pressure and temperature to be precise he noted that the mean pressure at which the measurement was determined should qualify air permeabilities. The mistake presented by not qualifying the permeability in this way increases as the permeability decreases and is significant for values less than one millidarcy.

The mathematical expression of the Klink Enberg equation can be written as:

$k = k_{\infty}[1 + b \ / \ P\_m \ ]$ (5.9)

Where:
k = Permeability. (Darcie's), k = Permeability of an infinite Mean Pressure, B = Klink Enberg Factor, Pm = Mean Pressure. (psia)

Klink Enberg permeability is not measured in this experiment using the PERG-200^{TM} Distinctions caused by Klink Enberg effects are decreased by keeping the mean pressure at a low level.

5.3.1.1 Principle of operation for air permeability measurements

The Buff Berea core plug is placed into the core holder. Air supply regulated to 20 psig is connected to the instrument. The valve V1 is opened and the regulator is used to adjust the flow pressure. The gas flow rate and the upstream pressure stabilizes in some minute's time. The stabilize temperature and upstream pressure are recorded. The regulator is moved in the clockwise direction to increase the gas flow rate which directly changes the upstream pressure. This display reading was taken after stabilizing. The process is repeated at different gas flow rate to make sure Darcian Flow occurs (flow pressure linearly increases with increase in gas flow rate). The Permeability is calculated when the recorded values are entered to the spreadsheet. The same procedure is repeated to determine the permeability of the Castle gate and Boise core samples.

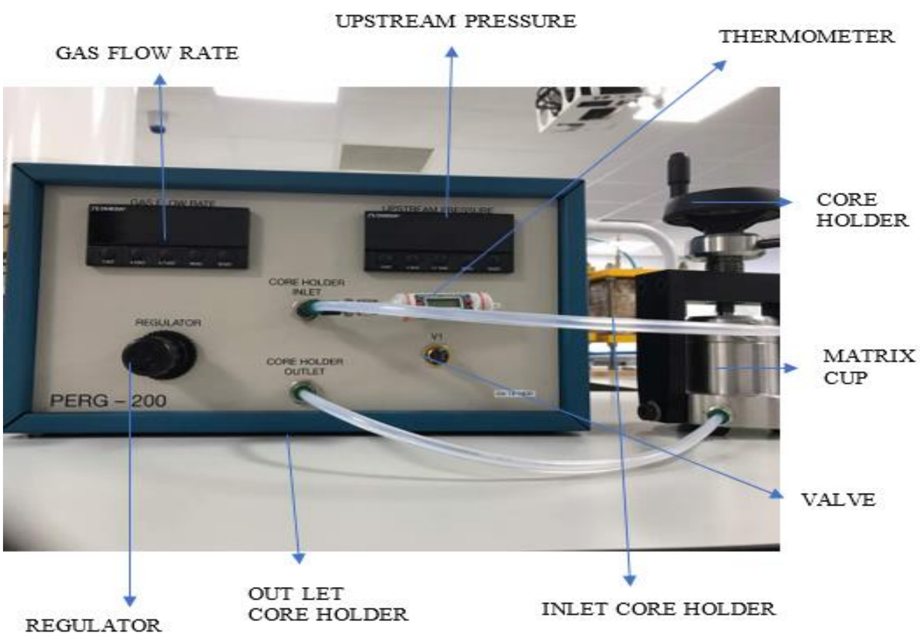

Figure 5-3: Gas Permeameter (PERG- 200^{TM})

5.3.1.2 Leak testing

Leaks are not usually problem with the PERG-200™ since it uses low- pressure air or nitrogen. Any leak suspected, it may be located or traced using a leak detector or soapy water. Care was taken by checking the valve packing, and at the Facher core holder. Care was taken not to wet the electronic components parts and connections. The Facher Core Holder was the most likely site of a leak. Inspection was thoroughly done on the rubber stopper for wear or pitting or Harding there was no wear and no necessary replacement made during the experiment.

5.3.1.3 Pressure transducer zeroing

With the core holder opened, the gas source was turned off and valve V1 was opened and the regulator handled was turned clock wise so that pressure line was depleted. The pressure reading on the digital until the value was zero. As a matter of fact, if the reading is was not zero, the procedure should be repeated to make sure all the pressure has been depleted. Care was also taken if the read out was still not zero, then adjustment was necessary until zero reading was obtained.

5.3.1.4 Pressure transducer calibration

The pressure transducer was calibrated at the factory by the equipment manufacturer, and this cannot be adjusted except for zero adjustment by the user. When repeatable, reliable measurements cannot be obtained, therefore the transducer may need to be replaced.

5.3.1.5 Flow Rate Meter Calibration

The meter can be removed from the instrument and recalibrated by a suitable NIST approved laboratory. If satisfactory recalibration is not possible or is not practical, the meter may be replaced.

5.4 Core flooding system

The Core Lab UFS-200 is a core flooding system student component designed for two-phase liquid movements under unsteady state or steady state circumstances and single-phase gas steady-state experiments. This arrangement is precisely designed to take benefit of Core Laboratories 50 years of perform water flooding and simulation experiments. The equipment is calibrated to 5,000 psig confining pressure, 3,500-psig pore pressure at room temperature. The inlet pressure into the core sample and outlet pressures on the other side of each core are measured with gauge pressure transducers. Fluids created through the core sample can be collected and produced gas can be measured from flasks on the electronic balance downstream. An integral part of the system is the Smart Flood software and computer data-acquisition-and-control system hardware which provides on-screen display of all measured values (pressures, temperatures, volumes etc.), automatic logging of test data to a computer data file, alarms, calculation of permeability.

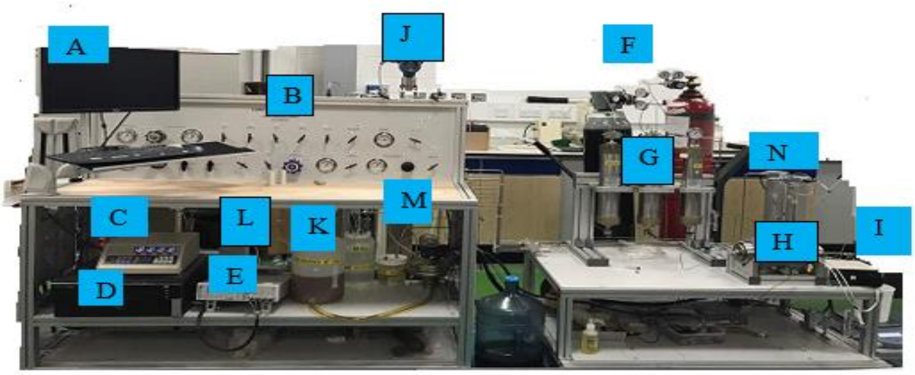

Figure 5-4: Cross-section of the UFS-200 core flooding equipment

Where:

A=Monitor, B=Control Panel, C=Pump Controller, D=CPU, E=Hameg Resistivity Control, F=Methane Gas Cylinder, G= Floating-Piston Accumulators, H=Core Holder, I=Hameg Balance, J=Rosemount Transducer, K=Back Pressure Oil, L=Isco Pump Reservoir,
M= Overburden Pressure, N=CC Cell

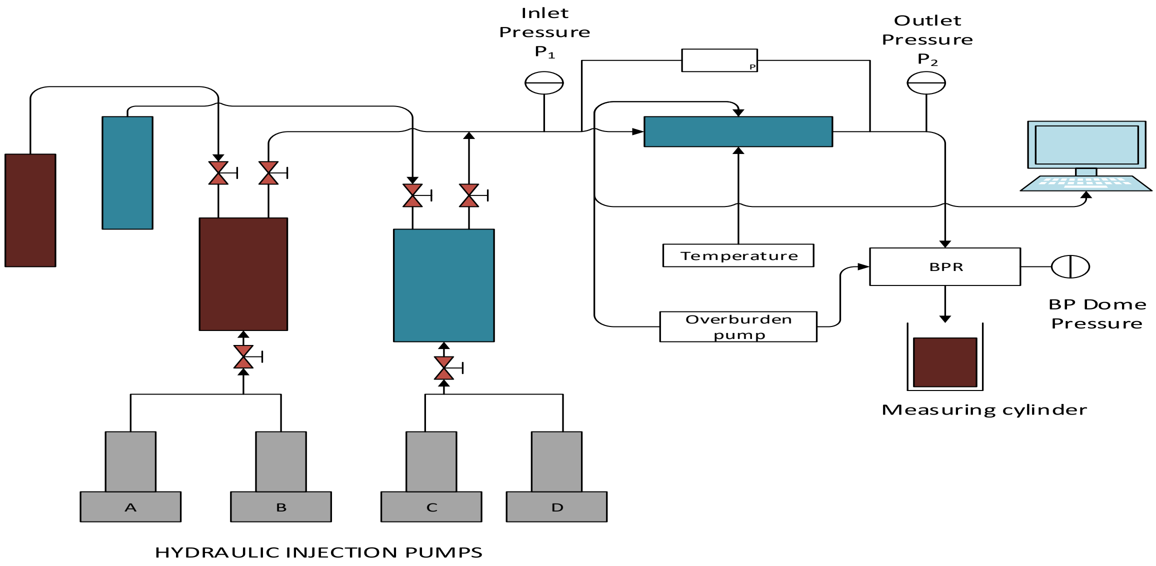

Figure 5-5: Schematics of the UFS-200 core flooding equipment

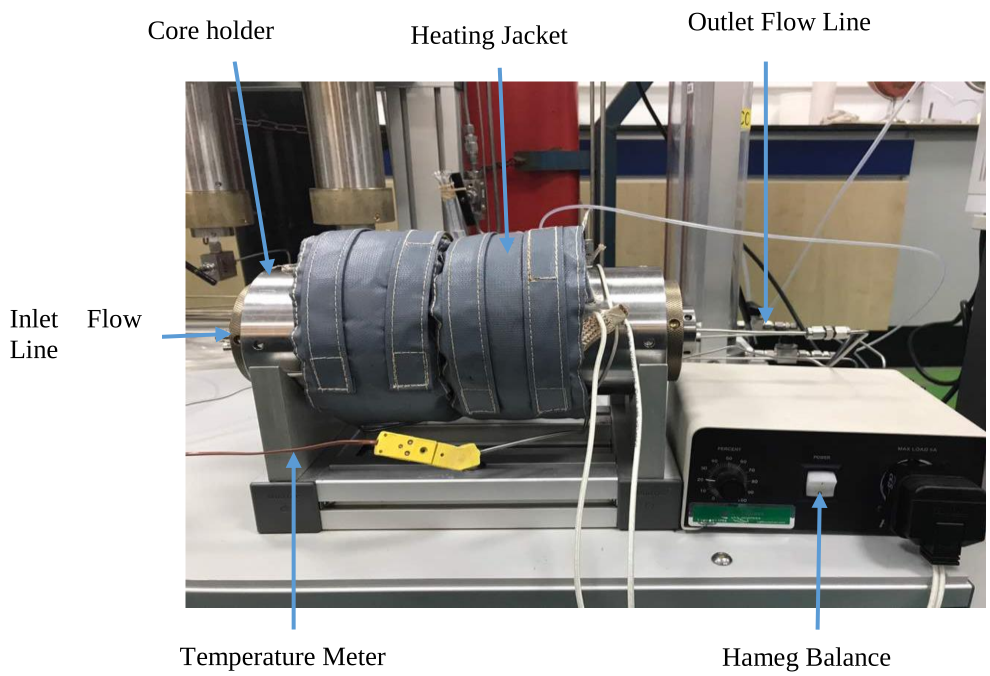

Figure 5-6: Core Holder

5.4.1 Core holder

This core holder is hassler-type core holder. Hassler can be defined as having radial loading only. They are used for gas and liquid permeability testing and water flooding experiments. The core sample is hold inside a rubber sleeve by radial confining pressure, which simulates reservoir overburden pressures. Inlet and outlet supply plugs permit fluids and gases are to be introduce through the core sample. All flow lines and internal volumes kept to a lowest, so that precise flow data can be determined. A core holder assembly, accommodating test samples 1.5 inches in diameter and up to 3 inches long. The core is confine and equivalent overburden stress applied via a rubber sleeve. The pressure is hydrostatic; that is, it is apply equally along the radial and axial axes.

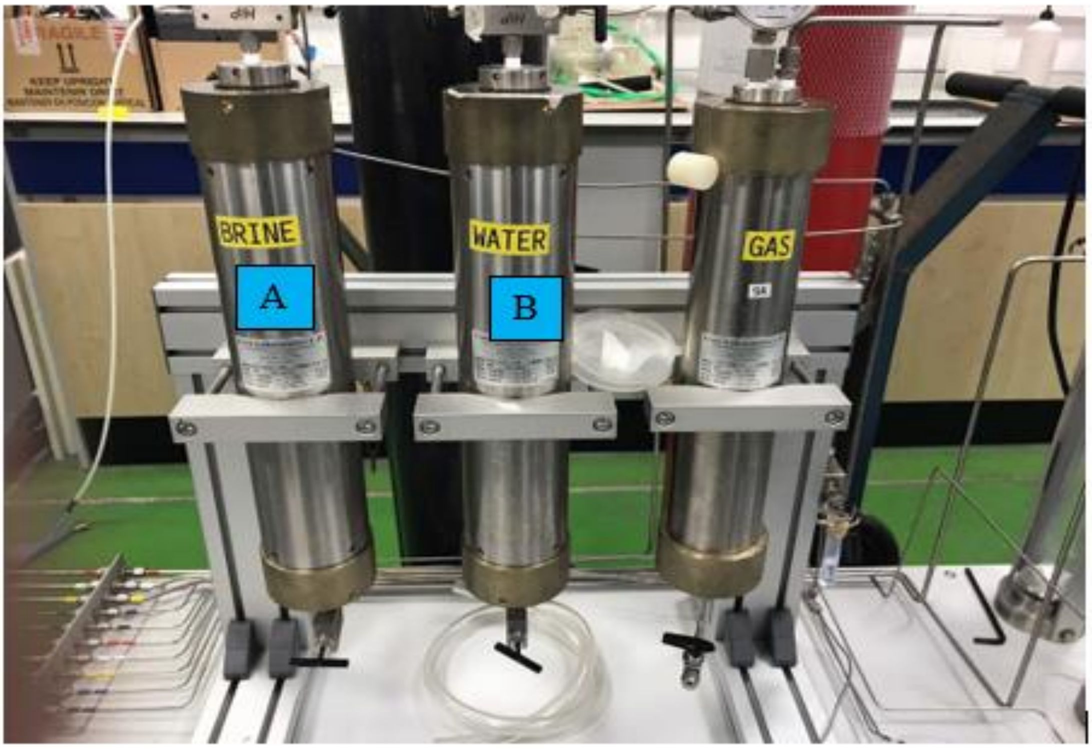

Figure 5-7*:* Floating-Piston accumulators

5.4.2 Floating-Piston accumulators

The floating- Piston accumulators were rated at 5,000 psig and 177 ºC (350 ºF), pressure and temperature, respectively. The volume was calibrated at 500 cc each and delivers for introducing liquid without permitting the fluid to come in communication with the metering pump. Furthermore, in this research the accumulator A (gas) and accumulator B (water) were used in saturation and flooding procedures. The fluid was injected into the preferred accumulator with the help of the Isco Pump.

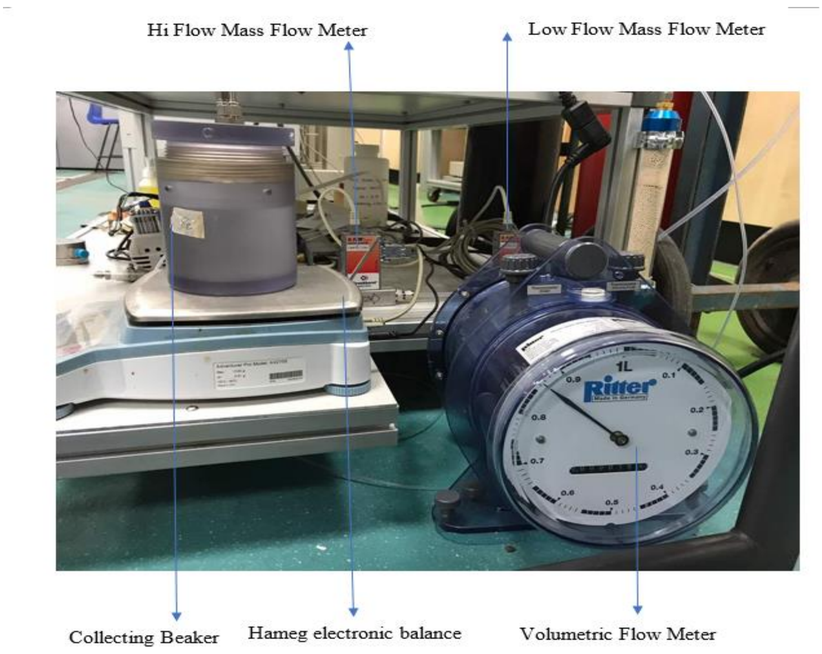

Figure 5-8: Collecting, weighing and volumetric flow meter.

5.4.3 Collecting, weighing and volumetric flow meter

The leak-off fluids produced through the core can be collected by the Electronic Balance at the outlet of the core's BPR. The liquids flow through the back-pressure regulator (BPR) and into a sealed container on the balance. In this study the Volumetric Flow meter was used to vent the gas from the core holder and measurements were taken tabulated and calculations were made for the produced gas.

Figure 5-9: Metering Isco Pumps.

5.4.4 Metering Isco pumps

The figure 5.11 Isco model 500D is a two- container metering pump co-ordination with a flow rate range of regulating from 0 - 200ml/min with a maximum of 3,750 psig pressure rating.

The pump`s boundary is established to turn off herself before it stretches excessively high pressure. The pumps can be controlled by the pump regulator and can be used to inject gas or fluid into the core sample through a floating piston accumulator. The most important procedure here is to close the valves to the confining pressure system and released pressure in the Isco pimps. When the valve is released to the accumulator and the valve at the bottommost of the accumulator, more so, opening the purge valve at the topmost of the accumulator to channel all air out of the stream lines. With an accurately filled accumulator, gas or liquid can now be introduced in to the core sample in question.

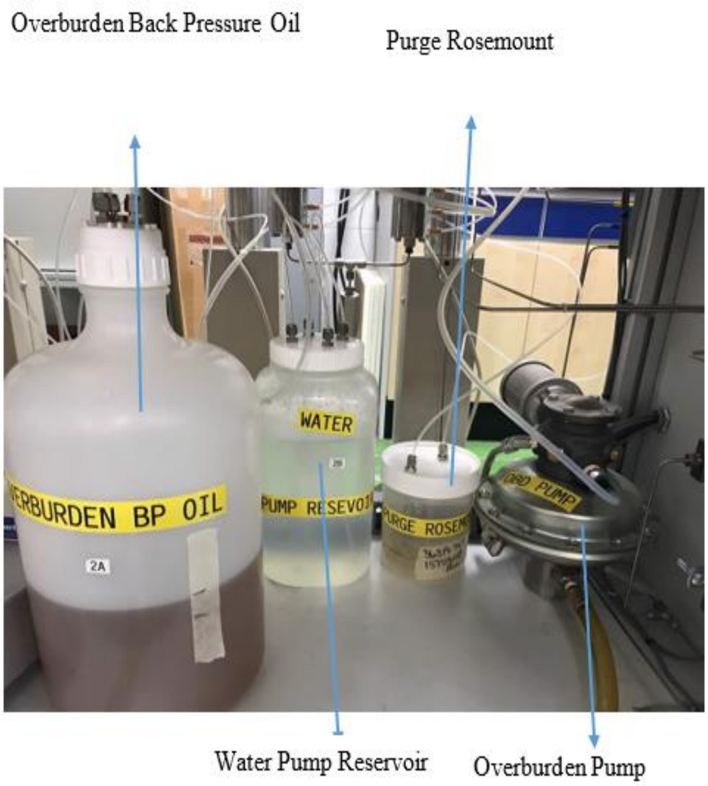

Figure 5-10: Overburden pump and relevant reservoirs.

5.4.5 Overburden pump and relevant reservoirs

Figure 5.12 characterize the overburden pressure pump; However, this is a hydraulic pupm Model S-216-JN-150 pump, with a maximum pressure yield of 10,000 psig. Consequently, the maximum overburden pressure ranking of the core holder and the system is 5,000 psig, it works by steadily pumping hydraulic oil into the annulus of the core holder to build up the looked-for overburden detaining pressure as well as the back pressure. 2.5-inch-dial pressure gauges are used to monitor the Overburden Pressure and the BPR Dome Pressure. The pressure range on these gauges is 15,000-psig full scale. A 160-psi gauge is provided to monitor the main inlet air going to the pump and air actuated valves.

5.5 Relative permeability

Permeability to a phase is reduced when a second or third phase is present.

$$\text{Relative Permeability} = \frac{Phase\ permeability\ when\ more\ than\ one\ phase\ is\ present}{Permeability\ to\ that\ phase\ alone}$$

Relative permeability is normally reported as a fraction or percentage.

It equals 1.0 or 100% when the phase is present on its own

$$K_e = K.K_r \tag{5.10}$$

$$K_r = \frac{K_e}{K} \tag{5.11}$$

Relative permeability provides an extension of Darcy's Law to the presence of more than a single fluid within the pore space.

Where:

K = Permeability (Darcies)

Ke = Effective permeability (Darcies)

Kr = Relative Permeability (Darcies)

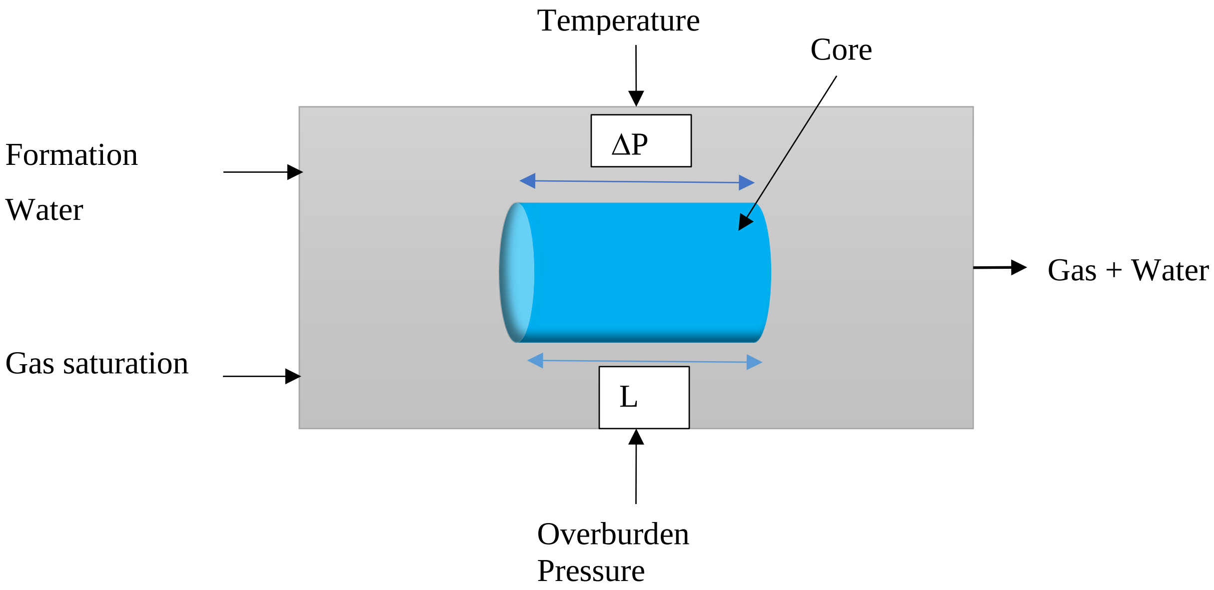

Figure 5-11: Reservoir

$$Q_w = \frac{KK_{rw}A}{\mu_w}\frac{dP}{dl} \tag{5.12}$$

$$Q_o = \frac{KK_{ro}A}{\mu_o}\frac{dP}{dl} \tag{5.13}$$

Where:

k	=	Permeability, (Darcies)
krw	=	Relative Permeability of Oil, (Darcies)
kro	=	Relative Permeability of Water, (Darcies)
μo	=	Viscosity of Oil, (centipoise)
μω	=	Viscosity of Water, (centipoise)
Qo	=	Oil Flow Rate, (cc / sec)
Qw	=	Water Flow Rate, (cc / sec)
A	=	Cross-Sectional Area of Flow, (cm^2)
dp	=	Pressure Drop Across Sample (Pascals)

5.6 Brine preparation

Brine with varying concentrations for the reservoir was prepared at 23^{O}C.The required quantity of NaCl (sodium Chloride was dissolved into an appropriate volume of distilled water using a measuring cylinder, a hot plate and a magnetic stirrer as shown in Figure 4.16. The salinity and concentration of salt in the fluid was determined at room temperature and pressure. This salt was purchased from the Fisher Scientific it comes a purity of Ninety-Nine percent (99.9%).

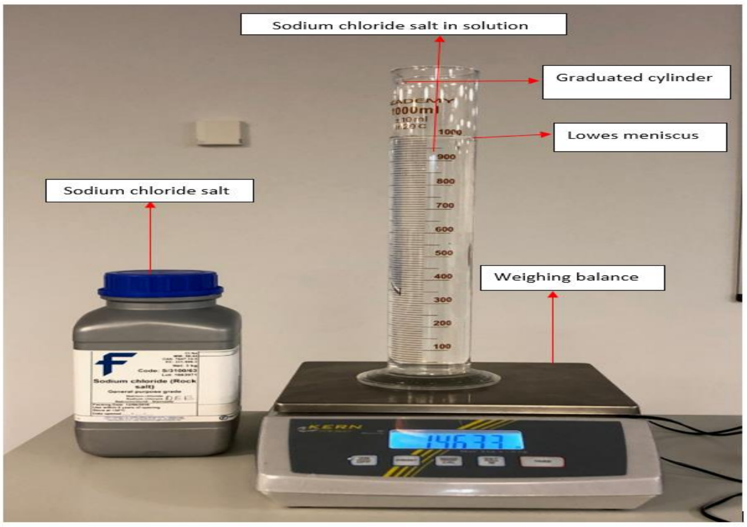

Figure 5-12: Brine preparation set up

5.7 : Core sample cleaning using soxhlet extraction

Before and during the experiment core samples get dirty it is only ideal to clean them using Soxhlet Extractor. This way any impurity within the core samples are cleaned up to achieve reliable and concise acceptable results. Having received the core samples from the manufactures, they are subjected to proper cleaning with the help of the Soxhlet Extractor where both organic and inorganic impurities resident in the core samples are removed. Since the experiments are repeated regularly, after some time the core samples are subjected to impurities removal as stated above. The extractor consists some attachments such as a Pyrex flask, a condenser, were cold water is circulated, a thimble, most importantly an electrical heater which provides the necessary energy to evaporate the toluene solvent within the system.

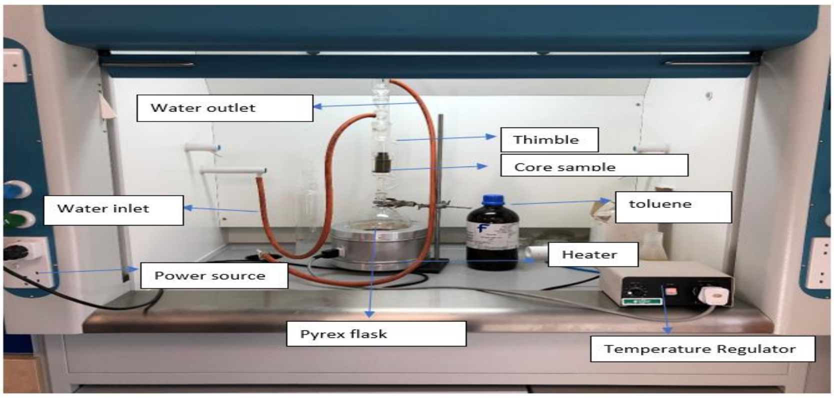

Figure 5-13: Soxhlet extraction set up

5.8 Chapter Summary

This chapter builds on the previous one and includes extensive details on the experimental Set-Up and Design for Helium porosimetry (equipment that is used to determine the porosity of the given core samples and the governing equations) and describes the principles of operation for Helium Porosimetry for porosity determination. A test is described which has been performed to ensure that the system is leak-tight. The system calibration and pressure testing procedures are also described. Furthermore, the gas permeameter for permeability determination for the given sandstone core samples is discussed and the principle of operation for permeability measurements included. The governing fundamental equation for flow in porous media (Darcy equation) is described. Factors affecting permeability measurement are also discussed particularly gas slippage (i.e. the Klink-Enberg effect). Also mentioned is the Core flooding system (Core Lab UFS-200) which is used for two-phase liquid movements under unsteady or steady flow conditions. Details of single-phase gas steady-state experiments are also included. Other relevant core flooding aspects have also been reviewed including the core holder (reservoir), floating-piston accumulators, collecting, weighing and volumetric flow meter, metering Isco pumps, overburden pump and relevant reservoirs. The concept of relative permeability has been introduced with associated equations and the reservoir schematics are included. The brine preparation procedure and set up is also presented as is the core sample cleaning procedure using Soxhlet extraction. The next chapter addresses in detail the extensive experimental Results generated in this study and detailed interpretations.

Chapter 6 Experimental Results and Discussions

6.1 Overview

This chapter presents result of experiment (Buff Brea, Boise, Castle gate sandstone) and mathematical modelling and computer simulation conducted to study the effect of parameters such as initial reservoir pressure, surface velocity, porosity and permeability on methane transport at pore scale using the sandstone samples. These parameters were measured using experimental methods in chapter 4, 5, and added to the model created to investigate their effect on fluid flow and gas production in sandstone reservoirs. This chapter is divided into six Phases.

I. Phase 1; Porosity and permeability (petrophysical results)
II. Phase 2: PVT Analysis for gas composition and fluid properties
III. Phase 3; Core flooding
IV. Phase 4; Single Phase flow of Buff Bera
V. Phase V: Ogba wet gas field production history results and discussions
VI. Phase VI: Material balance analysis Results and discussions

6.2 PHASE I: Petrophysical measurement

6.2.1 Porosity measurement

The experiment determines the grain volume values for the respective sandstones sample, which were used to calculate the porosity. The Boyle's law pressures obtained from the Helium Porosimeter equipment are shown in Table 6-1. These were obtained after calibration using the matrix cup and as mentioned, the equipment has an accuracy within ±2%.

Table 6-1: Porosity Measurement using Helium Porosimetry scenarios

Core Sample	Scenario A		Scenario B		Scenario C	
	P1(psi) Reference Pressure	P2(psi) Expanded Pressure	P1(psi) Reference Pressure	P2(psi) Expanded Pressure	P1(psi) Reference Pressure	P2(psi) Expanded Pressure
CASTLEGATE	90.26	21.40	91.64	21.12	92.96	22.00
BOISE	90.41	20.67	91.64	20.63	92.89	21.32
BUFF BEREA	90.40	23.23	91.66	23.37	92.97	23.80
BENDERA GRAY	90.40	24.79	91.63	24.91	92.88	13.37

The pressure values evaluated in Table 6-1 were then used to obtain the grain volumes of each core sample which was subsequently used to evaluate the pore volume and porosity. These were shown in Table 6-2 and a comparison was made in the table between the measured porosity and the porosity given from where the core samples were sourced.

Table 6-2: Porosity Measurement using Helium Porosimetry

Sample	**Measured Porosity (%)**	**Factory porosity (%)**
BUFF BEREA	24.55	20-22
CASTLE GATE	29.31	27-29
BOISE	30.35	28
BANDERA GREY	19.67	19-21
GREY BEREA	20.18	18-21

6.2.2 Permeability measurement

Furthermore, the absolute gas permeability was measured to ascertain the transmissivity of the core samples employed in this experimental run. With an accuracy of ± 3%, the gas permeater was able to measure the absolute permeability of each core sample based on the Darcy Equation. The results are shown in Table 6-3. Boise Berea had the highest permeability and it is within the range of the supplied permeability from the source.

Table 6-3: Permeability Measurement using PERG 200™

Sample	Flowrate (cm^3/s)	Pressure (Psig)	k (mD)	k (mD)
BUFF BEREA	65.2	0.3	458.1	350-600
CASTLEGATE	209.1	0.3	1434.8	1300-1500
BOISE	312.6	0.3	2196.4	2000-4000

The measured porosity and permeability clearly showed a deviation from those supplied by the source of the core samples. This is indicative of the need to accurately evaluate these properties during experiments to guarantee elimination of errors especially in flow behaviour measurements consisting of compressible components. Furthermore, the fluids used in this experiment were analysed to obtain the extensive properties using PVT cell for PVT analysis of the condensate and the gaseous components of the reservoir fluids.

6.3 Phase II: PVT Analysis

Given the unstable nature of condensates at ambient conditions, it was necessary to analyse the components present in order to devise a methodology to incorporate the fluid into the experimental set up which entailed exposing the fluid to ambient condition during the core flooding procedures. This was carried out using a quasi-differential liberation to analyse the components of the condensate. A summary of the sample is presented as follows;

Sample Summary

Fluid type: Sub surface Gas Condensate

Reservoir Name

Reservoir Conditions:

Pressure:	5621[psia]
Temperature:	224.6 [F]

Standard Conditions:

Pressure:	14.7[psia]
Temperature:	60 [F]

Summary of Fluid Properties:

Reservoir fluid mole % C7+	2.57 [%]
Reservoir fluid molecular wt	23.21 [g/mol]

<u>Propeties at initial Conditions</u>

Compressibility at 5621:	113.502 x E-06 [1/psia]
Density:	0.278 [g/cm^3]
Gas FVF (Bg):	0.00347 [cu ft/Scf]
Z-F actor	1.008

<u>Propeties at Saturation Conditions</u>

Dew point:	5621 [psia] at 224.6 [F]
Density:	0.278 [g/cm^3]
Gas FVF (Bg):	0.00347 [cu ft/Scf]
Compressibility 5621:	113.502 x E-06 [1/psia]
Z- factor	1.008

<u>Gas oil Ratio</u>

Flash	33,798.3 [Scf/Stb]
Multi stage separator test	25,656.8 [Scf/Stb]

<u>Gravity</u>

Constant volume depletion-residual oil	0.821 [g/cc], 40.8[°API]
Multi stage Separator test -STO	0.819 [g/cc], 40.6 [°API]

<u>CGR</u>

Flash	29.58 bbls/mmscf
Multistage separator stage	38.97 bbls/mmscf

The results from the PVT analysis are presented Table 6-4. The bulk fractions from the sample are C1 (methane) and this implies that the experiments can provide a good simulation of actual displacement and water influx.

Table 6-4*:* reservoir fluid composition

No	Component	Flash Gas [mol %]	Flash Oil [mol %]	Reservoir Fluid [mol %]
1	N2	0.34	0.00	0.06
2	CO2	0.06	0.00	8.11
3	H2S	0.00	0.00	0.00
4	C1	84.61	0.00	82.98
5	C2	4.09	0.06	4.01
6	C3	1.13	0.10	1.11
7	i-C4	0.27	0.08	0.27
8	n-C4	0.28	0.11	0.28
9	i-C5	0.16	0.21	0.16
10	n-C5	0.13	0.06	0.13
11	C6	0.30	1.26	0.32
12	C7	0.50	6.12	0.61
13	C8	0.20	7.87	0.35
14	C9	0.00	10.09	0.19
15	C10	0.00	7.08	0.14
16	C11	0.00	8.75	0.17
17	C12+	0.00	58.20	1.12
	TOTAL	100.00	100.00	100.00
	Density @ 60F		0.821	
	MW	20.43	164.59	23.21
	GOR			33,798.4
	Gravity	0.705		
	C7+	0.70	98.11	2.57
	C7+ MW	99.14	166.29	148.42
	C12+ MW	-	196.39	196.45
	CGR (bbls/mmscf)			29.58

The differential and flash vaporisation variation with some extensive fluid properties are shown in Figure 6-1 to 6-5. The interplay between the extensive properties and the intensive properties with respect to the liberation schemes are also presented. This facilitated the core flooding methodology and experimentation which is discussed next. It will investigate the effect of water influx into the retrograde condensate reservoir containing the hydrocarbon resource. By this, the volumetric reserve determination can be verified.

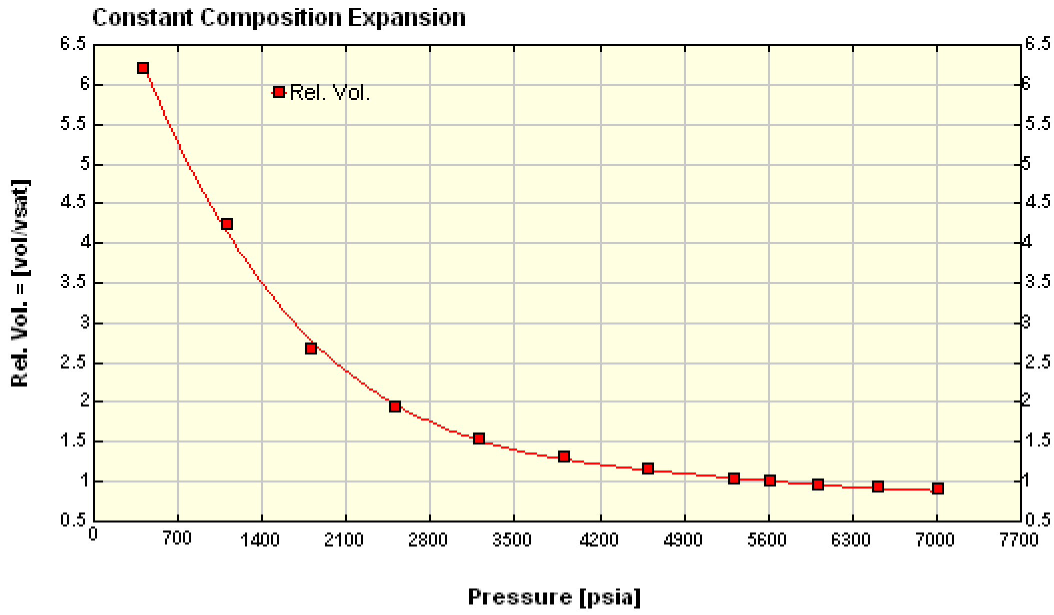

Figure 6-1: Constant Composition Expansion for Rel. Volume.

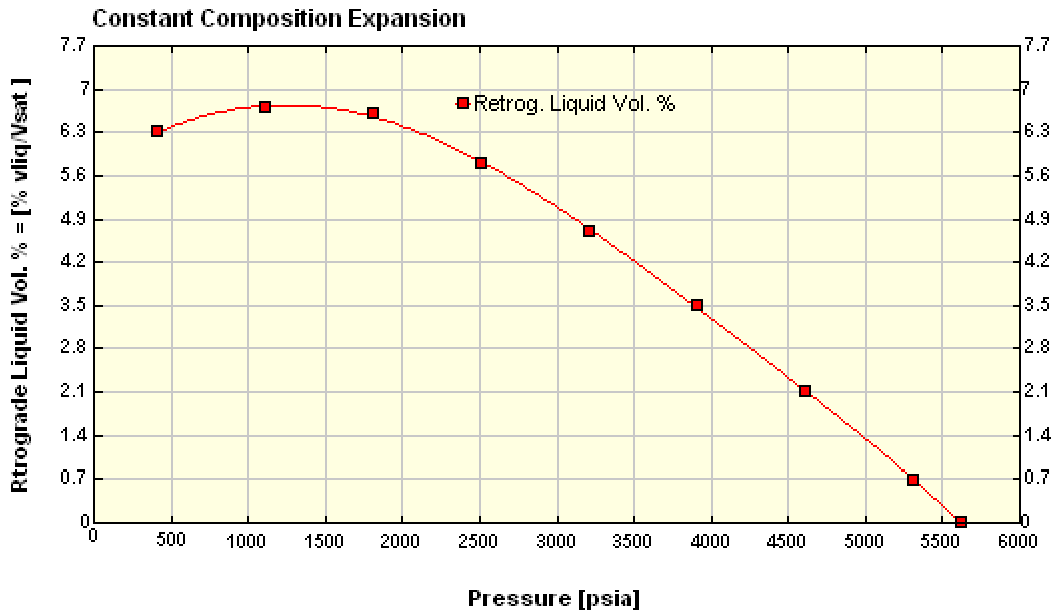

Figure 6-2*:* Constant Composition Expansion for Rel. Volume for Retrog. Liquid Expansion.

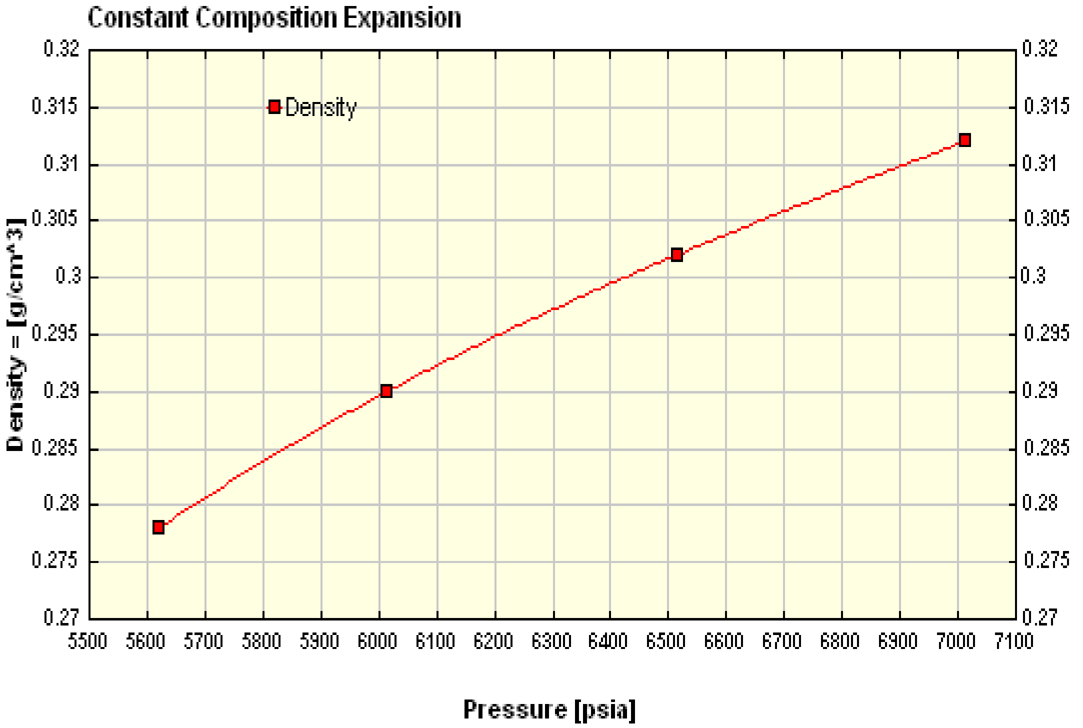

Figure 6-3*:* Constant Composition Expansion for Density.

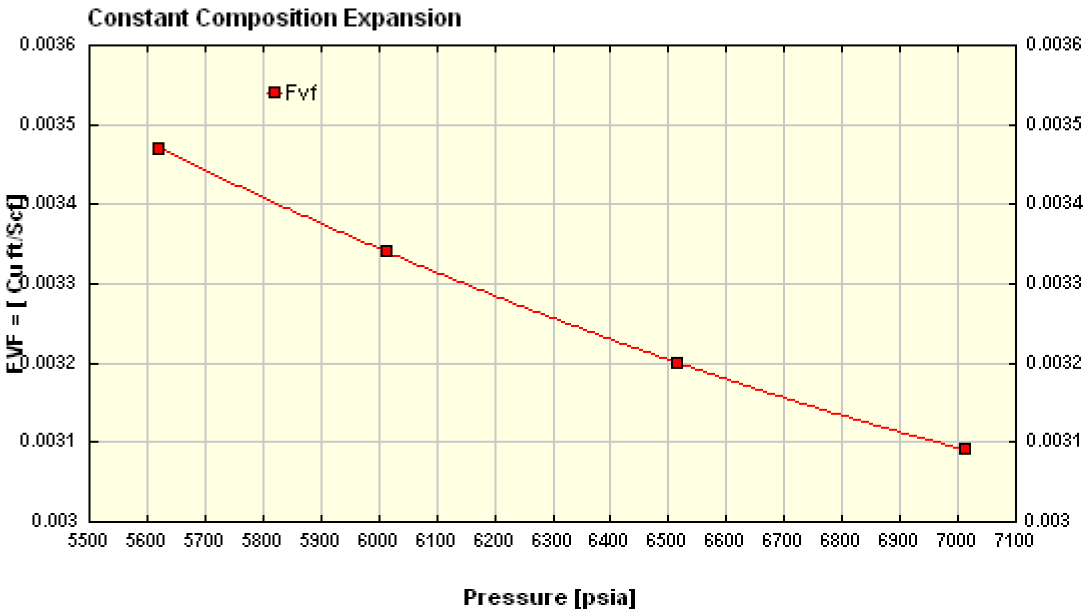

Figure 6-4*:* Constant Composition Expansion for formation volume factor.

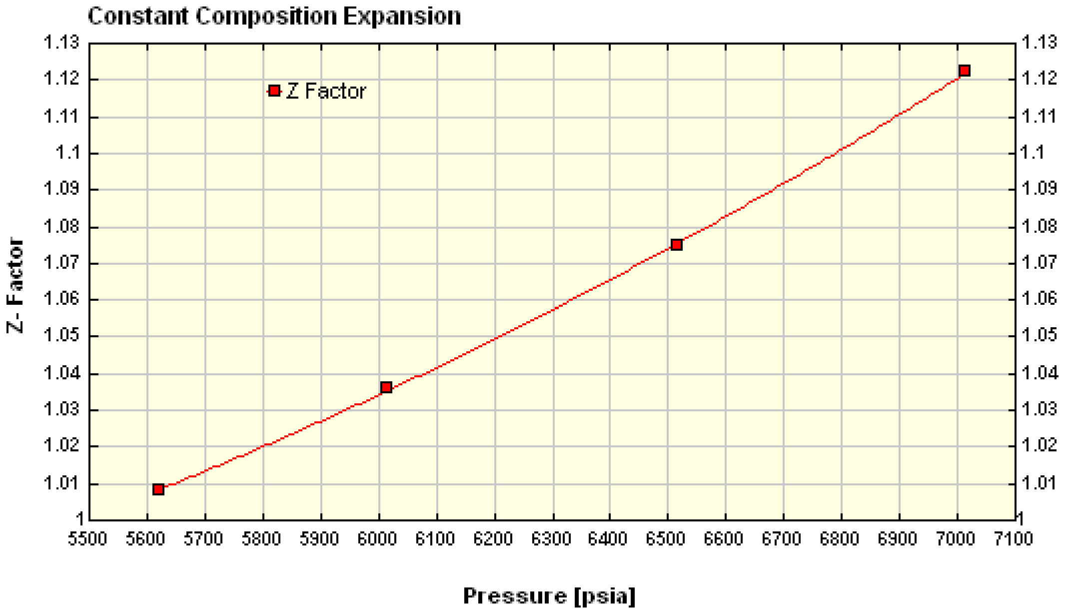

Figure 6-5*:* Constant Composition Expansion for Z Factor.

6.4 Phase III: Core flooding results

The performance of the laboratory simulated of water influx into the was carried at 1300 psig and at a temperature of 50C. Three different core floods using different brine salinities were carried out and presented. The influx rate of the water was set to 1ml/min into the simulated reservoir. Details are stated and presented in the core flooding process section.

6.4.1 Methane recovery and recovery factor

The original gas in place was evaluated using the volumetric method of reserve estimation for simplicity in calculation performed in this study and presented as:

$$G = \frac{V\phi(1 - S_w)}{B_g} \quad (6.0)$$

V is the bulk volume of the reservoir ft^3, ϕ is reservoir porosity, S_w is formation water saturation, and B_g is gas formation volume factor, ft^3/scf.

$$B_g = \frac{V_{p,T}}{V_{sc}} \quad (6.1)$$

Where B_g is gas formation volume factor, *v/v*, $V_{p,T}$ is gas volume at pressure *p* and temperature *T*, *v*, V_{sc} is the volume of the gas at standard condition.

Furthermore,

$$B_g = \frac{p_{sc}}{T_{sc}} \frac{zT}{p} \tag{6.2}$$

Where z is gas compressibility factor, p_{sc} and T_{sc} are pressure and temperature at standard conditions; p and T are pressure and temperatures at test conditions. Taking p_{sc} and T_{sc} to be 14.7 psia and 18°C, it becomes:

$$B_g = \frac{zT}{20p} \tag{6.3}$$

The pseudo-reduced properties of the system were also evaluated as done in the previous sections. These are as follows:

$$P_{pr} = \frac{1314.69}{670.13} = 1.97$$

$$T_{pr} = \frac{323.15}{190.2} = 1.70$$

And the gas formation volume factor was also evaluated to obtain the OGIP using the z obtained from Standing and Katz chart to be 0.91 and used in the expression.

$$B_g = \frac{0.91 \times 323.15}{20 \times 1314.7} = 0.01204 \frac{cm^3}{scm^3}$$

Now plugging the B_g into Eq 5 to compute the OGIP, the porosity value of the core sample (Bandera Grey) was 17.05% from Table 1, and the bulk volume, V_b was found to be 37.54 cm^3 using the core sample dimension in Table 1 and at $S_w = 0$

$$OGIP = \frac{37.54 \times 0.1705\ (1-0)}{0.01204} = 531.61\ cm^3$$

Having evaluated the original gas in place, the recoveries and recovery factors for each injection scenario of different brine salinities are presented as follows:

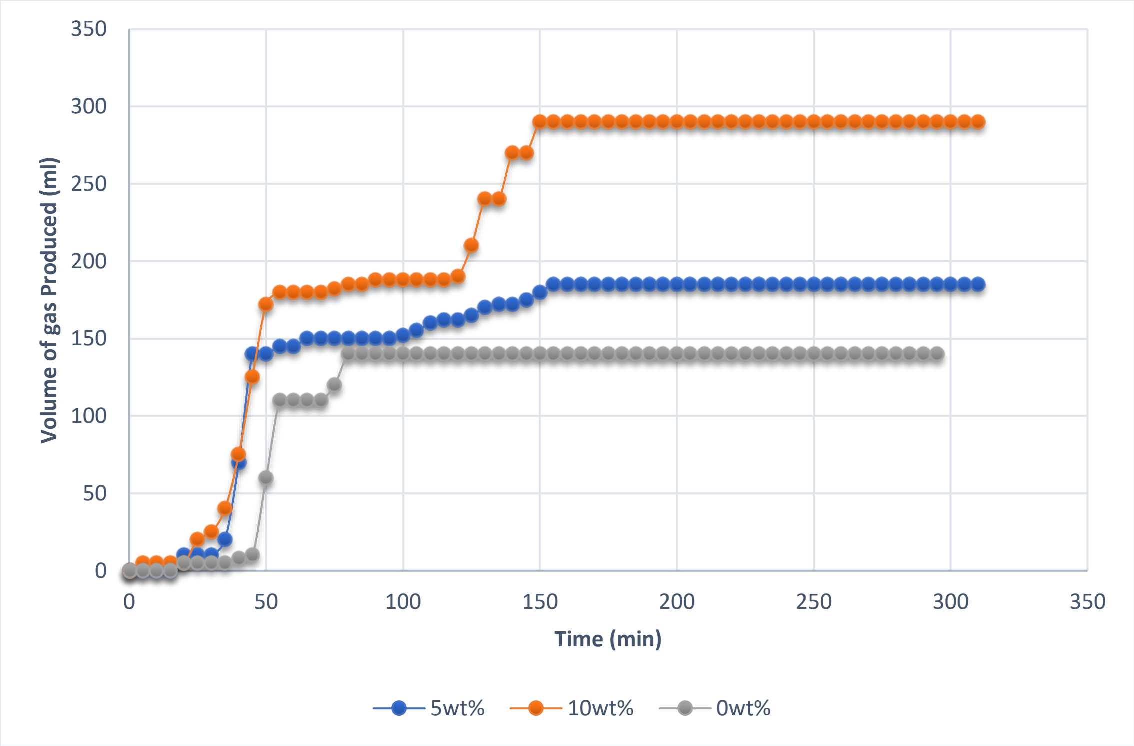

Figure 6-6: Natural gas production as a function of time

Given the OGIP obtained to be 531.61 cm^3, the recovery factor for both scenarios of 5wt% and 10wt% aquifer water are shown in Table 6.5.

Table 6-5*:* Recovery factor evaluation

SN	Aquifer salinity (wt% NaCl)	Cumulative gas produced (cm^3)	Recovery factor (%)
1	0	140	26.34
2	5	185	34.23
3	10	290	54.55

There is a clear relationship between the salinity of the aquifer and the recovery factor during the displacement process. At the same laboratory injection condition, the recovery factor was highest when the aquifer salinity was highest (10wt%), and this reduced as the salinity lowers. The relation is depicted in figure 2.

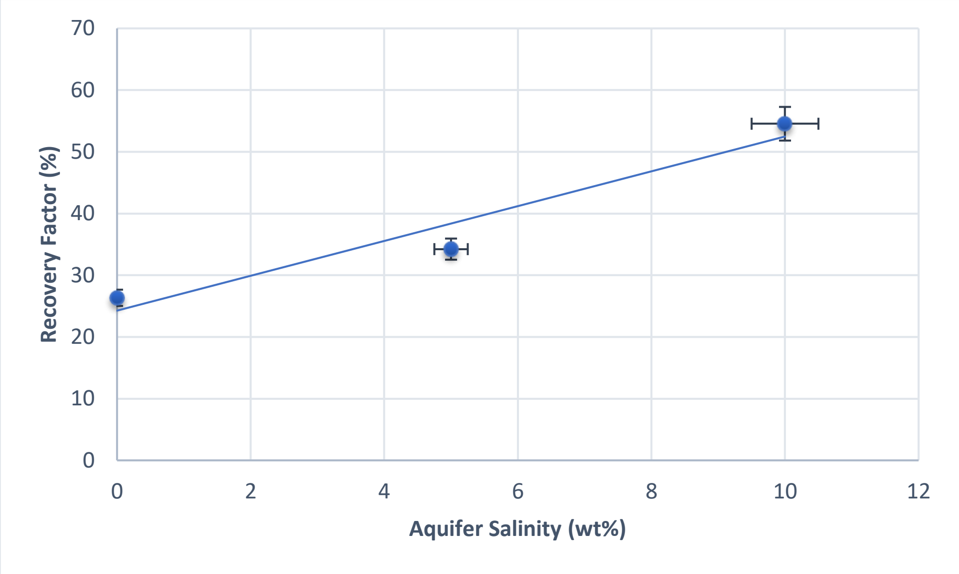

Figure 6-7*:* Recovery factor as a function of aquifer salinity.

It seems to be a perfect correlation, the two quantities and is an indication of the influence of salinity on the performance of the gas reservoir. Furthermore, the densities of the aquifer water play a vibrant character in the encroachment given that the viscosities increase with increase in the Newtonian density of the brines. A simulation of these properties of the aquifer connate water was carried out using PVT sim 20.0 to obtain the magnitudes and variations of these properties at the test conditions. This will help in the elucidation of the behaviour of the aquifer water during its encroachment/influx during the simulated natural gas production.

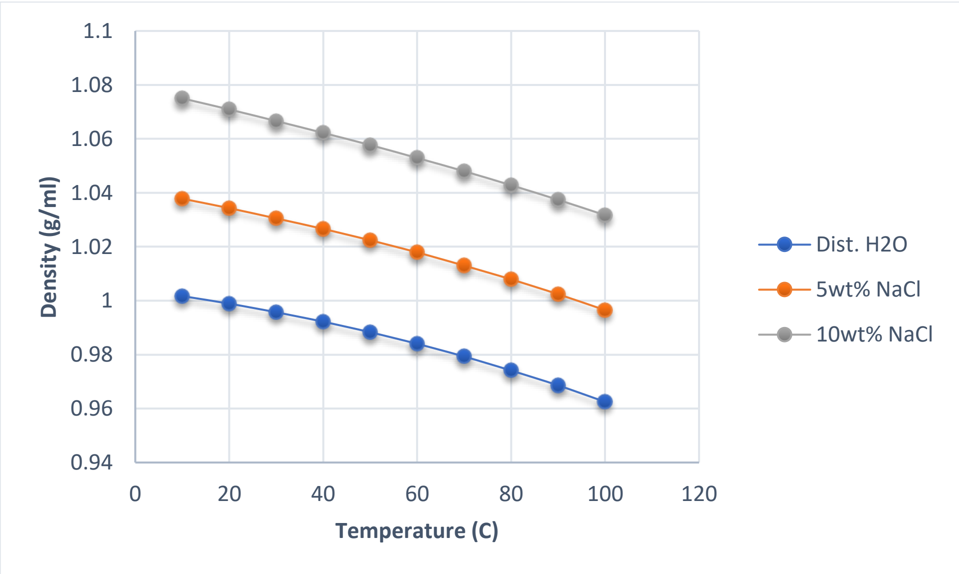

***Figure 6-8*:** Density assay at 1300 psia of different brine salinities.

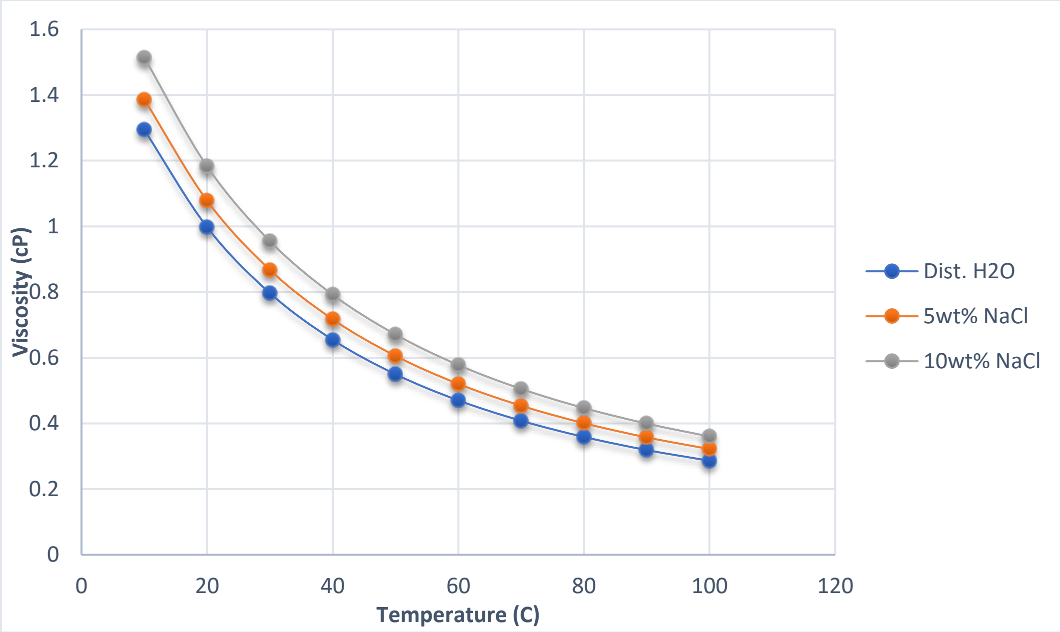

Figure 6-9: Viscosity assay at 1300 psia of different brine salinities.

From the figures, the viscosities and densities of the aquifer water were extracted, tabulated and presented below:

Table 6-6: Intrinsic properties table of different brine salinities/concentrations.

SN	Aquifer Water salinity (wt% NaCl)	Density (g/ml)	Viscosity (cP)
1	0	0.986	0.54
2	5	1.022	0.60
3	10	1.058	0.67

The densities and viscosities vary with increase in salinity of the aquifer water. This variation will affect the flow behaviour of the water at the conditions in the permeability of the water to the core sample will vary significantly and thus affect the influx rate and the performance of the reservoir.

Using a combination of the influx model described in the introduction section of the work and the Pots aquifer model (Ahmed and Meehan 2012b) , a comparison of the production rate against time was made to test the sensitivity of the experimental approach with the analytical adaptation. This is shown in figure 6-10 below. There is a strong similarity in the trends of the experimental and analytical approach to the natural gas recovery during the simulated production scheme. The error analysis is shown in Appendix A. This further reaffirms the accuracy of the experimental setup.

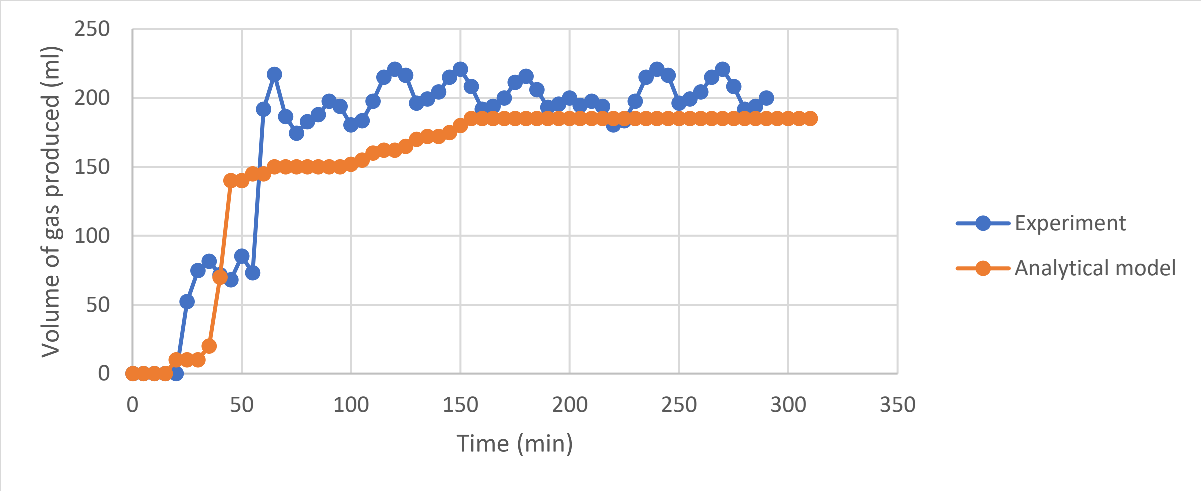

Figure 6-10: Comparison of model and experimental gas volume determination

Furthermore, the performance of the flooding scheme presents the impact of the formation water salinity (density) on the influx and subsequent production from the primary drive mechanism. This can be assessed through the water gas ratio which presents the ratio of the water produced to the gas produced at the onset and towards the end of the production life of the reservoir. It is presented next.

6.4.2 Water Gas ratio (WGR)

This parameter is a fraction which indicates the amount of water produced per unit volume of gas produced and it is a measure of the performance of the gas reservoir at the time of production. Figure 5 below shows the variation of the WGR during all the tests and its indicative of the nascent phenomenon of water influx during production from the reservoir. The tests where distilled water was used as the aquifer water showed the highest WGR which is an attribute of poor performance as seen in the previous section in that the recovery of the natural gas was poorest compared to the other tests. This confirms the points that the increase in salinity affects the production of the gas and its deliverability. Early water breakthrough was realised during the production from the tests where the salinity was lowest, however the volume of water produced was highest during in the lowest salinity test.

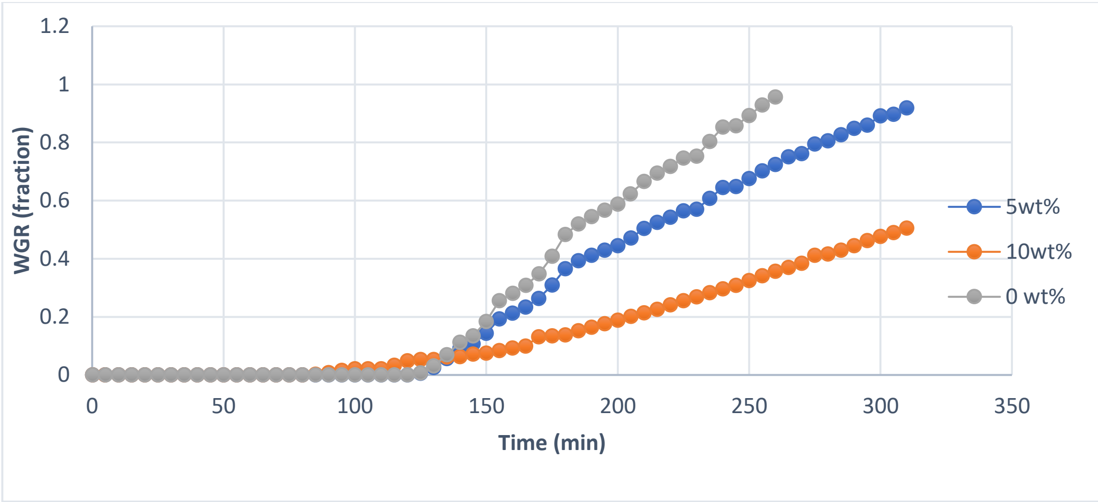

Figure 6-11: WGR as function of time for different influx scenarios.

It is expected that the higher the salinity of the aquifer water the better recovery realised as seen in the core flooding tests carried out. There is significant underperformance from the distilled water run in that the WGR is quite steep and higher than the other experiments. Consequently, the best performance was realised in the influx scheme where the salinity of the simulated formation water was highest. The is attributed to the relationship between the capillary pressure, wettability, and the interfacial tension. Interfacial tension is strongly dependent on the densities of the fluids in contact and capillary pressure is directly proportional to the interfacial tension. This phenomenon explains the performance seen in the scenarios with the higher salinity formation water occupying narrower pore spaces previously occupied by the gases and expelling the gases into the flow streams during production. The rock becomes water-wet and gases are further desorbed as the water influx takes place. The higher the salinity of the formation water the higher its density and the higher its interfacial tension with the gases. This increases the capillary forces exerted by the formation water within the pore matrix which helps in better production of the gases from the reservoir rock. To further investigate the flow behaviour of the gas transport within the pore matrix, a simulation was conducted on an SEM image of the core sample employed in the experiment to realistically present the fluid motion during production.

6.5 Phase IV: Simulation study of the flow behaviour of the core sample

The driving force that is very important for production and transport in gas reservoir is the initial reservoir pressure. In this model, the initial reservoir pressure effect at pore scale level is considered using different value of pressure (1000KPa, 2000KPa, 3000KPa and 4000KPa). The experimental porosity and permeability values and other parameter from table are kept constant while undergoing the investigation.

Figure 4.5: In chapter 4 (Four) gives the fluid velocity field of Grey Berea pore spaces using Navier-Stokes analysis as discussed previously in chapter 4. The black arrows indicate the direction of the gas moving from the inlet to the outlet within the slides and high-velocity magnitudes concentrated on the narrowest pores which decrease towards the outlet because of increase in cross-sectional area. In the slide mid-section, a high-velocity size within the area is recorded which point out that when channels commingle at lower pressures at a central point, a velocity of high magnitudes is obtained. The lowest flow velocity is several times less than the highest flow velocity within the Buff Berea sample. The streamlines represent the path of high-velocity gas flow in this model. The surface velocity is doubled because of 100% increase of the initial reservoir pressure which consequently increases methane gas production.

Figure 6.12 also clearly shows the change in the contour colours because of different initial reservoir pressure. The inlet has the highest pressure while the lowest pressure occurs at the outlet in the model. The pressure difference gives rise for more gas to flow through the pores of the model, with initial pressure of 4000Kpa producing the highest gas flow within and at the outlet of the model.

Figure 6.13 provides a plot that describes the velocity change at the outlet boundary using different reservoir pressure. The negative velocity values are because of the flow movement in the negative x-axis direction.

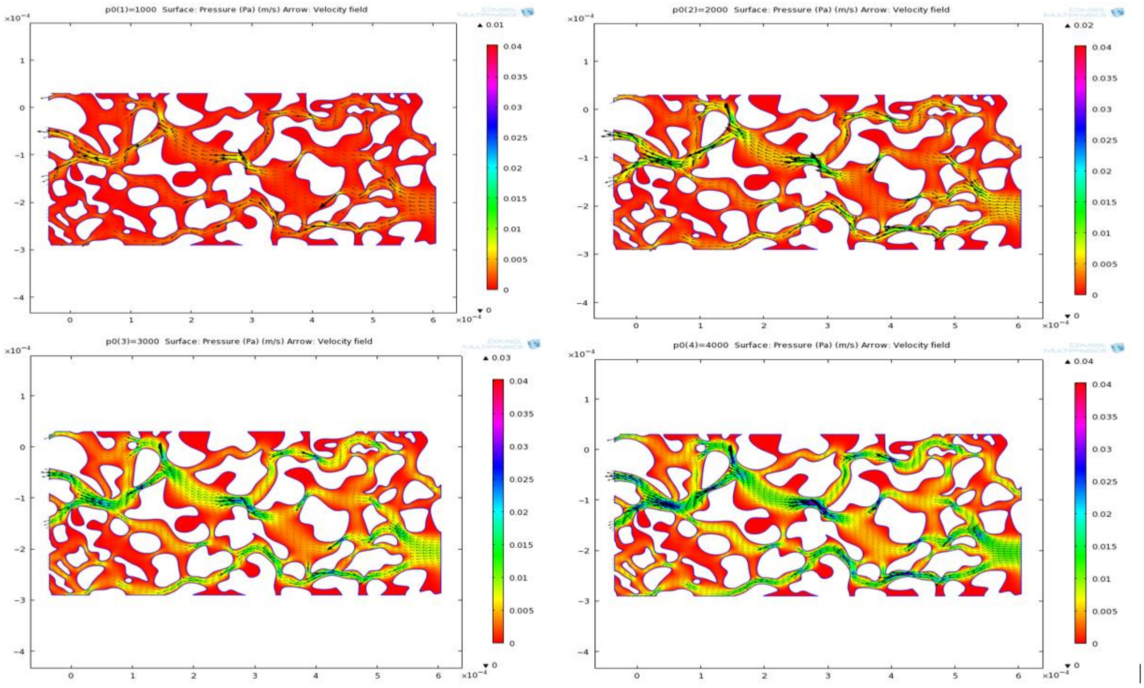

Figure 6-12: Surface Velocity with Arrows Using Navier-Stoke Equation.

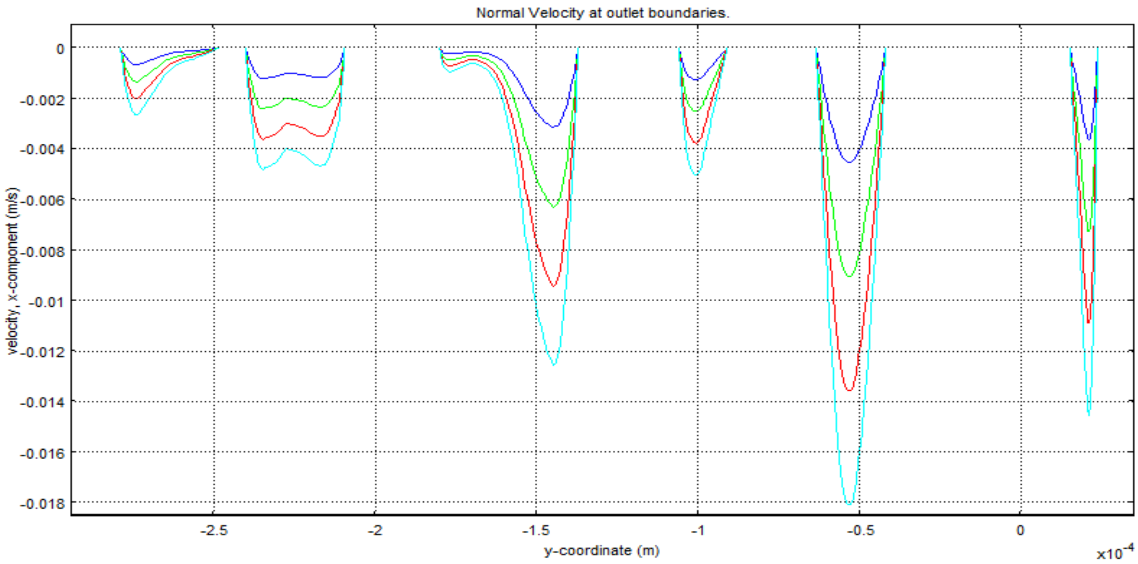

Figure 6-13: Outlet Velocity Boundary Plot of Different Reservoir Pressure.

- This presents the experimental result of porosity and permeability of various sandstone samples and implement the Grey Berea experiment result into COMSOL Multi physics software to characterize gas transport of single-phase flow at pore scale level.

- Considering the model, the Grey Berea SEM image is converted to a grey image of the pore-scale finite element mesh. A pore scale model was created when the SEM image is imported as a DXF into the COMSOL software which removed some part of the organic component of the sample.
- Navier-Stoke equation and Darcy Law were used to describe single-phase gas transport and free gas at the pore spaces. The inlet and outlet pressure, fluid pressure, porosity and permeability are the most important parameters which were known and recorded.
- The vital assumptions made in the model such as the same permeability through the formation reduce the number of unknowns for the result and problem encountered. Also, the distribution of pressure at the initial condition (t=0) of the pore system is assumed to be same through the formation.
- The simulation model at different initial reservoir pressure in the software give a satisfactory result on how changes in pressure is directly proportional to velocity of gas in sandstone reservoirs.

6.6 Phase V: Ogba wet gas field production history results and discussions

There are about twenty-four (24) discovered hydrocarbon bearing sands in OREDO field. Four (5) oil reservoirs namely

X8.2U, X8.2L X8.3,B1.0,A11and Nineteen(19) gas condensate reservoirs: X7.1, X8.0, X8.1,X9.0, X9.1, X10.1,X10.0A, X10.0B, Y1.1, Y2.1, Y3.0, Y5.0, Z1.0, Z2.0, Z2.1,Z3.0, Z4.1, Q2.0, Q3.0.

Production started in OGBA field in February 1996 from Wells 2, 4 and 5 in sand X8.2, other wells;7, 8 and 9 produced later from X8.2. Well7 was switched to Sand X8.3 while Wells 2, 4, 5, 7, 10, 11 and 12 produced from sands X8.1, X7.1, Y1.0, Y1.1 and Z2.0 through various strings. Only the above mentioned (7) reservoirs have produced so far in OGBA field.

The OGBA field has produced cumulatively, 18.02MMSTB of oil, 119.42BSCFof gas, and 2.27MMSTB of water as at December 2014.

6.6.1 Reservoir X8.2u

The Reservoir is saturated, with initial pressure of 4377 psia and bubble point pressure of 4377 psia. Strings (2LS, 4LS, 5LS, 7LS, 8bSS and 9SS) were completed in this reservoir. The reservoir started production in January 1996 and produced for about 14 years. Wells (5SS and 8bSS) are still on production, while the remaining boreholes remained closed in possibly owing to high water cut. The cumulative oil, gas and water produced as at end of history from reservoir X8.2 is about 12.24MMSTB, 45.07BSCF and 1.72MMSTB, respectively. Below is the production performance plot for ReservoirX8.2 as shown in Figure5.18 while the pressure profile plot and perforation panel plot are revealed in Figures 5.19 then 5.20 correspondingly.

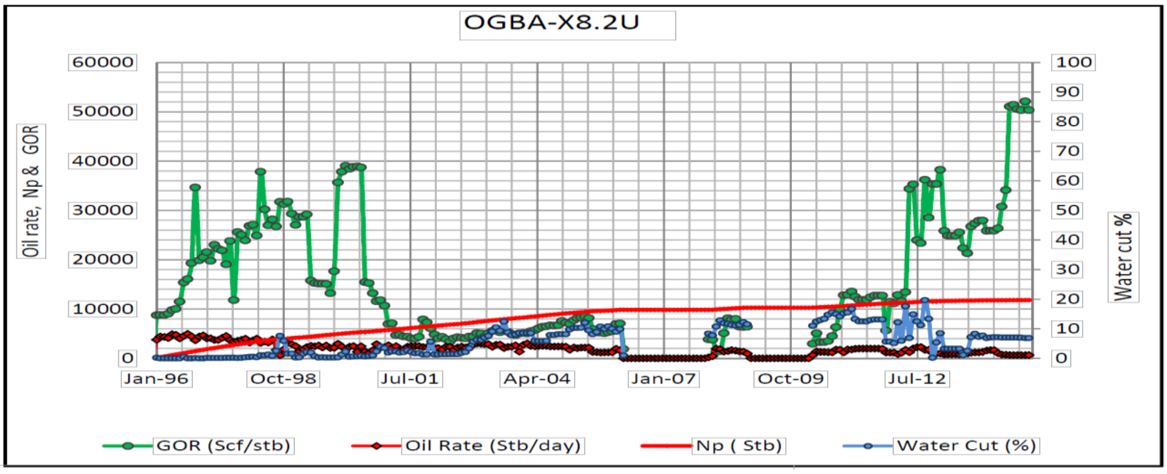

Figure 6-14: Shows the Np, GOR and WCUT for Reservoir X8.2

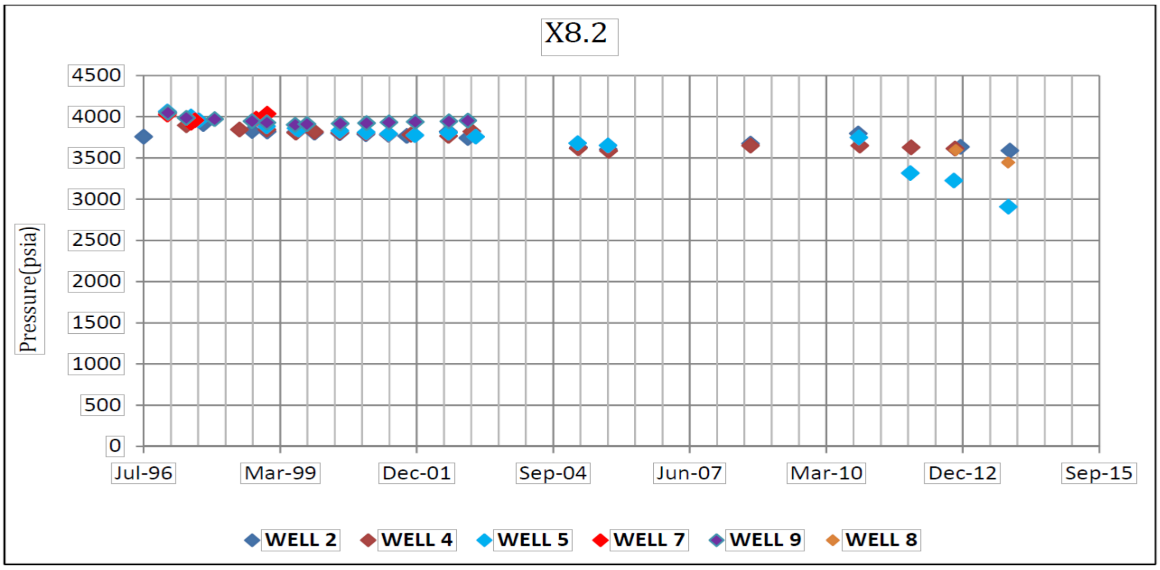

Figure 6-15: Shows the Pressure plot for Reservoir X8.2

6.6.2 Well 2LS

This string came on stream in February 1996 and water broke through 14 months later, the water cut steadily increased and was maintained at about 30% - 48% for about 3.16 years before first shut-in in February 2006. The string was reopened in 2008 and was shut-in that same year in December 2008 due to decline in production rate, it was reopened again in April 2010 and finally shut-in in January 2012 due to HWCT. See the Production Performance Plot in Figure 6.21.

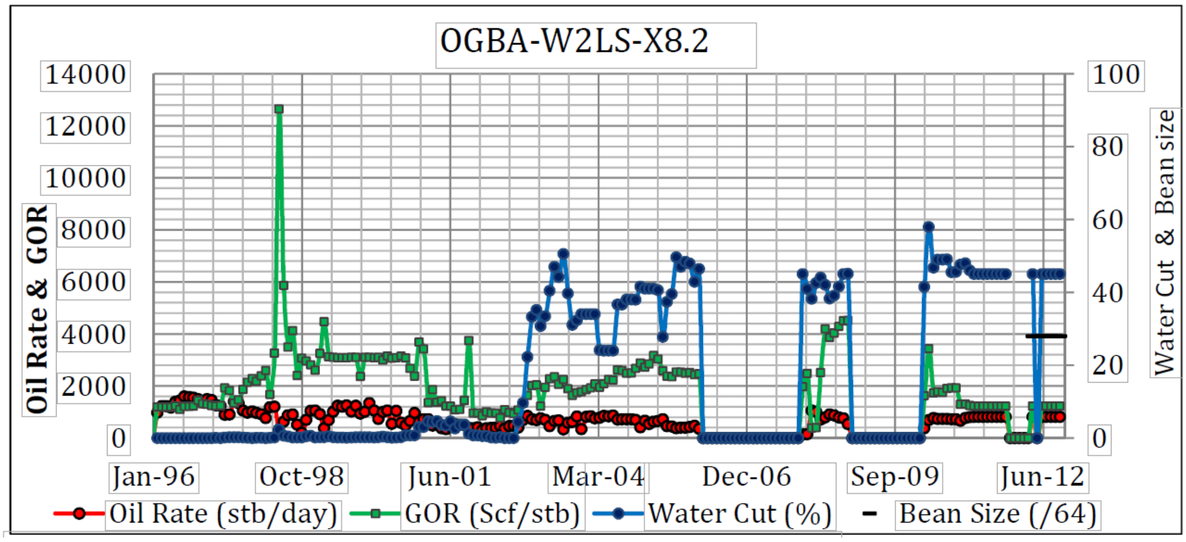

Figure 6-16: Shows the Oil rates, GOR and BSW plot for Well 2LS

6.6.3 Well 4LS

Well4 came on stream in February 1996 and was first shut-in, June 2005, it flowed intermittently between January 2008 and April 2010 and was finally shut-in possibly due to HWCT of about 63%in January 2013. The Production Performance Plots are shown in Figure 6.22 and 6.23

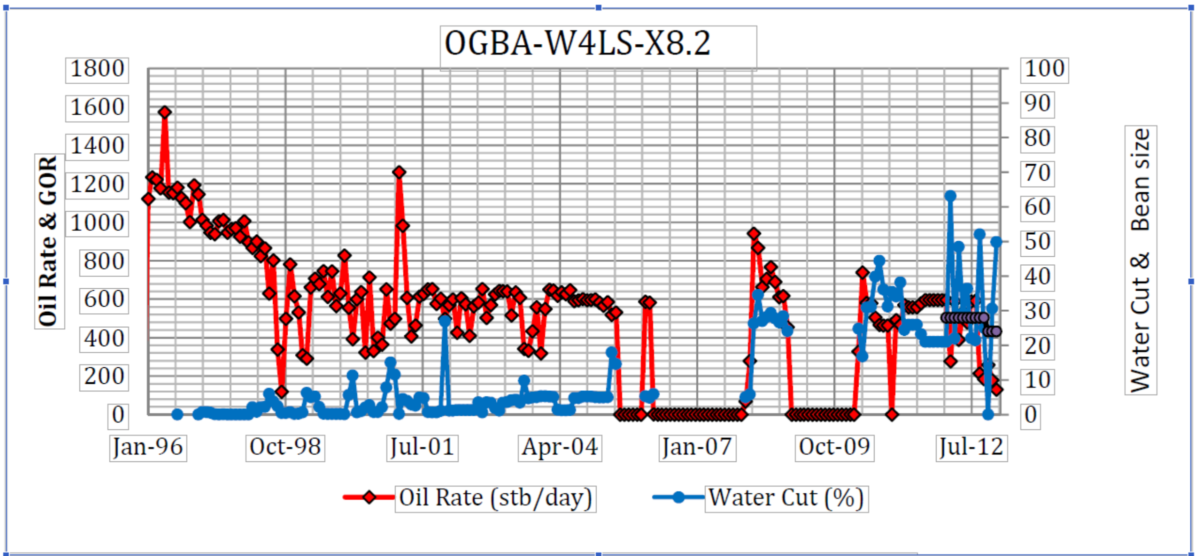

Figure 6-17: Shows the Oil rates, BSW and Bean size plot for Well 4LS

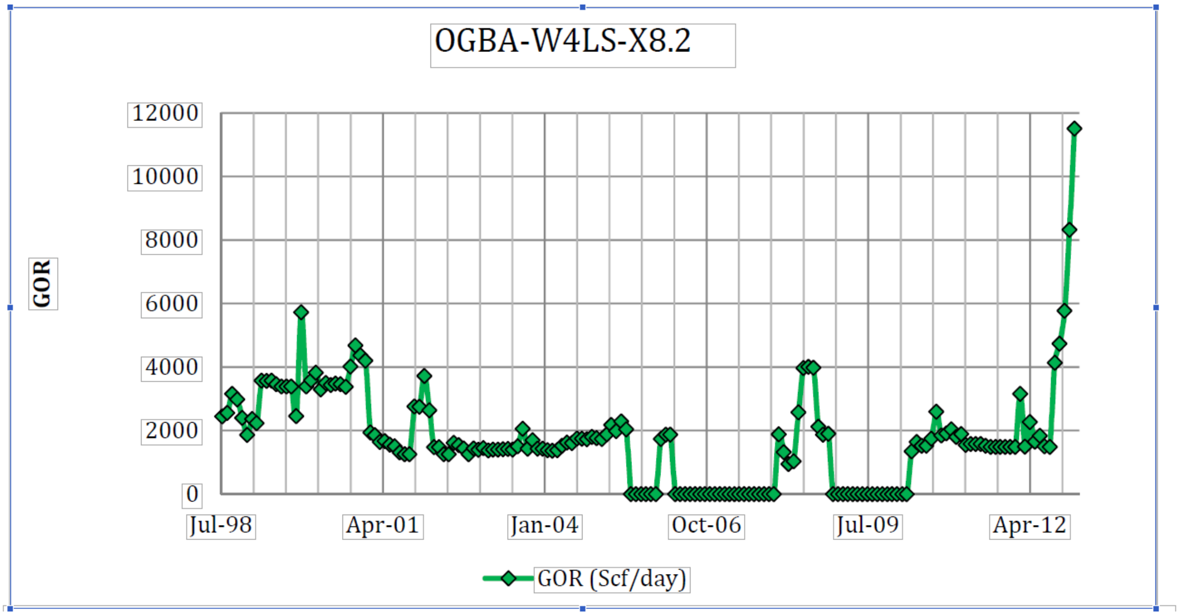

Figure 6-18: Shows the GOR for Well 4LS

6.6.4 Well 5LS

Well5 came on stream February 1996, first shut-in March 2006, reopened again in October 2010 and is still currently on production. The production performance plot is shown in Figure 6.24

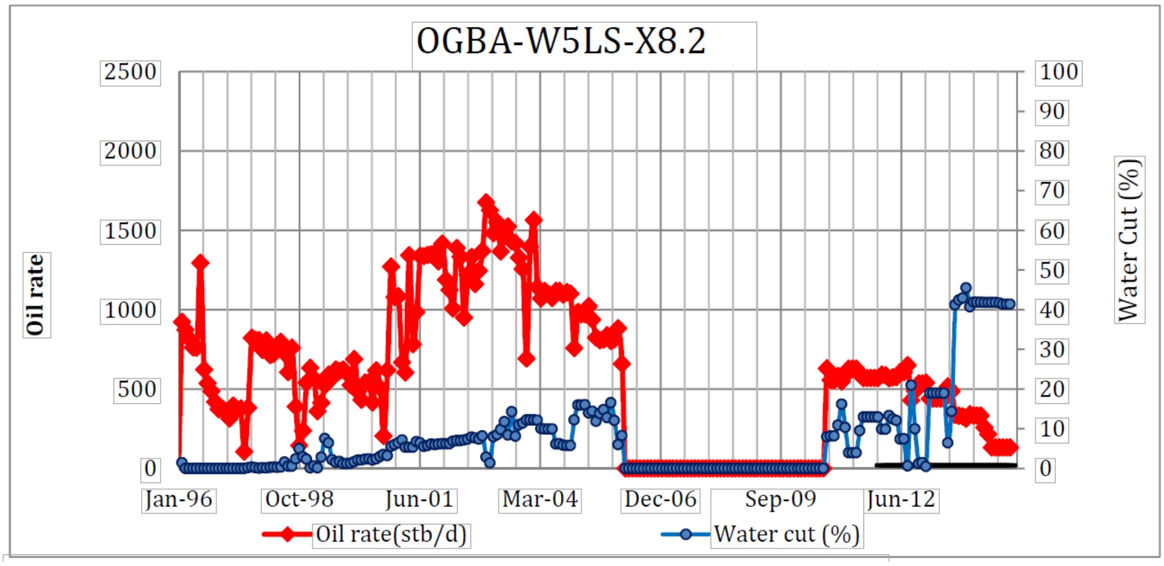

Figure 6-19: Shows the Oil rates, BSW and Bean Size plots for Well 5LS

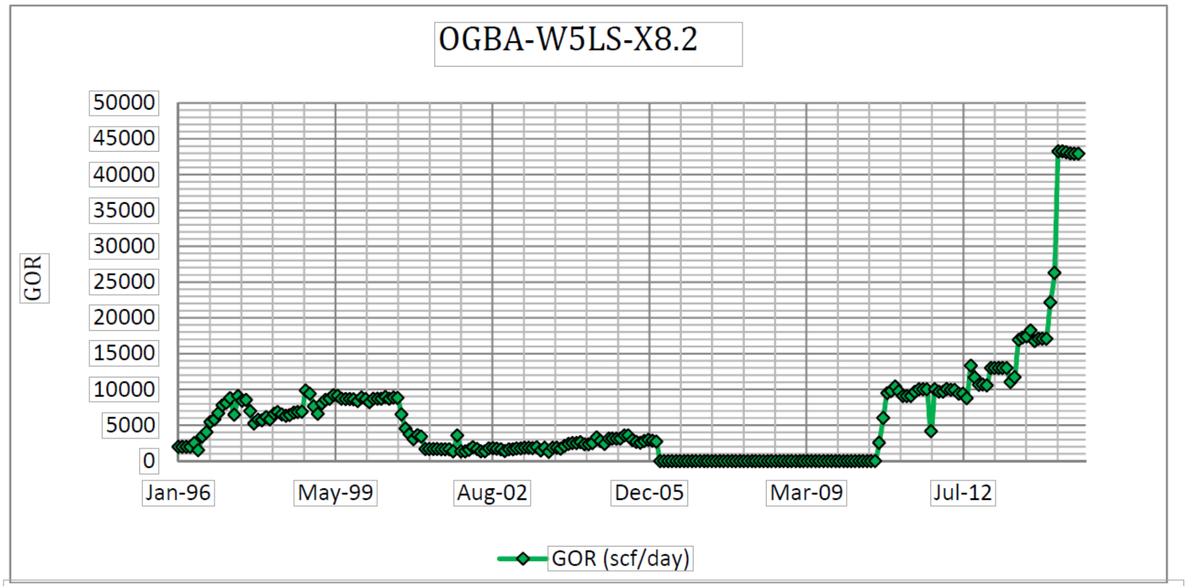

Figure 6-20: Shows the GOR for Well 5LS

6.6.5 Well 7LS.

Well 7 came on stream, January 1996 through sand X8.3, it was switched to X8.2 in September 1996 for unrecorded reasons, and it produced for about two (2) years and was taken back to X8.3 in January 1999.

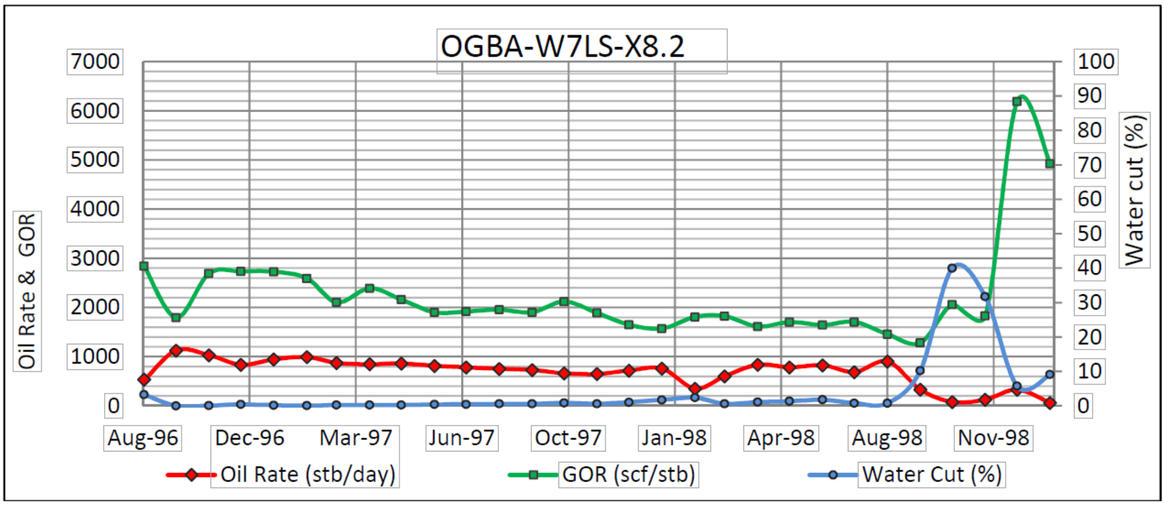

Figure 6-21: Shows the Oil rate, GOR and BSW plot for Well 7LS

6.6.6 Well 8Bss

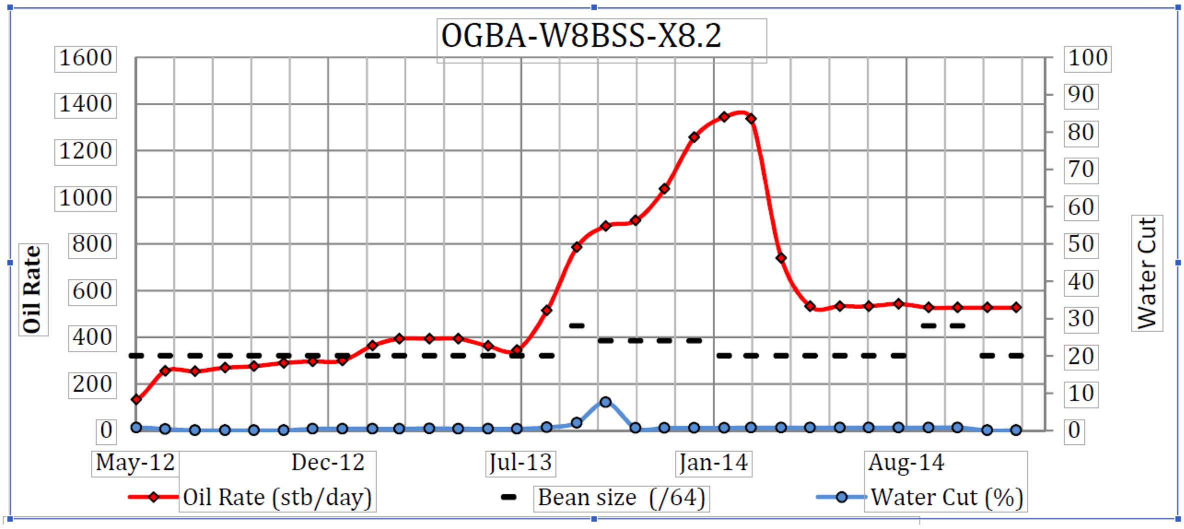

Figure 6-22: Shows the Oil Rates, Bean Size and BSW plots for Well 8bSS.

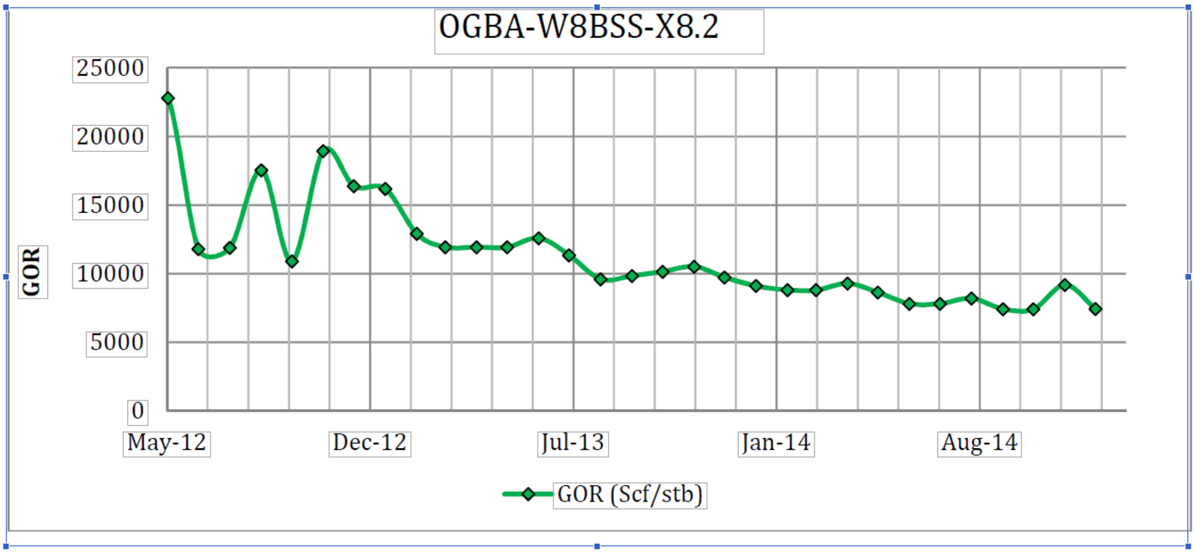

Figure 6-23: Shows the GOR for Well 8bSS

6.6.7 Well 9SS

This string came on stream in February 1996 with an initial GOR of 4447.07Scf/Stb, it was first shut-in May 1999 due to decline in production rate. It was reopened in January 2000 and was finally shut-in July 2000, possibly due to high GOR and low productivity. See the Production Performance Plots below;

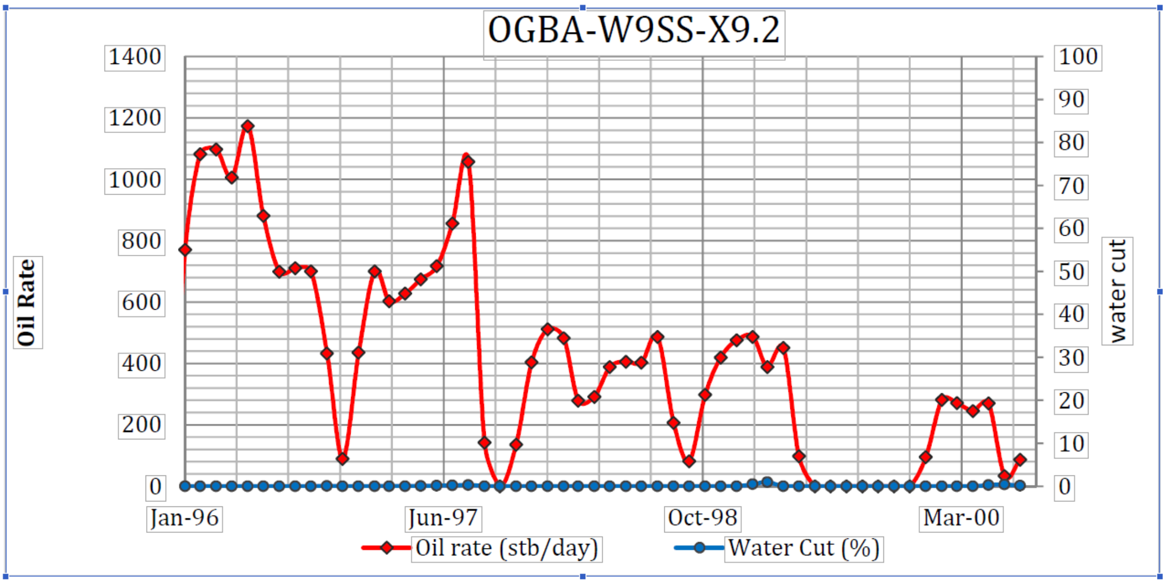

Figure 6-24: Shows the Oil rate and WCUT plots for Well 9SS

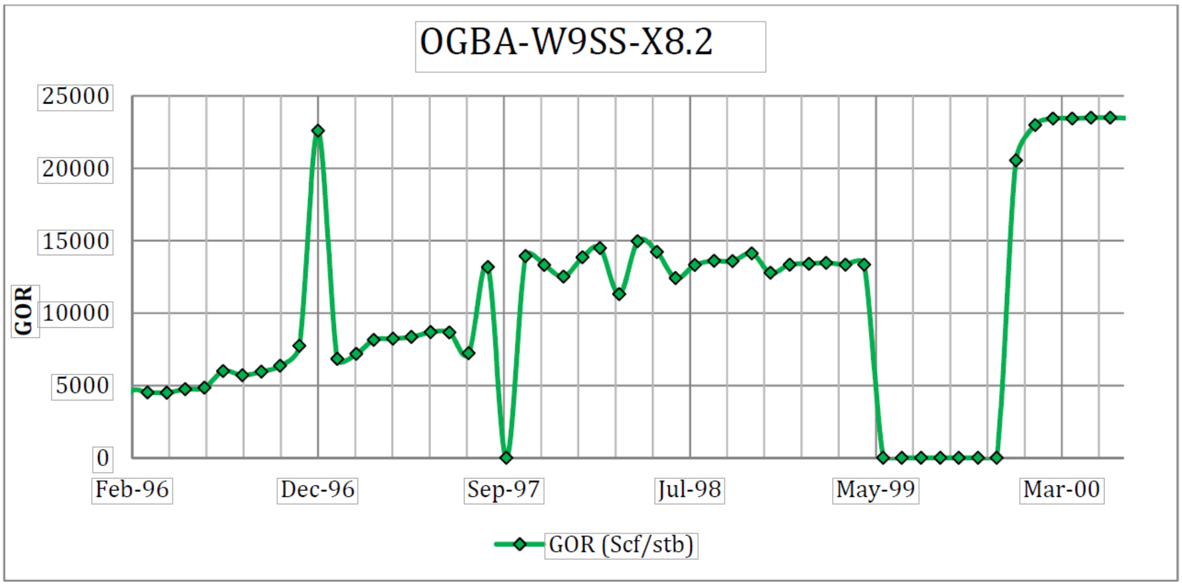

Figure 6-25: Shows the GOR for Well 9SS

Table 6-7: Summary for Reservoir X8.2

Status of Strings[wells] in X8.2									
S/N	**STRINGS**	**STATUS**	**MONTH OF PRODUCTION**	**Np [MMstb]**	**Gp [Bscf]**	**Wp [MMstb]**	**Qo [bopd]**	**GOR [scf/bbl]]**	**WCUT [%]**
1	2LS	Shut-In	156	3.60	7.77	1.020	808.96	1231	45
2	4LS	Shut-In	168	3.05	6.06	0.325	129.92	11514	49
3	5LS	Flowing	170	3.88	19.14	0.365	133.00	42932	41
4	7LS	Shut-In	27	0.68	1.27	0.010	57.19	4922	9
5	8LS	Flowing	31	0.42	4.34	0.005	527.01	7419	1
6	9SS	Shut-In	30	0.68	6.48	0.004	87.00	23461	0
	Total			12.24	45.07	1.72	-	-	-

6.6.8 Reservoir X8.3

Reservoir X8.3 is saturated, with initial pressure of 4303 psia and bubble point pressure of 4303 psia. The Reservoir came on production in January 1996 through well 7LS and was switched to X8.2 in September 1996. It flowed intermittently between January 1999 and January 2003 before the final shut-in January 2004. The cumulative oil, gas and water produced, as at end of history from this reservoir were about 0.77MMSTB, 1.42BSCF, and 0.275 MMSTB, respectively.

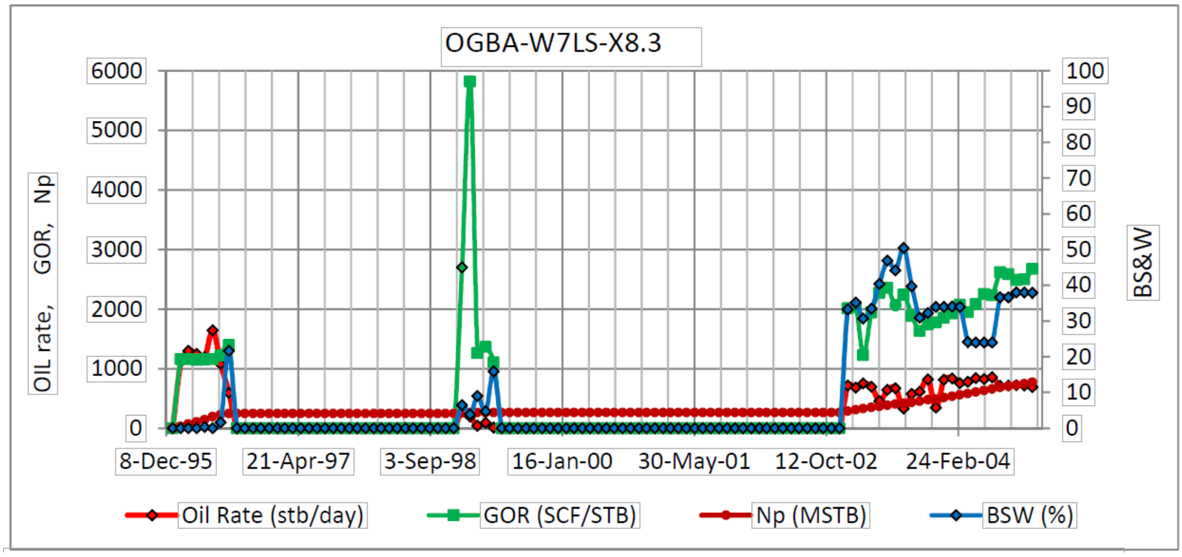

Figure 6-26: Shows the Np, Oil rate, GOR and Water cut plot for Well 7LS (Reservoir X8.3)

Table 6-8: Summary for Reservoir X8.3

Status of Strings [Wells] in X8.3									
S/N	Strings	Status	Months of Production	Np [MMstb]	Gp [Bscf]	Wp [MMstb]	Qo [bopd]	GOR [Scf/bbl]	Water Cut [%]
1	7LS	Shut-In	36	0.77	1.42	0.275	692	2675	37
	TOTAL			0.77	1.42	0.28	-	-	-

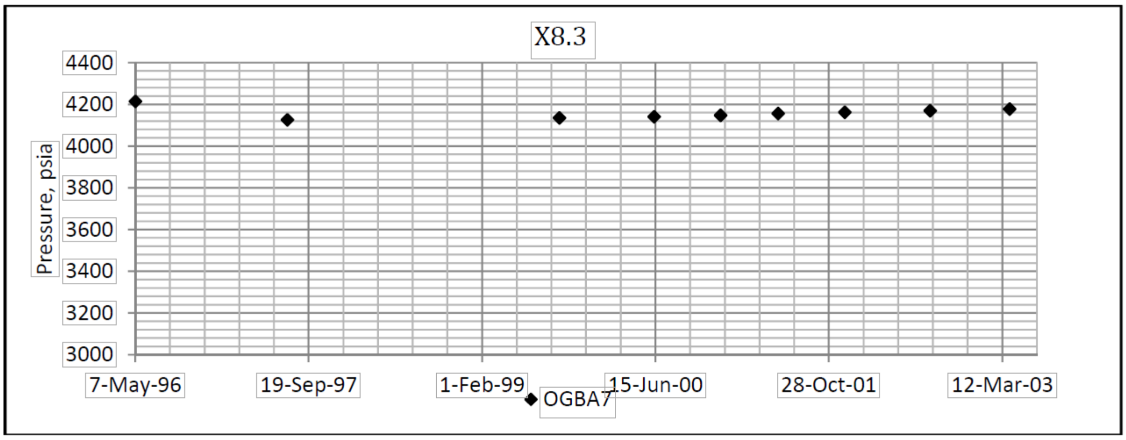

Figure 6-27: Shows the Pressure plot for Reservoir X8.3

6.6.9 FETKOVICH and Historical Regression for Gas wells

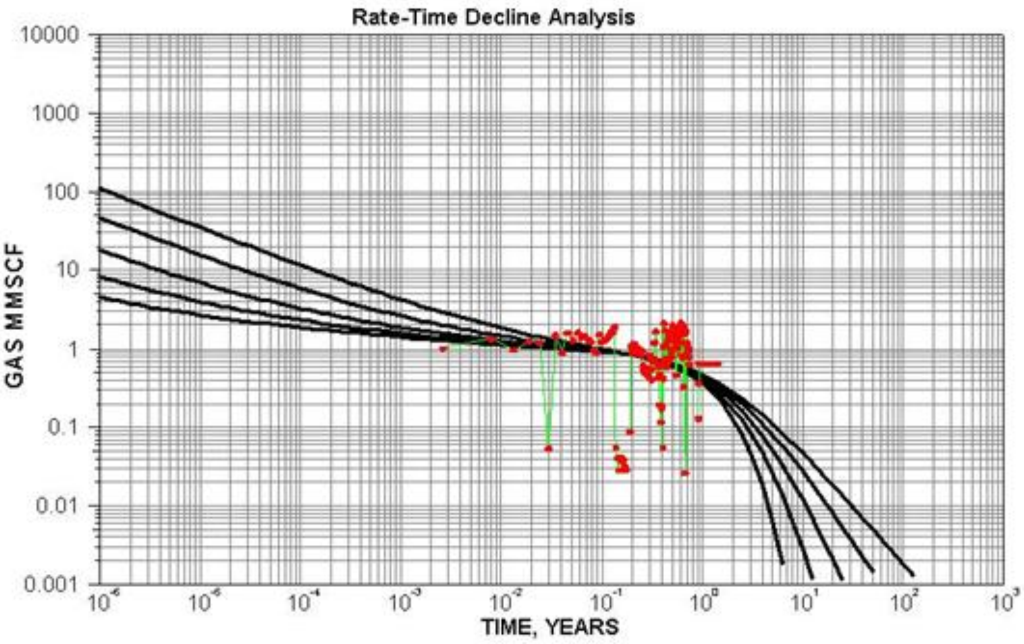

Figure 6-28: BS_25S Rate-Time Decline Analysis

The Cumulative Production is **120816 MMcf** through **12/31/2015** in this well at Ogba Essale the name of the well is BS_25S, this is a gas well. The well is at the middle time region as can be seen from the Rate-Time decline curve analysis in Figure 6.28.

Table 6-9: ARPS for BS 25S

Historical Regression									
	Cumulative Production 120816 MMcf thru 12/31/2015								
	b Value	**Di (A.e.)**	**qi (Mcf)**	**ti**					
	0	**-0.00004**	**432921.1**	**2/28/1994**					
Working forecast									
	EUR 1.51872e+006 MMcf								
#	**b Value**	**Di (A.e.)**	**qi (Mcf)**	**ti**	**te**	**qe (Mcf)**	**Res. (MMcf)**	**Ended By**	**Reserves Type**
1	**0**	**-0.00004**	**402738.5**	**12/31/2015**	**12/31/2025**	**402890.9**	**1397908**	**Time**	**Proven Developed**

Using the ARPS the well EUR 1.51872e+006 MMcf this is a proven and developed reserve and the forecast was extended by time from 12/31/2015 to 12/31/2025 for a period of ten years[10yrs]. This is evident in the table above table 6.12.

Working forecast	Parameters
Phase	: Gas
b	: 0
Di	: 0.0722597 A.e.
qi	: 402738 Mcf
ti	: 12/31/2015
te	: 12/31/2025
Final Rate	: 197484 Mcf
Cum. Prod.	: 120816 MMcf
Cum. Date	: 12/31/2015
Reserves	: 999544 MMcf
Reserves Date	: 12/31/2025
EUR	: 1.12036e+006 MMcf
Forecast Ended By	: Time
Reserve Type	: Proven-Developed

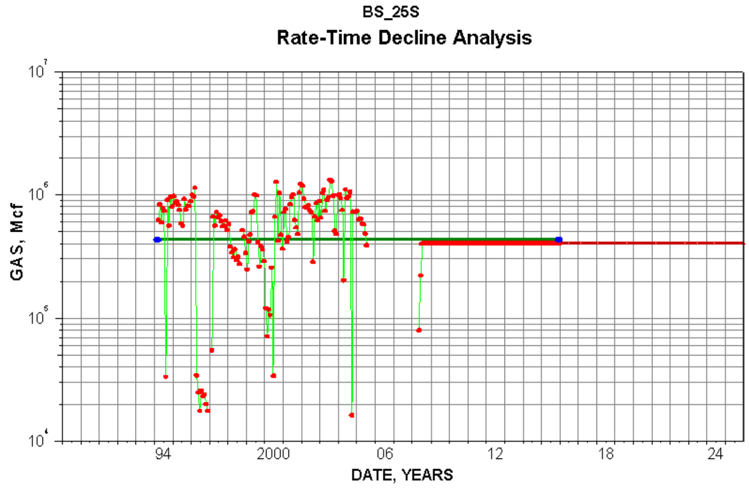

Figure 6-29*:*BS-25S Rate-Time Decline analysis**.**

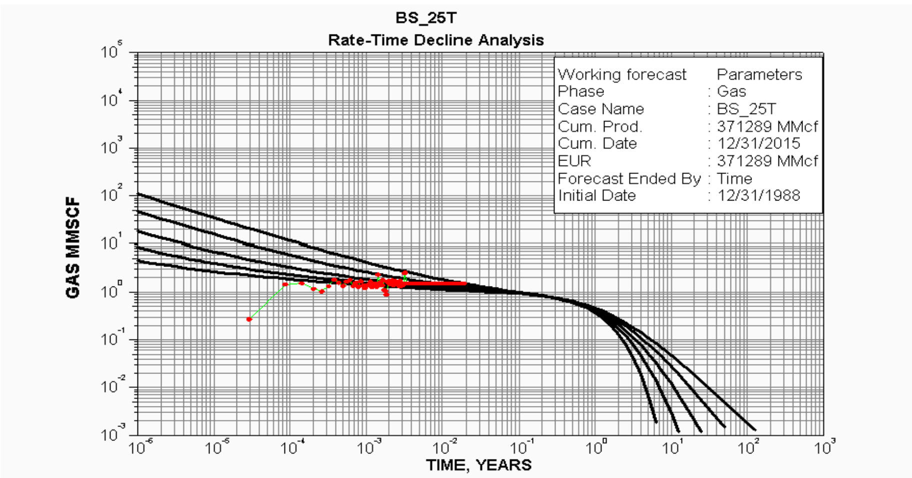

Figure 6-30*:* BS_25T: Rate-Time Decline analysis

The Historical Regression and Cumulative Production of **371289 MMcf** thru **12/31/2015** from this well at Ogba field, this well is tilting toward middle region left early time, so it is in between the early time to middle time region as indicated by the decline curve analysis curve in figure 6.30

Table 6-10: *ARPS for BS_25T*

BS_25T: Gas: UTOROGU_025: D4200X										
Historical Regression										
	Cumulative Production 371289 MMcf thru 12/31/2015									
	b Value	**Di (A.e.)**	**qi (Mcf)**	**ti**						
	0	**-0.00205**	**1081670.57**	**12/31/1988**						
Working forecast										
	EUR 4.39966e+006 MMcf									
#	**b Value**	**Di (A.e.)**	**qi (Mcf)**	**ti**	**te**	**qe (Mcf)**	**Res. (MMcf)**	**Ended By**	**Reserves Type**	
1	**0**	**-0.00205**	**1149551**	**12/31/2015**		**1172114**	**4028368**	**Time**	**None**	
Database Forecast										

Using the ARPS the well **EUR 4.39966e+006 MMcf** this is an undefined reserve and the forecast was extended by time from 12/31/2015 to 12/31/2025 for a period of ten years[10yrs]. This is evident in the table above table 6.13. The total reserve is **4028368 MMcf**

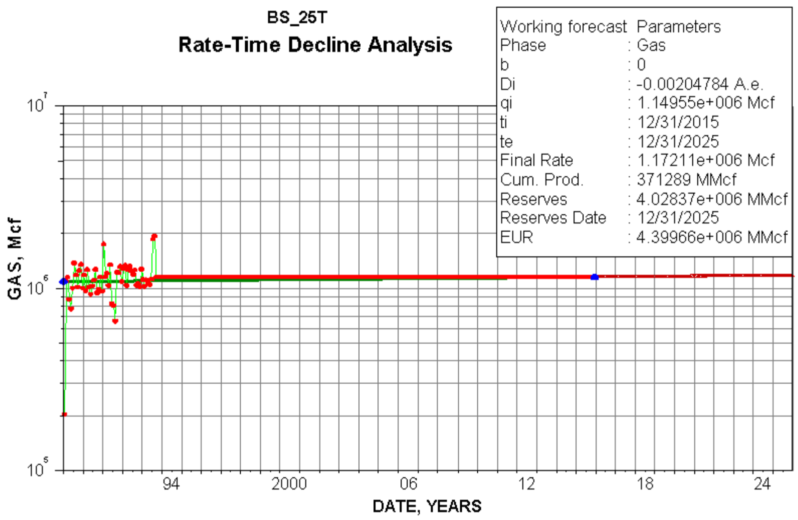

Figure 6-31: BS-25T Rate-Time Decline Analysis.

6.6.10 FETKOVICH and Historical Regression for Oil wells

Historical Regression

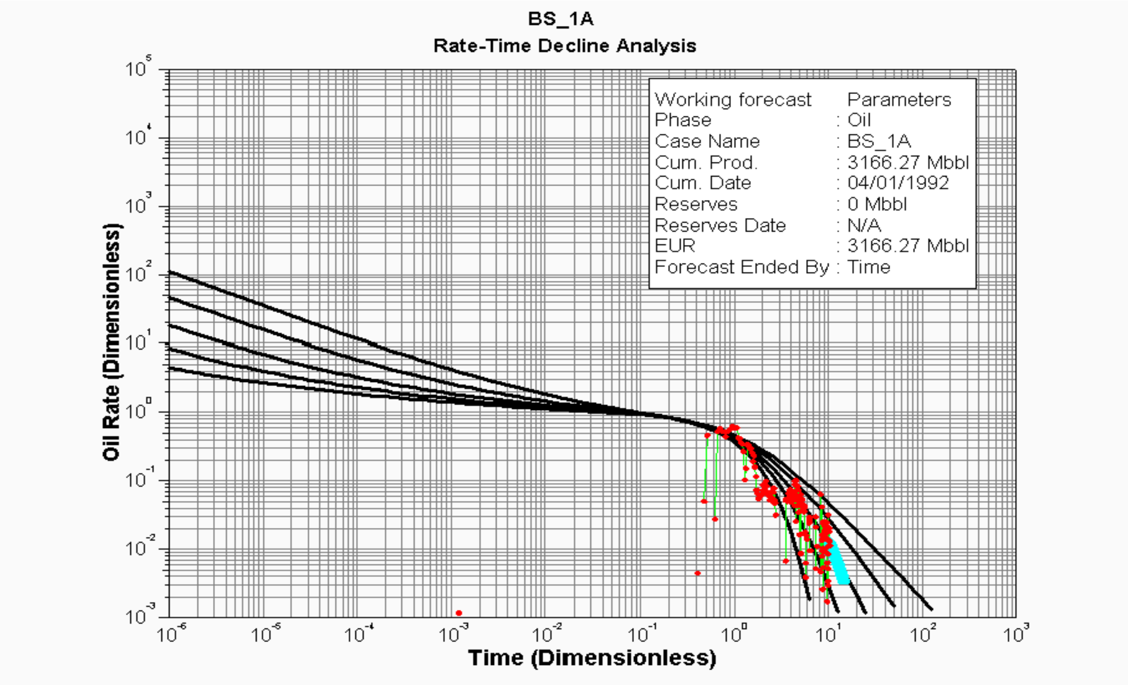

Figure 6-32:BS-1A Rate-Time Decline Analysis

Cumulative Production **3166.27 Mbbl** thru **04/01/1992** with an **EUR 7926.7 Mbbl** This well is already at the late time region of the decline curve analysis see figure 6.33 and this is an oil well, this is proven and developed reserve.

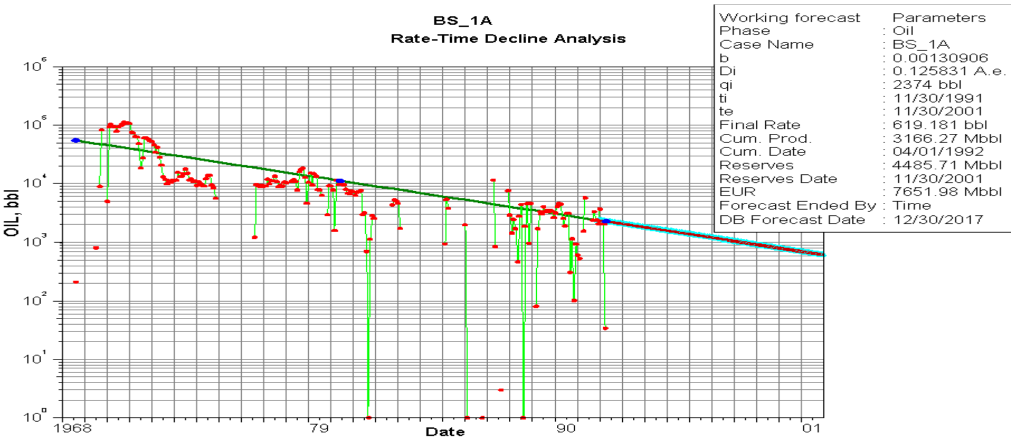

Figure 6-33*:* BS-1A

6.6.11 Reservoir summary

6.6.11.1 Field Gas Condensate Reserves.

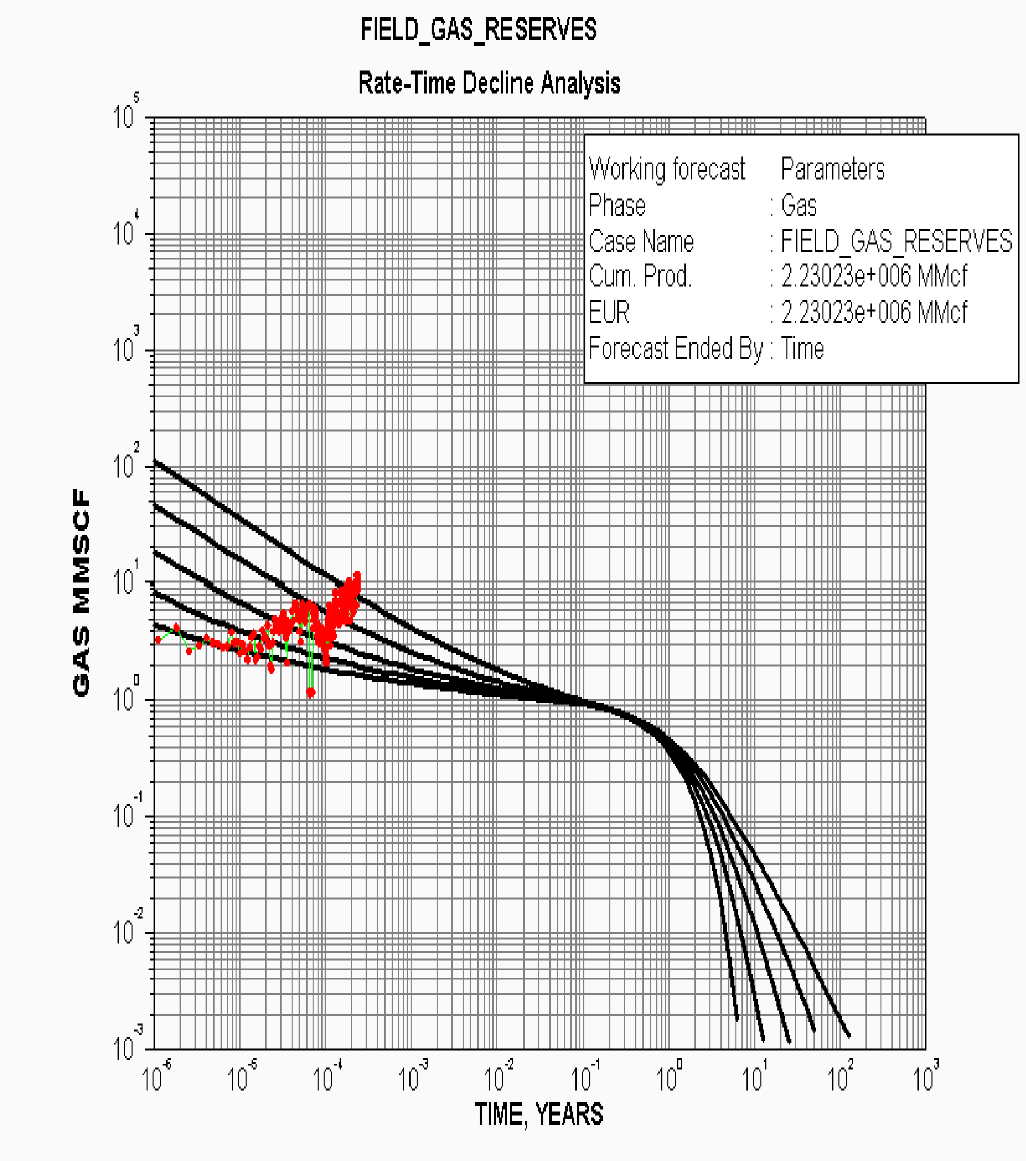

Figure 6-34*:* Gas Field Reserves

Cumulative Production 2.23023e+006 MMcf thru 12/31/2015 with an EUR of 2.23023e+006MMcf for the entire gas reserves in the field and the forecast was extended by time. Generally, the Gas field is in the early time region of the decline curve analysis see figure 6.34

Table 6-11: Arps For Entire Gas Fields.

FIELD_GAS_RESERVES: Gas: WELLTYPE: GASCOND										
Historical Regression										
	Cumulative Production 2.23023e+006 MMcf thru 12/31/2015									
	b Value	Di (A.e.)	qi (Mcf)	ti						
	0	-0.04695	3332502.7	12/31/1988						
Working forecast										
	EUR 5.2261e+007 MMcf									
#	b Value	Di (A.e.)	qi (Mcf)	ti	te	qe (Mcf)	Res. (MMcf)	Ended By	Reserves Type	
1	0	-0.04695	11501733	12/31/2015	12/31/2025	17786781	50030796	Time	None	

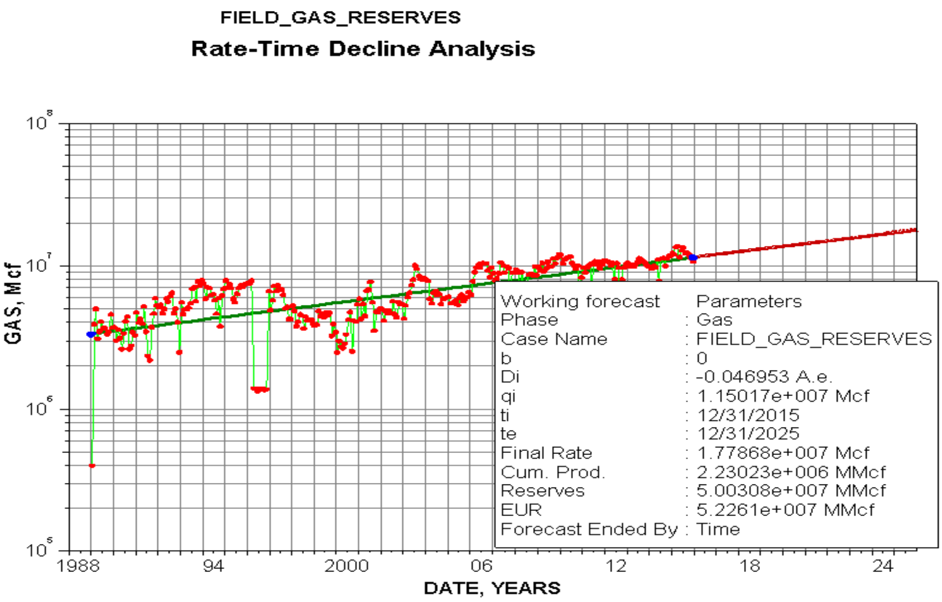

Figure 6-35*:* Field Gas Reserves

The Historical Regression and Cumulative Production of 371289 MMcf thru 12/31/2015 from this well at Ogba field, this well is tilting toward middle region left early time, so it is in between the early time to middle time region as indicated by the decline curve analysis curve in figure 6.35. This is total from Gas field at Ogba Essale field.

6.6.11.2 Field oil reserves

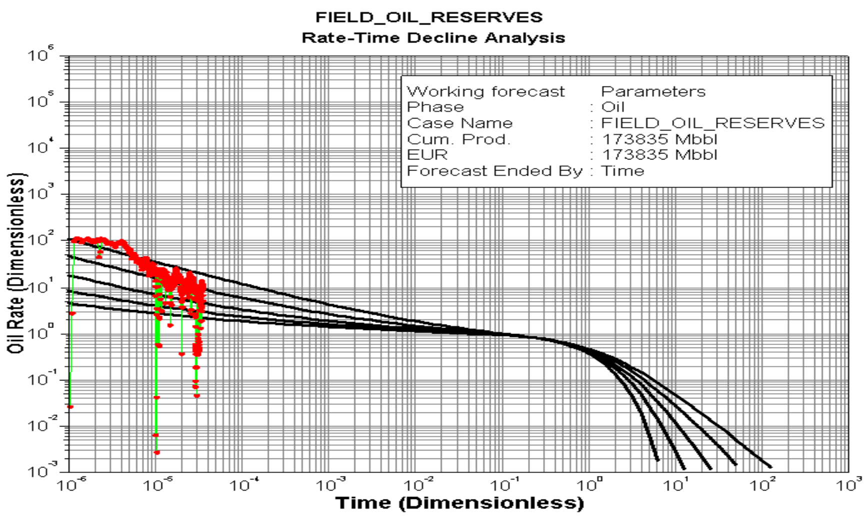

Figure 6-36*:* Oil Field Reserves

Figure 6.36 as shown above is in the middle region of the decline curve analysis, this is an oil phase with a cumulative production of 173835bll and the duration of forecast is ten years from 2014.

Table 6-12*:* Arps for the entire oil field

<table>
<tr><td colspan="4">FIELD_OIL_RESERVES: Oil: WELLTYPE: OIL</td><td></td><td></td><td></td><td></td><td></td><td></td></tr>
<tr><td colspan="3">Historical Regression</td><td></td><td></td><td></td><td></td><td></td><td></td><td></td></tr>
<tr><td></td><td colspan="5">Cumulative Production 173835 Mbbl thru 12/01/2014</td><td></td><td></td><td></td><td></td></tr>
<tr><td></td><td>b Value</td><td>Di (A.e.)</td><td>qi (bbl)</td><td>ti</td><td></td><td></td><td></td><td></td><td></td></tr>
<tr><td></td><td>1</td><td>0.13567</td><td>684567.5</td><td>7/31/1968</td><td></td><td></td><td></td><td></td><td></td></tr>
<tr><td colspan="2">Working forecast</td><td></td><td></td><td></td><td></td><td></td><td></td><td></td><td></td></tr>
<tr><td></td><td colspan="2">EUR Mbbl 452690</td><td></td><td></td><td></td><td></td><td></td><td></td><td></td></tr>
<tr><td>#</td><td>b Value</td><td>Di (A.e.)</td><td>qi (bbl)</td><td>ti</td><td>te</td><td>qe (bbl)</td><td>Res. (Mbbl)</td><td>Ended By</td><td>Reserves Type</td></tr>
<tr><td>1</td><td>1</td><td>0.01862</td><td>82745.56</td><td>12/1/2014</td><td>12/31/2024</td><td>69457.29</td><td>278855.1</td><td>Time</td><td>None</td></tr>
</table>

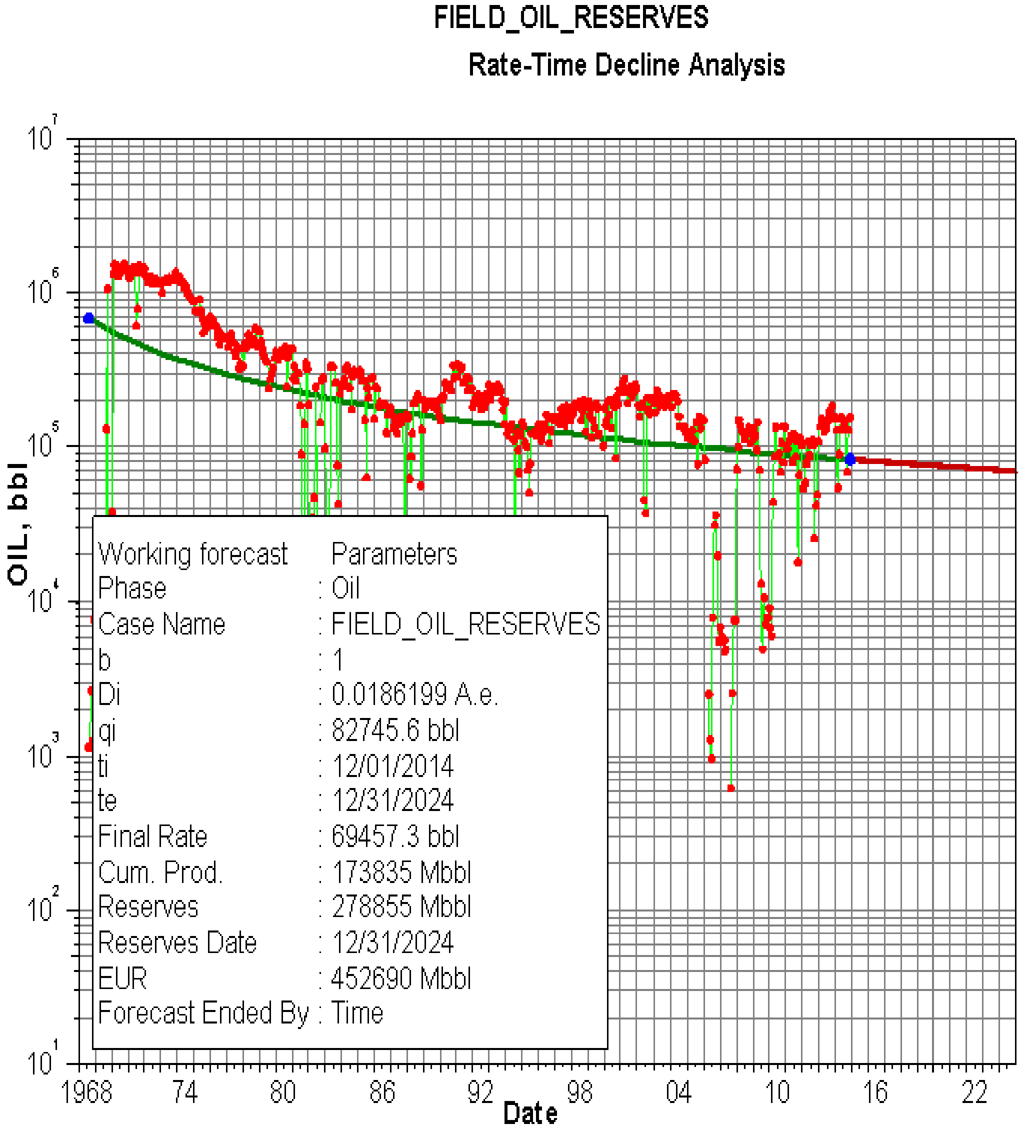

Figure 6-37*:* Oil Field Reserves Rate Decline Analysis.

The Historical Regression and Cumulative Production of 173835 Mbbl thru 12/01/2014 from this well at Ogba field, Final rate of production is 69457.3 bbl Total reserve stood at 278855 bbl reserve date 12/31/2024 this is forecasted in the next ten years from 2014 and finally the EUR stood at 452690 bbl as indicated by the decline curve analysis curve in figure 6.37

6.7 Phase VI: Material balance analysis Results and discussions

The matched result is shown in Table 6.5 and the material balance solution plot for each reservoir is shown below

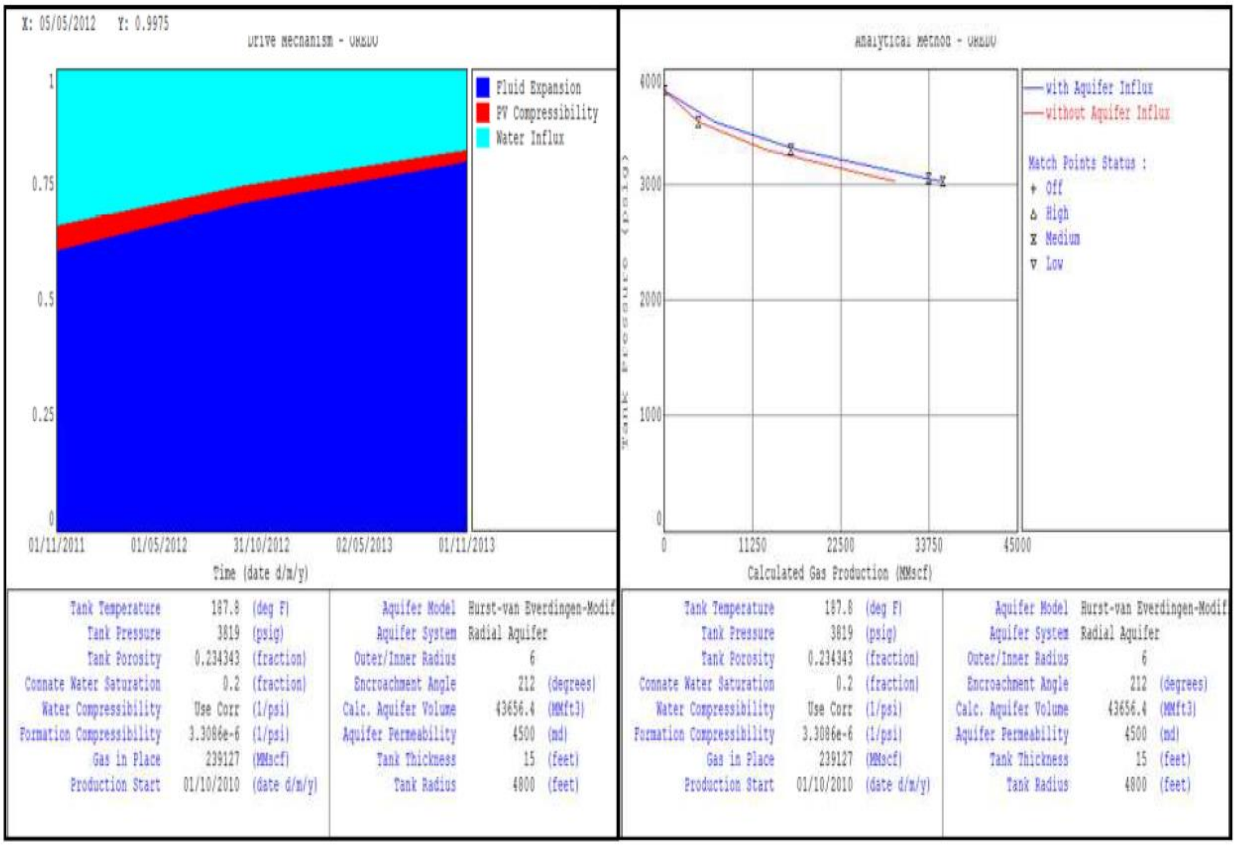

Figure 6-38: X8.1 Energy, pressure and simulated vs History plots

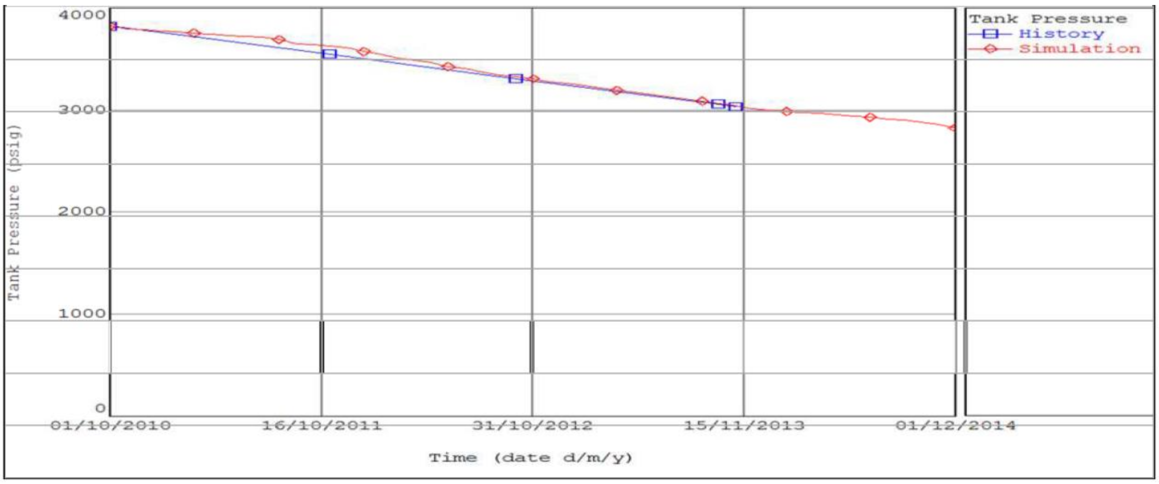

Figure 6-39: X8.1 Energy, pressure and simulated vs History plot

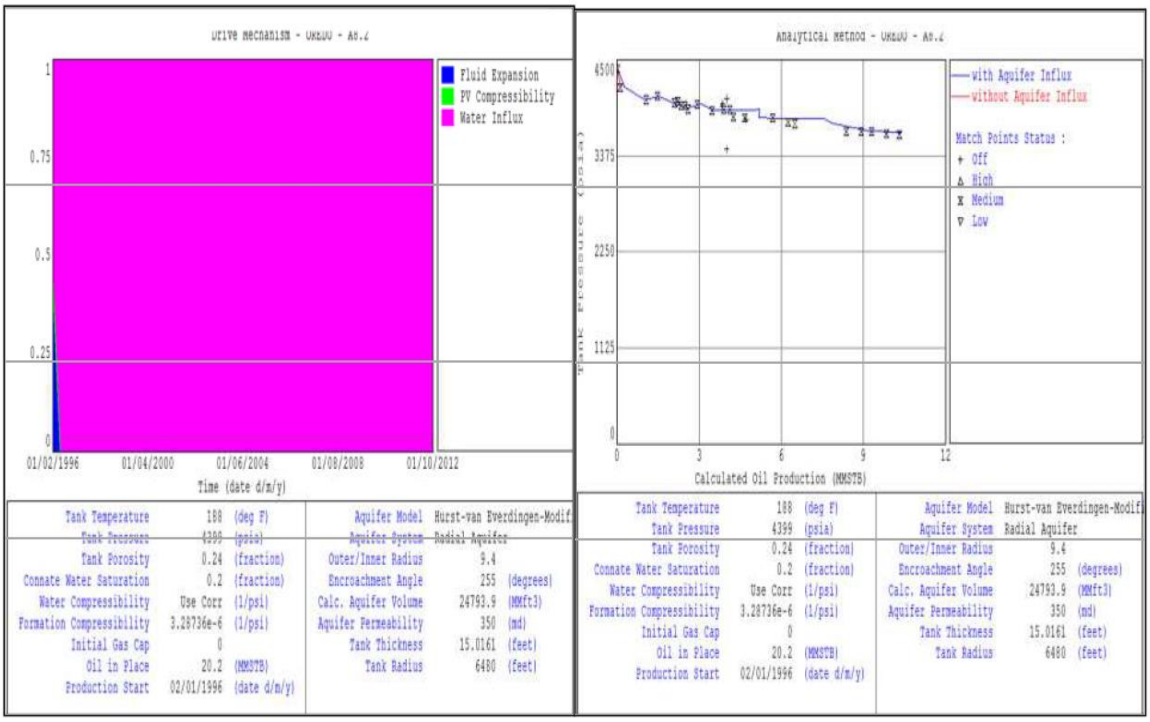

Figure 6-40*:* X8.2 Energy, pressure and Simulated vs History plots

X8.3

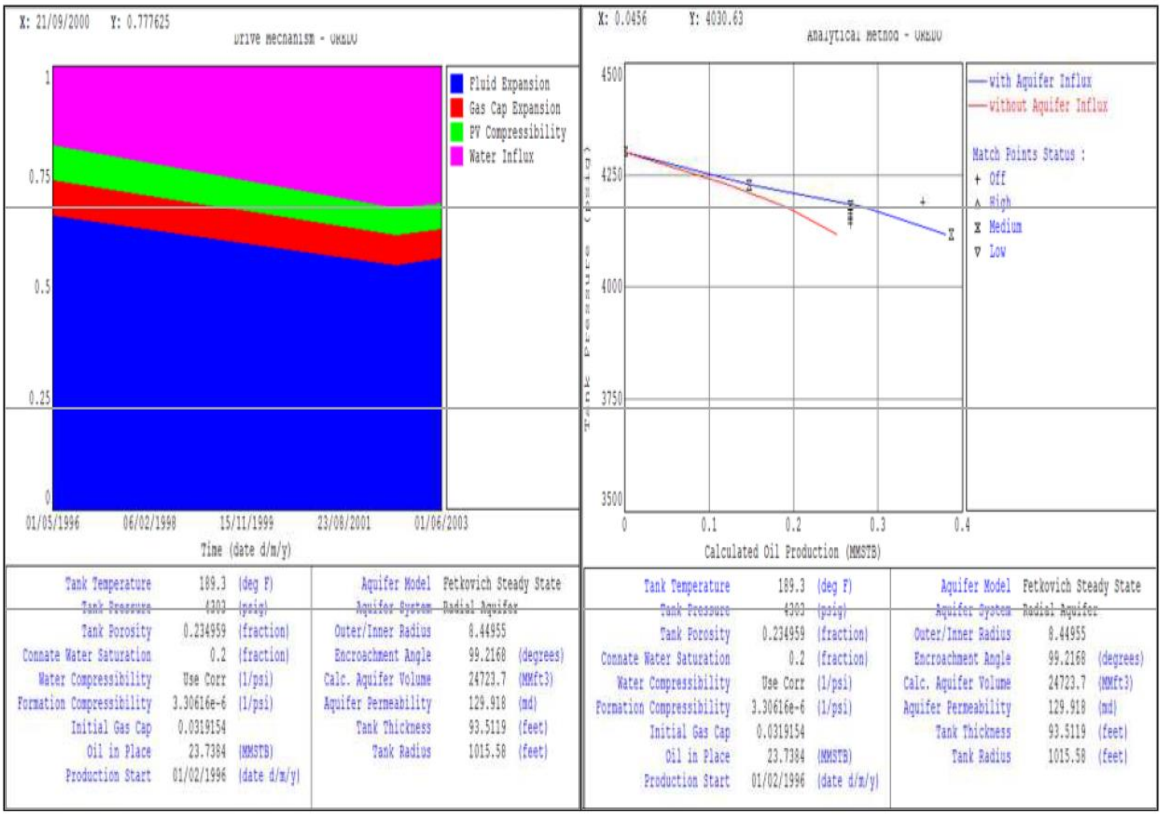

Figure 6-41: X8.3 Energy, pressure and Simulated vs History plots

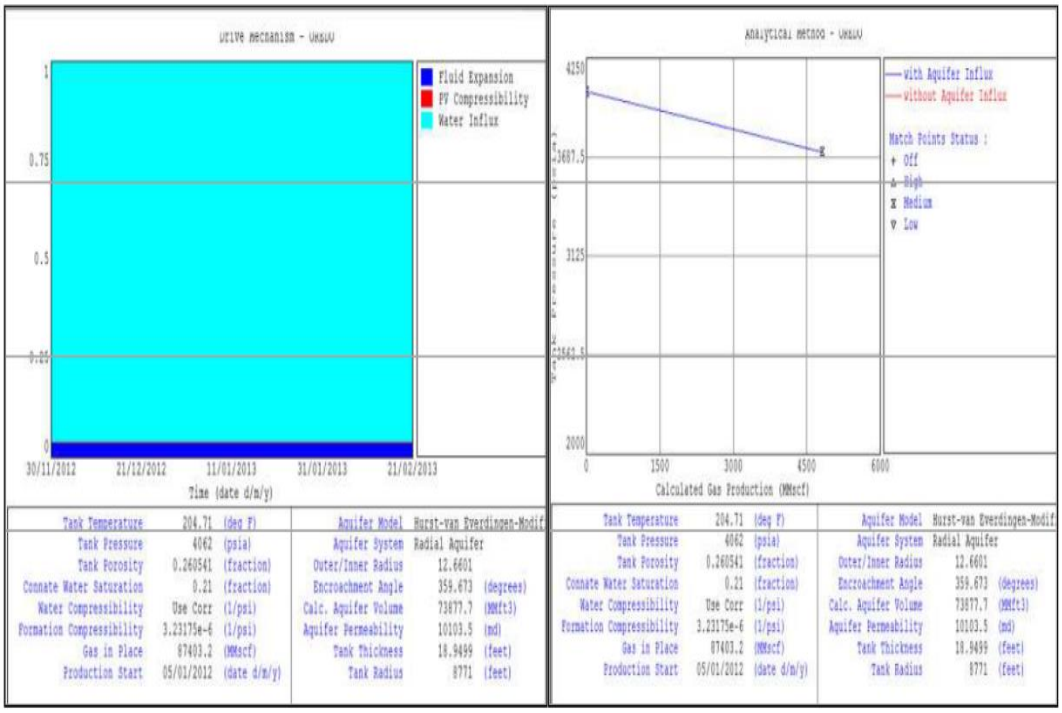

Figure 6-42*:* Y1.1 Energy, pressure and simulated vs History plots

Y1.1 Energy, pressure and Simulated vs History plots from the results of material balance analysis, water drive is the primary drive mechanism for most of the OGBA reservoirs.

The volume of initial hydrocarbon obtained from material balance analysis and static model volume estimates are comparable and within 2 -6% difference.

Table 6-13*:* Material Balance Result

RESERVOIR	AQUIFER MODEL	DRIVE MECHANISM	MATERIAL BALANCE VOLUME[MMSTB]	STATIC STOIIP [MMSTB]	PERCENTAGE DIFFERENCE
X8.1	Hurtst-van Everdigen modified	Combination drive	239.13	244.05	2
X8.2U	Hurtst-van Everdigen modified	Water Drive	20.2	21	3.8
X8.3	Fetchkovich Steady State	Combination drive	23.74	22.4	5.9
Y1.1	Hurtst-van Everdigen modified	Water Drive	87.4	89.8	2.7

6.8 Chapter Summary

This chapter summarizes research findings (Buff Brea, Boise, Castle gate sandstone) and computational modelling and computer simulation performed to look at the effects of parameters including such initial reservoir pressure, surface velocity, porosity and permeability on pore-scale methane transport using sandstone samples. Such parameters were calculated using experimental methods in chapter 4, 5 and applied to the model produced to investigate their impact in sandstone reservoirs on fluid flow and gas production. The section is broken down into three stages. The section is broken down into 6 (six) stages as follows: Phase 1; Porosity and permeability (petrophysical results), Phase 2: PVT Analysis for gas composition and fluid properties, Phase 3; Core flooding, Phase 4; Single Phase flow of Buff Bera, Phase V: Ogba wet gas field production history results and discussions, Phase VI: Material balance analysis Results and discussions. The next chapter will highlight recommendations and conclusions of the research.

Chapter 7 Conclusions and recommendations

The aims of the thesis were achieved through the cautious execution of the objectives. The core sample characterisation was carried out and the respective porosities and permeabilities of the core samples used in this experiment were obtained and analysed. The experiment has shown that the equipment and methodology used were accurate and well within the source company range for both the core taster with the aid of the equipment accuracy.

The volumetric results have shown an appreciable result. They were obtained by core flooding equipment and has simulated the real reservoir conditions. The consequence of the aquifer water salinity on the performance of the natural gas reservoir was experimentally evaluated and results show that the salinity plays a vital part in assessing the presentation of production from natural gas reservoir. The advanced the salinity of the aquifer the higher the natural gas production and the lower the produced water as seen in the WGR vs Time graph. There was a production increase of about 50% when 0wt% salt encroached the reservoir compared to when 10wt% NaCl aquifer water influx into the reservoir. With this development, a better characterisation of the natural gas reservoir will be carried out for adequate evaluation of the performance of the reservoirs.

This thesis also presented the experimental results of porosity and permeability of various sandstone samples and implement the core sample SEM result into COMSOL Multi physics software to characterize gas transport of single-phase flow at pore scale level. The porosity and permeability value by the experiment deviated slightly from the factory porosity values. The experimental result show that the instrument used for these determinations are highly efficient. The deviation might have occurred because of human errors and leak in the system.

Considering the model, the Buff Berea SEM image is converted to a grey image of the pore-scale finite element mesh. A pore scale model was created when the SEM image is imported as a DXF into the COMSOL software which removed some part of the organic component of the sample. Navier-Stoke equation and Darcy Law were used to describe single-phase gas transport and free gas at the pore spaces. The inlet and outlet pressure, fluid pressure, porosity and permeability are the most important parameters which were known and recorded.

The vital assumptions made in the model such as the same permeability through the formation reduce the number of unknowns for the result and problem encountered. Also, the distribution of pressure at the initial condition (t=0) of the pore system is assumed to be same through the formation. The simulation model at different initial reservoir pressure in the software give a satisfactory result on how changes in pressure is directly proportional to velocity of gas in sandstone reservoirs.

The following conclusions were derived from the Ogba Egase Ishelle Field Study:

Detailed 3D static and dynamic modelling has been carried out on the Ogba Egase Ishelle reservoirs. Several development scenarios ranging from completion of existing wells to drilling of new infill wells have been considered and evaluated. Do Nothing Case: An additional recovery for the field is about 30.23MMSTB and 27.8BSCF of oil and gas Respectively. Case 1: An additional recovery for the field is about 37.21MMSTB and 26.0BSCF of oil and gas respectively. Consequently, 75.9132 MMSTB of Oil and 2,188.54 BCF of Gas was obtained using simulation.

Table 7-1: Summary of results findings

METHOD	APPLICATION	VOLUMES	ACCURACY
VOLUMETRICS	OOIP, OGIP Recoverable reserves. Use early in the life of the field	STOOIP=1548.297365 MMSTB GIIP= 3007862.483 MMSCF	Dependent on the quality of reservoir description. Reserve estimate is often high because this method does not consider problem of reservoir heterogeneity
RESERVOIR SIMULATION	A simulation reservoir model reflects t a set of interconnected tanks each with fluid and rock characteristics. The model characterizes the reservoir by integrating the basic geological model and the dynamic flow model with the actual performance data of the reservoir (such as PVT data, rate of production, pressure, tests, etc.).	EUR=2,188.54 BCF EUR=75.9132 MMSTB	For any oil and gas recovery project, reservoir simulation can be used during any production phase to estimate directly both the original in-place and the recoverable quantities of petroleum or the EUR

MATERIAL BALANCE	OOIP, OGIP (assumes adequate production History available) recoverable reserves (assumes OOIP and OGIP known). Use in mature field with abundant geological, petrol physical, and engineering data.	GIIP=370.47MMSCF STOOIP=377.26	High dependent on the quality of reservoir description and amount of production data available. Reserve estimate is variable
PRODUCTION PERFORMANCE TREND (DECLINE CURVE ANALYSIS)	Recoverable reserves. Use after a moderate amount of production data is available	EUR=52261bscf GAS EUR=452.6MMSTB	Dependent on the amount of production history available. Reserve estimates tends to be realistic

Table 7.1 is the summary of reserve results finding from various, analytical, modelling and simulation.

Recommendations:

The following recommendations are made to optimize recovery from this asset:

- It is recommended that OGBA-3 and OGBA-15 be completed well and that six additional producers' wells be drilled to optimize recovery. It is also suggested to carry out profound exploration operations at D and C concentrations to improve reserves in OGBA ESSALE Field. A detailed management policy for reservoirs is suggested.
- For the core flooding experiment, the use of different core samples of different petrophysical properties and different simulated brine salinities and composition is recommended to cover a wider spectrum of different gas reservoirs.
- I recommend that other porous media modelling techniques could be explored as an extension to this study. These include using reconstructed media (developed by Professor P. Adler of CNRS France for fontainebleu sandstone systems) (Adler, 1992) and possibly Lattice Boltzmann methods (LBM) (Z.Benamram, 2015) as an alternative to finite element methods (used in COMSOL) for the numerical flow simulations which could resolve in greater detail the microscopic details of porous media flows. These approaches would certainly improve the methods used in the research I conducted, enhance accuracy of the simulation and would constitute good pathways for subsequent research.
- Additionally, it is noteworthy that, at the reservoir inlet/outlet due to inherent unsteady conditions, the Darcy model adopted in this study is not reliable. A non-Darcy flow model (F.A.L.Dullien, 1991) should be explored in which both Darcian (low velocity linear drag) and Forchheimer (high velocity quadratic drags) contributions are included. These are available in COMSOL Multiphysics software and also ANSYS FLUENT or CFX CFD software and details are given in (Beg, 2019), (O.Anwar Beg, 2016).
- Finally, the isotropic porous media case could be extended to anisotropic porous media to better simulate the reservoir structure (O.Anwar Beg M. U., 2016).

References

Adelman, M. A., & Watkins, G. C. (2005). U.S. oil and natural gas reserve prices, 1982-2003. *Energy Economics*, *27*(4), 553–571. http://doi.org/10.1016/j.eneco.2005.03.008

Akinwumi, F. V., Arochukwu, E. C., & Abdul-Kareem, A. S. (2004). Managing Uncertainties in Hydrocarbon-in-place Volumes in a Northern Depobelt Field, Niger Delta, Nigeria. In *28th Annual SPE International Technical Conference and Exhibition*. Abuja: Society of Petroleum Engineers. http://doi.org/10.2118/88880-MS

Al Salhi, M. S., Van Rijen, M. F., Alias, Z. a, Visser, F., Dijk, H., Lee, H. M., … Wei, L. (2005). Reservoir modelling for redevelopment of a giant fractured carbonate field, oman: Experimental design for uncertainty management and production forecasting. *2005 International Petroleum Technology Conference Proceedings*, 845–854. http://doi.org/10.2523/IPTC-10537-MS

Adelman, M. A., & Watkins, G. C. (2005). U.S. oil and natural gas reserve prices, 1982-2003. *Energy Economics*, *27*(4), 553–571. http://doi.org/10.1016/j.eneco.2005.03.008

Akinwumi, F. V., Arochukwu, E. C., & Abdul-Kareem, A. S. (2004). Managing Uncertainties in Hydrocarbon-in-place Volumes in a Northern Depobelt Field, Niger Delta, Nigeria. In *28th Annual SPE International Technical Conference and Exhibition*. Abuja: Society of Petroleum Engineers. http://doi.org/10.2118/88880-MS

Al Salhi, M. S., Van Rijen, M. F., Alias, Z. a, Visser, F., Dijk, H., Lee, H. M., … Wei, L. (2005). Reservoir modelling for redevelopment of a giant fractured carbonate field, oman: Experimental design for uncertainty management and production forecasting. *2005 International Petroleum Technology Conference Proceedings*, 845–854. http://doi.org/10.2523/IPTC-10537-MS

Anderson Jr, J. (1992). Governing equations of fluid dynamics *Computational fluid dynamics* (pp. 15-51): Springer.

Adler, P. (1992). *Porous Media-Geometry and Transport.* USA: Butterworth-Heinneman.

Aboukhedr, M., Vogiatzaki, K., Mitroglou, N. and Gavaises, M. (no date) 'A N Umerical S Imulation Of S Ingle A Nd T Wo - Phase Flow In P Orous M Edia ; A P Ore - Scale O Bservation Of Effective M Icroscopic F Orces'.

Akanji, L. T. and Matthai, S. K. (2009) 'Finite Element-Based Characterization of Pore-Scale Geometry and Its Impact on Fluid Flow'. doi: 10.1007/s11242-009-9400-7.

Akinlotan, O. (2016) 'Proceedings of the Geologists' Association Porosity and permeability of the English (Lower Cretaceous) sandstones', *Proceedings of the Geologists' Association*. The Geologists' Association., 127(6), pp. 681–690. doi: 10.1016/j.pgeola.2016.10.006.

Al-kharusi, A. S. and Blunt, M. J. (2007) 'Network extraction from sandstone and carbonate pore space images', 56, pp. 219–231. doi: 10.1016/j.petrol.2006.09.003.

Anovitz, L. M. and Cole, D. R. (2015) 'Characterization and Analysis of Porosity and Pore

Structures', 80, pp. 61–164.

Anon, (2017). [ebook] Available at: (https://mineralseducationcoalition.org/minerals-database/sandstone/) [Accessed 10 Sep. 2017].

Anovitz, L. M. and Cole, D. R. (2015) 'Characterization and Analysis of Porosity and Pore Structures', 80, pp. 61–164.

Arogundade, O. and Sohrabi, M. (2012) 'SPE 160869 A Review of Recent Developments and Challenges in Shale Gas Recovery', (April), pp. 8–11.

Anon, (2017). [eBook] Available at: (https://mineralseducationcoalition.org/minerals-database/sandstone/) [Accessed 10 Sep. 2017].

Anovitz, L. M. and Cole, D. R. (2015) 'Characterization and Analysis of Porosity and Pore Structures', 80, pp. 61–164.

Bistline, J. E. (2014). Natural gas, uncertainty, and climate policy in the US electric power sector. *Energy Policy*, *74*, 433–442. http://doi.org/10.1016/j.enpol.2014.08.017

Bistline, J. E. (2014). Natural gas, uncertainty, and climate policy in the US electric power sector. *Energy Policy*, *74*, 433–442. http://doi.org/10.1016/j.enpol.2014.08.017

Bistline, J. E. (2014). Natural gas, uncertainty, and climate policy in the US electric power sector. *Energy Policy*, *74*, 433–442. http://doi.org/10.1016/j.enpol.2014.08.017

Blunt, M. J., Bijeljic, B., Dong, H., Gharbi, O., Iglauer, S., Mostaghimi, P., Paluszny, A. and

Bogdanov, I. I., Guerton, F., Kpahou, J., Kamp, A. M. and Reservoirs, T. (2011) 'Direct Pore-Scale Modeling Of Two-Phase Flow Through Natural Media'.

Blunt, M. J., Bijeljic, B., Dong, H., Gharbi, O., Iglauer, S., Mostaghimi, P., Paluszny, A. and Pentland, C. (2013) 'Advances in Water Resources Pore-scale imaging and modelling', *Advances in Water Resources*. Elsevier Ltd, 51, pp. 197–216. doi: 10.1016/j.advwatres.2012.03.003.

Byrne, M., Jimenez, M. A., Rojas, E. and Castillo, E. (2011) 'SPE 144130 ComputationalFluid Dynamics for Reservoir and Well Fluid Flow Performance Modelling

C.A. Balanis, Advanced Engineering Electromagnetics, John Wiley & Sons Inc., 1989.

Council, W. P. (n.d.). Petroleum Resources Management System.

Ct, X., Boone, M. N., Jacobs, P., Cnudde, V., Boone, M., Dewanckele, J., Dierick, M., Hoorebeke, L. Van and Jacobs, P. (2011) '3D characterization of sandstone by means of', (January). doi: 10.1130/GES00563.1

Chengzao, J., Min, Z., & Yongfeng, Z. (2012) 'Unconventional hydrocarbon resources in China and the prospect of exploration and development'. Petroleum Exploration and Development, *39*(2), 139-146.

Chengzao, J., Min, Z., & Yongfeng, Z. (2012) ‘Unconventional hydrocarbon resources in China and the prospect of exploration and development’. Petroleum Exploration and Development, *39*(2), 139-146

Council, W. P. (n.d.). Petroleum Resources Management System.

Demirmen, F. (2007). Reserves Estimation: The Challenge for the Industry. *Journal of Petroleum Technology*, *59*(May), 80–89. http://doi.org/10.2118/103434-MS

Demirmen, F. (2007). Reserves Estimation: The Challenge for the Industry. *Journal of Petroleum Technology*, *59*(May), 80–89. http://doi.org/10.2118/103434-MS

Framework, V. A. (2012). Reserves and Resources Technical Standards and Guidelines, (May).

F.A.L.Dullien. (1991). *Porous Media: Fluid Transport and Pore Structure, 2nd Edition.* USA: Elservier.

Framework, V. A. (2012). Reserves and Resources Technical Standards and Guidelines, (May).

Framework, V. A. (2012). Reserves and Resources Technical Standards and Guidelines, (May)

Feynman, "Differential Calculus of Vector Fields", The Feynman Lectures on Physics, Caltech's Division of Physics, Mathematics and Astronomy, 2013.

Harrell, D. R., Hodgin, J. E., & Wagenhofer, T. (2004). Oil and Gas Reserves Estimates: Recurring Mistakes and Errors. In *SPE Annual Technical Conference and Exhibition*. Houston: Society of Petroleum Engineers. http://doi.org/10.2118/91069-MS

Hinkley, R., Gu, Z., Wong, T. and Camilleri, D. (2013) ‘SPE 167146 Multi-Porosity Simulation of Unconventional Reservoirs’, (November), pp. 5–7.

Javadpour, F., D. Fisher, and M. Unsworth, (2007) Nanoscale gas flow in shale gas sediments: Journal of Canadian Petroleum Technology, 46, 55-61.

J.A. Stratton, Electromagnetic Theory, McGraw-Hill Company Inc., 1941.

Kamali, M. R., Omidvar, A., & Kazemzadeh, E. (2013). 3D Geostatistical Modeling and Uncertainty Analysis in a Carbonate Reservoir, SW Iran. *Journal of Geological Research*, 1–7. http://doi.org/10.1155/2013/687947

Kazimierz, T. and Jacek, T. (2004) ‘Evaluation of Rock Porosity Measurement Accuracy with a Helium Porosimeter’, 9, pp. 316–318.

Klaja, J. and Przelaskowska, A. (2015) ‘Helium porosity measurements for rocks from unconventional reservoirs performed on crushed samples’, (11), pp. 856–863. doi: 10.18668/NG2015.11.07.

Lopez, O., Mock, A., Skretting, J., Boye, E. And Jr, P. (2010) 'Investigation Into The Reliability Of Predictive Pore-Scale Modeling For Siliciclastic Reservoir Rocks', Pp. 1–12.

Lock, P. A., Jing, X., Schlueter, R. W. Z. M., Lock, P. A., Jing, X., Zimmerman, R. W. and Schlueter, E. M. (2002) 'Predicting the permeability of sandstone from image analysis of pore structure Predicting the permeability of sandstone from image analysis of pore structure', 6311. doi: 10.1063/1.1516271.

Lyons, C., & Plisga, J. G. (2005) 'Standard Handbook of Petroleum and Natural Gas'. Oxford: Gulf Professional Publishing

MacDonald, A., & Tollesfrud, J. L. (2008). 3D Reservoir Uncertainty Modelling – workflows, products & benefits.

Mata, T., Rojas, L., Salil, B., & Camacho, M. (1997). Probabilistic Reserves Estimation of Mara West Field, Maracaibo Basin, Venezuela: Case Study. In *SPE Annual Technical Conference and Exhibition*. San Antonio: Society of Petroleum Engineers. http://doi.org/10.2118/38805-MS

Manger GE (1963) Porosity and Bulk Density of Sedimentary Rocks. Geol Surv Bull 1114–E

okane, A., Jain, S., Deshpande, Y. and Crespo, F. (2013) 'SPE 165952 Computational Fluid Dynamics (CFD) Study and Investigation of Proppant Transport and Distribution in Multistage Fractured Horizontal Wells'

M. Sajben, J.C. Kroutil, and C.P. Chen, "A High-Speed Schlieren Investigation of Diffuser Flows with Dynamic Distortion", AIAA Paper 77-875, 1977

O.Anwar Bég *et al.*. (2016). Spectral quasilinear numerical simulation of micropolar convective wall plumes in Higher permeability (non-Darcy) porous media. *J. Engineering Thermophysics*, 25.

O.Anwar Bég *et al*. (2016). Numerical simulation of self-smilar and thermal convection from spinning cone in anisotropic porous media. *J. Hydrodynamics Series B*, 184-194.

Pentland, C. (2013) 'Advances in Water Resources Pore-scale imaging and modelling', *Advances in Water Resources*. Elsevier Ltd, 51, pp. 197–216. doi: 10.1016/j.advwatres.2012.03.003.

Plessis, D. (2008) 'Predicting the Permeability of Very Low Porosity', pp. 39–55. doi: 10.1007/s11242-007-9168-6.

Raza, A., Bing, C. H., Nagarajan, R. and Ali, M. (no date) 'Experimental Investigation on Sandstone Rock Permeability of Pakistan Gas Fields'. doi: 10.1088/1757-899X/78/1/012007.

Rezazadeh, M. and Technology, I. (2015) 'Porosity And Permeability In Tight Supervisor ':, (October).

Rexer, T. F., Mathia, E. J., Aplin, A. C. and Thomas, K. M. (2014) 'High-Pressure Methane Adsorption and Characterization of Pores in Posidonia Shales and Isolated Kerogens'

Senturk, Y. (2011). Essence of the SPE Petroleum Resources Management System Definitions and Guiding Principles for Classification, Categorization and Assessment

Process. In *SPE/DGS Saudi Arabia Section Technical Symposium and Exhibition*. Al-Khoba: Society of Petroleum Engineers. http://doi.org/10.2118/149078-MS

SPE. (2011). Guidelines for Application of The Petroleum Resources Management System. Society of Petroleum Engineers.

Spe1398z/L Probabilistic Hydrocarbon Reserves Estimation: A Novel Monte Carlo Approach P Bebrenbruch, G. (n.d.).

Saadi, A., Biotechnol, J. P. E., Saadi, F. Al, Wolf, K. and Kruijsdijk, C. Van (2017) 'Journal of Petroleum & Characterization of Fontainebleau Sandstone: Quartz Overgrowth and its Impact on Pore-Throat Framework', 8(3). doi: 10.4172/2157-7463.1000328.

Schwartz, L. M., Toksoz, M. N., Wave, C., Morgan, F. D., Modelling, P., Zhan, X., Schwartz, L. M., Toksöz, M. N., Smith, W. C. and Morgan, F. D. (2017) 'Pore-scale modelling of electrical and fluid transport in Berea sandstone

R.D. Bird, W.E. Stewart, E.N. Lightfoot,Transport Phenomena, 2nd ed., NY: John Wiley & Sons Inc., 2002

Tye, B. and Tye, R. S. (2015) 'Permeability characterization of distributary mouth bar sandstones in Prudhoe Bay field, Alaska: How ... Permeability characterization of distributary mouth bar field, Alaska: How horizontal deltaic reservoirs', (May).

Umavathi, J.C. and O.Anwar Bég (2019). Numerical study of double-diffusive dissipative reactive convective flow in an open vertical duct containing a non-Darcy porous medium with Robin boundry condition,. *J.Engineering Mathematics*, 13.

Wilkinson, J. (1996). Reserve and resource definition: dealing with uncertainty. *Norwegian Petroleum Society Special Publications*, *6*, 71–76. http://doi.org/10.1016/S0928-8937(07)80008-7

Wright, J. D. (2003). Irreducible Uncertainty -- A Fact of Life in Reserve Estimates. In *SPE Annual Technical Conference and Exhibition*. Denver: Society of Petroleum Engineers Inc. http://doi.org/10.2118/84146-MS

Wang, S., Song, Z., Cao, T. and Song, X. (2013) 'The methane sorption capacity of Paleozoic shales from the Sichuan', *Marine and Petroleum Geology*. Elsevier Ltd, 44, pp. 112–119. doi: 10.1016/j.marpetgeo.2013.03.007.

Wang, C. (1991). Exact solutions of the steady-state Navier-Stokes equations. *Annual Review of Fluid Mechanics, 23*(1), 159-177.

Appendices

List of Appendices

APPENDIX A The calibration tables, graphs used in determining the grain volumes.

1/3 BUFF BEREA CALIBRATION

Calibration Table				
		Reference	Expanded	
Disc	Volume	Pressure	Pressure	P1/P2
No.	cc	psig (P1)	psig (P2)	
empty	0	92.72	10.64	8.714
1	1.596	91.23	10.8	8.447
2	4.791	92.13	11.88	7.755
3	6.408	91.8	11.95	7.682
4	9.615	91.84	12.87	7.136
5	16.024	91.83	15.11	6.077
5+1	17.620	91.75	16.13	5.688
5+3	22.431	91.76	18.57	4.941
5+4	25.639	91.72	20.66	4.439
5+4+3	32.047	91.7	27.19	3.373
5+4+3+2	36.838	91.68	35.04	2.616

Testing Table			
P1	P2	P1/P2	Grain Vol
91.66	23.37	3.922122379	28.712

1/3 CASTLE GATE CALIBRATION

Calibration Table				
		Reference	Expanded	
Disc	Volume	Pressure	Pressure	P1/P2
No.	cc	psig (P1)	psig (P2)	
empty	0	92.72	10.64	8.714
1	1.596	91.23	10.8	8.447
2	4.791	92.13	11.88	7.755
3	6.408	91.8	11.95	7.682
4	9.615	91.84	12.87	7.136
5	16.024	91.83	15.11	6.077
5+1	17.620	91.75	16.13	5.688
5+3	22.431	91.76	18.57	4.941
5+4	25.639	91.72	20.66	4.439
5+4+3	32.047	91.7	27.19	3.373
5+4+3+2	36.838	91.68	35.04	2.616

Testing Table			
P1	P2	P1/P2	**Grain Vol**
91.64	21.12	4.339015152	**26.159**

1/3 BOISE CALIBRATION

Calibration Table				
		Reference	Expanded	
Disc	Volume	Pressure	Pressure	P1/P2
No.	cc	psig (P1)	psig (P2)	
empty	0	92.72	10.64	8.714
1	1.596	91.23	10.8	8.447
2	4.791	92.13	11.88	7.755
3	6.408	91.8	11.95	7.682
4	9.615	91.84	12.87	7.136
5	16.024	91.83	15.11	6.077
5+1	17.620	91.75	16.13	5.688
5+3	22.431	91.76	18.57	4.941
5+4	25.639	91.72	20.66	4.439
5+4+3	32.047	91.7	27.19	3.373
5+4+3+2	36.838	91.68	35.04	2.616

Testing Table			
P1	P2	P1/P2	**Grain Vol**
91.64	20.63	4.442074649	**25.530**

CALCULATION OF POROSITY FOR BUFF BEREA, BOISE AND CASTLEGATE SAMPLES

BASIS:

1 cubic in = 16.3871cc

Bulk Volume= $\pi r^2 h$, Pore volume= Bulk volume – Grain volume

$$\emptyset = \frac{Pore\ volume}{Bulk\ volume}$$

1/3 BUFF BERA

Length= 3.0025in, Diameter= 0.9920in, Weight= 75.77g

$$Bulk\ Volume = 3.144 * \frac{0.9920^2}{4} * 3.0025 = 2.3223ci$$

Bulk volume= 38.05576233cc

Pore volume= 38.05576233 – 28.712 = 9.3438cc

$$\emptyset = \frac{9.3438}{38.05576233} = 0.2455 = 24.55\%$$

1/3 CASTLE GATE

Length= 2.9965in, Diameter= 0.9795in, Weight= 69.95g

$$Bulk\ Volume = 3.144 * \frac{0.9795^2}{4} * 2.9965 = 2.2596ci$$

Bulk volume= 37.0053cc

Pore volume= 37.0053 – 26.159 = 10.8463cc

$$\emptyset = \frac{10.8463}{37.0053} = 0.2931 = 29.31\%$$

1/3 BOISE

Length= 2.9940in, Diameter= 0.9755in, Weight= 66.77g

$$Bulk\ Volume = 3.144 * \frac{0.9755^2}{4} * 2.9940 = 2.2393ci$$

Bulk volume= 36.69563303cc

Pore volume= 36.69563303 – 25.559 = 11.1366cc

$$\emptyset = \frac{11.1366}{36.69563303} = 0.3035 = 30.35\%$$

The calibration tables and graphs used in determining the permeability for the various sandstone samples are presented below;

Length (cm)	2.54	**Area (cm2)**	5.07
Diameter (cm)	2.54	**Mean Pres (atmos)**	1.01
Viscosity (cp)	0.0174	**Upstream Pres (atmos)**	1.02
Transducer Pres (psig)	0.3	**Downstream Pres (atmos)**	1.00
Flow Rate (cc/min)	65.2	**Flow Rate (cc/sec)**	1.09
		Permeability (md)	**458.1**

Length (cm)	2.54	**Area (cm2)**	5.07
Diameter (cm)	2.54	**Mean Pres (atmos)**	1.01
Viscosity (cp)	0.0174	**Upstream Pres (atmos)**	1.02
Transducer Pres (psig)	0.3	**Downstream Pres (atmos)**	1.00
Flow Rate (cc/min)	209.1	**Flow Rate (cc/sec)**	3.49
		Permeability (md)	**1469.2**

Length (cm)	2.54	**Area (cm2)**	5.07
Diameter (cm)	2.54	**Mean Pres (atmos)**	1.01
Viscosity (cp)	0.0174	**Upstream Pres (atmos)**	1.02
Transducer Pres (psig)	0.3	**Downstream Pres (atmos)**	1.00
Flow Rate (cc/min)	312.6	**Flow Rate (cc/sec)**	5.21
		Permeability (md)	**2196.4**

APPENDIX B Data from production published journal used in the numerical model.

.

S/N	Reservoir Parameter	Value	Units
1	Matrix porosity	24.55	%
2	Matrix permeability	1.0*10^-4	mD
3	Fluid Viscosity	0.0184	cP
4	Fluid Density	0.66	Kg/m^3
5	Initial Reservoir Pressure	1000	psi
6	Fluid Compressibility	2.5*10^-4	Psi^-1
7	Well-bore radius	0.25	ft
8	Reservoir Length	500	ft
9	Reservoir thickness	250	ft
10	Reservoir Width	2000	ft

The Model Geometry

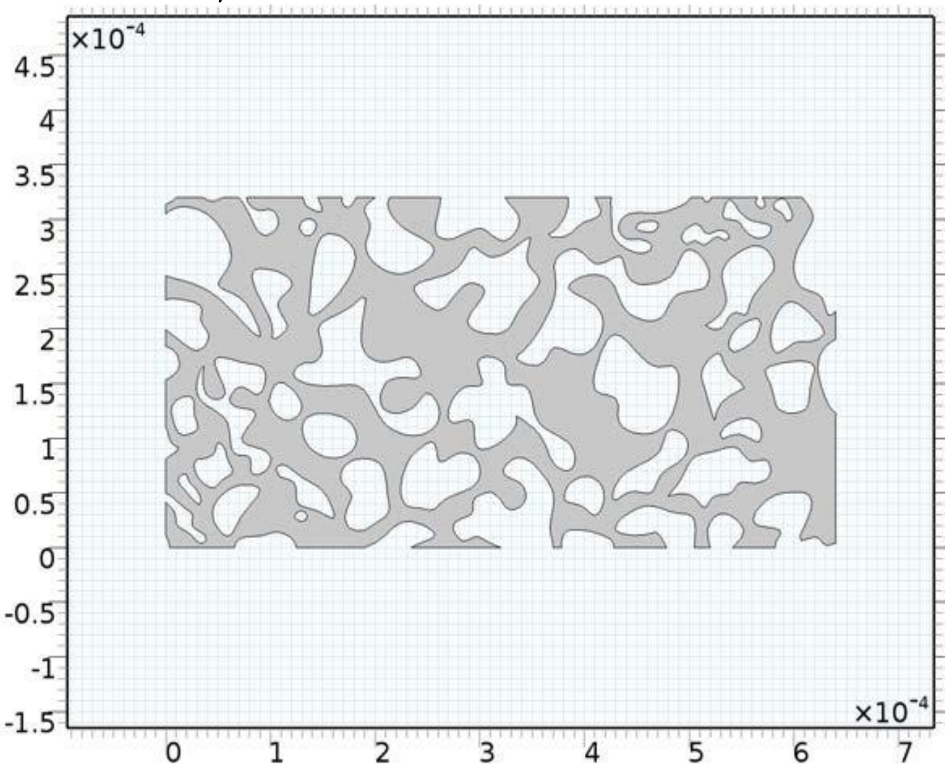

Pore scale Mesh

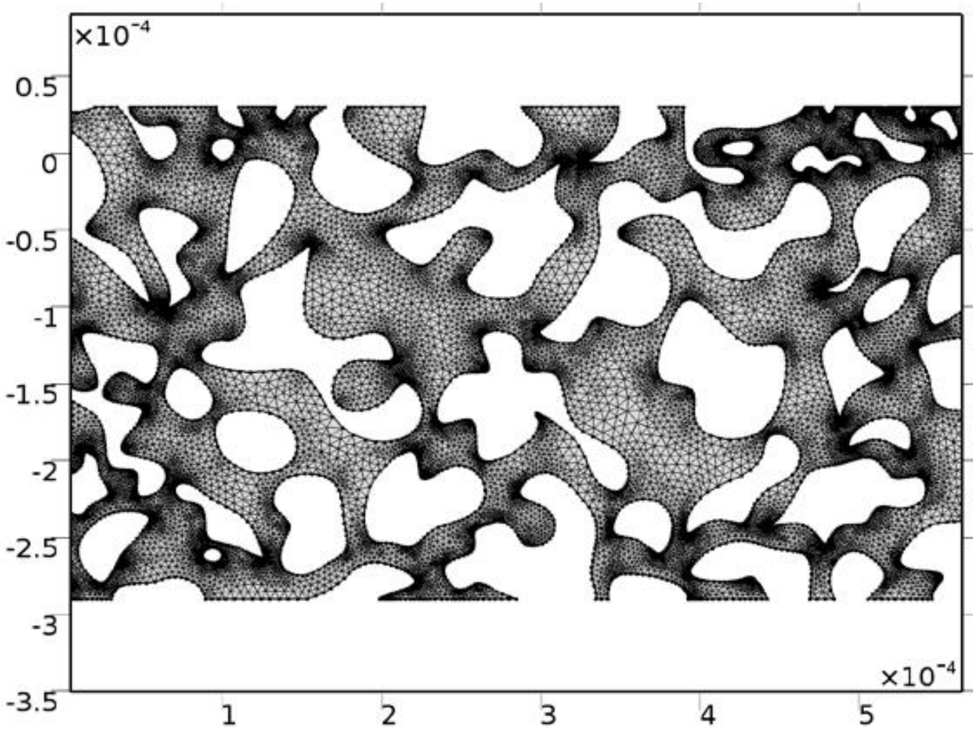

APPENDIX C Results of decline curve analysis using Oil Field Manager

BS_25U: Gas: OGBA_025: E1000X
Historical Regression

Cumulative Production 72050.7 MMcf thru 12/31/2015

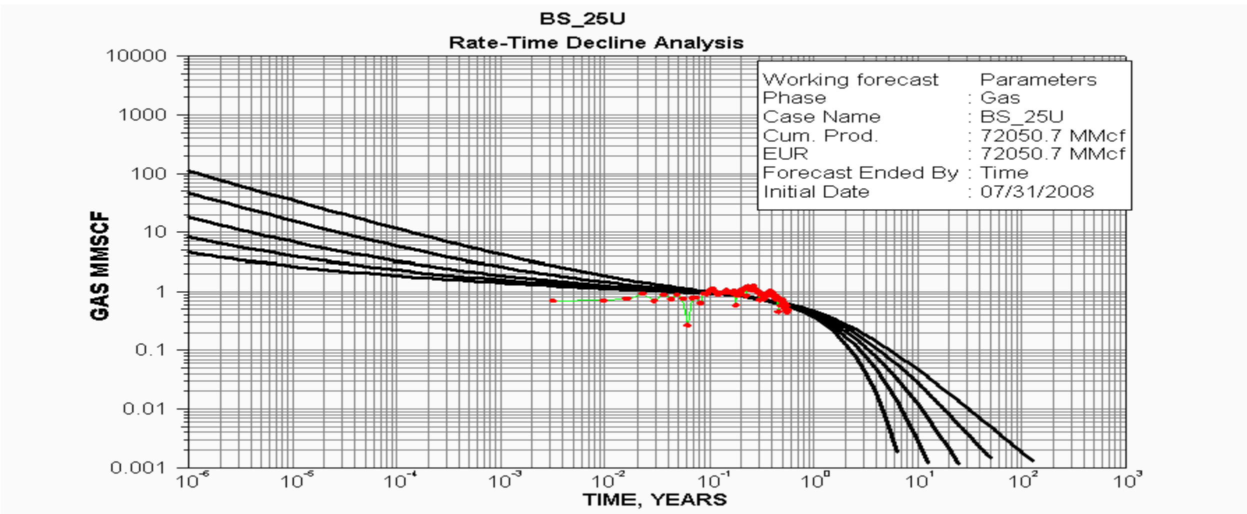

BS_25U: Gas: OGBA_025: E1000X									
Historical Regression									
	Cumulative Production 72050.7 MMcf thru 12/31/2015								
	b Value	Di (A.e.)	qi (Mcf)	ti					
	0	0.04795	939711.7	7/31/2008					
Working forecast									
	EUR 1.38967e+006 MMcf								
#	b Value	Di (A.e.)	qi (Mcf)	ti	te	qe (Mcf)	Res. (MMcf)	Ended By	Reserves Type
1	0	0.04795	475190	12/31/2015	12/31/2025	297914.5	1317621	Time	
Database Forecast									
None									

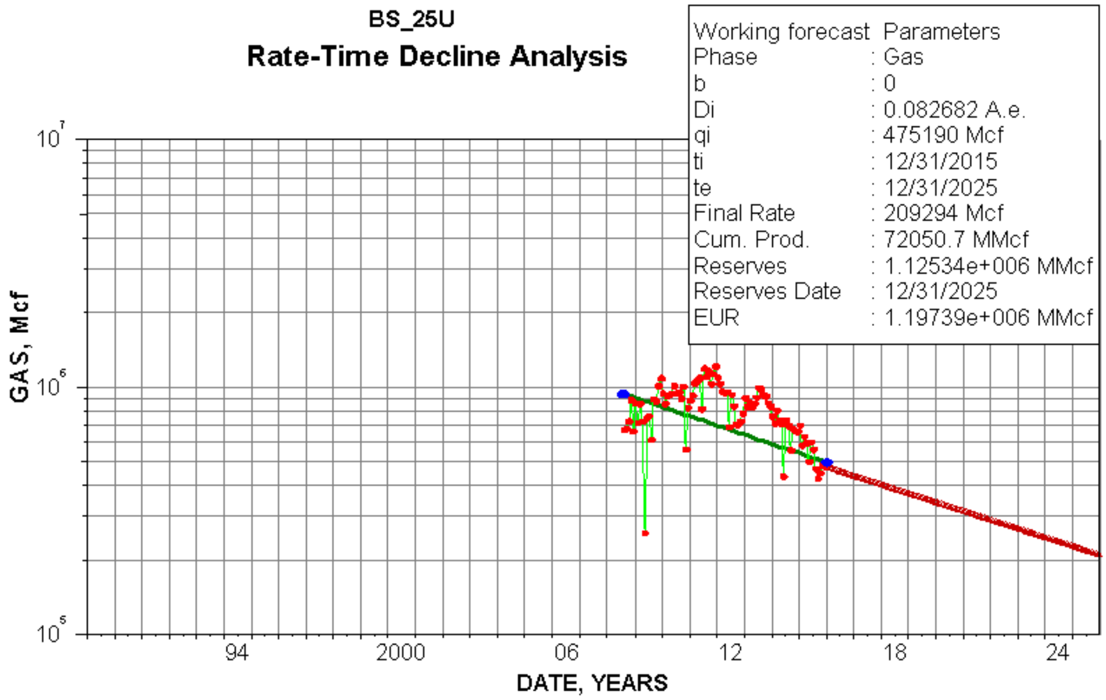

BS_26V: Gas: OGBA_026: F4000X				
Historical Regression				
	Cumulative Production 267282 **MMcf** thru 12/31/2015			

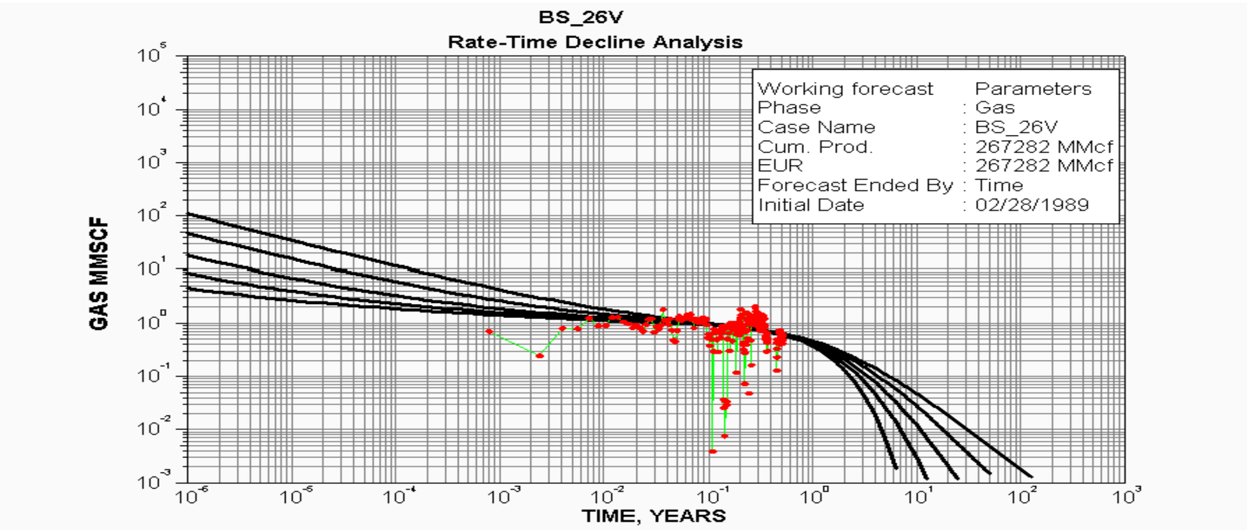

BS_26V: Gas: OGBA_026:F4000X										
Historical Regression										
	Cumulative Production 267282 MMcf thru 12/31/2015									
	b Value	Di (A.e.)	qi (Mcf)	ti						
	0	0.01514	935108.2	2/28/1989						
Working forecast										
	EUR 2.19237e+006 MMcf									
#	b Value	Di (A.e.)	qi (Mcf)	ti	te	qe (Mcf)	Res. (MMcf)	Ended By	Reserves Type	
1	0	0.01514	595890	12/31/2015	12/31/2025	515500.3	1925089	Time	None	
Database Forecast										

BS_29Z: Gas: OGBA_029:F7100X

Historical Regression

Cumulative Production 233310 MMcf thru 12/31/2015

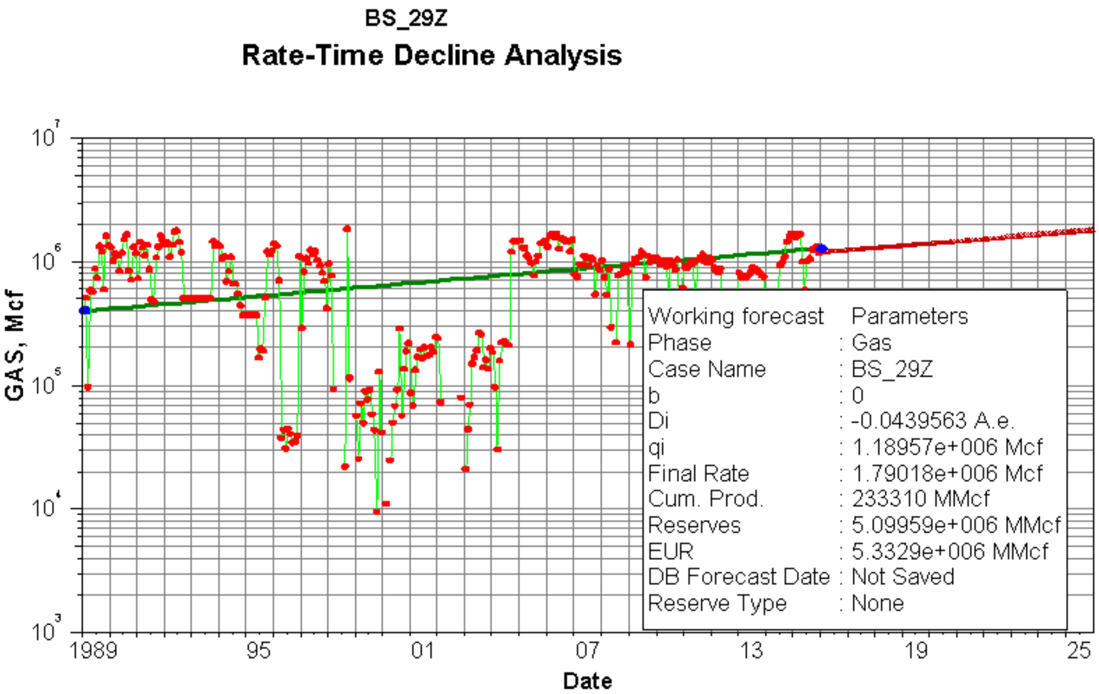

BS_30AA: Gas: OGBA_030:F5700X

Historical Regression

Cumulative Production 80027.5 MMcf thru 12/31/2014

b	Value	Di (A.e.)qi	(qi (Mcf)Mcf	ti
	0	0	0	1/1/1900

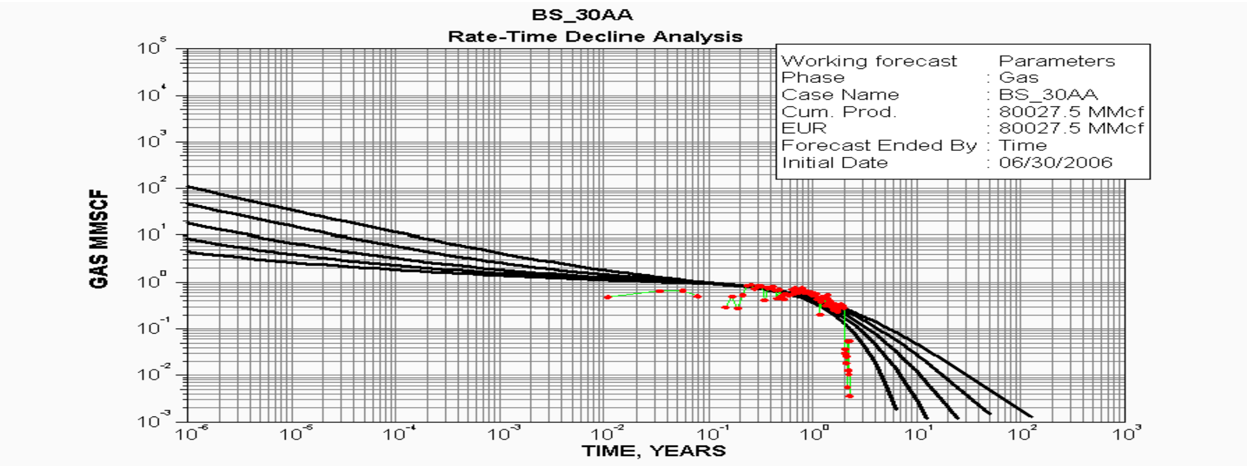

BS_30AA: Gas: OGBA_030:F5700X										
Historical Regression										
	Cumulative Production 80027.5 MMcf thru 12/31/2014									
	b Value	Di (A.e.)	qi (Mcf)	ti						
	0	0.19571	2352695	6/30/2006						
Working forecast										
	EUR 564277 MMcf									
#	b Value	Di (A.e.)	qi (Mcf)	ti	te	qe (Mcf)	Res. (MMcf)	Ended By	Reserves Type	
1	0	0.19571	825362.1	5/31/2011	5/31/2021	104217.5	1209382	Time	None	

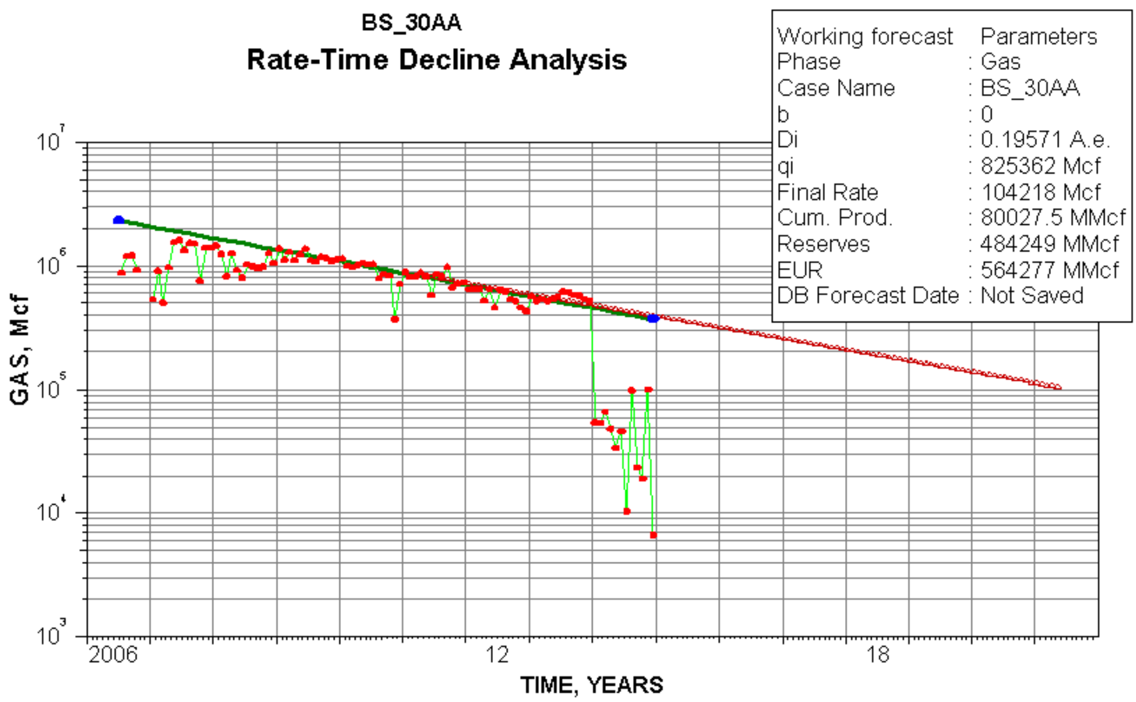

BS_30AB: Gas: OGBA_030:G4000X

Historical Regression

Cumulative Production 121066 MMcf thru 11/30/2003

b ValueDi Di (A.e.) qi (Mcf)A.e.) qi (Mcf ti

0 0 0 1/1/1900

Working forecast

Database Forecast

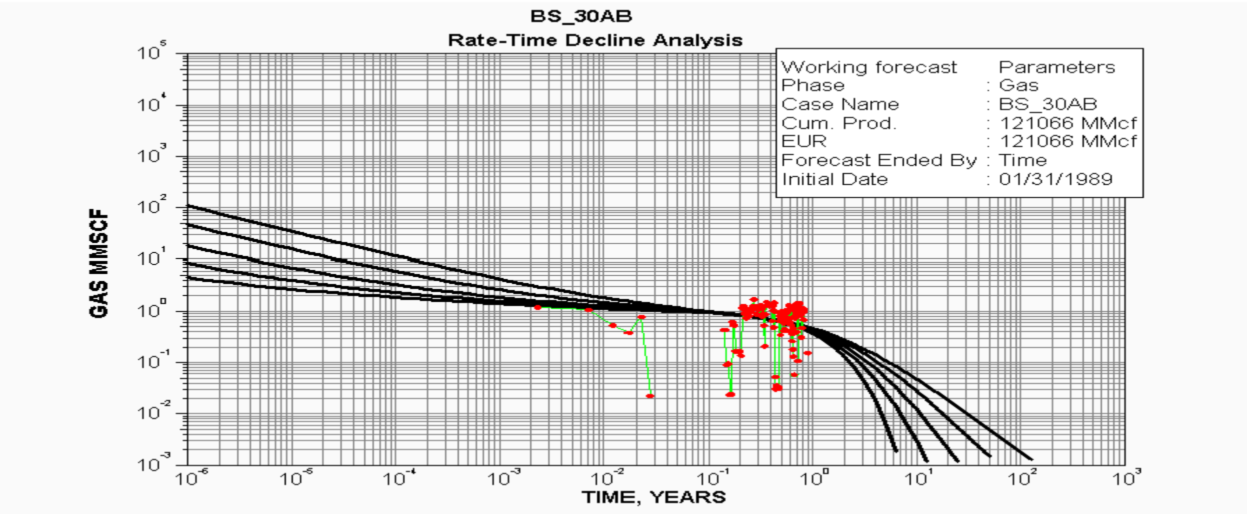

BS_30AB: Gas: OGBA_030:G4000X									
Historical Regression									
	Cumulative Production 121066 MMcf thru 11/30/2003								
	b Value	Di (A.e.)	qi (Mcf)	ti					
	0	0.06439	1980722	4/8/1992					
Working forecast									
	EUR 2.49301e+006 MMcf								
#	b Value	Di (A.e.)	qi (Mcf)	ti	te	qe (Mcf)	Res. (MMcf)	Ended By	Reserves Type
1	0	0.06439	1114487	7/31/2002	7/31/2012	592155.2	2866428	Time	None

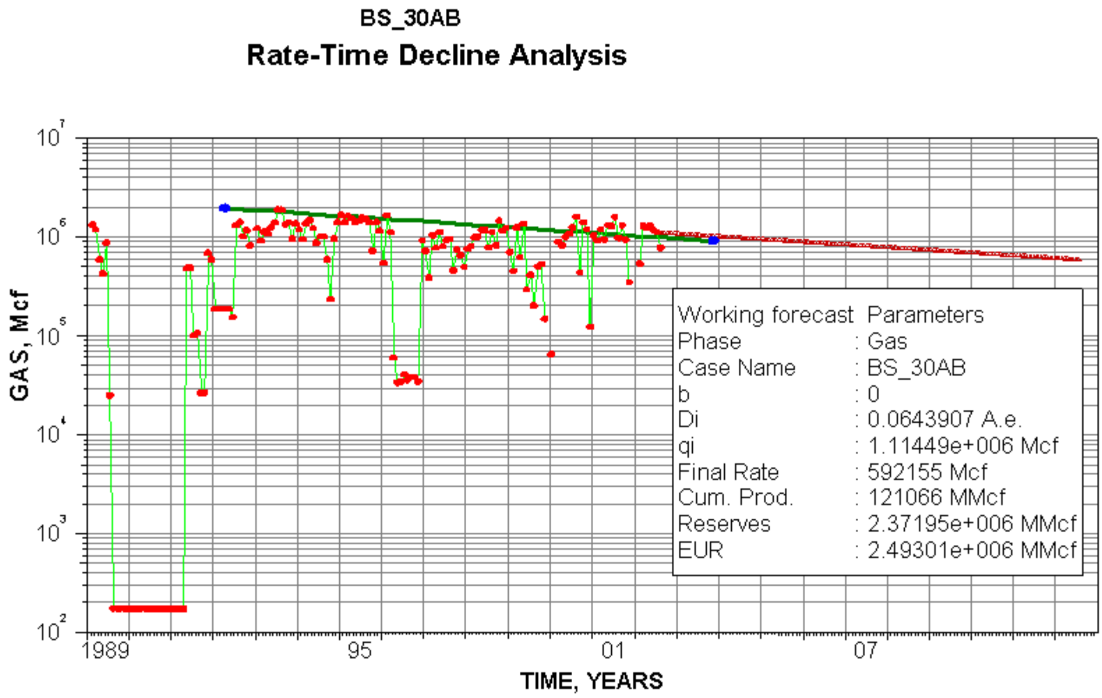

BS_31AC: Gas: OGBA_031:F1000X

Historical Regression

Cumulative Production 173038 MMcf thru 11/30/2015

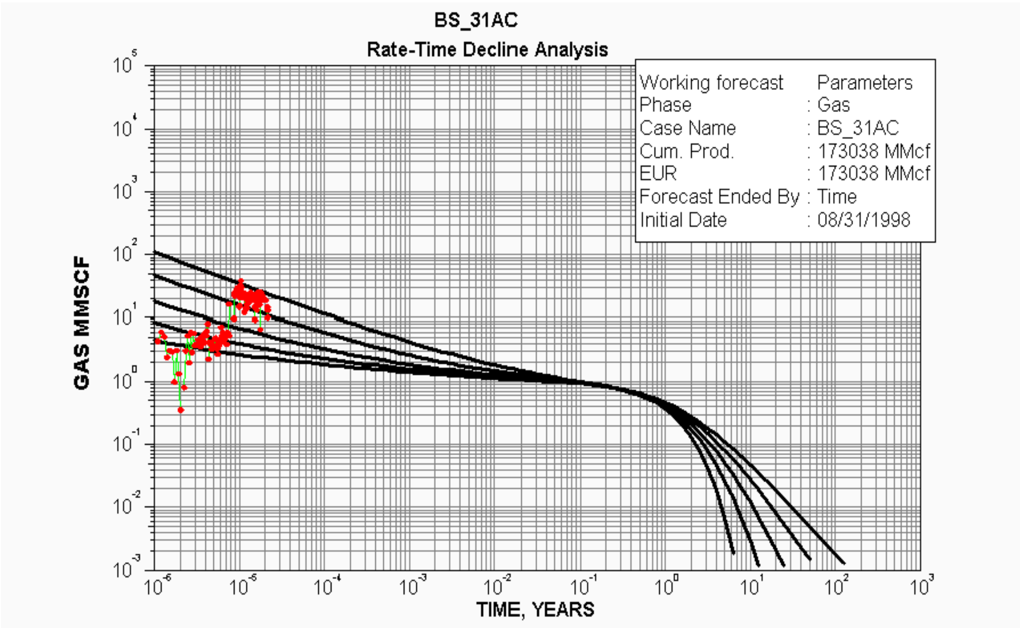

BS_31AC: Gas: OGBA_031:F1000X										
Historical Regression										
	Cumulative Production 173038 MMcf thru 11/30/2015									
	b Value	Di (A.e.)	qi (Mcf)	ti						
	0	0.01643	1452563	12/2/2003						
Working forecast										
	EUR 3.89283e+006 MMcf									
#	b Value	Di (A.e.)	qi (Mcf)	ti	te	qe (Mcf)	Res. (MMcf)	Ended By	Reserves Type	
1	0	0.01643	1213154	6/30/2015	6/30/2025	1036519	3895542	Time	None	
Database Forecast										

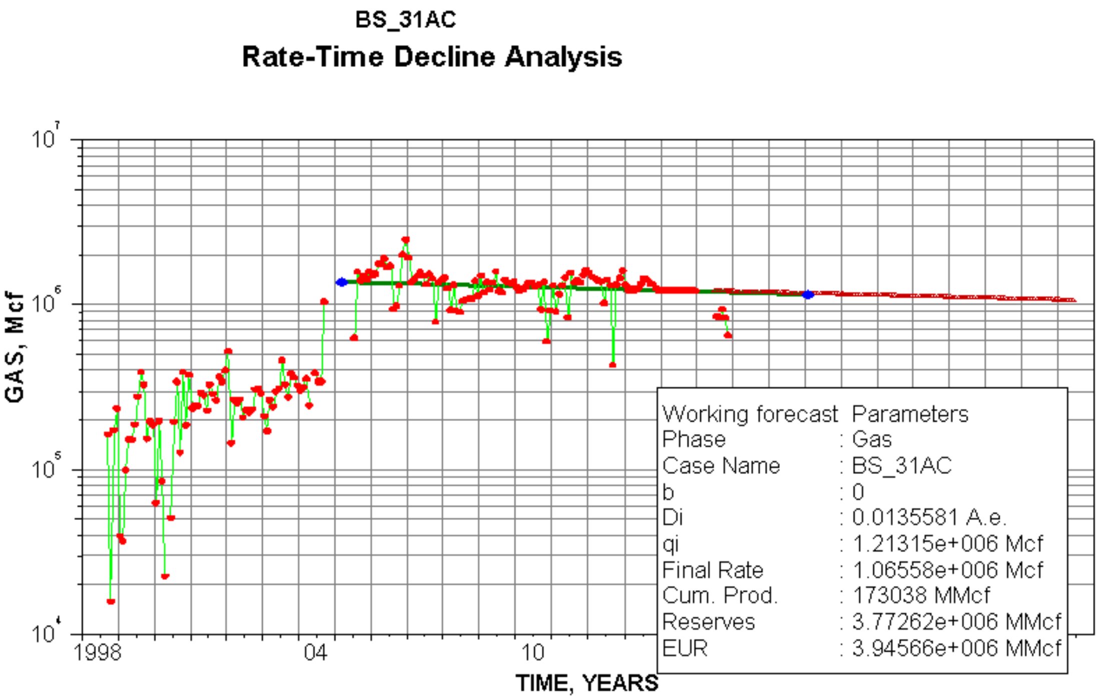

BS_32AD: Gas: OGBA_032: **G1000X**

Historical Regression

Cumulative Production 91494.2 MMcf thru 12/31/2015

b Value	Di (A.e.)	qi (Mcf)A.e.) qi (	Mcf) ti
0	0	0	1/1/190

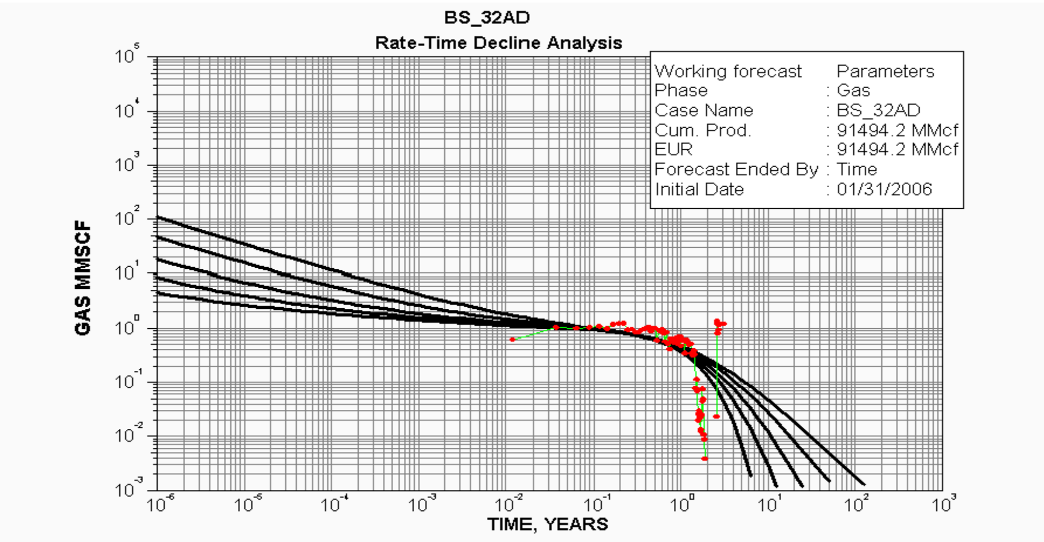

BS_32AD: Gas: OGBA_032:G1000X										
Historical Regression										
	Cumulative Production 91494.2 MMcf thru 12/31/2015									
	b Value	Di (A.e.)	qi (Mcf)	ti						
	0.06	0.5568	1760078	1/31/2006						
Working forecast										

	EUR 92884.8 MMcf									
#	b Value	Di (A.e.)	qi (Mcf)	ti	te	qe (Mcf)	Res. (MMcf)	Ended By	Reserves Type	
1	0.06	0.48223	36728.45	3/31/2011	3/31/2021	158.572	21074.09	Time	None	
Database Forecast										

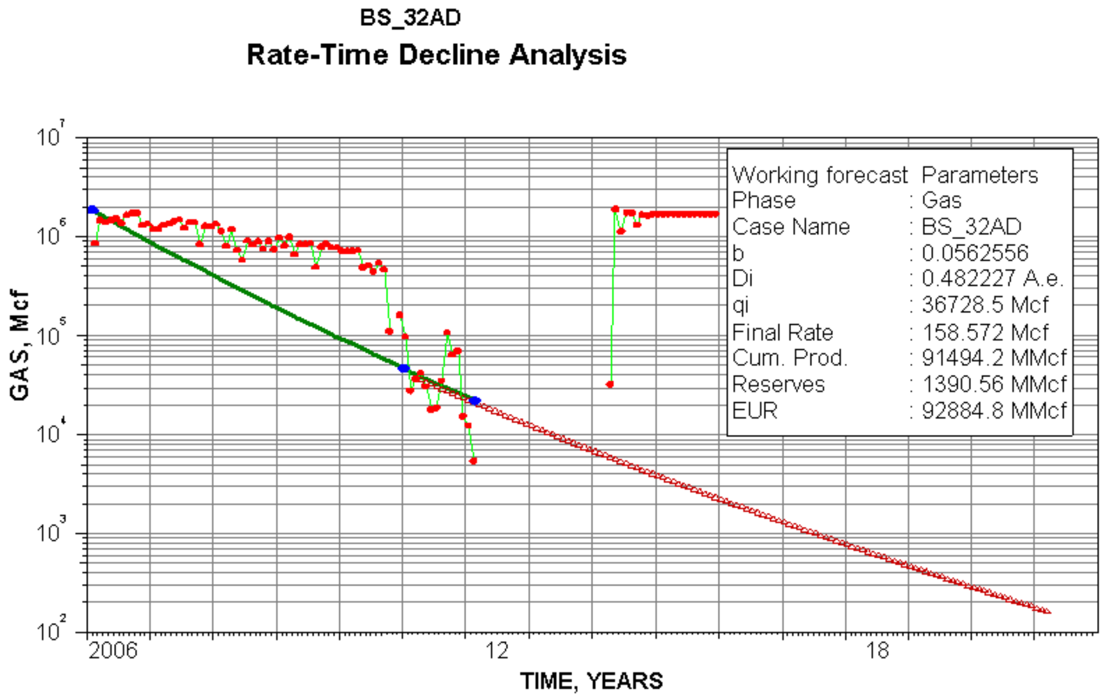

BS_32AE: Gas: OGBA_032:G5000X

Historical Regression

Cumulative Production 18315.4 MMcf thru 12/31/2015

b Value Di (A.e.)qi (qi (Mcf)Mcf ti

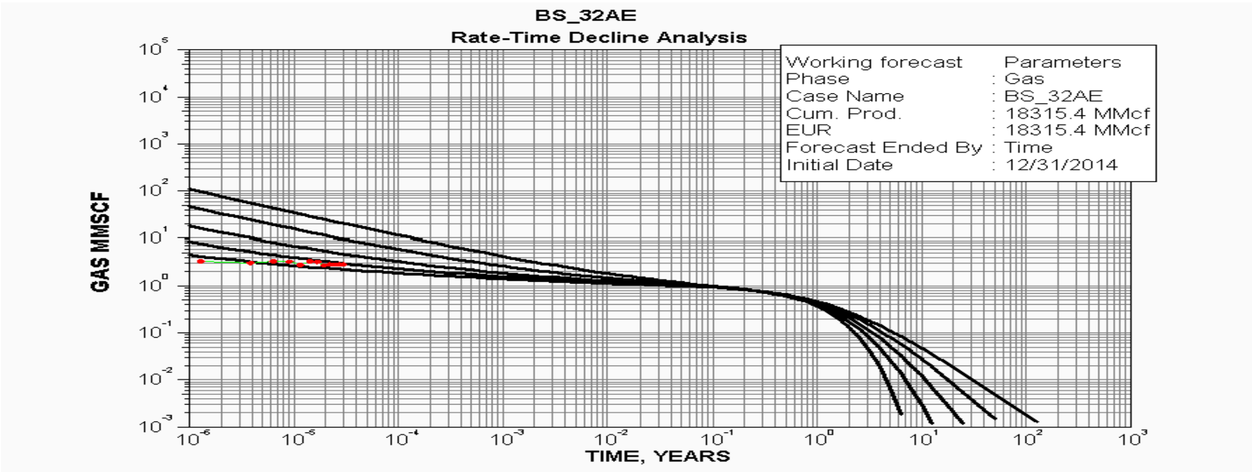

BS_32AE: Gas: OGBA_032: G5000X										
Historical Regression										
	Cumulative Production 18315.4 MMcf thru 12/31/2015									
	b Value	Di (A.e.)	qi (Mcf)	ti						
	1	0.15062	1654569.124	12/31/2014						
Working forecast										
	EUR 3.12661e+006 MMcf									
#	b Value	Di (A.e.)	qi (Mcf)	ti	te	qe (Mcf)	Res. (MMcf)	Ended By	Reserves Type	
1	1	0.13092	1442950	12/31/2015	12/31/2025	593504.3	3108290	Time	None	
Database Forecast										

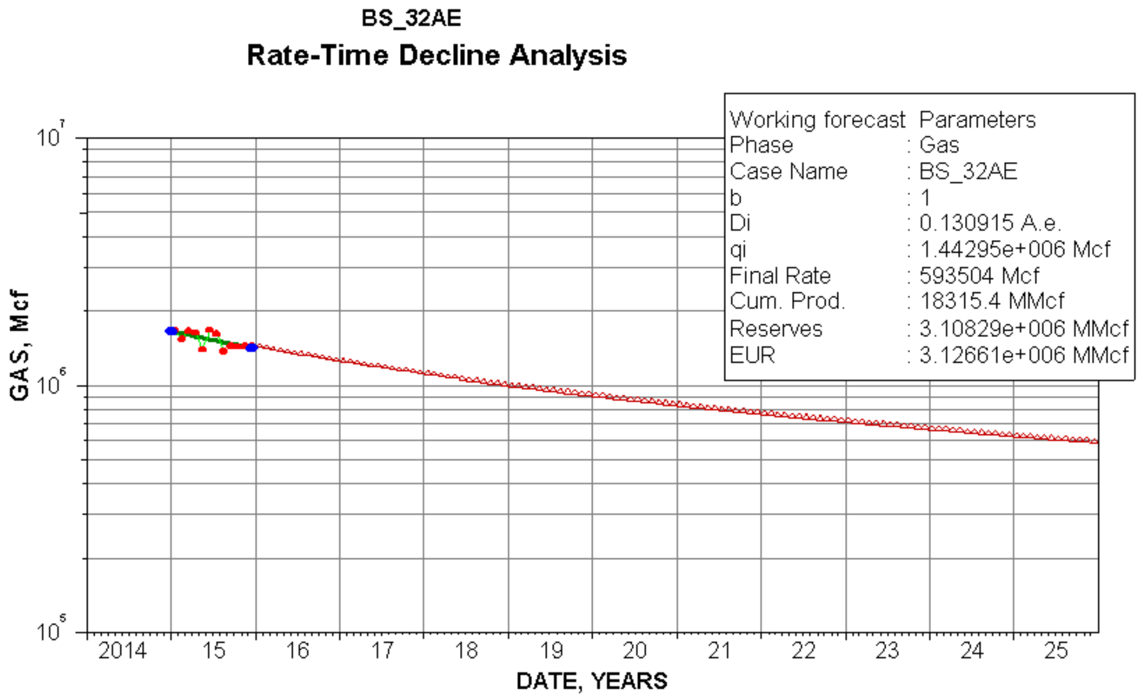

BS_33AF: Gas: OGBA_033:G3000X

Historical Regression

Cumulative Production 87080.4 MMcf thru 12/31/2015

b	Value	Di (A.e.)qi (qi (Mcf)Mcf		ti
0	0	0	1/1/1900	

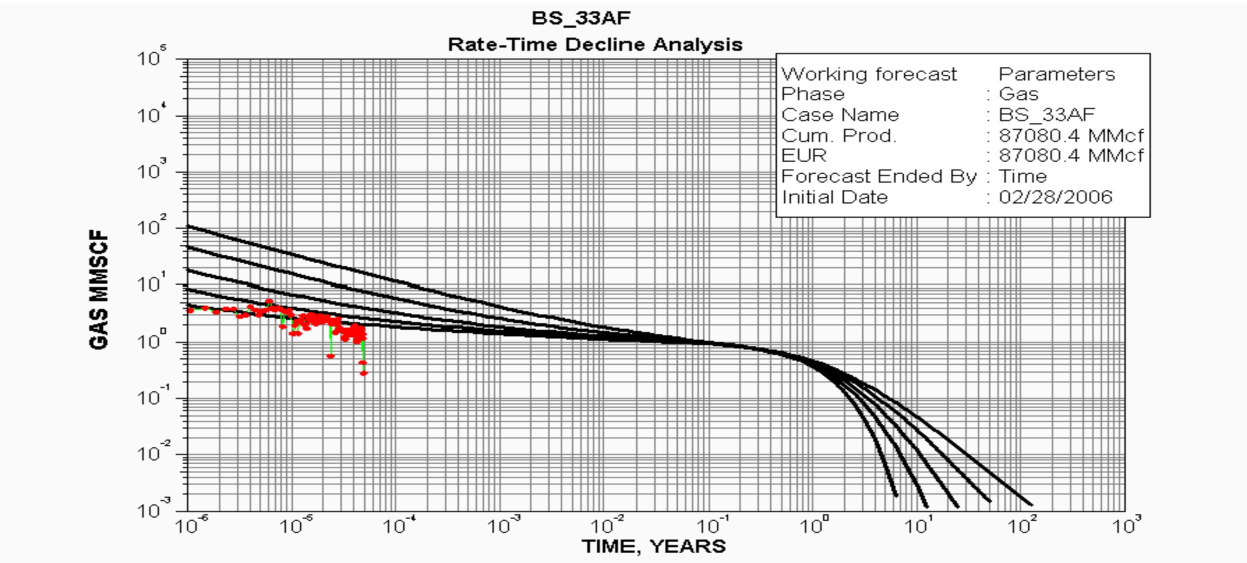

BS_33AF: Gas: OGBA_033:G3000X										
Historical Regression										
	Cumulative Production 87080.4 MMcf thru 12/31/2015									
	b Value	Di (A.e.)	qi (Mcf)	ti						
	0	0.0956	1198741	2/28/2006						
Working forecast										
	EUR 1.08439e+006 MMcf									
#	b Value	Di (A.e.)	qi (Mcf)	ti	te	qe (Mcf)	Res. (MMcf)	Ended By	Reserves Type	
1	0	0.0956	470050	8/31/2015	8/31/2025	180933.4	1050932	Time	None	

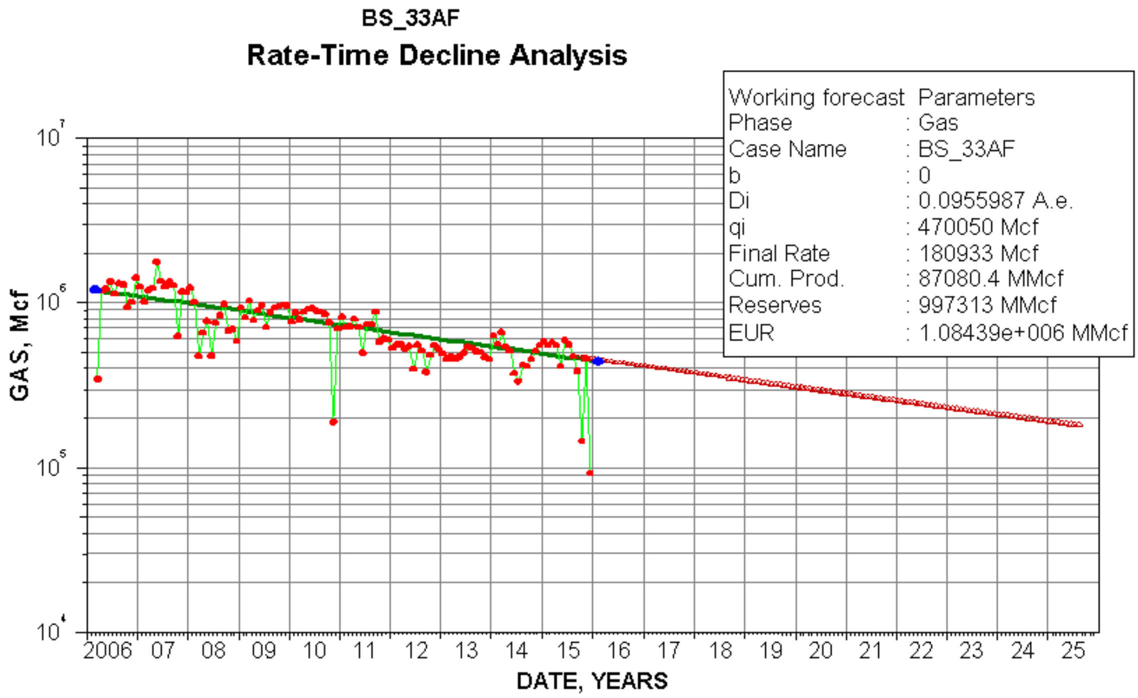

BS_34AG: Gas: OGBA_034:E3000X

Historical Regression

Cumulative Production 67294.7 MMcf thru 12/31/2015

b Value Di (A.e.)qi (qi (Mcf)Mcf ti

0 0 0 1/1/1900

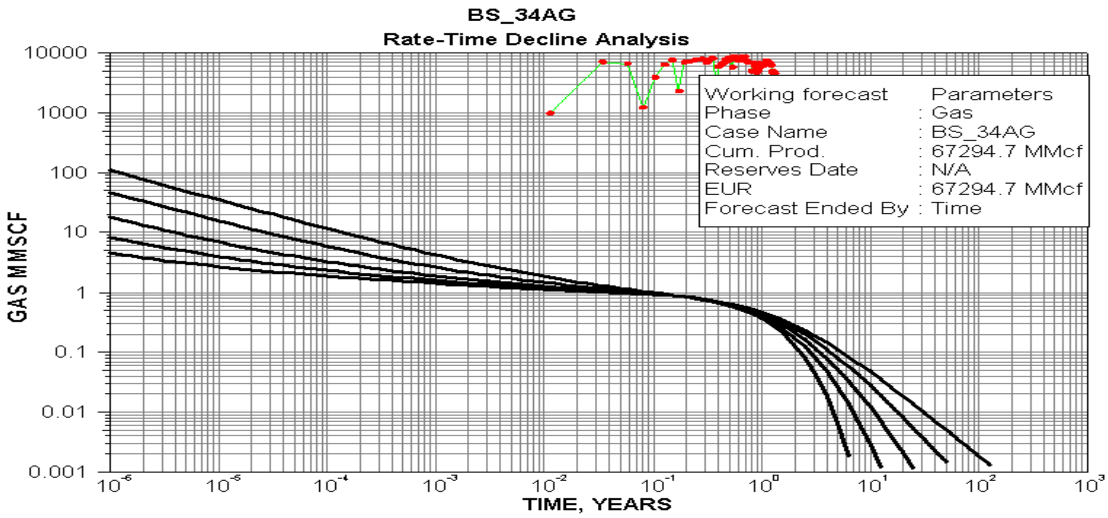

Historical Regression										
	Cumulative Production 67294.7 MMcf thru 12/31/2015									
	b Value	Di (A.e.)	qi (Mcf)	ti						
	0	0.10477	1085411	6/30/2009						
Working forecast										
	EUR 987842 MMcf									
#	b Value	Di (A.e.)	qi (Mcf)	ti	te	qe (Mcf)	Res. (MMcf)	Ended By	Reserves Type	
1	0	0.10477	428790	11/30/2017	11/30/2027	149867.4	920547	Time	None	

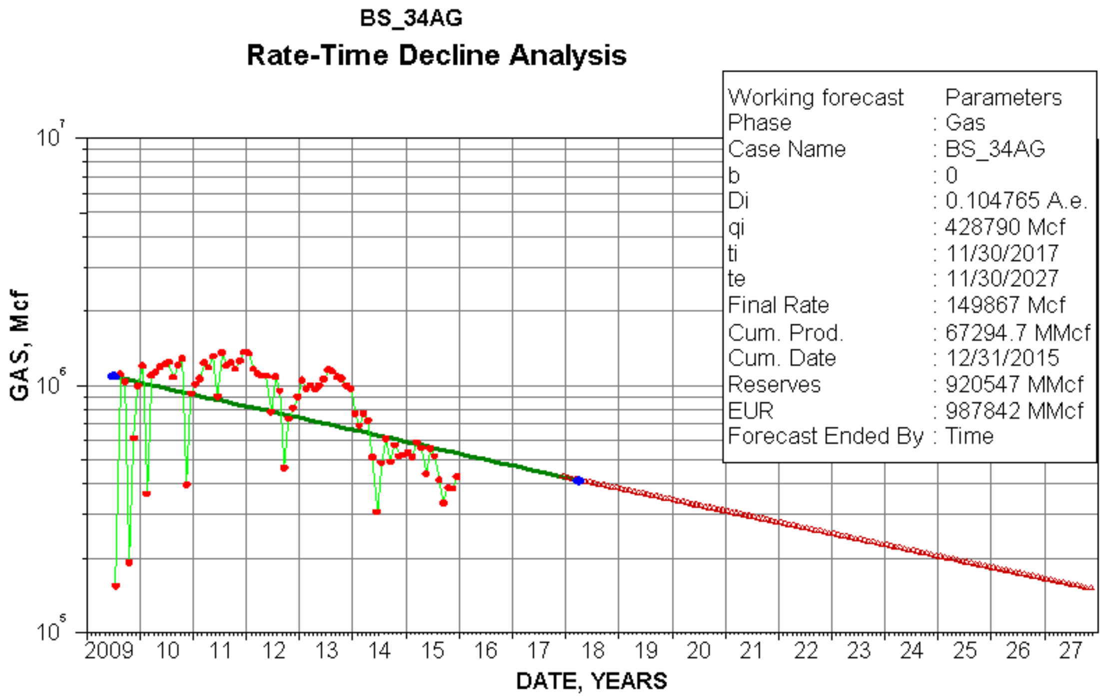

APPENDIX D Constant volume depletion Test at 224.6 F – Retrograde liquid deposit, Cumulative Produced Fluid (CPF)

	Pressure [Psia]	Retrograde liquid vol.[1] [%]	CPF[2] [%]
Psat=Pres	**5621**	**0.00**	**0.00**
Step A	5315	0.67	3.87
Step B	4515	2.01	13.83
Step C	3715	3.53	25.99
Step D	2915	4.78	40.03
Step E	2115	5.66	54.50
Step F	1315	5.51	69.70
Step G	515	4.86	86.70

a. Condensed liquid volume at indicated pressure @ reservoir temperature as a percent of the hydrocarbon pore volume at the dew point pressure and reservoir temperature.

b. Percent Cumulative produced Moles of gas at step pressure per Total moles at saturation pressure.

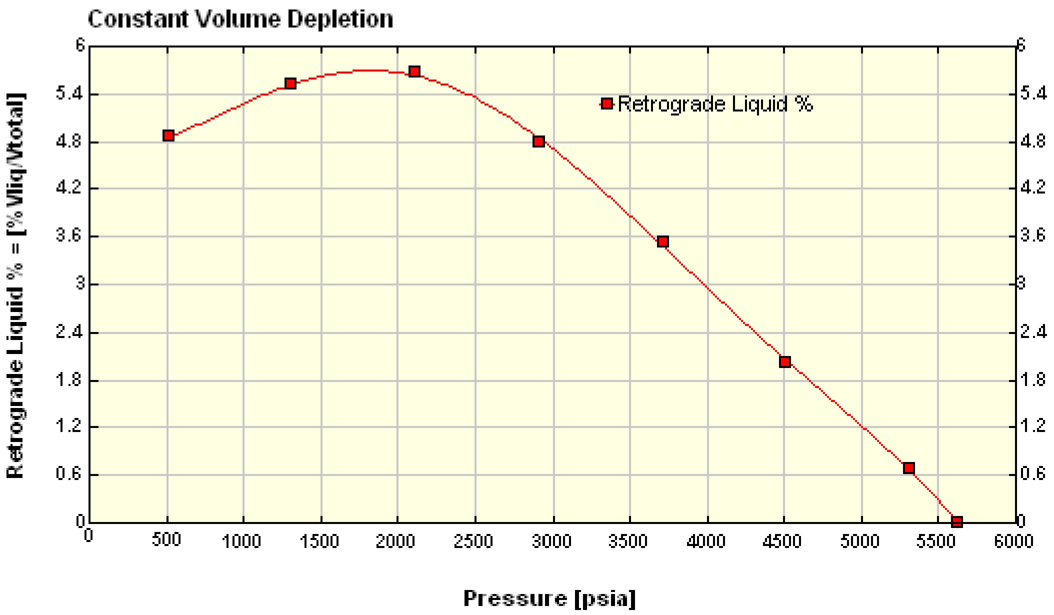

Figure Constant Volume Depletion for retrograde Liquid %

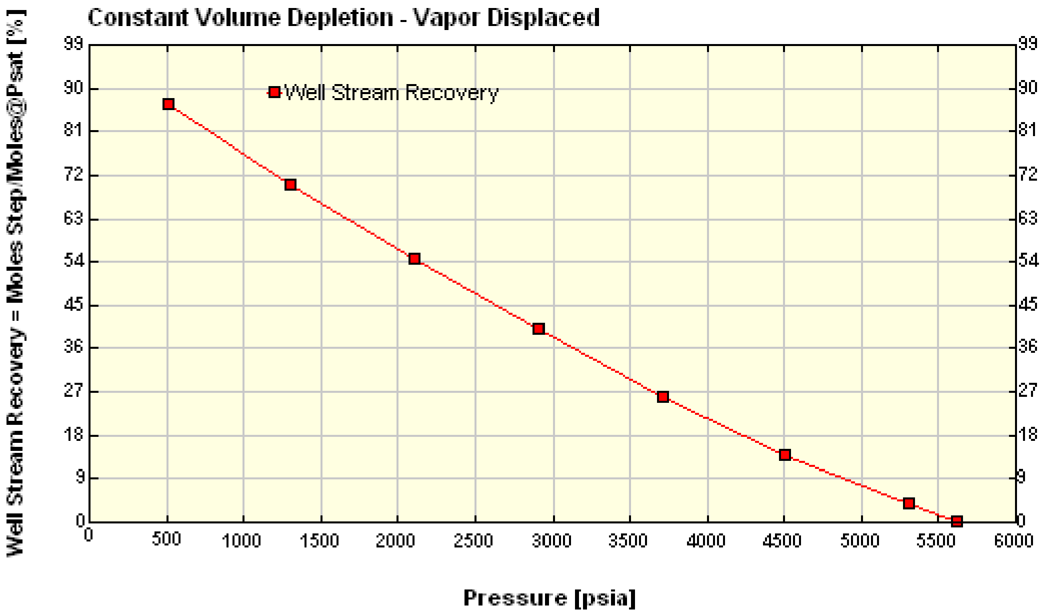

Figure: Constant Volume Depletion – Vapour Displaced

Table: Produced vapor properties

No	Pressure	Vap[1] Density	Vap Z-factor	Vap [2] Viscosity	Vap [3] FVF
	[psia]	[g/cm^3]		[cP]	[cu ft/scf]
1	5315	0.236	0.991	0.0291	0.0036
2	4515	0.190	0.957	0.0258	0.0041
3	3715	0.158	0.929	0.0228	0.0048
4	2915	0.133	0.910	0.0200	0.0060
5	2115	0.106	0.908	0.0175	0.0083
6	1315	0.077	0.926	0.0155	0.0136
8	515	0.051	0.965	0.0141	0.0362

a. Gravimetric density at indicated pressure and reservoir temperature

2. Calculated from Lee-Gonzalez correlation

3. Cu ft of gas at indicated pressure and reservoir temp. per standard cubic feet of gas at 14.7 psia ,60 F

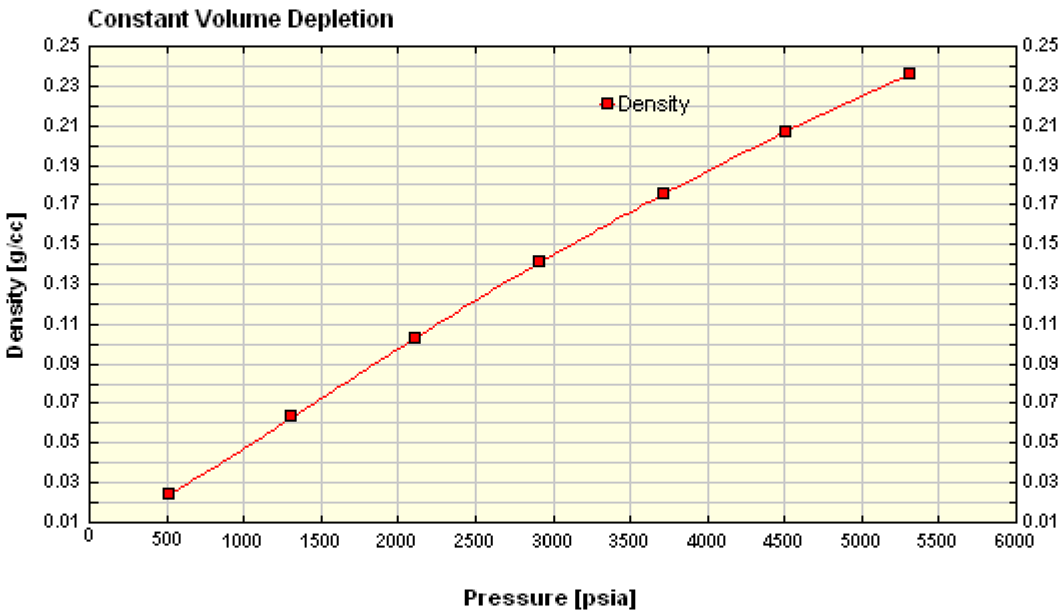

Figure Constant Volume Depletion for Density

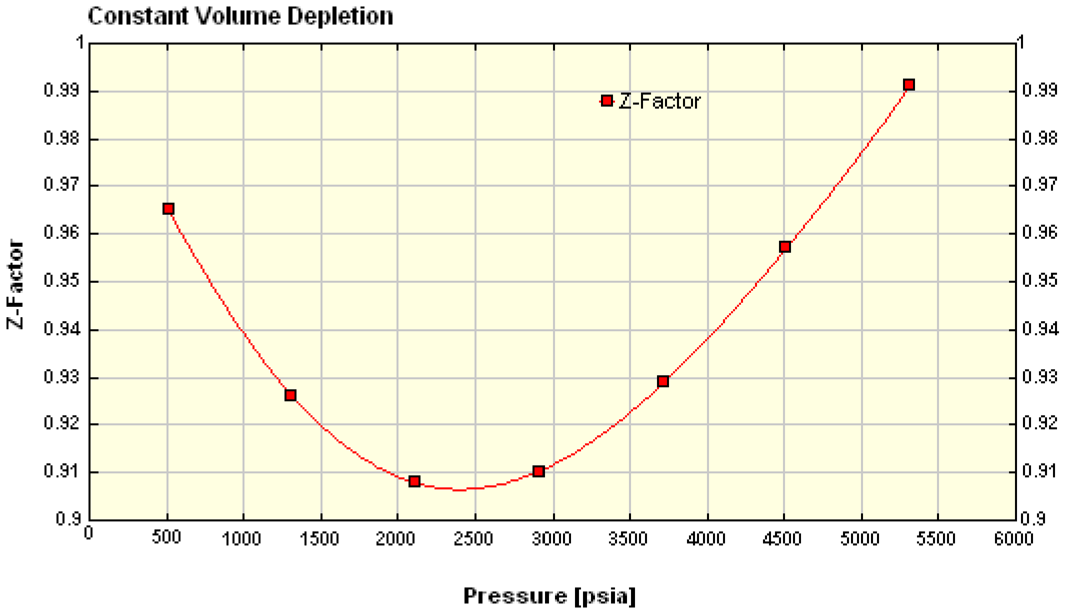

Figure: Constant Volume Depletion for Z-Factor

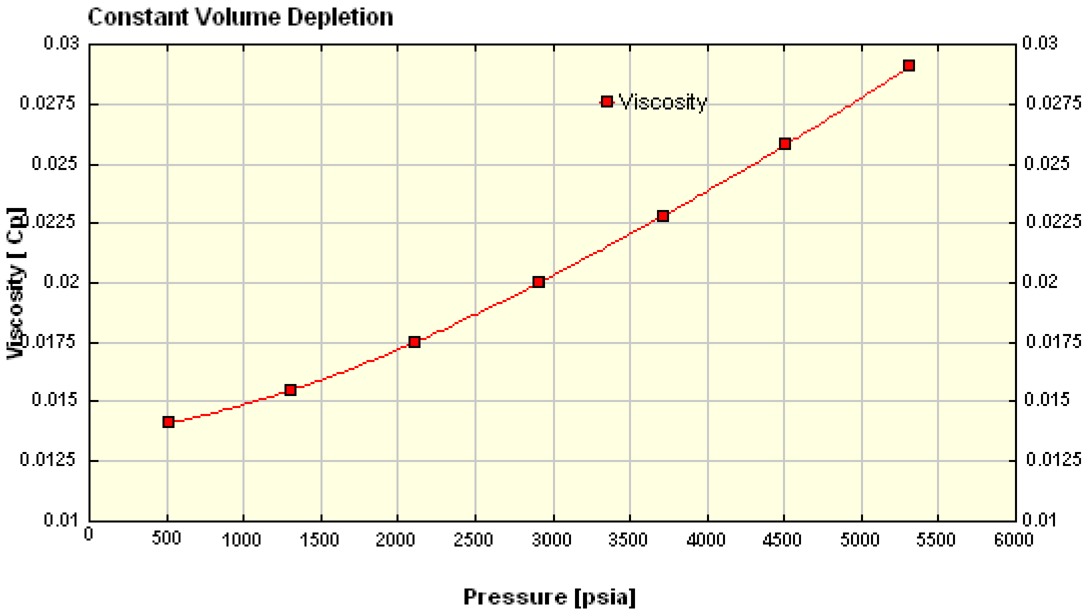

***Figure* Constant** Volume Depletion for Viscosity

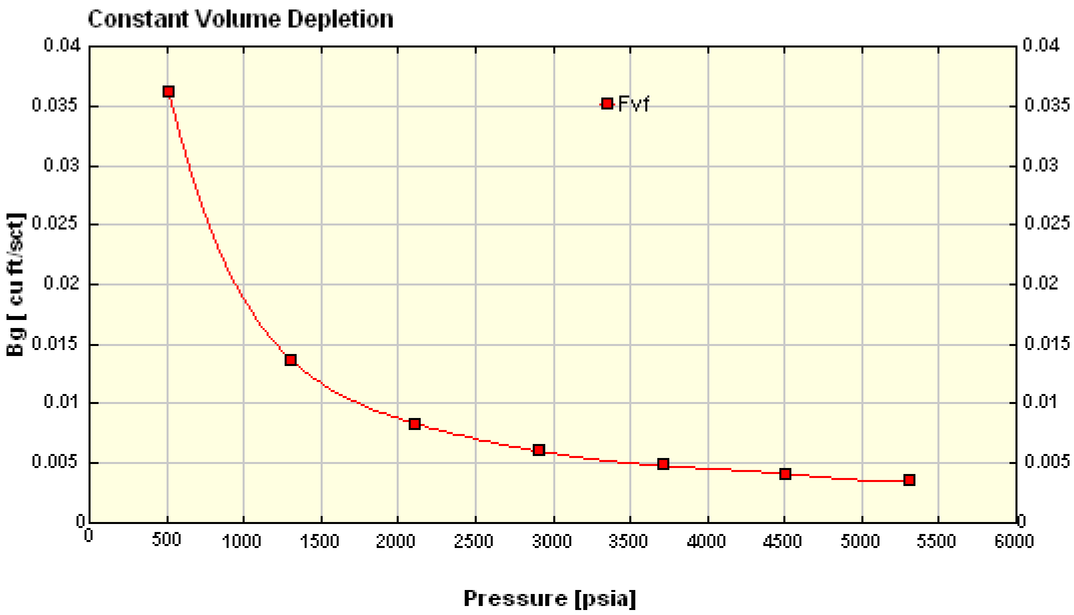

Figure Constant Volume Depletion for Formation Volume Factor

Time	Analytical Method production	Experimental Production	Standard Error of Mean (%)
0.2	0.0	0.0	0.0
5.0	0.0	0.0	0.0
10.0	0.0	0.0	0.0
15.0	0.0	0.0	0.0
20.0	10.0	0.0	2.9
25.0	10.0	52.3	12.2
30.0	10.0	74.8	18.7
35.0	20.0	81.5	17.8
40.0	70.0	71.8	0.5
45.0	140.0	68.0	20.8
50.0	140.0	85.3	15.8
55.0	145.0	73.3	20.7
60.0	145.0	191.8	13.5
65.0	150.0	217.3	19.4
70.0	150.0	186.5	10.5
75.0	150.0	174.5	7.1
80.0	150.0	182.8	9.5
85.0	150.0	188.0	11.0
90.0	150.0	197.8	13.8
95.0	150.0	194.0	12.7
100.0	152.0	180.5	8.2
105.0	155.0	183.5	8.2
110.0	160.0	197.8	10.9
115.0	162.0	215.0	15.3

120.0	162.0	221.0	17.0
125.0	165.0	216.5	14.9
130.0	170.0	196.3	7.6
135.0	172.0	199.3	7.9
140.0	172.0	204.5	9.4
145.0	175.0	215.0	11.5
150.0	180.0	221.0	11.8
155.0	185.0	208.3	6.7
160.0	185.0	191.8	1.9
165.0	185.0	194.0	2.6
170.0	185.0	200.0	4.3
175.0	185.0	211.3	7.6
180.0	185.0	215.8	8.9
185.0	185.0	206.0	6.1
190.0	185.0	193.3	2.4
195.0	185.0	195.5	3.0
200.0	185.0	200.0	4.3
204.9	185.0	194.8	2.8

Table *Constant Volume Depletion Test – Composition.*

	Pressure->psia	**5315**	**4515**	**3715**	**2915**	**2115**	**1315**		**515**		**Residual Liquid**
No.	**Component**	**[mol %]**	**[mol %]**	**[mol %]**	**[mol %]**	**[mol %]**	**[mol %]**		**[mol %]**		**[mol %]**
1	**N2**	**0.06**	**0.06**	**0.07**	**0.07**	**0.07**	**0.06**		**0.06**		**0.00**
2	**CO2**	**8.27**	**8.24**	**8.24**	**8.39**	**8.57**	**8.75**		**8.75**		**0.00**
3	**H2S**	**0.00**	**0.00**	**0.00**	**0.00**	**0.00**	**0.00**		**0.00**		**0.00**
4	**C1**	**84.86**	**84.97**	**85.02**	**84.89**	**84.70**	**84.46**		**84.36**		**0.00**
5	**C2**	**4.09**	**4.09**	**4.07**	**4.08**	**4.11**	**4.16**		**4.32**		**0.03**
6	**C3**	**1.12**	**1.11**	**1.11**	**1.11**	**1.11**	**1.12**		**1.13**		**0.20**
7	**i-C4**	**0.27**	**0.27**	**0.27**	**0.27**	**0.27**	**0.27**		**0.28**		**0.23**
8	**n-C4**	**0.28**	**0.28**	**0.28**	**0.28**	**0.28**	**0.28**		**0.28**		**0.38**
9	**i-C5**	**0.16**	**0.15**	**0.14**	**0.14**	**0.14**	**0.14**		**0.15**		**0.66**
10	**n-C5**	**0.13**	**0.12**	**0.12**	**0.12**	**0.11**	**0.12**		**0.12**		**0.31**
11	**C6**	**0.30**	**0.29**	**0.27**	**0.26**	**0.26**	**0.25**		**0.26**		**1.66**
12	**C7**	**0.25**	**0.23**	**0.22**	**0.22**	**0.21**	**0.21**		**0.21**		**4.20**
13	**C8**	**0.21**	**0.19**	**0.18**	**0.18**	**0.17**	**0.17**		**0.17**		**6.39**
14	**C9**	**0.00**	**0.00**	**0.00**	**0.00**	**0.00**	**0.00**		**0.00**		**6.49**
15	**C10**	**0.00**	**0.00**	**0.00**	**0.00**	**0.00**	**0.00**		**0.00**		**4.47**
16	**C11**	**0.00**	**0.00**	**0.00**	**0.00**	**0.00**	**0.00**		**0.00**		**5.66**
17	**C12+**	**0.00**	**0.00**	**0.00**	**0.00**	**0.00**	**0.00**		**0.00**		**69.34**
	TOTAL	**100.00**	**100.00**	**100.0**	**100.00**	**100.00**	**100.00**		**100.00**		**100.00**
	MW[g/mol]	**20.24**	**20.17**	**20.14**	**20.17**	**20.21**	**20.27**		**20.30**		**187.24**
	Gas G [air=1]	**0.698**	**0.696**	**0.695**	**0.696**	**0.697**	**0.699**		**0.700**		**0.821g/cc**

	C7+ MW[g/mol]	**101.06**	**100.91**	**100.94**	**100.87**	**100.88**	**100.91**		**100.91**		**191.33**
	C7+ [mol %]	**0.46**	**0.42**	**0.40**	**0.40**	**0.38**	**0.38**		**0.38**		**96.53**
Sample: Sample1											
Reservoir Temperature = 224.6 [F]											

Table Multi-Stage Separator Test - 1755 psia at 104 F to 1127 psia @ 60F to 15 psia @ 60F

Stage	**Pressure**	**Temp.**	**GOR**	**Liq. Density**	**Vap. Gravity**	**Sep.Vol. factor**
	[psia]	**[F]**	**[SCF/STB]**	**[g/cm^3]**	**[air=1]**	**[Sep. bbl/STB]**
Stage 1	**1755**	**104**	**24,585.8**	**0.714**	**0.691**	**1.205**
Stage 2	**1127**	**60**	**286**	**0.750**	**0.666**	**1.271**
Stage 3	**15**	**60**	**785**	**0.819**	**0.787**	
Total Separator Gas-Oil Ratio			**25,656.8**	**[SCF/STB]**		
TOTAL CGR			**38.97**	**[Bbls/mmscf]**		
Stock Tank Oil Gravity at 60F			**47.8**	**[API]**		
Separator Formation Vol. factor			**16.89**			
(bbl Res.Gas @ Saturation Condition/bbl STL @ 60 F)						

		Stage 1	Stage 2	Stage 3	Stock tank
N0.	**Component**	**Vapor**	**Vapor**	**Vapor**	**Liquid**
		[mol %]	[mol %]	[mol %]	[mol %]
1	N2	0.10	0.08	0.02	0.00
2	CO2	8.49	8.39	11.83	0.00
3	H2S	0.00	0.00	0.00	0.00
4	C1	85.36	87.34	72.93	0.00
5	C2	3.91	3.03	9.27	0.02
6	C3	0.94	0.58	3.80	0.16
7	i-C4	0.18	0.18	0.67	0.20
8	n-C4	0.17	0.17	0.63	0.33
9	i-C5	0.14	0.06	0.31	0.61
10	n-C5	0.10	0.04	0.21	0.28
11	C6	0.19	0.05	0.15	1.56
12	C7	0.24	0.04	0.09	4.06
13	C8	0.18	0.04	0.09	6.30
14	C9	0.00	0.00	0.00	6.43
15	C10	0.00	0.00	0.00	4.46
16	C11	0.00	0.00	0.00	5.67
17	C12+	0.00	0.00	0.00	69.91
	TOTAL	**100.00**	**100.00**	**100.00**	**100.00**
	MW	20.01	19.30	19.69	188.18
Sample: BHS					

APPENDIX E summary of the database for seismic interpretation

Data Type	No	Coverage	Data Format
3D Seismic	2	Ogba Egase Ishelle (Area~200Sq.Km)	SEG-Y, ZGY
Well Logs	18	Wells 1,2,3,4,5,6,7,8,8B,9,9ST,10ST,11,12,12ST,13,14 &15	LAS
check shot	2	Wells: 3, 5	Ascii
Deviation Survey	8	8B,10ST,11,13,14,15,6,12ST,9ST	LAS
Ogba Egase Ishelle Field Report	1	Previous Study Report, 2004	MS Word
Core Analysis Report	1	WELL 8: SAND X8.1, X8.2, X9.2	PDF
Concession Boundary	1	OML AAA Concession Boundary	WORD & LAS
End of Well Report	4	Wells 10ST, 11,12,8B	WORD
Sand file	1	For Wells: 1, 2, 3, 4, 5, 6, 7, 8, 8B, 9, 9ST, 10ST, 11,12, 12ST,13,14,15.	PDF

***Table*:**Data Base

WELL HEADER	NO	HEADER INFORMATION FOR WELLS 1-15	LAS
PRODUCTION HISTORY	1	X.8.1(2SS,4SS,5SS,7SS) X.8.2(2LS,4LS,5LS,7LS,9SS) A.8.3(7LS)	MS Excel
PVT	7	X.8.1, X.8.2, X.8.3, Y.2.1, Y.3.0, Z.20	PDF
BHP	1	2LS,2SS,4LS,5LS,7SS,7LS,9SS	MS Excel
WELL SCHEMATICS	9	Wells; 2SS,4LS,4SS,5LS,5SS,7LS,9LS,9SS,7SS	MS Excel & PDF

Table: Shows the available log suites for each of Ogba Egase Ishelle Wells

LOGS	WELLS																	
WELL ID	X1	X2	X3	X4	X5	X6	X7	X8	X8B	X9	X9ST	X10ST	X11	X12	AX12ST	X13	X14	X15
GAMMA RAY	1	1	1	1	1	1	1	1	1	1	1	1		1	1	1	1	1
RESISTIVITY	1	1	1	1	1	1		1	1	1	1	*	1	1	1	0	0	1
DENSITY	0	1	1	1	1	0	0	1	1	1	1	0	1	1	1	0	0	1
SP	1	1	1	1	1	1	1	0	0	0	0	0	0	0	0	0	0	0
SONIC	1	1	1	0	1	0	0	1	0	0	0	0	0	0	0	0	0	0
NEUTRON	0	0	1	1	0	0	0	1	1	0	1	0	1	1	1	0	0	1

KEYS
AVAILABLE = 1
INCOMPLETE = *
NOT AVAILABLE = 0

Table Well Header Information

S/No	Name	Surface X	Surface Y	KB	TD(MD)	TD (TVDSS)
1	X-1	347340	226220.00	16.30	4000.01	3983.70
2	X-2	349970	227660.00	21.20	3515.56	3983.70
3	X-3	350800	227025.00	24.70	3864.81	3840.10
4	X-4	352770	228345.00	25.60	3833.48	3807.90
5	X-5	348900	228880.00	24.70	3449.99	3425.30
6	X-6	352770	228345.00	24.70	3599.99	3389.30
7	X-7	348750	229320.00	26.70	3299.91	3273.20
8	X-8	350785	228275.00	23.10	3682.83	3659.70
9	X-8B	350020	229477.60	27.04	3626.51	3203.30
10	X-9	352000	228000.00	21.70	3289.94	3268.20
11	X-9ST	325000	228000.00	11.10	3453.40	3383.00
12	X-10ST	350018.00	229469.96	27.04	3428.7	2944.10
13	X-11	350018.00	229465.44	27.00	4877.41	3231.10
14	X-12	349839.00	225943.00	26.50	4003.24	3976.70
15	X-12ST	349839.00	225943.00	11.18	3658.21	3589.70
16	X-13	349842.00	225943.00	29.19	4150.00	3898.60
17	X-14	351993.20	227998.85	11.12	3863.34	3619.00
18	X-15	351998.80	227994.75	11.12	3747.52	3610.20

TABLE Summary Average Reservoir Property and Volumetric Estimates

SAND	Bgi Cu.ft/scf	Boi	PSO STOIIP (MMSTB)	PSO GIIP (BCF)	POR.	NTG	SW	CONTACT	
								OWC/ODT	GOC/GDT/GWC
A7.1	0.0040			66.74	0.2105	0.96640	0.24360		2908.85 GDT
A8.0	0.0044			169.14	0.1183	0.85960	0.37053		2958.45 GDT
A8.1	0.0044			249.19	0.2467	0.82410	0.22905		2967.64 GDT
A9.0	0.0044			88.35	0.1900	0.82000	0.34000		3046.15 GDT
A9.1	0.0043			28.62	0.2200	0.92000	0.15000		3050.88 GDT
A10.1	0.0043			82.96	0.2000	0.90000	0.36220		3086.10 GWC
A10.0a	0.0043			5.48	0.2000	0.92000	0.15000		3082.59 GWC
A10.0b	0.0043			8.05	0.1710	0.90840	0.45770		3089.15 GWC
B1.1	0.0043			89.76	0.2140	0.86430	0.31720		3217.99 GWC
B2.1	0.0042			50.92	0.1927	0.70790	0.42632		3271.30 GDT
B3.0	0.0033			204.20	0.2673	0.91900	0.24520		3262.77 GDT
B5.0	0.0041			4.78	0.1645	0.83430	0.63427		3425.08 GDT
C1.0	0.0033			504.47	0.2359	0.88500	0.30310		3572.31 GDT
C2.0	0.0036			93.85	0.2167	0.89070	0.32049		3607.04 GWC

C2.1	0.0040			17.09	0.1770	0.68020	0.31880		3614.22 GWC
C3.0	0.0040			6.25	0.1288	0.90520	0.66630		3601.67 GDT
C4.1	0.0039			17.53	0.1691	0.89000	0.33590		3732.39 GDT
D2	0.0039			2.90	0.1438	0.83850	0.37840		3745.1 GDT
D3	0.0039			1.55	0.1535	0.85140	0.23660		3791.93 GDT
A8.2U	0.0044	2.0500	21.1700	131.79	0.2100	0.88000	0.35000	2986.79 OWC	2967.27 GOC
A8.2L		2.0500	7.6215		0.1561	0.87290	0.42480	2989.22 ODT	
A8.3	0.004	2.1500	24.5750	87.74	0.2197	0.8209	0.3804	3003.47 OWC	3000.53 GOC
A11	0.0043	2.9500	17.1231	79.71	0.2230	0.8969	0.2985	3129.41 0WC	3124.72 GOC
B1.0	0.0043	1.3800	5.4236	133.52	0.8133	0.8133	0.3684	3204.07 ODT	3187 GOC
TOTAL			75.9132	2,188.54					

The word 1P is often used to denote proven reserves, 2P is the total of proven and likely reserves and 3P is the number of proven, probable and potential reserves.

SPE. (2011). Guidelines for Application of The Petroleum Resources Management System. Society of Petroleum Engineers.